Electronic Supplementary Material (ESI) for Chemical Science.

Hit-optimization using target-directed dynamic combinatorial chemistry: Development of inhibitors of the anti-infective target 1-deoxy-D-xylulose-5-phosphate synthase

Ravindra P. Jumde,[a] Melissa Guardigni,[a,d] Robin M. Gierse,[a,b,c] Alaa Alhayek,[a,b] Di Zhu,[a,b,c] Zhoor Hamid,[a,b] Sandra Johannsen,[a,b] Walid A. M. Elgaher,[a] Philipp J. Neusens,[a,b] Christian Nehls,[e] Jörg Haupenthal,[a] Norbert Reiling,[f,g] Anna K. H. Hirsch[a,b*]

[a] Department of Drug Design and Optimization, Helmholtz Institute for Pharmaceutical Research Saarland (HIPS) – Helmholtz Centre for Infection Research (HZI), Campus Building E8.1, 66123 Saarbrücken, Germany

[b] Department of Pharmacy, Saarland University, Campus Building E8.1, 66123 Saarbrücken, Germany

[c] Stratingh Institute for Chemistry, University of Groningen, Nijenborgh 7, 9747 AG Groningen, The Netherlands

[d] D3-PharmaChemistry, Istituto Italiano di Tecnologia, Via Morego 30, 16163 Genoa, Italy

[e] RG Biophysics, Research Center Borstel, Leibniz Lung Center, Borstel, Germany.

[f] RG Microbial Interface Biology, Research Center Borstel, Leibniz Lung Center, Borstel, Germany.

[g] German Center for Infection Research (DZIF), Partner site Hamburg-Lübeck-Borstel-Riems, Borstel, Germany.

*Corresponding author: Anna.Hirsch@helmholtz-hips.de

TABLE OF CONTENTS

Supplementary methods 3

General information 3

Chemicals 3

General procedure for DCC experiments 4

General procedure for molecular docking studies (GP-7): 5

General procedure for acylhydrazone formation (GP-8): 5

General procedure for amide bioisostere formation (GP-9): 6

General procedure for oxadiazole bioisostere formation (GP-10): 6

DCC-experiments 7

DCC-1: 7

DCC-2: 8

DCC-3: 8

DCC-4 9

DCC-5 (Competition experiment with ThDP): 9

DCC-6 (Competition experiment with ThDP and BAP): 10

Characterization of acylhydrazones 10

Identification of different conformers of acylhydrazone 10

Determination of IC_{50} values 19

Determination of antibacterial activity 19

DLS measurements 20

Mycobacterium tuberculosis growth analysis in liquid culture 20

Binding affinity (K_D) determinations by surface plasmon resonance (SPR) 20

Mode-of-inhibition (MOI) study 21

Protein stability study by thermal shift assay 22

Supplementary Figures 23

Supplementary references 128

SUPPLEMENTARY METHODS

General information

All reactions using oxygen- and/or moisture-sensitive materials were carried out in dry solvents (*vide infra*) under a nitrogen atmosphere using oven-dried glassware. Reactions were monitored by a Liquid chromatography-mass spectrometry (LC-MS) system equipped with Dionex UltiMate 3000 pump, autosampler, column compartment, detector, and ESI quadrupole MS (MSQ Plus or ISQ EC) from Thermo Fisher Scientific, Dreieich, Germany. Purification of the final products, when necessary, was performed using preparative HPLC (Dionex UltiMate 3000 UHPLC+ focused, Thermo Scientific) on a reversed-phase column (C18 column, 5 µM, Macherey-Nagel, Germany). The solvents used for the chromatography were water (0.1 % formic acid) and MeCN (0.1% formic acid). High-resolution mass (HRMS) of final products was determined by LCMS/MS using a Thermo Scientific Q Exactive Focus Orbitrap LC-MS/MS system. NMR data were collected on a Bruker Avance Neo 500 MHz (^{1}H at 500.0 MHz; ^{13}C at 126.0 MHz; ^{19}F NMR at 470 MHz), equipped with a Prodigy Cryo-probe. Chemical shifts are reported in parts per million (ppm) relative to residual solvent peak (DMSO-d_6, ^{1}H: 2.54 ppm; ^{13}C: 39.9 ppm). Coupling constants are reported in Hertz (Hz). Multiplicity is reported with the usual abbreviations (s: singlet, br s: broad singlet, d: doublet, dd: doublet of doublets, ddd: doublet of doublet of doublets, t: triplet, dt: doublet of triplets, q: quartet, p: pentet, dp: doublet of pentets, m: multiplet).

The periodic progress and analysis of DCC were monitored by UPLC-MS (ThermoScientific Dionex Ultimate 3000 UHPLC System coupled to a ThermoScientific Q Exactive Focus with an electrospray ion source) using an Acquity Waters Column (BEH, C8 1.7 µm, 2.1 × 150 mm, Waters, Germany) at a flow rate of 0.250 mL/min with detection set at 210, 254, 290, and 310 nm, and the mass spectrum recorded in a positive mode in the range of 100−700 m/z. The solvent system was 0.1% formic acid in H_2O (Solvent-A) and 0.1% formic acid in MeCN (Solvent-B). The gradient program began with 5% of Solvent-B for 1 min and was then increased to 95% of Solvent-B over 17 min and held for 2 min, followed by a decrease of Solvent-B to 5% over 0.1 min, where it was held for 2 min.

Chemicals

Unless indicated otherwise, reagents and substrates were purchased from commercial sources and used as received. Solvents not required to be dry were purchased as technical grade and used as received. Dry solvents were purchased from commercial sources in Sure/Seal™ bottles and used as received and stored under a dry inert gas (N_2 or Ar). Inert atmosphere experiments were performed with standard Schlenk techniques with dried (P_2O_5) nitrogen gas. Unless indicated otherwise, the acylhydrazone products were purified by precipitation of the product at lower temperature followed by filtration and successive washing with cold solvents to remove soluble impurities (for details, see purification method-1). All reported compounds were characterized by ^{1}H and ^{13}C NMR and compared with literature data. All new compounds were fully characterized by ^{1}H and ^{13}C NMR and HRMS techniques. The purity of the final products was determined by LC-MS and found to be >95%.

General procedure for DCC experiments

DCL preparation (GP-1): To a 1.5 mL Eppendorf Tube® containing phosphate buffer (pH 6.25 or 7.04), were added hydrazides (300−2000 μM each, in DMSO), aldehydes (100 μM each, in DMSO), aniline (10 mM, in DMSO), and an additional amount of DMSO to reach a final concentration of 5% in the DCL with 1 mL of end-volume. The DCL was allowed to gently mix on a rotating wheel (7 rpm) at room temperature and was frequently monitored via UPLC-MS. For analysis, 10 μL of the corresponding library was mixed with 90 μL acetonitrile and 2 μL of NaOH (2 M), the mixture was centrifuged, and the supernatant was used for the analysis.

Protein-templated DCL preparation (GP-2): To a 1.5 mL Eppendorf Tube® containing phosphate buffer (pH 6.25 or 7.04), were added hydrazides (300−2000 μM each, in DMSO), aldehydes (100 μM each, in DMSO), aniline (10 mM, in DMSO), the protein drDXPS (20−40 μM in phosphate buffer at pH 6.25 or 7.04), and an additional amount of DMSO to reach a final concentration of 5% in the DCL with 1 mL of end-volume. The DCL with the protein was allowed to gently mix on a rotating wheel (7 rpm) at room temperature and was frequently monitored via UPLC-MS, and the traces were compared with the blank composition. For analysis, 10 μL of the corresponding library were mixed with 90 μL acetonitrile and 2 μL of NaOH (2 M), the mixture was centrifuged and the supernatant was used for the analysis.

Note: The protein-templated DCL-2 and -3 were run as duplicate.

DCL preparation (pre-equilibrated) (GP-3): To a 1.5 mL Eppendorf Tube® containing phosphate buffer (pH 6.25, 512.5 μL), were added hydrazides (300 μM each, in DMSO), aldehydes (100 μM each, in DMSO), aniline (10 mM, in DMSO), and an additional amount of DMSO to reach a final concentration of 5% in the DCL. The DCL was allowed to gently mix on a rotating wheel (7 rpm) at room temperature for six hours and was frequently monitored via UPLC-MS. The additional amount of phosphate buffer (pH 6.25, 437.5 μL) was added after six hours to reach 1 mL of end-volume. For analysis, 10 μL of the corresponding library was mixed with 90 μL acetonitrile and 2 μL of NaOH (2 M), the mixture was centrifuged, and the supernatant was used for the analysis.

Protein-templated DCL preparation (pre-equilibrated) (GP-4): To a 1.5 mL Eppendorf Tube® containing phosphate buffer (pH 6.25, 512.5 μL), were added hydrazides (300 μM each, in DMSO), aldehydes (100 μM each, in DMSO), aniline (10 mM, in DMSO), and an additional amount of DMSO to reach a final concentration of 5% in the DCL. The DCL was allowed to gently mix on a rotating wheel (7 rpm) at room temperature for six hours and was frequently monitored via UPLC-MS. After six hours, the protein drDXPS (437.5 μL, 20 μM in phosphate buffer at pH 6.25) was added to the pre-equilibrated library. The DCL with the protein was allowed to gently mix on a rotating wheel (7 rpm) at room temperature and was frequently monitored for the next 6 h via UPLC-MS and the traces were compared with the blank composition. For analysis, 10 μL of the corresponding library was mixed with 90 μL acetonitrile and 2 μL of NaOH (2 M), the mixture was centrifuged, and the supernatant was used for the analysis.

Protein-templated DCL preparation for competition experiment with ThDP (GP-5): To a 1.5 mL Eppendorf Tube® containing phosphate buffer (pH 6.25), were added hydrazides (300 μM each, in DMSO), aldehydes (100 μM each, in DMSO), aniline (10 mM, in DMSO), an additional amount of DMSO to reach a final concentration of 5%, and a pre-incubated mixture of drDXPS protein (40 μM in phosphate buffer at pH 6.25), ThDP (100 μM in water), and $MgCl_2$ (100 μM in water) in the DCL with 1 mL of end-volume. The DCL with the protein was allowed to gently mix on a rotating wheel (7 rpm) at room temperature and was frequently monitored via UPLC-MS, and the traces were compared with the blank composition. For analysis, 10 μL of the corresponding library was mixed with 90 μL acetonitrile and 2 μL of NaOH (2 M), the mixture was centrifuged, and the supernatant was used for the analysis.
Note: The blank-DCL composition for competition experiments was similar except for the added protein. The protein- templated DCL was run as duplicate.

Protein-templated DCL preparation for competition experiment with ThDP and BAP (GP-6): To a 1.5 mL Eppendorf Tube® containing phosphate buffer (pH 6.25), were added hydrazides (300 μM each, in DMSO), aldehydes (100 μM each, in DMSO), aniline (10 mM, in DMSO), an additional amount of DMSO to reach a final

concentration of 5%, and a pre-incubated mixture of drDXPS protein (40 μM in phosphate buffer at pH 6.25), ThDP (100 μM in water), $MgCl_2$ (100 μM in water), and BAP (100 μM in water) in the DCL with 1 mL of end-volume. The DCL with the protein was allowed to gently mix on a rotating wheel (7 rpm) at room temperature and was frequently monitored via UPLC-MS, and the traces were compared with the blank composition. For analysis, 10 μL of the corresponding library was mixed with 90 μL acetonitrile and 2 μL of NaOH (2 M) to raise pH > 8. The mixture was centrifuged, and the supernatant was used for the analysis.
Note: The blank-DCL composition for the competition experiments was the same except for the added protein. The protein-templated DCL was run as duplicate.

Assessment of DCL composition: The library composition was assessed after the equilibrium of acylhydrazone formation was reached as reported in the literature.[1,2] All the DCLs in this study reached an equilibrium between four to six hours. The "amplification factor" was determined with the relative peak area (RPA), which is the percent of each peak when the sum of all peak areas was set to 100%. The "normalized RPA" was used for the final assessment of amplification of the acylhydrazone products in the DCL.

$$amplification\ factor\ = \frac{RPA_{(templated)}}{RPA_{(blank)}}$$

$$normalized\ change\ of\ RPA\ = \frac{(RPA_{(templated)} - RPA_{(blank)})}{RPA_{(blank)}}$$

General procedure for molecular docking studies (GP-7):

The X-ray crystal structure of *Deinococcus radiodurans* (drDXPS) (PDB code: 2O1X) was used for our docking studies.[3] The binding site of drDXPS was defined to include residues within a 6.5 Å radius around the cofactor thiaminediphosphate in the LeadIT program. The binding site includes 43 amino acid residues and a magnesium ion. All 21 possible acylhydrazones products from DCL-1 were used as ligands for docking using the FlexX docking module in the LeadIT suite v2.3.2.[4] Top-30 (FlexX)-scored solutions were retained and subsequently post-scored with the HYDE module in LeadIT v2.3.2. After careful visualization to exclude poses with significant inter- or intramolecular clash terms or unfavorable conformations, the resulting solutions were subsequently ranked according to their binding energies. The top-ranked pose from each compound was chosen and used for the comparison. The 2D-figures were generated with Pose View[5] as implemented in the LeadIT suite. The program SeeSAR 10.0 was used to visualize the acylhydrazone hits from the DCL-1 inside the active site of enzyme drDXPS and to generate the figures.[6]

General procedure for acylhydrazone formation (GP-8):

To a heat-dried Schlenk tube equipped with a magnetic stirring bar, the hydrazide (1−1.2 equiv.) and the corresponding aldehyde (1 equiv.) were dissolved/suspended in MeOH under nitrogen atmosphere. The reaction mixture was stirred at 65 °C until completion. After cooling the reaction to room temperature, the reaction mixture was precipitated by cooling the Schlenk tube to 0 °C in an ice bath. The resulting crude was purified either by filtration and washing sequences (Purification method-1) or by preparative HPLC, affording the corresponding acylhydrazone products in 21−94% isolated yields.

Purification method-1: The precipitated reaction mixture was transferred to an Eppendorf Tube® and centrifuged for 2 min, the supernatant liquid was removed, and 1 mL ice-cold MeOH was added to the residue, which was resuspended by vigorous agitation by a vortex mixer. The cold suspension was centrifuged again for 2 min, followed by removal of supernatant liquid. This process was repeated at least three times or until the sufficiently pure product (residue) was isolated, which was monitored on LC-MS. The solvents were removed from the final residue under reduced pressure to obtain the pure acylhydrazone product.

Purification method-2: After cooling to room temperature, the reaction mixture was concentrated *in vacuo* and purified by preparative HPLC on a reversed-phase column (C18 column, 5 μM, Macherey-Nagel, Germany), using 15–100% gradient (MeCN (0.1% formic acid) in water (0.1% formic acid)). After removing water and acetonitrile from the pure fractions *in vacuo* followed by lyophilization, the pure acylhydrazone products were obtained.

General procedure for amide bioisostere formation (GP-9):

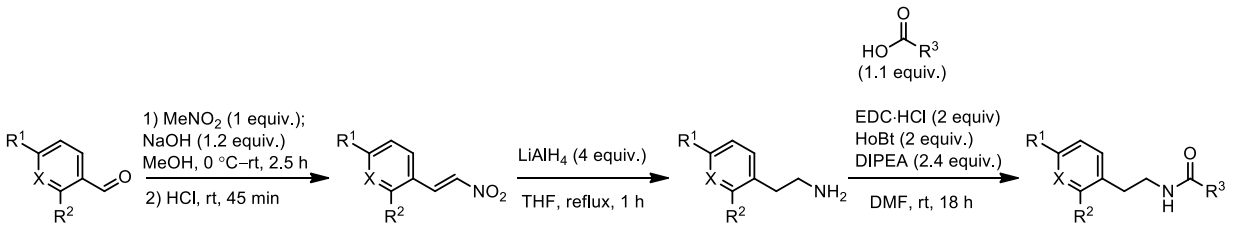

a: X = N, R^1 = CF_3, R^2 = H
b: X = CH, R^1 = OH, R^2 = F

38: X = N, R^1 = CF_3, R^2 = H
39: X = CH, R^1 = OH, R^2 = F

Step 1: To a 50 mL round-bottomed flask were added aldehyde (1 equiv.), nitromethane (1 equiv.) and MeOH (2 mL). The reaction mixture was cooled to 0 °C, and an aqueous solution of NaOH (1.2 equiv. In 1.5 mL water) was added. The reaction was kept stirring for 2.5 hours while slowly warming to rt. After, the reaction mixture was poured into an aqueous solution of HCl (0.6 mL in 1 mL of water) and kept stirring at rt for an additional 45 minutes. The reaction progress was monitored on LCMS. After full conversion, water (5 mL) was added to the reaction mixture and extracted with DCM (3 × 20 mL). The combined organic phases were dried over Na_2SO_4, filtered, and volatiles were removed on a rotary evaporator. The crude nitrostyrene derivative obtained was used in the next step without further purification.

Step 2: The crude nitrostyrene derivative (approx, 1 mmol) from the first step was added to a two-necked round-bottomed flask, and the flask was purged using vacuum-argon cycles. The dry-THF (16 mL) was added to the reaction flask followed by portion-wise addition of $LiAlH_4$ (4 equiv.), and the reaction mixture was kept stirring at rt for one hour. After the disappearance of starting material by LCMS, 1 M NaOH (10 mL) was slowly added to the reaction flask, and the resulting reaction mixture was filtered through Celite. The Celite pad was washed with EtOAc (3 × 20 mL), and the organic phase was separated, the aqueous phase was extracted with EtOAc and combined organic phases were treated with brine. After separation, the organic phases were dried over Na_2SO_4, filtered, and volatiles were removed on a rotary evaporator. The crude ethylamine derivative obtained was used in the next step without further purification.

Step 3: To a 50 mL round-bottomed flask, were added ethanamine (1equiv.), carboxylic acid (1.1 equiv.), HOBt.H_2O (2 equiv.), and 2 mL DMF. To the resulting solution were added EDC·HCl (2 equiv.), and DIPEA (2.5 equiv.). The reaction was kept stirring at rt for 18 hours before treating it with water (5 mL) and extracting it with EtOAc (3 × 10 mL). The combined organic phases were dried over Na_2SO_4, filtered and volatiles were removed on a rotary evaporator. The crude obtained was purified by preparative HPLC (H_2O:MeCN + 0.1% formic acid, gradient 5% to 100% MeCN) to afford the amide product.

General procedure for oxadiazole bioisostere formation (GP-10):

Oxadiazole compounds were prepared according to the reported procedure of Farshori *et al.* (2017) under microwave conditions.[7] The original procedure was adapted as follows:

The hydrazide (1 equiv.), corresponding carboxylic acid (1 equiv.), and neutral active aluminum oxide (100 mg / 50 mg of hydrazide) were ground to a fine powder in a mortar. This powder was transferred into a microwave (MW) glass tube and phosphorous oxytrichloride was added in excess (14 equiv.). The MW reaction tube was capped under air, and the reaction mixture was heated in a laboratory microwave oven at 90 °C for 30 min. For purification, the crude was washed with ice-cold distilled water and ice-cold concentrated sodium bicarbonate solution. The residue was further washed with cold MeOH to provide the final pure product. Further purification by preparative HPLC was needed for compound **41**.

DCC-experiments

DCC-1:

This experiment library consists of three aldehydes (**A1**–**A3**) and seven hydrazides (**H1**–**H7**).

DCL-1 (40 mol% protein): The DCC-experiment was carried out according to the GP-1 (blank) and GP-2 (protein-templated) in phosphate buffer at pH 6.25 and 5% DMSO.

The DCL-composition is as below:

Entry	Blank		Protein-templated (I)		Protein-templated (II)	
	amount	*Final conc. in DCL*	*amount*	*Final conc. in DCL*	amount	Final conc. in DCL
Phosphate buffer	950 µL	-	76 µL	-	15.2 µL	-
Hydrazide (100 mM)	7 × 3 µL (21 µL)	(7 × 300 µM)	7 × 3 µL (21 µL)	(7 × 300 µM)	7 × 0.6 µL[a] (4.2 µL)	(7 × 300 µM)
Aldehyde (100 mM)	3 × 1 µL (3 µL)	(3 × 100 µM)	3 × 1 µL (3 µL)	(3 × 100 µM)	7 × 0.2 µL[b] (0.6 µL)	(3 × 100 µM)
Aniline (1 M)	10 µL	10 mM	10 µL	10 mM	2 µL	10 mM
DMSO	16 µL	-	16 µL	-	3.2 µL	-
drDXPS (45.7 µM)*	0	-	874 µL	40 µM	174.8 µL	40 µM

*drDXPS, 45.7 µM in phosphate buffer at pH 6.25. [a] to minimize the error, the 21 µL stock solution was prepared by mixing 3 µL of each hydrazide from the initial 100 mM stock, and 4.2 µL were taken from this stock. [b] to minimize the error, the 6 µL stock solution was prepared by mixing 2 µL of each aldehyde from the initial 100 mM stock, and 0.6 µL were taken from this stock.

DCL-1 (20 mol% protein): The DCC-experiment was carried out according to the GP-1 (blank), GP-2 (protein-templated) in phosphate buffer at pH 6.25 and 5% DMSO.

The DCL-composition is as below:

Entry	Blank		Protein-templated (I)		Protein-templated (II)	
	amount	*Final conc. in DCL*	*amount*	*Final conc. in DCL*	*amount*	*Final conc. in DCL*
Phosphate buffer	950 µL	-	512.5 µL	-	102.5 µL	-
Hydrazide (100 mM)	7 × 3 µL (21 µL)	(7 × 300 µM)	7 × 3 µL (21 µL)	(7 × 300 µM)	7 × 0.6 µL[a] (4.2 µL)	(7 × 300 µM)
Aldehyde (100 mM)	3 × 1 µL (3 µL)	(3 × 100 µM)	3 × 1 µL (3 µL)	(3 × 100 µM)	7 × 0.2 µL[b] (0.6 µL)	(3 × 100 µM)
Aniline (1 M)	10 µL	10 mM	10 µL	10 mM	2 µL	10 mM
DMSO	16 µL	-	16 µL	-	3.2 µL	-
drDXPS (45.7 µM)*	0	-	437.5 µL	20 µM	87.5 µL	20 µM

* drDXPS, 45.7 µM in phosphate buffer at pH 6.25. [a] to minimize the error, the 21 µL stock solution was prepared by mixing 3 µL of each hydrazide from the initial 100 mM stock, and 4.2 µL were taken from this stock. [b] to minimize the error, the 6 µL stock solution was prepared by mixing 2 µL of each aldehyde from the initial 100 mM stock, and 0.6 µL were taken from this stock.

DCL-1 (20 mol% protein 'pre-equilibrated'): The DCC-experiment was carried out according to GP-3 (blank) and GP-4 (protein-templated) in phosphate buffer at pH 6.25 and 5% DMSO.

The DCL-composition is as below:

Entry	Blank		Protein-templated	
	amount	*Final conc. in DCL*	*amount*	*Final conc. in DCL*
Phosphate buffer	512.5 + 437.5 µL	-	512.5 µL	-
Hydrazide (100 mM)	7 × 3 µL (21 µL)	(7 × 300 µM)	7 × 3 µL (21 µL)	(7 × 300 µM)
Aldehyde (100 mM)	3 × 1 µL (3 µL)	(3 × 100 µM)	3 × 1 µL (3 µL)	(3 × 100 µM)
Aniline (1 M)	10 µL	10 mM	10 µL	10 mM
DMSO	16 µL	-	16 µL	-
drDXPS (45.7 µM)*	0	-	437.5 µL	20 µM

* drDXPS, 45.7 µM in phosphate buffer at pH 6.25

DCC-2:

This experiment's library consists of three aldehydes (**A4**–**A6**) and seven hydrazides (**H2, H5, H6, H8–H11**).

This DCC-experiment was carried out according to the GP-1 (blank) and GP-2 (protein-templated) in phosphate buffer at pH 7.04 and 5% DMSO.

The DCL-composition is as below:

Entry	Blank		Protein-templated (I)		Protein-templated (II)	
	amount	*Final conc. in DCL*	*amount*	*Final conc. in DCL*	*amount*	*Final conc. in DCL*
Phosphate buffer	950	-	524.5 µL	-	524.5 µL	-
Hydrazide (100 mM)	7 × 3 µL (21 µL)	(7 × 300 µM)	7 × 3 µL (21 µL)	(7 × 300 µM)	7 × 3 µL (21 µL)	(7 × 300 µM)
Aldehyde (100 mM)	3 × 1 µL (3 µL)	(3 × 100 µM)	3 × 1 µL (3 µL)	(3 × 100 µM)	3 × 1 µL (3 µL)	(3 × 100 µM)
Aniline (1 M)	10 µL	10 mM	10 µL	10 mM	10 µL	10 mM
DMSO	16 µL	-	16 µL	-	16 µL	-
drDXPS (94 µM)*	0	-	425.5 µL	40 µM	425.5 µL	40 µM

* drDXPS, 94 µM in phosphate buffer at pH 7.04

DCC-3:

DCC-3a: This experiment's library consists of eleven aldehydes (**A1, A2, A7**–**A15**) and two hydrazides (**H11** and **H12**).

This DCC-experiment was carried out according to the GP-1 (blank) and GP-2 (Protein-templated) in phosphate buffer at pH 7.04 and 5% DMSO.

The DCL-composition is as below:

Entry	Blank		Protein-templated (I)		Protein-templated (II)	
	amount	*Final conc. in DCL*	*amount*	*Final conc. in DCL*	*amount*	*Final conc. in DCL*
Phosphate buffer	950	-	590 µL	-	590 µL	-
Hydrazide (200 mM)	2 × 10 µL (20 µL)	(2 × 2000 µM)	2 × 10 µL (20 µL)	(2 × 2000 µM)	2 × 10 µL (20 µL)	(2 × 2000 µM)
Aldehyde (100 mM)	11 × 1 µL (11 µL)	(11 × 100 µM)	11 × 1 µL (11 µL)	(11 × 100 µM)	11 × 1 µL (11 µL)	(11 × 100 µM)
Aniline (1 M)	10 µL	10 mM	10 µL	10 mM	10 µL	10 mM
DMSO	9 µL	-	9 µL	-	9 µL	-
drDXPS (111 µM)*	0	-	360 µL	40 µM	360 µL	40 µM

* drDXPS, 111 µM in phosphate buffer at pH 7.04

DCC-3b: This experiment library consists of eleven aldehydes (**A16** –**A26**) and two hydrazides (**H11** and **H12**). This DCC-experiment was carried out according to the GP-1 (blank) and GP-2 (Protein-templated) in phosphate buffer at pH 7.04 and 5% DMSO.

The DCL-composition is as below:

Entry	Blank		Protein-templated (I)		Protein-templated (II)	
	amount	*Final conc. in DCL*	*amount*	*Final conc. in DCL*	*amount*	*Final conc. in DCL*
Phosphate buffer	950 µL	-	590 µL	-	590 µL	-
Hydrazide (200 mM)	2 × 10 µL (20 µL)	(2 × 2000 µM)	2 × 10 µL (20 µL)	(2 × 2000 µM)	2 × 10 µL (20 µL)	(2 × 2000 µM)
Aldehyde (100 mM)	11 × 1 µL (11 µL)	(11 × 100 µM)	11 × 1 µL (11 µL)	(11 × 100 µM)	11 × 1 µL (11 µL)	(11 × 100 µM)
Aniline (1 M)	10 µL	10 mM	10 µL	10 mM	10 µL	10 mM
DMSO	9 µL	-	9 µL	-	9 µL	-
drDXPS (111 µM)*	0	-	360 µL	40 µM	360 µL	40 µM

* drDXPS, 111 µM in phosphate buffer at pH 7.04

DCC-4

This DCC-experiment was carried out according to the GP-1 (blank) and GP-2 (Protein-templated) in phosphate buffer at pH 7.04 and 5% DMSO.
The DCL-composition is as below:

Entry	Blank		Protein-templated (I)		Protein-templated (II)	
	amount	*Final conc. in DCL*	*amount*	*Final conc. in DCL*	*amount*	*Final conc. in DCL*
Phosphate buffer	950	-	590 µL	-	590 µL	-
Hydrazide (100 mM)	7 × 3 µL (21 µL)	(7 × 300 µM)	7 × 3 µL (21 µL)	(7 × 300 µM)	7 × 3 µL (21 µL)	(7 × 300 µM)
Aldehyde (100 mM)	3 × 1 µL (3 µL)	(11 × 100 µM)	3 × 1 µL (3 µL)	(11 × 100 µM)	3 × 1 µL (3 µL)	(11 × 100 µM)
Aniline (1 M)	10 µL	10 mM	10 µL	10 mM	10 µL	10 mM
DMSO	9 µL	-	16 µL	-	9 µL	-
drDXPS (111 µM)*	0	-	360 µL	40 µM	360 µL	40 µM

* drDXPS, 111 µM in phosphate buffer at pH 7.04

DCC-5 (Competition experiment with ThDP):

This DCC-experiment was carried out according to the GP-5 (blank and protein-templated) in phosphate buffer at pH 6.25 and 5% DMSO using the DCL-1.
The DCL-composition is as below:

Entry	Blank		Protein-templated (I)		Protein-templated (II)	
	amount	*Final conc. in DCL*	*amount*	*Final conc. in DCL*	*amount*	*Final conc. in DCL*
Phosphate buffer	948 µL	-	587.6µL	-	587.6µL	-
Hydrazide (100 mM)	7 × 3 µL (21 µL)	(7 × 300 µM)	7 × 3 µL (21 µL)	(7 × 300 µM)	7 × 3 µL (21 µL)	(7 × 300 µM)
Aldehyde (100 mM)	3 × 1 µL (3 µL)	(3 × 100 µM)	3 × 1 µL (3 µL)	(3 × 100 µM)	3 × 1 µL (3 µL)	(3 × 100 µM)
Aniline (1 M)	10 µL	10 mM	10 µL	10 mM	10 µL	10 mM
DMSO	16 µL	-	16 µL	-	16 µL	-
ThDP (100 mM)	1 µL	100 µM	1 µL	100 µM	1 µL	100 µM
$MgCl_2$ (100 mM)	1 µL	100 µM	1 µL	100 µM	1 µL	100 µM
drDXPS (111 µM)*	0	-	360.4 µL	40 µM	360.4 µL	40 µM

* drDXPS, 111 µM in phosphate buffer at pH 6.25, ThDP = Thiamine diphosphate.

DCC-6 (Competition experiment with ThDP and BAP):

This DCC-experiment was carried out according to the GP-6 (blank and protein-templated) in phosphate buffer at pH 6.25 and 5% DMSO using the DCL-1.

The DCL-composition is as below:

Entry	Blank		Protein-templated (I)		Protein-templated (II)	
	amount	*Final conc. in DCL*	*amount*	*Final conc. in DCL*	*amount*	*Final conc. in DCL*
Phosphate buffer	947µL	-	586.6µL	-	586.6µL	-
Hydrazide (100 mM)	7 × 3 µL (21 µL)	(7 × 300 µM)	7 × 3 µL (21 µL)	(7 × 300 µM)	7 × 3 µL (21 µL)	(7 × 300 µM)
Aldehyde (100 mM)	3 × 1 µL (3 µL)	(3 × 100 µM)	3 × 1 µL (3 µL)	(3 × 100 µM)	3 × 1 µL (3 µL)	(3 × 100 µM)
Aniline (1 M)	10 µL	10 mM	10 µL	10 mM	10 µL	10 mM
DMSO	16 µL	-	16 µL	-	16 µL	-
ThDP (100 mM)	1 µL	100 µM	1 µL	100 µM	1 µL	100 µM
$MgCl_2$ (100 mM)	1 µL	100 µM	1 µL	100 µM	1 µL	100 µM
BAP	1 µL	100 µM	1 µL	100 µM	1 µL	100 µM
drDXPS ((111 µM)*	0	-	360.4 µL	40 µM	360.4 µL	40 µM

* drDXPS, 111 µM in phosphate buffer at pH 6.25, ThDP = Thiamine diphosphate, BAP = butylacetylphosphonate

Characterization of acylhydrazones

Identification of different conformers of acylhydrazone

Analysis of ^{1}H NMR spectra of acylhydrazone products reported in this study gave two sets of signals. The two-dimensional Nuclear Overhauser Effect Spectroscopy (2D NOESY) experiments revealed (See Figure 21) that acylhydrazone **24** presents the relative configuration *E* of imine double bond (C=N) and the splitting of signals can be attributed to the existence of *cis*/*trans*-amide conformers.

***(E)-N*'-((6-(Trifluoromethyl)pyridin-3-yl)methylene)-4,5,6,7-tetrahydrobenzo[*b*]thiophene-2-carbohydrazide (1):**

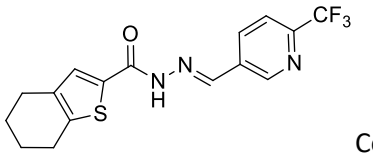

Compound **1** was synthesized according to GP-8, starting with aldehyde **A3** (87.6 mg, 0.5 mmol) and hydrazide **H1** (100 mg, 0.51 mmol). The crude was purified by using purification method-1 to afford **1** as a mixture of *cis* and *trans* conformers of amide (*cis*:*trans* = 50:50) as a pale yellow solid (133.7 mg, 0.38 mmol, 75.7%).

^{1}H NMR (500 MHz, DMSO-d_6) δ 12.10 (s, 2H, 1*trans* and 1*cis*), 9.08 (d, *J* = 36.6 Hz, 2H, 1*trans* and 1*cis*), 8.51 (s, 1H, *trans*), 8.40 (d, *J* = 7.3 Hz, 2H, 1*trans* and 1*cis*), 8.19 (s, 1H, *cis*), 8.01 (br s, 2H, 1*trans* and 1*cis*), 7.69 (d, *J* = 38.2 Hz, 2H, 1*trans* and 1*cis*), 2.79 (br s, 4H, 2*trans* and 2*cis*), 2.62 (t, *J* = 5.8 Hz, 4H, 2*trans* and 2*cis*), 1.95 – 1.66 (m, 8H, 4*trans* and 4*cis*).
^{13}C NMR (126 MHz, DMSO-d_6) δ 162.1, 158.5, 149.2, 147.1, 145.8, 143.0, 139.9, 136.4, 136.0, 135.3, 134.1, 130.5, 128.6, 125.32 123.1, 121.5, 121.0, 118.8, 25.1, 23.2, 22.6.
^{19}F NMR (470 MHz, DMSO) δ −66.4.
HRMS (ESI$^+$): m/z calcd. for $C_{16}H_{15}F_3N_3OS$ ([M+H]$^+$) 354.08879, measured 354.08773.

***(E)*-*N*'-((2-Methylpyrimidin-5-yl)methylene)-4,5,6,7-tetrahydrobenzo[*b*]thiophene-2-carbohydrazide (2):**

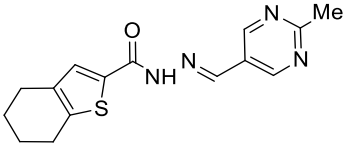

Compound **2** was synthesized according to GP-8, starting with aldehyde **A1** (61.2 mg, 0.5 mmol) and hydrazide **H1** (100 mg, 0.51 mmol). The crude was purified by using purification method-1 to afford **1** as a mixture of *cis* and *trans* conformers of amide (*cis*:*trans* = 50:50) as a pale yellow solid (79.0 mg, 0.38 mmol, 52.6%).

^{1}H NMR (500 MHz, DMSO-d_6) δ 11.98 (s, 2H, 1*trans* and 1*cis*), 9.00 (d, *J* = 28.0 Hz, 4H, 2*trans* and 2*cis*), 8.40 (s, 1H,*trans*), 8.07 (s, 1H, *cis*), 7.67 (d, *J* = 45.9 Hz, 2H, 1*trans* and 1*cis*), 2.78 (br s, 4H, 2*trans* and 2*cis*, 2.66 (s, 6H, 3trans and 3*cis*), 2.61 (t, *J* = 5.8 Hz, 4H, 2*trans* and 2*cis*), 1.85 – 1.69 (m, 8H, 4trans and 4*cis*).

^{13}C NMR (126 MHz, DMSO-d_6) δ 168.3, 168.1, 162.0, 158.4, 155.6, 145.6, 142.6, 142.2, 138.7, 136.6, 136.2, 135.2, 134.0, 130.3, 128.7, 125.9, 26.1, 25.4, 25.2, 25.0, 23.2, 22.7.

HRMS (ESI$^+$): m/z calcd. for $C_{15}H_{17}N_4OS$ ([M+H]$^+$) 301.11231, measured 301.11126.

***(E)*-*N*'-((2-Aminopyrimidin-5-yl)methylene)-4,5,6,7-tetrahydrobenzo[*b*]thiophene-2-carbohydrazide (3):**

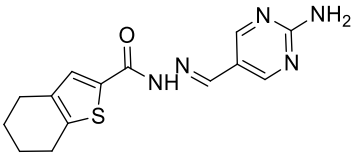

Compound **3** was synthesized according to GP-8, starting with aldehyde **A2** (61.5 mg, 0.5 mmol) and hydrazide **H1** (100 mg, 0.51 mmol). The crude was purified by using purification method-1 to afford **3** as a mixture of *cis* and *trans* conformers of amide (*cis*:*trans* = 50:50) as a pale yellow solid (136.1 mg, 0.45 mmol, 90.1%).

^{1}H NMR (500 MHz, DMSO-d_6) δ 11.61 (d, *J* = 11.9 Hz, 2H, 1*trans* and *1cis*), 8.56 (d, *J* = 29.9 Hz, 4H, 2*trans* and 2cis), 8.21 (s, 1H,*trans*), 7.88 (s, 1H, *cis*), 7.68 (s, 1H,*trans*), 7.56 (s, 1H, *cis*), 7.17 (s, 4H, 2*trans* and 2*cis*), 2.84 – 2.67 (m, 4H, 2*trans* and 2*cis*), 2.58 (t, *J* = 5.7 Hz, 4H, 2*trans* and 2*cis*), 1.88 – 1.58 (m, 8H, 4*trans* and 4*cis*).

^{13}C NMR (126 MHz, DMSO-d_6) δ 164.2, 164.0, 161.6, 158.1, 157.6, 157.5, 145.2, 143.8, 141.9, 140.1, 136.5, 135.7, 135.0, 134.5, 129.7, 129.2, 117.6, 25.4, 25.1, 24.9, 23.3, 22.7, 22.6.

HRMS (ESI$^+$): m/z calcd. for $C_{14}H_{16}N_5OS$ ([M+H]$^+$) 302.10756, measured 302.10656.

***(E)*-2-(1*H*-Indol-3-yl)-N'-((6-(trifluoromethyl)pyridin-3-yl)methylene)acetohydrazide (4):**

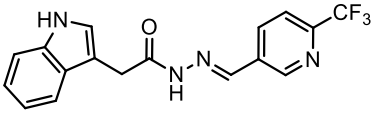

Compound **4** was synthesized according to GP-8, starting with aldehyde **A3** (92.63 mg, 0.53 mmol) and hydrazide **H7** (100 mg, 0.53 mmol). The crude was purified by using purification method-1 to afford **4** as a mixture of *cis* and *trans* conformers of amide (*cis*:*trans* = 59:41) as a white solid (71.9 mg, 0.21 mmol, 40.0 %).

^{1}H NMR (500 MHz, DMSO-d_6) δ 11.91 (br s, 1H, *trans*), 11.69 (br s,1H, *cis*), 10.97 (s, 1H,*trans*), 10.91 (s, 1H, *cis*), 9.07 (d, *J* = 2.0 Hz, 1H, *cis*), 9.00 (d, *J* = 2.0 Hz, 1H, *trans*), 8.41 (dd, *J* = 8.3, 2.1 Hz, 1H, *cis*), 8.37 (s, 1H, *trans*), 8.34 (dd, *J* = 8.2, 2.1 Hz, 1H, *trans*), 8.10 (s, 1H, *cis*), 7.96 (d, *J* = 8.0 Hz, 2H, 1*trans* and 1*cis*), 7.59 (t, *J* = 7.2 Hz, 2H, 1*trans* and 1*cis*), 7.42 – 7.32 (m, 2H, 1*trans* and 1*cis*), 7.27 (dd, *J* = 8.1, 2.4 Hz, 2H, 1*trans* and 1*cis*), 7.14 – 7.03 (m, 2H, 1*trans* and 1*cis*), 7.03 – 6.93 (m, 2H, 1*trans* and 1*cis*), 4.11 (s, 2H, *cis*), 3.69 (s, 2H, *trans*).

^{13}C NMR (126 MHz, DMSO-d_6) δ 173.6, 168.1, 149.2, 149.0, 147.1, 147.1, 146.8, 146.8, 146.6, 146.5, 146.3, 142.3, 138.6, 136.6, 136.5, 135.9, 135.8, 134.15, 134.1, 127.8, 127.6, 125.4, 125.3, 123.2, 123.15, 121.0, 121.0, 118.8, 111.9, 111.8, 108.3, 32.2, 29.7.

^{19}F NMR (470 MHz, DMSO) δ −66.4, −66.4.

HRMS (ESI$^+$): m/z calcd. for $C_{17}H_{14}F_3N_4O$ ([M+H]$^+$) 347.11197, measured 347.11080.

***(E)*-*N*'-((2-Aminopyrimidin-5-yl)methylene)-2-(1*H*-indol-3-yl)acetohydrazide (5):**

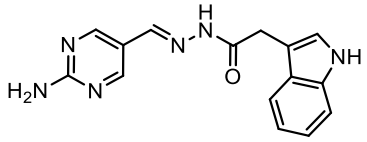

Compound **5** was synthesized according to GP-8, starting with aldehyde **A2** (135.34 mg, 1.1 mmol) and hydrazide **H7** (228.1 mg, 1.2 mmol). The crude was purified by using purification method-1 to afford **5** as a mixture of *cis* and *trans* conformers of amide (*cis*:*trans* = 53:47) as a white solid (132.0 mg, 0.45 mmol, 40.8%).

^{1}H NMR (500 MHz, DMSO-d_6) δ 11.42 (s, 1H, *trans*), 11.17 (s, 1H, *cis*), 10.91 (s, 1H, *trans*), 10.86 (s, 1H, *cis*), 8.55 (s, 2H, *cis*), 8.49 (s, 2H, *trans*), 8.04 (s, 1H, *trans*), 7.80 (s, 1H, *cis*), 7.56 (t, *J* = 7.5 Hz, 2H, 1*trans* and 1*cis*), 7.33 (t, *J* = 8.4 Hz, 2H, 1*trans* and *1cis*), 7.21 (dd, *J* = 12.3, 2.4 Hz, 2H, 1*trans* and *1cis*), 7.12 (d, *J* = 10.2 Hz, 4H, *2trans* and 2cis), 7.10 – 7.00 (m, 2H, 1*trans* and *1cis*), 7.00 – 6.91 (m, 2H, 1*trans* and 1*cis*), 4.00 (s, 2H, *cis*), 3.59 (s, 2H, *trans*).

^{13}C NMR (126 MHz, DMSO-d_6) δ 162.2, 158.5, 149.2, 147.1, 146.6, 145.8, 142.9, 139.9, 136.7, 136.4, 136.0, 135.3, 134.1, 133.9, 130.5, 128.6, 125.3, 123.2, 121.5, 121.0, 118.8, 25.2, 23.2, 22.6.

HRMS (ESI$^+$): m/z calcd. for $C_{15}H_{15}N_6O$ ([M+H]$^+$) 295.13073, measured 295.12972.

***(E)*-2-(2,4-Dichlorophenoxy)-*N*'-((4,5,6,7-tetrahydrobenzo[*b*]thiophen-2-yl)methylene)acetohydrazide (6)**:

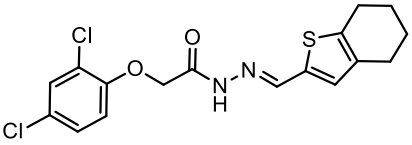

Compound **6** was synthesized according to GP-8, starting with aldehyde **A4** (25.5 mg, 0.15 mmol) and hydrazide **H9** (30.0 mg, 0.13 mmol). The crude was purified by using purification method-1 to afford **6** as a mixture of *cis* and *trans* conformers of amide (*cis*:*trans* = 40:60) as a pale yellow solid (40.0 mg, 0.10 mmol, 80.0%).

^{1}H NMR (500 MHz, DMSO-d_6) δ 11.52 (d, *J* = 32.5 Hz, 2H, 1*trans* and 1*cis*), 8.35 (s, 1H, *trans*), 8.07 (s, 1H, *cis*), 7.61 (d, *J* = 2.6 Hz, 1H, *trans*), 7.57 (d, *J* = 2.6 Hz, 1H, *cis*), 7.38 (dd, *J* = 8.9, 2.6 Hz, 1H, *trans*), 7.32 (dd, *J* = 8.9, 2.6 Hz, 1H, *cis*), 7.22 – 6.94 (m, 4H, 2*trans* and 2cis), 5.15 (s, 2H, *cis*), 4.75 (s, 2H, *trans*), 2.78 – 2.65 (m, 4H, 2*trans* and 2cis), 2.59 – 2.50 (m, 4H, 2*trans* and 2cis), 1.84 – 1.61 (m, 8H, 4trans and 4cis).

^{13}C NMR (126 MHz, DMSO-d_6) δ 167.7, 163.1, 152.8, 152.6, 143.2, 139.5, 138.9, 138.4, 135.7, 134.7, 134.6, 132.2, 131.4, 129.4, 129.3, 128.1, 127.9, 125.1, 124.5, 122.5, 122.2, 115.4, 115.1, 67.1, 65.4, 24.84, 24.79, 24.7, 22.8, 22.2.

HRMS (ESI$^+$): m/z calcd. for $C_{17}H_{17}Cl_2N_2O_2S$ ([M+H]$^+$) 383.03878, measured 383.03655.

***(E)*-*N*'-((4,5,6,7-Tetrahydrobenzo[*b*]thiophen-2-yl)methylene)thiophene-2-carbohydrazide (7):**

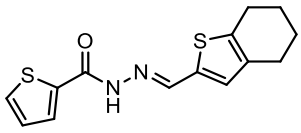

Compound **7** was synthesized according to GP-8, starting with aldehyde **A4** (42.0 mg, 0.25 mmol) and hydrazide **H11** (30.0 mg, 0.21 mmol). The crude was purified by using purification method-1 to afford **7** as a mixture of *cis* and *trans* conformers of amide (*cis*:*trans* = 54:46) as a pale yellow solid (25.0 mg, 0.086 mmol, 41.0%).

^{1}H NMR (500 MHz, DMSO-d_6) δ 11.72 (d, *J* = 4.3 Hz, 2H, 1*trans* and 1*cis*), 8.53 (s, 1H,*trans*), 8.17 (s, 1H, *cis*), 8.02 (d, *J* = 3.7 Hz, 1H,*trans*), 7.95 (d, *J* = 5.0 Hz, 1H,*trans*), 7.85 (d, *J* = 4.5 Hz, 2H, 1*trans* and 1*cis*), 7.20 (t, *J* = 4.5 Hz, 2H, 1*trans* and 1*cis*), 7.14 (d, *J* = 8.3 Hz, 2H, 1*trans* and 1*cis*), 2.80 – 2.68 (m, 4H, 2*trans* and 2cis), 2.59 – 2.51 (m, 4H, 2*trans* and 2cis), 1.87 – 1.61 (m, 8H, 4trans and 4cis).

^{13}C NMR (126 MHz, DMSO-d_6) δ 160.9, 157.5, 143.0, 138.8, 138.3, 135.8, 135.7, 135.0, 134.9, 134.5, 133.4, 132.0, 131.7, 128.7, 128.1, 126.6, 24.9, 24.8, 22.9, 22.2.

HRMS (ESI$^+$): m/z calcd. for $C_{14}H_{15}N_2OS_2$ ([M+H]$^+$) 291.06258, measured 291.06025.

***(E)*-2-((1*H*-Benzo[*d*]imidazole-2-yl)thio)-*N*'-((4,5,6,7-tetrahydrobenzo[*b*]thiophen-2-yl)methylene)acetohydrazide (8):**

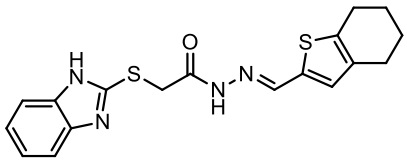

Compound **8** was synthesized according to GP-8, starting with aldehyde **A4** (26.0 mg, 0.16 mmol) and hydrazide **H6** (30.0 mg, 0.13 mmol). The crude was purified by using purification method-1 to afford **8** as a mixture of *cis* and *trans* conformers of amide (*cis*:*trans* = 54:46) as a white solid (16.0 mg, 0.04 mmol, 33.2%).

^{1}H NMR (500 MHz, DMSO-d_6) δ 12.64 (br s, 1H,*trans*), 12.57 (br s, 1H, *cis*), 11.70 (s, 1H,*trans*), 11.52 (s, 1H, *cis*), 8.30 (s, 1H,*trans*), 8.09 (s, 1H, *cis*), 7.49 (t, *J* = 7.4 Hz, 2H, 1*trans* and 1*cis*), 7.37 (t, *J* = 8.8 Hz, 2H, 1*trans* and 1*cis*), 7.19 – 7.03 (m, 6H, 3*trans* and 3*cis*), 4.46 (s, 2H, 1*trans* and 1*cis*), 4.12 (s, 2H, 1*trans* and 1*cis*), 2.70 (q, *J* = 6.6 Hz, 4H, 2*trans* and 2*cis*), 2.54 (t, *J* = 6.3 Hz, 4H, 2*trans* and 2*cis*), 1.84 – 1.63 (m, 8H, 4*trans* and 4*cis*).
^{13}C NMR (126 MHz, DMSO-d_6) δ 169.0, 164.0, 150.4, 150.1, 142.9, 139.5, 139.3, 138.8, 136.2, 135.2, 135.2, 132.6, 131.8, 121.9, 117.8, 110.6, 34.7, 34.0, 25.3, 25.3, 25.24, 25.19, 23.3, 22.7, 22.6.
HRMS (ESI$^+$): m/z calcd. for $C_{18}H_{19}N_4OS_2$ ([M+H]$^+$) 371.10003, measured 371.09790.

***(E)*-*N*'-((1*H*-Indol-3-yl)methylene)-2-(2,4-dichlorophenoxy)acetohydrazide (9):**

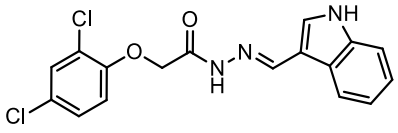

Compound **9** was synthesized according to GP-8, starting with aldehyde **A5** (22.1 mg, 0.15 mmol) and hydrazide **H9** (30.0 mg, 0.13 mmol). The crude was purified by using purification method-1 to afford **9** as a mixture of *cis* and *trans* conformers of amide (*cis*:*trans* = 76:24) as a white solid (20.0 mg, 0.055 mmol, 42.5%).

^{1}H NMR (500 MHz, DMSO-d_6) δ 11.69 – 11.47 (m, 2H, 1*trans* and 1*cis*), 11.33 (d, *J* = 49.8 Hz, 2H, 1*trans* and 1*cis*), 8.42 (s, 1H, *trans*), 8.21 (s, 1H, *trans*), 8.20 (s, 1H, *cis*), 8.11 (d, *J* = 7.9 Hz, 1H, *cis*), 7.82 (d, *J* = 2.2 Hz, 2H, 1*trans* and 1*cis*), 7.63 (d, *J* = 2.6 Hz, 1H, *trans*), 7.60 (d, *J* = 2.6 Hz, 1H, *cis*), 7.44 (d, *J* = 8.1 Hz, 2H, 1*trans* and 1*cis*), 7.40 (dd, *J* = 8.9, 2.6 Hz, 1H, *trans*), 7.35 (dd, *J* = 8.9, 2.6 Hz, 1H, *cis*), 7.24 – 7.17 (m, 2H, 1*trans* and 1*cis*), 7.17 – 7.02 (m, 4H, 2*trans* and 2cis), 5.35 (s, 4H, *trans*), 4.78 (s, 4H, *cis*).
^{13}C NMR (126 MHz, DMSO-d_6) δ 167.8, 163.0, 153.4, 153.2, 145.4, 142.0, 137.5, 131.2, 129.9, 129.7, 128.6, 128.4, 125.5, 124.8, 124.7, 124.5, 123.1, 123.0, 122.6, 122.4, 122.3, 121.1, 120.9, 115.9, 115.5, 112.3, 111.8, 111.7, 67.8, 66.3.
HRMS (ESI$^+$): m/z calcd. for $C_{17}H_{14}Cl_2N_3O_2$ ([M+H]$^+$) 362.04631, measured 362.04400.

***(E)*-*N*'-((5-Bromopyridin-2-yl)methylene)-2-(2,4-dichlorophenoxy)acetohydrazide (10):**

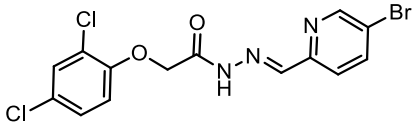

Compound **10** was synthesized according to GP-8, starting with aldehyde **A6** (22.1 mg, 0.15 mmol) and hydrazide **H9** (30.0 mg, 0.13 mmol). The crude was purified by using purification method-1 to afford **10** as a mixture of *cis* and *trans* conformers of amide (*cis*:*trans* = 77:23) as a white solid (33.0 mg, 0.08 mmol, 63.0%).

^{1}H NMR (500 MHz, DMSO-d_6) δ 11.94 (d, *J* = 12.1 Hz, 2H, 1*trans* and 1*cis*), 8.81 – 8.66 (m, 2H, 1*trans* and 1*cis*), 8.24 (s, 1H, *trans*), 8.17 – 8.09 (m, 2H, 1*trans* and 1*cis*), 8.00 (s, 1H, *cis*), 7.95 (d, *J* = 8.5 Hz, 1H, *cis*), 7.86 (d, *J* = 8.5 Hz, 1H, *trans*), 7.62 (d, *J* = 2.6 Hz, 1H, *trans*), 7.58 (d, *J* = 2.6 Hz, 1H, *cis*), 7.38 (dd, *J* = 8.9, 2.6 Hz, 1H,*trans*), 7.33 (dd, *J* = 8.9, 2.6 Hz, 1H, *cis*), 7.11 (dd, *J* = 8.9, 4.1 Hz, 2H, 1*trans* and 1*cis*), 5.34 (s, 2H, *cis*), 4.84 (s, 2H, *trans*).
^{13}C NMR (126 MHz, DMSO-d_6) δ 168.6, 164.0, 152.8, 152.6, 151.8, 151.6, 150.3, 146.8, 143.2, 139.7, 139.5, 129.5, 129.3, 128.1, 127.9, 125.2, 124.6, 122.5, 122.2, 121.6, 121.5, 121.0, 120.8, 115.4, 115.2, 67.1, 65.7.
HRMS (ESI$^+$): m/z calcd. for $C_{14}H_{11}BrCl_2N_3O_2$ ([M+H]$^+$) 401.94117, measured 401.93877

***(E)-N'*-((1*H*-Imidazol-2-yl)methylene)thiophene-2-carbohydrazide (11)**

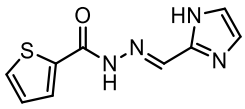

Compound **11** was synthesized according to GP-8, starting with aldehyde **A12** (50.0 mg, 0.52 mmol) and hydrazide **H11** (73.98 mg, 0.52 mmol). The crude was purified by using purification method-2 (Prep-HPLC) to afford **11** as a mixture of *cis* and *trans* conformers of amide (*cis*:*trans* = 28:72) as a white solid (25 mg, 0.11 mmol, 21.8%).

^{1}H NMR (500 MHz, DMSO-d_6) δ 14.60 (br s, 1H, *trans*), 13.57 (br s, 1H, *cis*), 13.09 (s, 2H, 1*trans* and 1*cis*), 8.12 (br s, 1H, *cis*), 7.95 (d, *J* = 5.0 Hz, 2H, 1*trans* and 1*cis*), 7.78 (br s, 1H, *trans*), 7.66 – 7.31 (m, 6H, 3*trans* and 3*cis*), 7.33 – 7.18 (m, 2H, 1*trans* and 1*cis*).

^{13}C NMR (126 MHz, DMSO-d_6) δ 162.2, 158.3, 141.9, 141.4, 138.3, 135.6, 133.1, 132.8, 130.1, 130.0, 129.3, 129.0, 127.4, 127.0 119.4.

HRMS (ESI$^+$): m/z calcd. for $C_9H_9N_4OS$ ([M+H]$^+$) 221.04971, measured 221.04888.

***(E)-N'*-((1*H*-Imidazol-2-yl)methylene)-4-(2,4-dichlorophenoxy)butanehydrazide (12):**

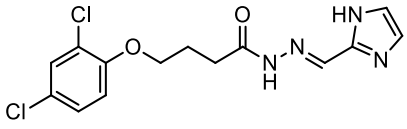

Compound **12** was synthesized according to GP-8, starting with aldehyde **A12** (54.8 mg, 0.21 mmol) and hydrazide **H12** (20 mg, 0.21 mmol). The crude was purified by using purification method-1 (Prep-HPLC) to afford **12** as a mixture of *cis* and *trans* conformers of amide (*cis*:*trans* = 56:44) as a white solid (53.9 mg, 0.16 mmol, 76.2%).

^{1}H NMR (500 MHz, DMSO-d_6) δ 12.76 (br s, 1H, *trans*), 12.51 (br s, 1H, *cis*), 11.45 (s, 1H, *trans*), 11.32 (s, 1H, *cis*), 8.06 (s, 1H, *trans*), 7.88 (s, 1H, *cis*), 7.64 – 7.50 (m, 2H, 1*trans* and 1*cis*), 7.43 – 7.33 (m, 2H, 1*trans* and 1*cis*), 7.24 (br s, 1H, *trans*), 7.23 – 7.14 (m, 2H, 1*trans* and 1*cis*), 7.04 (br s, 1H, *cis*), 4.12 (dt, *J* = 13.6, 6.3 Hz, 4H, 2*trans* and 2*cis*), 2.83 (t, *J* = 7.3 Hz, 2H, *cis*), 2.43 (t, *J* = 7.4 Hz, 2H, *trans*), 2.05 (dp, *J* = 13.7, 6.8, 6.4 Hz, 4H, 2*trans* and 2*cis*).

^{13}C NMR (126 MHz, DMSO-d_6) δ 174.2, 168.4, 153.4, 143.0, 142.9, 138.3, 134.8, 130.3, 130.1, 129.8, 128.6, 124.9, 124.78, 122.83, 119.8, 119.3, 115.5, 115.4, 68.9, 30.9, 28.6, 24.7, 24.1.

HRMS (LC-MS/MS): m/z calcd. for $C_{14}H_{15}Cl_2N_4O_2$ ([M+H]$^+$) 341.05721, measured 341.05618.

***(E)*-4-(2,4-Dichlorophenoxy)-*N'*-(thiophen-2-ylmethylene)butanehydrazide (16):**

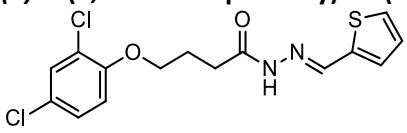

Compound **16** was synthesized according to GP-8, starting with aldehyde **A7** (54.8 mg, 0.21 mmol) and hydrazide **H12** (23.3 mg, 0.21 mmol). The crude was purified by using purification method-1 to afford **16** as a mixture of *cis* and *trans* conformers of amide (*cis*:*trans* = 58:42) as a white solid (51.9 mg, 0.14 mmol, 69.4 %).

^{1}H NMR (500 MHz, DMSO-d_6) δ 11.39 (s, 1H,*trans*), 11.30 (s, 1H, *cis*), 8.37 (s, 1H, *trans*), 8.15 (s, 1H, *cis*), 7.64 (d, *J* = 5.1 Hz, 1H, *trans*), 7.60 (d, *J* = 5.0 Hz, 1H, *cis*), 7.57 (dd, *J* = 4.5, 2.6 Hz, 2H, 1*trans* and 1*cis*), 7.47 – 7.31 (m, 4H, 2*trans* and 2*cis*), 7.19 (dd, *J* = 8.9, 1.5 Hz, 2H, 1*trans* and 1*cis*), 7.15 – 7.06 (m, 2H, 1*trans* and 1*cis*), 4.12 (dt, *J* = 15.4, 6.3 Hz, 4H, 2*trans* and 2*cis*), 2.76 (t, *J* = 7.3 Hz, 2H, 1*trans* and 1*cis*), 2.40 (t, *J* = 7.4 Hz, 2H, 1*trans* and 1*cis*), 2.12 – 1.91 (m, 4H, 2*trans* and 2*cis*).

^{13}C NMR (126 MHz, DMSO-d_6) δ 173.9, 168.3, 153.4, 141.5, 139.6, 139.5, 138.3, 131.1, 130.6, 129.7, 129.1, 128.6, 128.6, 128.3, 128.3, 124.8, 124.8, 122.9, 122.8, 115.5, 68.8, 68.8, 30.8, 28.6, 24.7, 24.0.

HRMS (ESI$^+$): m/z calcd. For $C_{15}H_{15}Cl_2N_2O_2S$ ([M+H]$^+$) 357.02313, measured 357.02189.

***(E)-N'*-(4-(Diethylamino)-2-hydroxybenzylidene)thiophene-2-carbohydrazide (21):**

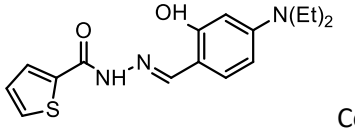

Compound **21** was synthesized according to GP-8, starting with aldehyde **A25** (135.8 mg, 0.70 mmol) and hydrazide **H11** (100.0 mg, 0.70 mmol). The crude was purified by using purification

method-1 to afford **21** as a mixture of *cis* and *trans* conformers of amide (*cis*:*trans* = 81:19) as a white solid (115.3mg, 0.36 mmol, 51.9%).

^{1}H NMR (500 MHz, DMSO-d_6) δ 11.85 (s, 1H, *trans*), 11.47 (s, 1H, *cis*), 11.30 (s, 1H, *trans*), 9.72 (s, 1H, *cis*), 8.41 (s, 1H, *trans*), 8.26 (s, 1H, *cis*), 8.00 (d, *J* = 2.9 Hz, 1H, *cis*), 7.92 (d, *J* = 5.0 Hz, 1H, *cis*), 7.90 – 7.82 (m, 2H, 1*trans,* 1*trans*), 7.67 (d, *J* = 8.9 Hz, 1H, *cis*), 7.29 – 7.13 (m, 3H, 1*trans*; 1*trans* and 1*cis*), 6.36 – 6.23 (m, 2H, 1*trans* and 1*cis*), 6.13 (d, *J* = 2.4 Hz, 2H, 1*trans* and 1*cis*), 3.42 – 3.30 (m, 8H, 4*trans* and 4*cis*), 1.11 (t, *J* = 7.0 Hz, 12H, 6*trans* and 6*cis*).

^{13}C NMR (126 MHz, DMSO-d_6) δ 161.0, 160.1, 158.6, 157.4, 150.64, 150.29, 150.0, 142.6, 138.6, 134.8, 134.5, 134.1, 132.1, 131.9, 129.1, 128.6, 128.2, 127.0, 108.3, 106.9, 104.8, 104.1, 97.9, 97.6, 44.34, 44.28, 13.0.

HRMS (ESI$^+$): m/z calcd. For $C_{16}H_{20}N_3O_2S$ ([M+H]$^+$) 318.1276, measured 318.12665.

***(E)*-*N*'-((1*H*-Indazol-4-yl)methylene)-4-(2,4-dichlorophenoxy)butanehydrazide (22):**

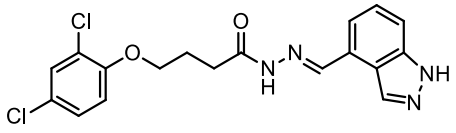

Compound **22** was synthesized according to GP-8, starting with aldehyde **A22** (6.8 mg, 0.046 mmol) and hydrazide **H12** (12.2 mg, 0.046 mmol). The crude was purified by using purification method-1 to afford **22** as a mixture of *cis* and *trans* conformers of amide (*cis*:*trans* = 71:29) as a white solid (7.6 mg, 0.0019 mmol, 41.9%).

^{1}H NMR (500 MHz, DMSO-d_6) δ 13.31 (s, 2H, 1*trans* and *1cis*), 11.59 (s, 1H, *trans*), 11.43 (s, 1H, *cis*), 8.60 (d, *J* = 1.0 Hz, 1H, *trans*), 8.49 (d, *J* = 1.0 Hz, 1H, *cis*), 8.35 (s, 1H, *trans*), 8.21 (s, 1H, *cis*), 7.61 (d, *J* = 8.4 Hz, 2H, 1*trans* and 1*cis*), 7.59 (d, *J* = 2.6 Hz, 1H, *trans*), 7.56 (d, *J* = 2.6 Hz, 1H, *cis*), 7.43 – 7.33 (m, 4H, 2*trans* and 2*cis*), 7.30 (d, *J* = 7.0 Hz, 1H, *trans*), 7.25 (d, *J* = 7.0 Hz, 1H, *1cis*), 7.24 – 7.19 (m, 2H, 1*trans* and 1*cis*), 4.20 (t, *J* = 6.3 Hz, 2H, 1*cis* and 1*trans*), 4.14 (t, *J* = 6.3 Hz, 2H, 1*trans* and 1*cis*), 2.97 (t, *J* = 7.3 Hz, 2H, 1*trans* and 1*cis*), 2.47 (t, *J* = 7.3 Hz,, 2H, 1*trans* and 1*cis*), 2.10 (dt, *J* = 12.2, 6.8 Hz, 4H, 2*trans* and 2*cis*).

^{13}C NMR (126 MHz, DMSO-d_6) δ 174.1, 168.6, 153.5, 146.1, 143.9, 140.7, 135.0, 134.4, 129.7, 128.6, 128.6, 128.0, 127.6, 126.4, 126.3, 124.8, 124.8, 123.7, 123.4, 123.0, 122.8, 119.0, 118.6, 115.6, 112.6, 68.9, 68.8, 30.8, 28.8, 24.7, 23.9.

HRMS (ESI$^+$): m/z calcd. For $C_{18}H_{17}Cl_2N_4O_2$ ([M+H]$^+$) 391.07286, measured 391.07179.

***(E)*-4-(2,4-Dichlorophenoxy)-*N*'-(2-fluoro-4-hydroxybenzylidene)butanehydrazide (23):**

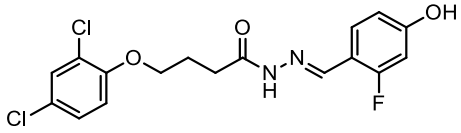

Compound **23** was synthesized according to GP-8, starting with aldehyde **A26** (35.0 mg, 0.25 mmol) and hydrazide **H12** (65.8 mg, 0.25 mmol). The crude was purified by using purification method-1 to afford **23** as a mixture of *cis* and *trans* conformers of amide (*cis*:*trans* = 65:35) as a white solid (50.3 mg, 0.13 mmol, 55.2%).

^{1}H NMR (500 MHz, DMSO-d_6) δ 11.36 (s, 1H, *trans*), 11.24 (s, 1H, *cis*), 10.41 (br s, 2H, 1*trans* and 1*cis*), 8.26 (s, 1H, *trans*), 8.07 (s, 1H, *cis*), 7.67 (dt, *J* = 15.7, 8.7 Hz, 2H, 1*trans* and 1*cis*), 7.57 (dd, *J* = 4.1, 2.6 Hz, 2H, 1*trans* and 1*cis*), 7.36 (ddd, *J* = 8.8, 7.5, 2.6 Hz, 2H, 1*trans* and 1*cis*), 7.19 (dd, *J* = 8.9, 1.8 Hz, 2H, 1*trans* and 1*cis*), 6.70 (dd, *J* = 8.7, 2.3 Hz, 1H, *trans*), 6.66 (dd, *J* = 8.7, 2.3 Hz, 1H, *cis*), 6.60 (ddd, *J* = 12.7, 4.9, 2.3 Hz, 2H, 1*trans* and 1*cis*), 4.12 (dt, *J* = 15.5, 6.3 Hz, 4H, 2*trans* and 2cis), 2.80 (t, *J* = 7.4 Hz, 2H, *cis*), 2.39 (t, *J* = 7.3 Hz, 2H, *trans*), 2.11 – 1.96 (m, 4H, 2*trans* and 2cis).

^{13}C NMR (126 MHz, DMSO-d_6) δ 174.0, 168.2, 163.2, 163.0, 161.3, 161.2, 161.1, 161.1, 161.0, 153.4, 139.5, 139.5, 136.4, 136.4, 129.7, 128.6, 127.7, 127.6, 127.4, 127.3, 124.8, 124.7, 122.8, 115.5, 115.4, 113.2, 113.1, 103.06, 102.9, 68.8, 30.8, 28.8, 24.7, 24.2.

^{19}F NMR (470 MHz, DMSO) δ -119.91, -119.99.

HRMS (ESI$^+$): m/z calcd. for $C_{17}H_{16}Cl_2FN_2O_3$ ([M+H]$^+$) 385.05220, measured 385.05120.

***(E)*-*N*'-((1*H*-|Pyrrol-2-yl)methylene)-4-(2,4-dichlorophenoxy)butanehydrazide (24):**

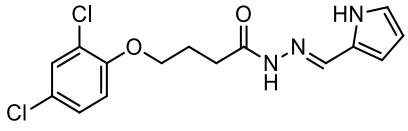

Compound **24** was synthesized according to GP-8, starting with aldehyde **A20** (19.8 mg, 0.21 mmol) and hydrazide **H12** (54.8 mg, 0.21 mmol). The crude was purified by using purification method-1 to afford **24** as a mixture of *cis* and *trans* conformers of amide (*cis*:*trans* = 53:47) as a white solid (52.5 mg, 0.15 mmol, 73.7%).

^{1}H NMR (500 MHz, DMSO-d_6) δ 11.43 (s, 1H, *trans*), 11.24 (s, 1H, *cis*), 11.07 (s, 1H, *trans*), 10.97 (s, 1H, *cis*), 8.00 (s, 1H, *trans*), 7.82 (s, 1H, *cis*), 7.57 (dd, *J* = 4.0, 2.5 Hz, 2H, 1*trans* and 1*cis*), 7.36 (ddd, *J* = 9.5, 7.2, 2.6 Hz, 2H, 1*trans* and 1*cis*), 7.24 – 7.14 (m, 2H, 1*trans* and 1*cis*), 6.88 (dq, *J* = 9.8, 2.3 Hz, 2H, 1*trans* and 1*cis*), 6.47 – 6.35 (m, 2H, 1*trans* and 1*cis*), 6.18 – 6.03 (m, 2H, 1*trans* and 1*cis*), 4.14 (t, *J* = 6.5 Hz, 2H, *cis*), 4.10 (t, *J* = 6.2 Hz, 2H, *trans*), 2.78 (t, *J* = 7.3 Hz, 2H, *cis*), 2.38 (t, *J* = 7.4 Hz, 2H, *trans*), 2.09 – 1.97 (m, 4H, 2*trans* and 2*cis*).

^{13}C NMR (126 MHz, DMSO-d_6) δ 173.7, 167.8, 153.5, 139.6, 136.1, 129.7, 128.6, 127.7, 127.5, 124.9, 124.8, 122.9, 122.7, 122.1, 115.6, 115.5, 113.4, 112.3, 109.6, 69.0, 68.9, 30.8, 28.7, 24.9, 24.2.

HRMS (ESI$^+$): m/z calcd. for $C_{15}H_{16}Cl_2N_3O_2$ ([M+H]$^+$) 340.06196, measured 340.06112.

***(E)*-4-(2,4-Dichlorophenoxy)-*N*'-(2-hydroxy-3-methoxybenzylidene)butanehydrazide (25):**

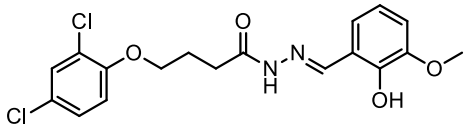

Compound **25** was synthesized according to GP-8, starting with aldehyde **A24** (38.0 mg, 0.25 mmol) and hydrazide **H12** (65.8 mg, 0.25 mmol). The crude was purified by using purification method-1 to afford **25** as a mixture of *cis* and *trans* conformers of amide (*cis*:*trans* = 45:55) as a white solid (49.4 mg, 0.12 mmol, 49.7%).

^{1}H NMR (500 MHz, DMSO-d_6) δ 11.64 (s, 1H, *trans*), 11.28 (s, 1H, *cis*), 10.90 (s, 1H,*trans*), 9.45 (s, 1H, *cis*), 8.35 (s, 1H, *trans*), 8.29 (s, 1H, *cis*), 7.57 (t, *J* = 2.8 Hz, 2H, 1*trans* and 1*cis*), 7.36 (td, *J* = 8.6, 2.6 Hz, 2H, 1*trans* and 1*cis*), 7.22 (dd, *J* = 8.0, 1.4 Hz, 1H, *cis*), 7.20 (d, *J* = 8.9 Hz, 2H, 1*trans* and 1*cis*), 7.10 (dd, *J* = 7.9, 1.5 Hz, 1H, *trans*), 7.01 (dd, *J* = 8.1, 1.4 Hz, 1H, *trans*), 6.98 (dd, *J* = 8.1, 1.5 Hz, 1H, *cis*), 6.84 (t, *J* = 7.9 Hz, 1H, *trans*), 6.79 (t, *J* = 8.0 Hz, 1H, *cis*), 4.13 (dt, *J* = 12.2, 6.3 Hz, 4H, 2*trans* and 2*cis*), 3.81 (d, *J* = 4.9 Hz, 6H, 3*trans* and 3*cis*), 2.79 (t, *J* = 7.4 Hz, 2H, *cis*), 2.44 (t, *J* = 7.3 Hz, 2H, *trans*), 2.16 – 1.95 (m, 4H, 2*trans* and 2*cis*).

^{13}C NMR (126 MHz, DMSO-d_6) δ 173.9, 168.3, 153.44, 148.4, 148.3, 147.4, 146.8, 146.3, 140.9, 129.7, 128.6, 124.8, 124.75, 122.8, 121.2, 121.0, 119.6, 119.4, 119.3, 118.2, 115.5, 115.5, 114.0, 113.2, 68.8, 56.3, 56.2, 30.7, 28.8, 24.6, 24.1.

HRMS (ESI$^+$): m/z calcd. for $C_{18}H_{19}Cl_2N_2O_4$ ([M+H]$^+$) 397.07219, measured 397.07097.

***(E)*-*N*'-((1*H*-Indol-6-yl)methylene)-4-(2,4-dichlorophenoxy)butanehydrazide (26):**

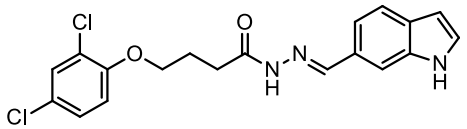

Compound **26** was synthesized according to GP-8, starting with aldehyde **A23** (36.3 mg, 0.25 mmol) and hydrazide **H12** (65.8 mg, 0.25 mmol). The crude was purified by using purification method-1 to afford **26** as a mixture of *cis* and *trans* conformers of amide (*cis*:*trans* = 62:38) as a white solid (40.3 mg, 0.10 mmol, 41.3%).

^{1}H NMR (500 MHz, DMSO-d_6) δ 11.29 (br s, 1H, *trans*), 11.27 (s, 1H, *trans*), 11.25 (br s, 1H, *cis*), 11.15 (s, 1H, *cis*), 8.22 (s, 1H, *trans*), 8.06 (s, 1H, *cis*), 7.69 (s, 1H, *trans*), 7.61 (s, 1H, *cis*), 7.59 – 7.51 (m, 4H, 2*trans* and 2*cis*), 7.46 (t, *J* = 2.8 Hz, 1H, *trans*), 7.44 (t, *J* = 2.7 Hz, 1H, *cis*), 7.41 – 7.32 (m, 4H, 2*trans* and 2*cis*), 7.20 (dd, *J* = 9.0, 2.3 Hz, 2H, 1*trans* and 1*cis*), 6.46 (q, *J* = 2.4 Hz, 2H, 1*trans* and 1*cis*), 4.16 (t, *J* = 6.4 Hz, 2H, *cis*), 4.12 (t, *J* = 6.3 Hz, 2H, *trans*), 2.85 (t, *J* = 7.4 Hz, 2H, *cis*), 2.42 (t, *J* = 7.3 Hz, 2H, *trans*), 2.14 – 2.00 (m, 4H, 2*trans* and 2*cis*).

^{13}C NMR (126 MHz, DMSO-d_6) δ 173.9, 168.1, 153.5, 148.0, 144.9, 136.3, 136.22, 129.7, 129.5, 128.6, 127.9, 127.8, 124.8, 124.8, 122.9, 120.8, 120.7, 118.4, 117.6, 115.5, 115.47, 111.49, 111.28, 102.0, 102.0, 68.8, 30.8, 28.8, 24.8, 24.1.

HRMS (ESI$^+$): m/z calcd. for $C_{19}H_{18}Cl_2N_3O_2$ ([M+H]$^+$) 390.07761, measured 390.07634.

***(E)-N'*-((1*H*-Indol-6-yl)methylene)-4,5,6,7-tetrahydrobenzo[*b*]thiophene-2-carbohydrazide (35):**

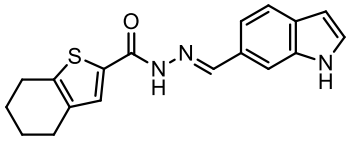

Compound **35** was synthesized according to GP-8, starting with aldehyde **A23** (37.0 mg, 0.25 mmol) and hydrazide **H1** (50 mg, 0.25 mmol). The crude was purified by using purification method-1 to afford **35** as a mixture of *cis* and *trans* conformers of amide (*cis*:*trans s* = 49:51) as a white solid (76.7 mg, 0.24 mmol, 94.9%).

^{1}H NMR (500 MHz, DMSO-d_6) δ 11.59 (d, *J* = 32.2 Hz, 2H, 1*trans* and 1*cis*), 11.35 (d, *J* = 24.0 Hz, 2H, 1*trans* and 1*cis*), 8.46 (s, 1H, *trans*), 8.15 (s, 1H, *cis*), 7.74 (br s, 3H, 1*trans*; 1*trans* and 1*cis*), 7.68 – 7.55 (m, 3H, 1*cis*; 1*trans* and 1*cis*), 7.51 (d, *J* = 8.3 Hz, 1H, *trans*), 7.48 (t, *J* = 2.7 Hz, 2H, 1*trans* and 1*cis*), 7.40 (d, *J* = 8.2 Hz, 1H, *cis*), 6.48 (br s, 2H, 1*trans* and 1*cis*), 2.80 (dt, *J* = 31.7, 6.0 Hz, 4H, 2*trans* and 2*cis*), 2.62 (q, *J* = 6.5, 5.9 Hz, 4H, 2*trans* and 2*cis*), 1.97 – 1.56 (m, 8H, 4trans and 4*cis*).

^{13}C NMR (126 MHz, DMSO-d_6) δ 161.7, 158.4, 149.2, 146.0, 145.1, 141.8, 136.48, 136.3, 135.6, 135.0, 134.7, 129.8, 129.7, 129.5, 128.1, 127.8, 127.7, 121.0, 120.8, 118.6, 118.2, 112.0, 111.3, 102.1, 102.0, 25.4, 25.2, 25.1, 23.3, 23.3, 22.8, 22.6.

HRMS (ESI$^+$): m/z calcd. for $C_{18}H_{18}N_3OS$ ([M+H]$^+$) 324.11706, measured 324.11588.

(*S,E*)-tert-butyl (1-(2-((1H-indol-6-yl)methylene)hydrazinyl)-1-oxo-3-phenylpropan-2-yl)carbamate (37):

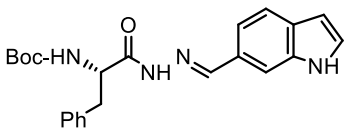

Compound **37** was synthesized according to GP-8, starting with aldehyde **A23** (30.19 mg, 0.21 mmol) and hydrazide **H14** (58.1 mg, 0.21 mmol). The crude was purified by using purification method-1 to afford **37** as a mixture of *cis* and *trans* conformers of amide (*cis*:*trans* = 53:47) as a white solid (34.1 mg, 0.08 mmol, 39.9%).

^{1}H NMR (500 MHz, DMSO-d_6) δ 11.43 (s, 1H, *trans*), 11.37 (s, 1H, *cis*), 11.34 (s, 1H, *trans*), 11.25 (s, 1H, *cis*), 8.25 (s, 1H, *trans*), 8.09 (s, 1H, *cis*), 7.71 (s, 2H, 1*trans* and 1*cis*), 7.60 (dd, *J* = 16.9, 8.3 Hz, 2H, 1*trans* and 1*cis*), 7.48 (q, *J* = 2.5 Hz, 2H, 1*trans* and 1*cis*), 7.44 (dd, *J* = 8.2, 1.4 Hz, 1H, *trans*), 7.39 (dd, *J* = 8.3, 1.4 Hz, 1H, *cis*), 7.37 – 7.26 (m, 8H, 4*trans* and 4*cis*), 7.26 – 7.16 (m, 3H, 1*trans*; 1*trans* and 1*cis*), 7.10 (d, *J* = 8.8 Hz, 1H, *cis*), 6.48 (dt, *J* = 7.6, 2.4 Hz, 2H, 1*trans* and *1cis*), 5.11 (ddd, *J* = 10.5, 8.8, 3.6 Hz, 1H, *cis*), 4.22 (ddd, *J* = 10.1, 8.3, 4.8 Hz, 1H, *trans*), 3.09 – 2.91 (m, 2H, 1*trans* and 1*cis*), 2.90 – 2.71 (m, 2H, 1*trans* and 1*cis*), 1.32 (d, *J* = 4.7 Hz, 18H, 9*trans* and 9*cis*).

^{13}C NMR (126 MHz, DMSO-d_6) δ 173.4, 168.6, 156.0, 155.9, 149.0, 145.7, 139.1, 138.5, 136.3, 129.8, 129.7, 129.7, 129.7, 128.7, 128.6, 128.0, 128.0, 127.7, 127.6, 126.8, 126.7, 120.9, 120.8, 118.4, 117.9, 111.5, 111.4, 102.1, 102.0, 78.5, 78.4, 55.6, 53.6, 37.8, 36.9, 28.6, 28.3.

HRMS (ESI$^+$): m/z calcd. for $C_{23}H_{27}N_4O_3$ ([M+H]$^+$) 407.20832, measured 407.20696.

N-(2-(6-(Trifluoromethyl)pyridin-3-yl)ethyl)-4,5,6,7-tetrahydrobenzo[b]thiophene-2-carboxamide (38):

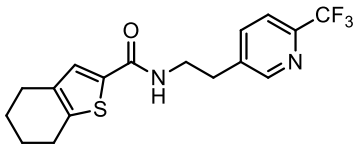

Compound **38** was synthesized according to GP-9. The first step product (*E*)-5-(2-nitrovinyl)-2-(trifluoromethyl)pyridine was prepared by starting with 6-(trifluoromethyl)nicotinaldehyde (175.1 mg, 1 mmol, 1 equiv.), nitromethane (61.1 mg, 1 mmol, 1 equiv.), and MeOH (2 mL) followed by treating with HCl (0.6 mL in 1 mL of water). After workup, the obtained crude was treated with $LiAlH_4$ (151.8 mg, 4 mmol) in dry-THF (16 mL) to afford the second step product 2-(6-(trifluoromethyl)pyridin-3-yl)ethanamine. This crude (127.5 mg, aprrox. 0.67 mmol, 1 equiv.) was reacted with 4,5,6,7-tetrahydrobenzo[*b*]thiophene-2-carboxylic acid (133.8 mg, 0.74 mmol, 1.1 equiv.), HOBt.H_2O (204.7 mg, 1.34 mmol, 2 equiv.), EDC·HCl (256.27 mg, 1.34 mmol, 2 equiv.), and DIPEA (279.4 uL, 1.67 mmol, 2.5 equiv.) in

DMF (2 mL). The crude obtained after the workup was purified by preparative HPLC (H_2O:MeCN + 0.1% formic acid, gradient 5% to 100% MeCN) to afford **38** as a pale yellow solid (75 mg, 0.21 mmol, 21%).
^{1}H NMR (500 MHz, $CDCl_3$) δ 8.51 (d, *J* = 2.3 Hz, 1H), 7.67 (dd, *J* = 8.1, 2.2 Hz, 1H), 7.57 (d, *J* = 8.0 Hz, 1H), 7.07 (s, 1H), 5.97 (bs, 1H), 3.60 (q, *J* = 6.7 Hz, 2H), 2.95 (t, *J* = 7.0 Hz, 2H), 2.69 (td, *J* = 5.9, 1.8 Hz, 2H), 2.54 – 2.47 (m, 2H), 1.82 – 1.67 (m, 4H).
^{13}C NMR (126 MHz, $CDCl_3$) δ 162.5, 150.4, 146.6 (q, *J* = 34.8 Hz), 141.7, 138.0, 137.7, 136.4, 133.6, 129.4, 121.6 (q, *J* = 273.6 Hz), 120.4, 40.6, 32.9, 25.4, 25.3, 23.2, 22.6.
^{19}F NMR (470 MHz, $CDCl_3$) δ −67.73.
HRMS (ESI$^+$): m/z calcd. for $C_{17}H_{18}F_3N_2OS$ ([M+H]$^+$) 355.10919, measured 355.10776

4-(2,4-Dichlorophenoxy)-N-(2-fluoro-4-hydroxyphenethyl)butanamide (39):

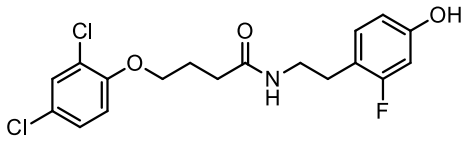

Compound **39** was synthesized according to GP-9. The first step product (*E*)-3-fluoro-4-(2-nitrovinyl)phenol was prepared by starting with 2-fluoro-4-hydroxybenzaldehyde (140.1 mg, 1 mmol, 1 equiv.), nitromethane (61.1 mg, 1 mmol, 1 equiv.), and MeOH (2 mL) followed by treating with HCl (0.6 mL in 1 mL of water). After workup, the obtained crude was treated with $LiAlH_4$ (151.8 mg, 4 mmol) in dry-THF (16 mL) to afford the second step product 4-(2-aminoethyl)-3-fluorophenol. This crude (78 mg, aprrox. 0.5 mmol, 1equiv.) was reacted with 4-(2,4-dichlorophenoxy)butanoic acid (73 mg, 0.55 mmol, 1.1 equiv.), HOBt.H_2O (168.5 mg, 1.1 mmol, 2 equiv.), EDC·HCl (210.9 mg, 1.1 mmol, 2 equiv.), and DIPEA (239 uL, 1.37 mmol, 2.5 equiv.) in DMF (2 mL). The crude obtained after the workup was purified by preparative HPLC (H_2O:MeCN + 0.1% formic acid, gradient 5% to 100% MeCN) to afford **39** as a pale yellow solid (35 mg, 0.09 mmol, 9%).
^{1}H NMR (500 MHz, $CDCl_3$) δ 7.26 (d, *J* = 2.5 Hz, 1H), 7.08 (dd, *J* = 8.8, 2.5 Hz, 1H), 6.85 (t, *J* = 8.6 Hz, 1H), 6.71 (d, *J* = 8.8 Hz, 1H), 6.50 – 6.42 (m, 2H), 5.83 (bt, *J* = 5.8 Hz, 1H), 3.90 (t, *J* = 5.8 Hz, 2H), 3.41 (q, *J* = 6.6, 5.9 Hz, 2H), 2.65 (t, *J* = 6.8 Hz, 2H), 2.35 (t, *J* = 7.1 Hz, 2H), 2.04 (p, *J* = 6.7 Hz, 2H).
^{13}C NMR (126 MHz, $CDCl_3$) δ 173.2, 162.6, 160.6, 156.8, 156.7, 153.0, 131.2, 131.2, 129.9, 127.7, 125.8, 123.5, 116.3, 116.2, 114.1, 111.4, 111.4, 103.3, 103.1, 68.0, 40.0, 32.8, 28.5, 24.9.
^{19}F NMR (470 MHz, $CDCl_3$) δ -116.90.
HRMS (ESI$^+$): m/z calcd. for Chemical Formula: $C_{18}H_{19}Cl_2FNO_3$ ([M+H]$^+$) 386.07260, measured 386.07151

2-(4,5,6,7-tetrahydrobenzo[b]thiophen-2-yl)-5-(6-(trifluoromethyl)pyridin-3-yl)-1,3,4-oxadiazole (40):

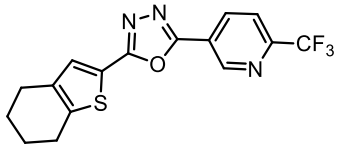

Compound **40** was synthesized according to GP-10, starting with 6-(trifluoromethyl)nicotinic acid (101.5 mg, 0.53 mmol, 1 equiv.), 4,5,6,7-tetrahydrobenzo[b]thiophene-2-carbohydrazide (104.1 mg, 0.53 mmol, 1 equiv.), aluminum oxide (200 mg), and phosphorous oxytrichloride (1.14 g, 7.44 mmol, 14 equiv.). The crude purified by washing with ice-cold distilled water and ice-cold concentrated sodium bicarbonate solution. The residue was further washed with cold MeOH to provide the **40** as a white solid (115.5 mg, 0.33 mmol, 62%).
^{1}H NMR (500 MHz, $CDCl_3$) δ 9.34 (d, *J* = 1.8 Hz, 1H), 8.51 (dd, *J* = 8.2, 1.7 Hz, 1H), 7.80 (d, *J* = 8.2 Hz, 1H), 7.49 (s, 1H), 2.79 (t, *J* = 6.1 Hz, 2H), 2.63 (t, *J* = 6.2 Hz, 2H), 1.81-1.70 (m, 4H).
^{13}C NMR (126 MHz, $CDCl_3$) δ 162.2, 160.5, 150.1 (q, *J* = 35.7 Hz), 147.8, 143.2, 137.2, 135.5, 131.49, 123.0, 120.8, 121.1 (q, *J* = 270.1 Hz) 120.8, 120.0, 25.4, 25.4, 23.1, 22.5.
^{19}F NMR (470 MHz, $CDCl_3$) δ −68.1.
HRMS (ESI$^+$): m/z calcd. for Chemical Formula: $C_{16}H_{13}F_3N_3OS$ ([M+H]$^+$) 352.07314, measured 352.07090

4-(5-(3-(2,4-dichlorophenoxy)propyl)-1,3,4-oxadiazol-2-yl)-3-fluorophenol (41):

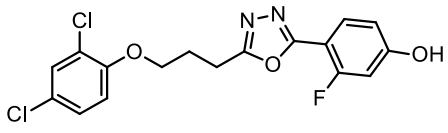

Compound **41** was synthesized according to GP-10, starting with 2-fluoro-4-hydroxybenzoic acid (32.4 mg, 0.19 mmol, 1 mmol), 4-(2,4-dichlorophenoxy)butanehydrazide (32.4 mg, 0.19 mmol, 1 equiv.), aluminum oxide (121 mg), and phosphorous oxytrichloride (408 mg, 2.66 mmol, 14 equiv.). The crude purified by washing with ice-cold distilled water and ice-cold concentrated sodium bicarbonate solution. The residue was further washed with cold MeOH and the crude was purified by preparative HPLC (H_2O:MeCN + 0.1% formic acid, gradient 20% to 100% MeCN) to afford **41** as a white solid (9.1 mg, 0.024 mmol, 12.5%).
^{1}H-NMR (500 MHz, MeOD) δ 7.76 (t, 1H, *J* = 8.4 Hz), 7.34 (d, 1H, *J* = 2.6 Hz), 7.24 (dd, 1H, *J* = 8.7 Hz, 2.4 Hz), 7.06 (d, 1H, *J* = 8.9 Hz), 6.75 (dd, 1H, *J* = 9.0 Hz, 2.2 Hz), 6.69 (dd, 1H, *J* = 12.5 Hz, 2.4 Hz), 4.20 (t, 2H, *J* = 5.7 Hz), 3.20 (t, 2H, *J* = 7.3 Hz), 2.38 (m, 2H).
^{13}C-NMR (500 MHz, MeOD) δ 167.8, 164.3, 164.2, 163.8, 163.4, 161.8, 154.6, 131.6, 130.7, 123.0, 126.8, 124.6, 115.5, 113.5, 104.8, 104.6, 104.1, 104.0, 69.2, 27.0, 23.2.
^{19}F NMR (470 MHz, MeOD) δ −108.62.
HRMS (ESI$^+$): m/z calcd. for Chemical Formula: $C_{17}H_{14}Cl_2FN_2O_3$ ([M+H]$^+$) 383.03655, measured 383.03428

Determination of IC_{50} values

The inhibition of the DXPS enzyme was analyzed in a previously reported photometric assay using the NADPH consumption of the downstream enzyme IspC as readout with minor modifications.[9,10] The assay was conducted in transparent, flat bottom 384 well-plates (Greiner BioOne) and the absorbance measured using a microplate reader (PHERAstar, BMG Labtech). The assay mixture contained 100 mM Tris-HCl with a pH of 7.6, 2 mM dithiotreithol (DTT), 5 mM $MnCl_2$, 0.5 mM NADPH, and 1.5 µM IspC (*E. coli*, expressed and purified in-house according to literature report).[9] The amount of DXPS used in the assays was determined experimentally by a dilution series of the enzyme. The concentration, which showed a reaction velocity in the range of −0.1 to −0.2 OD over a time range of 10 mins was chosen for further experiments. For compounds that were known aggregators, 0.01% v/v of Triton X-100 detergent was added to the assay.

The assay was prepared using two buffers, buffer A containing Tris-HCl and most of the components of the reaction in 2x the final concentration and buffer B, consisting of only 100 mM Tris-HCl, pH 7.6 and the substrates, 0.5 mM pyruvate and 0.5 mM D/L glyceraldehyde 3-phosphate. After the addition of 60 µL of buffer A to the plate with a pre-made inhibitor dilution series in 6 µL DMSO the reaction was started by the addition of 60 µL buffer B. The plate was centrifuged for 1 min at 2000 rpm and 25 °C to remove possible air bubbles. The plate was then immediately supplied to the microplate reader and the absorbance measured at 340 nm using the mode slow kinetics with a cycle time of 30 sec and 60 cycles at RT.

Blank correction and linear fitting of the raw data was performed using the program Origin2019. The obtained initial velocities were converted to percent inhibition and plotted against the inhibitor concentration. The IC_{50} values were determined by nonlinear curve fitting using Origin2019.

Determination of antibacterial activity

Experiments to determine the minimum inhibitory concentration (MIC) have been carried out as described recently.[10] Briefly, our studies were performed with the efflux-pump deficient *E. coli* knockout strain ΔtolC. In case MIC values could not be measured for activity reasons, the percentage (%) inhibition was determined at 100 µM (or lower, depending on the solubility of the compounds).

DLS measurements

Compounds were analyzed for aggregate formation using dynamic light scattering (DLS) on a Zetasizer Nano ZS90 (Malvern Instruments Ltd, Worcestershire, UK). Disposable cuvettes (3.2 mL, 67.758, Sarstedt AG & Co, Nümbrecht, Germany) were filled with a total sample volume of 50 µL and equilibrated to 25 °C for 60 sec prior to the experiments. Analyses were performed in the absence or presence of compounds using 7H9 medium supplemented with 10% OADC and 1% DMSO. Count rate data for all samples were determined from three measurements of at least three cycles of 10 sec each. The count rate at high scattering intensities is reduced by an automatic attenuator, so the derived count rate, which is corrected with the attenuation factor, was used as a measure for the degree of aggregate formation. Derived count rate values of the compounds were compared with the derived count rate of the medium at the concentrations as indicated. This allowed the determination of the highest sample concentration at which the respective compound was not yet present with an increased degree of aggregate formation.

Mycobacterium tuberculosis growth analysis in liquid culture

Bacteria

M. tuberculosis (Mtb) strain H37Rv (ATCC 25618) carrying a mCherry-expressing plasmid (pCherry10)[11] was cultured in 7H9 complete medium (BD Difco; Becton Dickinson) supplemented with oleic acid-albumin-dextrose-catalase (OADC, 10%; BD), 0.2% glycerol, and 0.05% Tween80 as previously described.[12] At mid-log phase (OD_{600} = 0.4) cultures were harvested and frozen in aliquots at −80 °C.

Frozen aliquots of mCherry-Mtb H37Rv were thawed and centrifuged (3700 × g, 10 min). Supernatants were discarded and bacteria were thoroughly resuspended in 7H9 medium (10% OADC) in the absence of glycerol and Tween80 by use of a syringe and a 26-gauge syringe needle. The bacterial suspension was passed in and out of the syringe about 10 times. Non-precipitating compounds - identified and determined by DLS - were tested in triplicates (2 × 10e5 bacteria, volume 100 µL) for their anti-tubercular activity in 2-fold serial dilutions starting from 64 µM using 96-well flat clear bottom black polystyrene microplates (Corning® CellBIND®, New York, USA). Each plate was prepared with rifampicin (National Reference Center, Borstel) as a reference compound. Plates were sealed with an air-permeable membrane (Porvair Sciences, Wrexham, UK) in a 37 °C incubator with mild agitation (TiMix5, Edmund Bühler, Germany), as previously described.[13] Bacterial growth was measured as relative light units (RLU) from the fluorescence intensity obtained at an excitation wavelength of 575 nm and an emission wavelength of 635 nm (microplate reader, Synergy 2, BioTek Instruments, Vermont, USA) after 9 days (Figure 9, in the main text) and 10 days of culture (Supplementary Figures 164 and 165). Obtained values were normalized to RLU values of the solvent control (1% DMSO-treated bacteria set to 100%).

Binding affinity (K_D) determinations by surface plasmon resonance (SPR)

The SPR binding studies were performed using a Reichert SR7500DC surface plasmon resonance spectrometer (Reichert Technologies, Depew, NY, USA), and medium density carboxymethyl dextran hydrogel CMD500M sensor chips (XanTec Bioanalytics, Düsseldorf, Germany). Milli-Q water was used as the running buffer for immobilization. The *Deinococcus radiodurans* DXPS (drDXPS, 69.96 kDa) or truncated *Mycobacterium tuberculosis* DXPS (ΔmtDXPS, 66.61 kDa) was immobilized in one of the two flow cells according to reported amine-coupling protocols.[14-16] The other flow cell was left blank to serve as a reference. The system was initially primed with borate buffer 100 mM (pH 9.0), then the carboxymethyldextran matrix was activated by a 1:1 mixture of *N*-ethyl-*N*'-(3-dimethylaminopropyl)carbodiimide hydrochloride (EDC)

100 mM and *N*-hydroxysuccinimide (NHS) 100 mM at a flow rate of 10 µL/min for 7 min. The drDXPS or ΔmtDXPS was diluted to a final concentration of 70 µg/mL in 10 mM sodium acetate buffer (pH 5.5 or 5.0), respectively, and was injected at a flow rate of 5 µL/min for 10 min. The non-reacted surface was quenched by 1 M ethanolamine hydrochloride (pH 8.5) at a flow rate of 25 µL/min for 3 min. A series of 10 buffer injections was run initially on both reference and active surfaces to equilibrate the system resulting in a stable immobilization level of approximately 5000 (13000 for ΔmtDXPS) µ refractive index unit (µRIU) (Supplementary Figures 109 and 127), respectively. Phosphate buffered saline (PBS) buffer (10 mM Na_2HPO_4, 1.8 mM KH_2PO_4, 137 mM NaCl, 2.7 mM KCl, 0.05% v/v Tween 20, pH 7.4) or HEPES buffer (50 mM HEPES, 150 mM NaCl, 0.05% v/v Tween 20, 1 mM $MgCl_2$, pH 8.0) containing 5% v/v DMSO was used as the running buffer for binding studies with drDXPS and ΔmtDXPS, respectively. All running buffers were filtered and degassed prior to use. Binding experiments were performed at 20 °C. Compounds dissolved in DMSO were diluted with the running buffer (final DMSO concentration of 5% v/v) and were injected at a flow rate of 30 µL/min. Single-cycle kinetics were applied for K_D determination. The association time was set to 60 s, and the dissociation phase was recorded for 120 sec. Ethylene glycol 80% in the running buffer was used for regeneration of the surface. Differences in the bulk refractive index due to DMSO were corrected by a calibration curve (nine concentrations: 3–7% v/v DMSO in the running buffer). Data processing and analysis were performed by Scrubber software (Version 2.0c, 2008, BioLogic Software). Sensorgrams were calculated by sequential subtractions of the corresponding curves obtained from the reference flow cell and the running buffer (blank). SPR responses are expressed in the resonance unit (RU). The K_D values were calculated by the fitting of the steady-state binding responses to a 1:1 Langmuir interaction model (Hill equation was used for compound **3**).

Mode-of-inhibition (MOI) study

MOI study followed a previously reported protocol and was performed against *D. radiodurans* DXPS.[17] The experiments were performed in duplicates.

Inhibitor competition with ThDP: The Michaelis–Menten constant K_m^{ThDP} was determined with an assay mixture containing 100 mM Tris-HCl (pH 7.6), 2.0 mM $MgCl_2$, 2.0 mM DTT, 0.5 mM NADPH, 0.5 mM sodium pyruvate, 0.5 mM D-GAP, 8.3 µM *E. coli* IspC, 0.4 µM *D. radiodurans* DXPS and 5% DMSO. Buffer A contained 100 mM Tris-HCl (pH 7.6), 4.0 mM $MgCl_2$, 4.0 mM DTT, 1.0 mM NADPH, 16.6 µM *E. coli* IspC, 0.8 µM *D. radiodurans* DXPS. Buffer B contained 100 mM Tris-HCl (pH 7.6), 1.0 mM sodium pyruvate, and 1.0 mM D-GAP. ThDP was titrated in the 0.1–200 µM range, and K_m^{ThDP} was calculated using the program Dynafit.[18] Four ThDP concentrations were taken for IC_{50} determination, spanning from 1x K_m^{ThDP} to 16x K_m^{ThDP}. Assay mixtures contained ThDP concentrations 0.3 µM, 1 µM, 2 µM, and 5 µM, respectively. Buffer A1–A4 contained ThDP concentrations 0.6 µM, 2 µM, 4 µM, and 10 µM respectively. The rest of the procedure followed the protocol of IC_{50} determination.

Inhibitor competition with pyruvate: The Michaelis-Menten constant $K_m^{pyruvate}$ was determined with assay mixture containing 100 mM Tris-HCl (pH 7.6), 2.0 mM $MgCl_2$, 2.0 mM DTT, 0.5 mM NADPH, 100 µM ThDP, 0.5 mM D-GAP, 8.3 µM *E. coli* IspC, 0.4 µM *D. radiodurans* DXPS and 5% DMSO. Buffer A contained 100 mM Tris-HCl (pH 7.6), 4.0 mM $MgCl_2$, 4.0 mM DTT, 1.0 mM NADPH, 200 µM ThDP, 16.6 µM *E. coli* IspC, 0.8 µM *D. radiodurans* DXPS. Buffer B contained 100 mM Tris-HCl (pH 7.6) and 1.0 mM D-GAP. Pyruvate was titrated in 1–500 µM range, and $K_m^{pyruvate}$ was calculated using the program Dynafit. Four pyruvate concentrations were taken for IC_{50} determination, spanning from 1x $K_m^{pyruvate}$ to 5x $K_m^{pyruvate}$. Assay mixtures contained pyruvate concentrations 0.1 mM, 0.2 mM, 0.4 mM, and 0.6 mM respectively. Buffer B1–B4 contained pyruvate concentrations 0.2 mM, 0.4 mM, 0.8 mM, and 1.2 mM, respectively. The rest of the procedure followed the protocol of IC_{50} determination.

Inhibitor competition with D-GAP: The Michaelis–Menten constant $K_m^{D\text{-}GAP}$ was determined with assay mixture containing 100 mM Tris-HCl (pH 7.6), 2.0 mM $MgCl_2$, 2.0 mM DTT, 0.5 mM NADPH, 100 µM ThDP, 0.2 mM sodium pyruvate, 8.3 µM *E. coli* IspC, 0.4 µM *D. radiodurans* DXPS and 5% DMSO. Buffer A contained 100 mM Tris-HCl (pH 7.6), 4.0 mM $MgCl_2$, 4.0 mM DTT, 1.0 mM NADPH, 200 µM ThDP, 16.6 µM *E. coli* IspC, 0.8 µM *D. radiodurans* DXPS. Buffer B contained 100 mM Tris-HCl (pH 7.6) and 0.4 mM sodium pyruvate. D-GAP

was titrated in 0.1–0.8 mM range, and $K_m^{D\text{-}GAP}$ was calculated using the program Dynafit. Four D-GAP concentrations were taken for IC_{50} determination, spanning from 1 x $K_m^{D\text{-}GAP}$ to 7 x $K_m^{D\text{-}GAP}$. Assay mixtures contained D-GAP concentration 0.1 mM, 0.2 mM, 0.4 mM, and 0.8 mM, respectively. Buffer B1–B4 contained D-GAP concentration 0.2 mM, 0.4 mM, 0.8 mM, and 1.6 mM, respectively, without significant substrate inhibition. The rest of the procedure followed the protocol of IC_{50} determination.

Protein stability study by thermal shift assay

Analysis was performed using an ABI StepOneplus real-time PCR instrument. The protein samples were measured in white 96-well plates and denatured using a continuous heating rate of 0.5°C /min from 25°C up to 95 °C. The total sample volume was 25 µL of which 20 µL were buffer (100 mM phosphate buffer of pH ranges 5.8, 6.2, 7.0, and 7.5), 2.5 µL protein (2 µg), and 2.5 µL dye (Sypro Orange 50x). The melting curves were analyzed using Protein Thermal Shift 1.3 software. The most stabilizing buffer pH for drDXS, which showed the highest Tm was then used in our following experiments.

Time/hr	**Melting temperature of drDXS (°C)**			
	pH 7.5	pH 7.0	pH 6.2	pH 5.8
0	51.2	51.8	48.4	41.4
3	51.5	51.8	48.4	42.3
6	51.7	51.8	48.4	45.2
24	51.5	51.7	48.4	44.9

Supplementary Table 1 Melting temperature of drDXS protein at different pH over time

SUPPLEMENTARY FIGURES

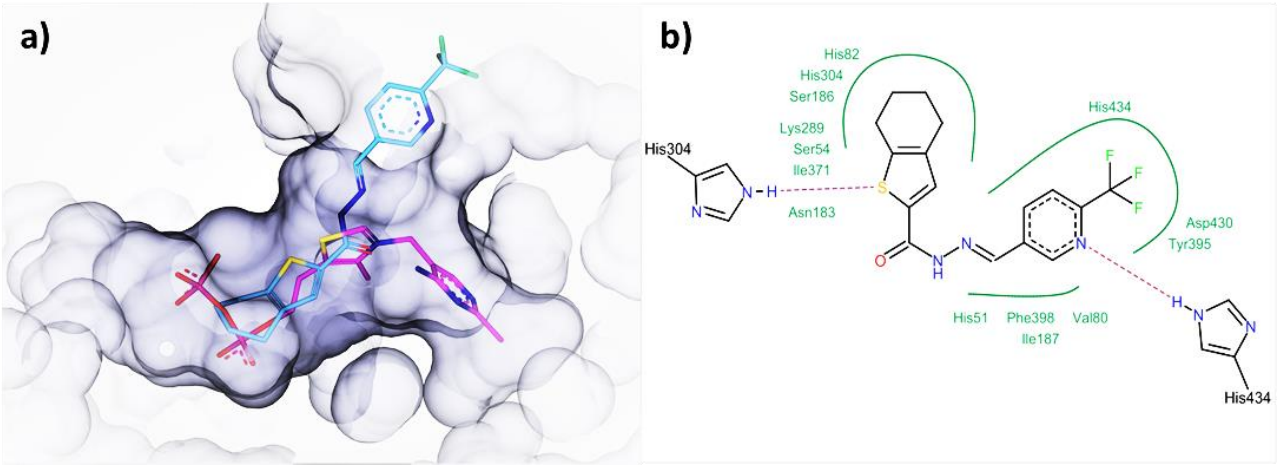

Supplementary Figure 1 a) Binding mode of compound **1** (cyan) compared to the ThDP (pink) in the active site of drDXPS, b) Interaction of compound **1** with the residues in the active site of drDXPS.

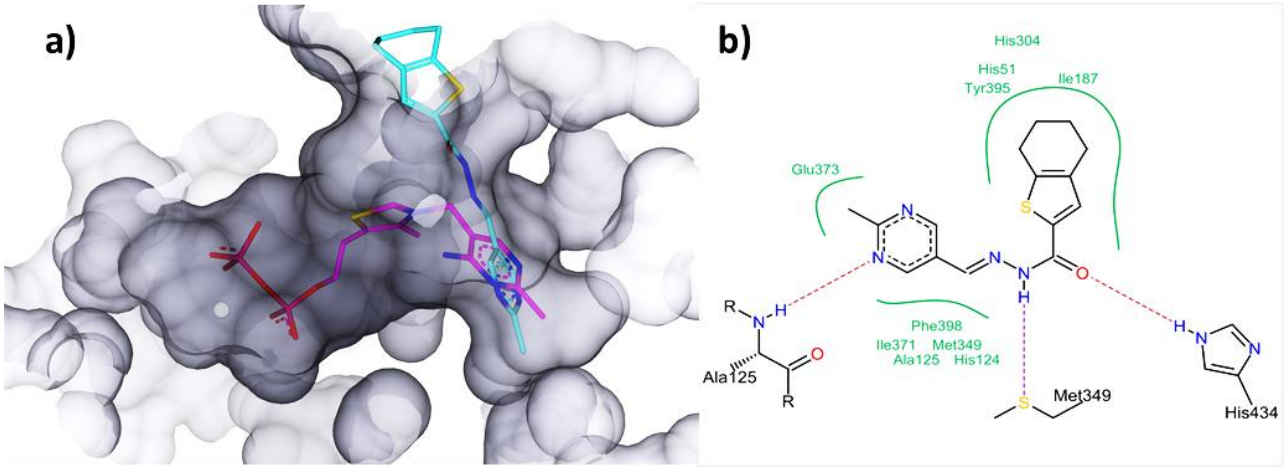

Supplementary Figure 2 a) Binding mode of compound **2** (cyan) compared to the ThDP (pink) in the active site of drDXPS, b) Interaction of compound **2** with the residues in the active site of drDXPS.

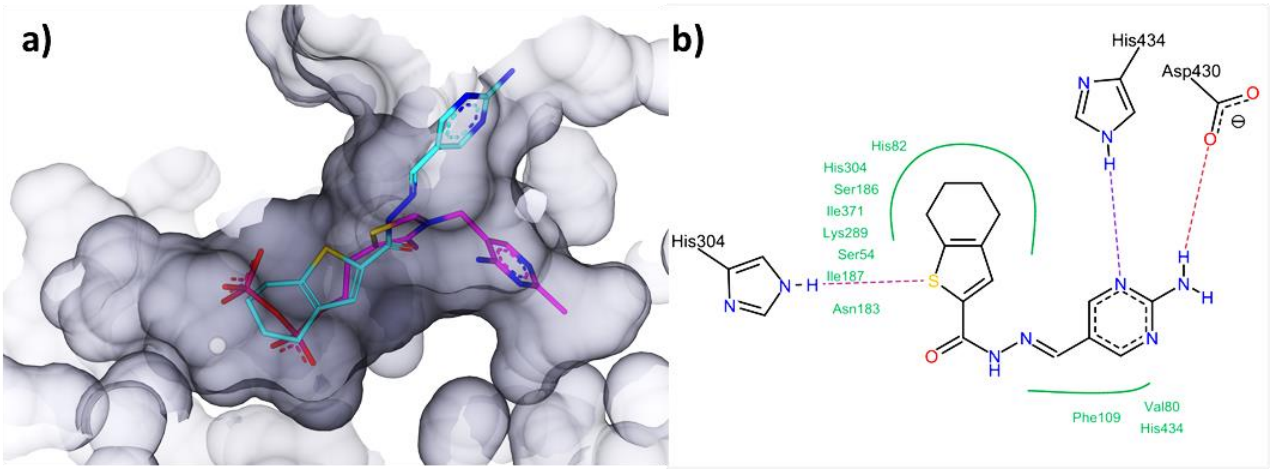

Supplementary Figure 3 a) Binding mode of compound **3** (cyan) compared to the ThDP (pink) in the active site of drDXPS, b) Interaction of compound **3** with the residues in the active site of drDXPS.

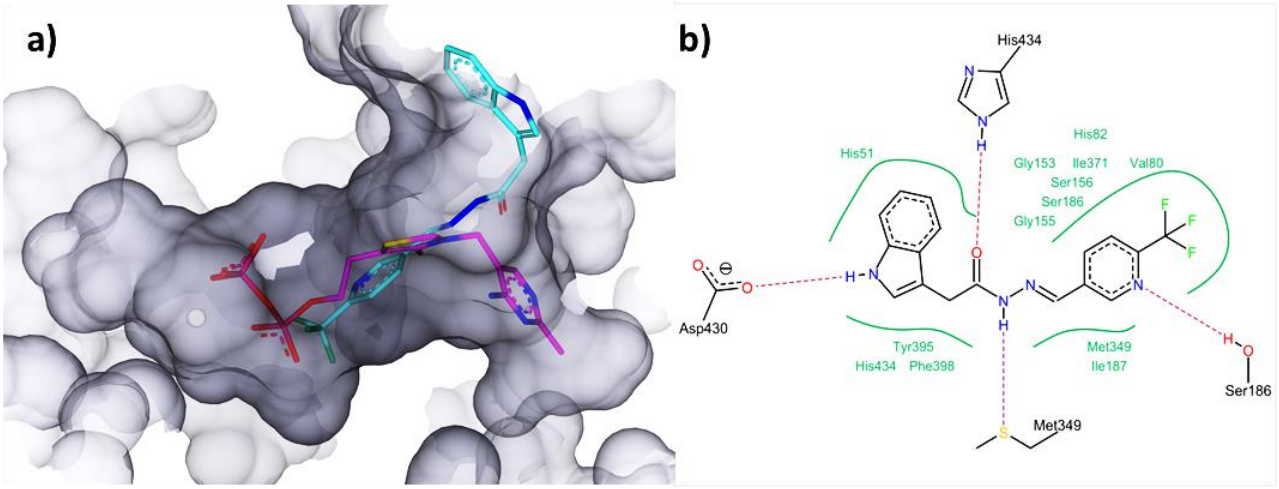

Supplementary Figure 4 a) Binding mode of compound **4** (cyan) compared to the ThDP (pink) in the active site of drDXPS, b) Interaction of compound **4** with the residues in the active site of drDXPS.

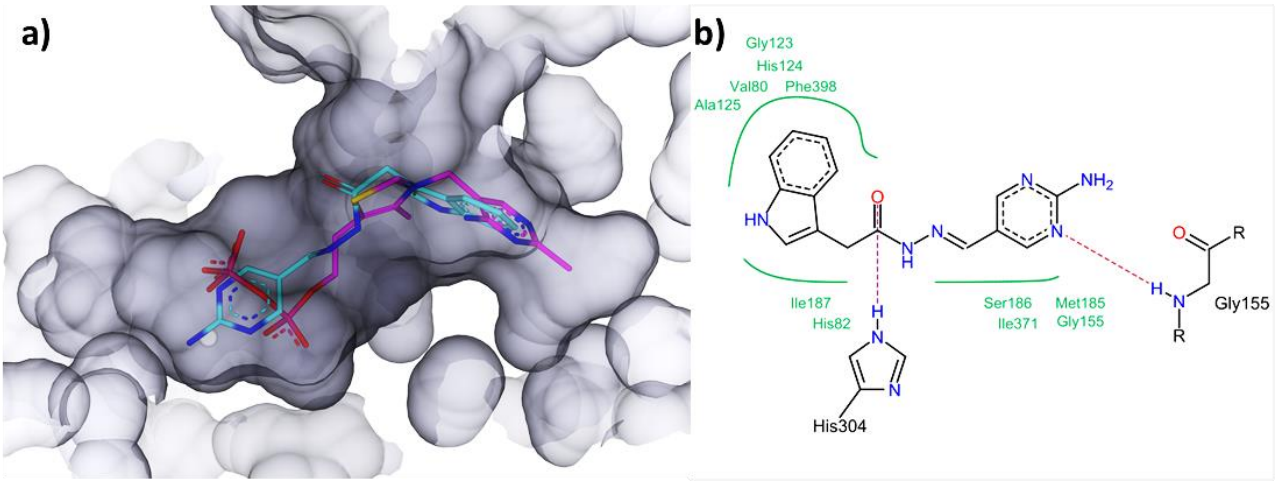

Supplementary Figure 5 a) Binding mode of compound **5** (cyan) compared to the ThDP (pink) in the active site of drDXPS, b) Interaction of compound **5** with the residues in the active site of drDXPS.

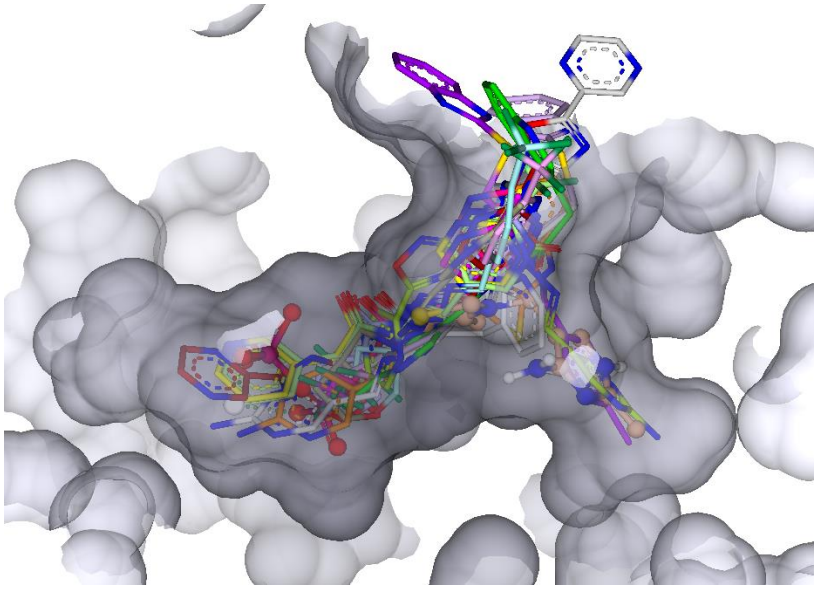

Supplementary Figure 6 Binding mode comparison of other 16 possible acylhydrazones to the ThDP in the active site of drDXPS

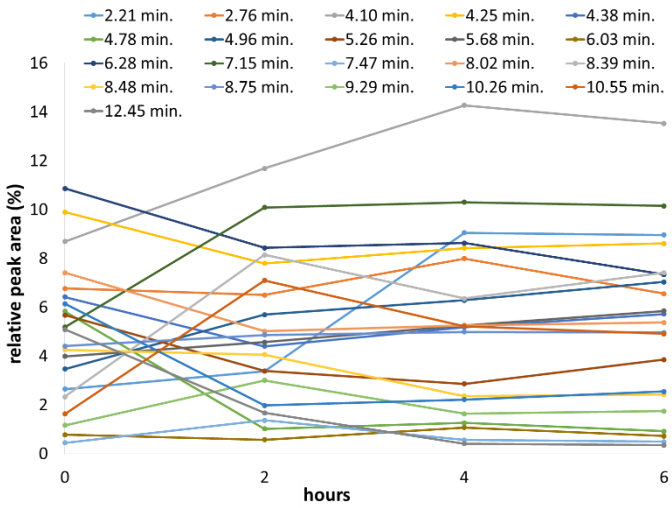

Supplementary Figure 7 Evaluation of the equilibrium state of acylhydrazone formation in blank **DCL-1** by comparing relative peak areas of products formed over time.

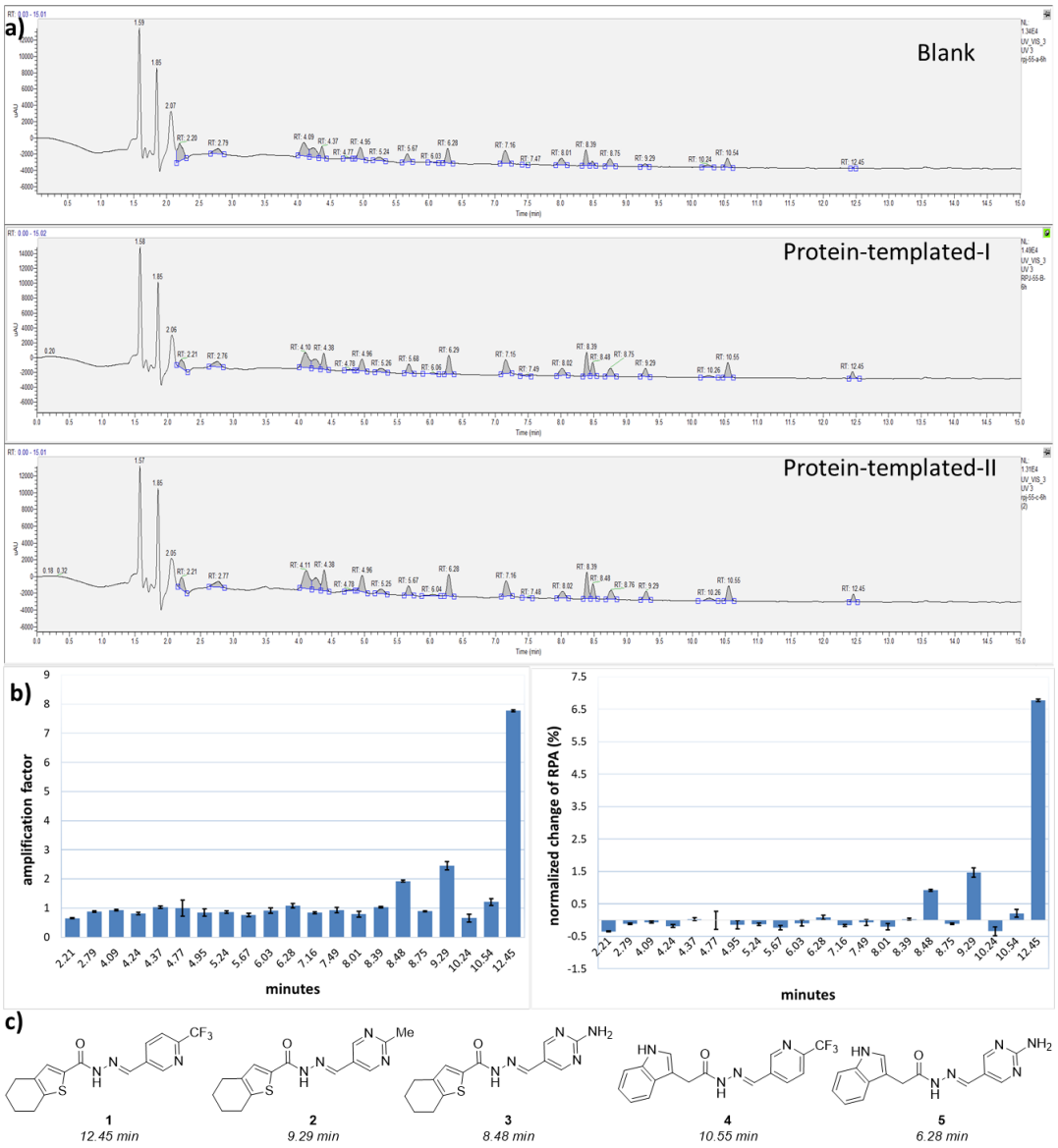

Supplementary Figure 8 a) Comparison between blank and protein-templated **DCC-1 (40 mol% protein)** at 6 h, b) amplification factor and normalized change of RPA of products, c) amplified acylhydrazone products in protein-templated DCC.

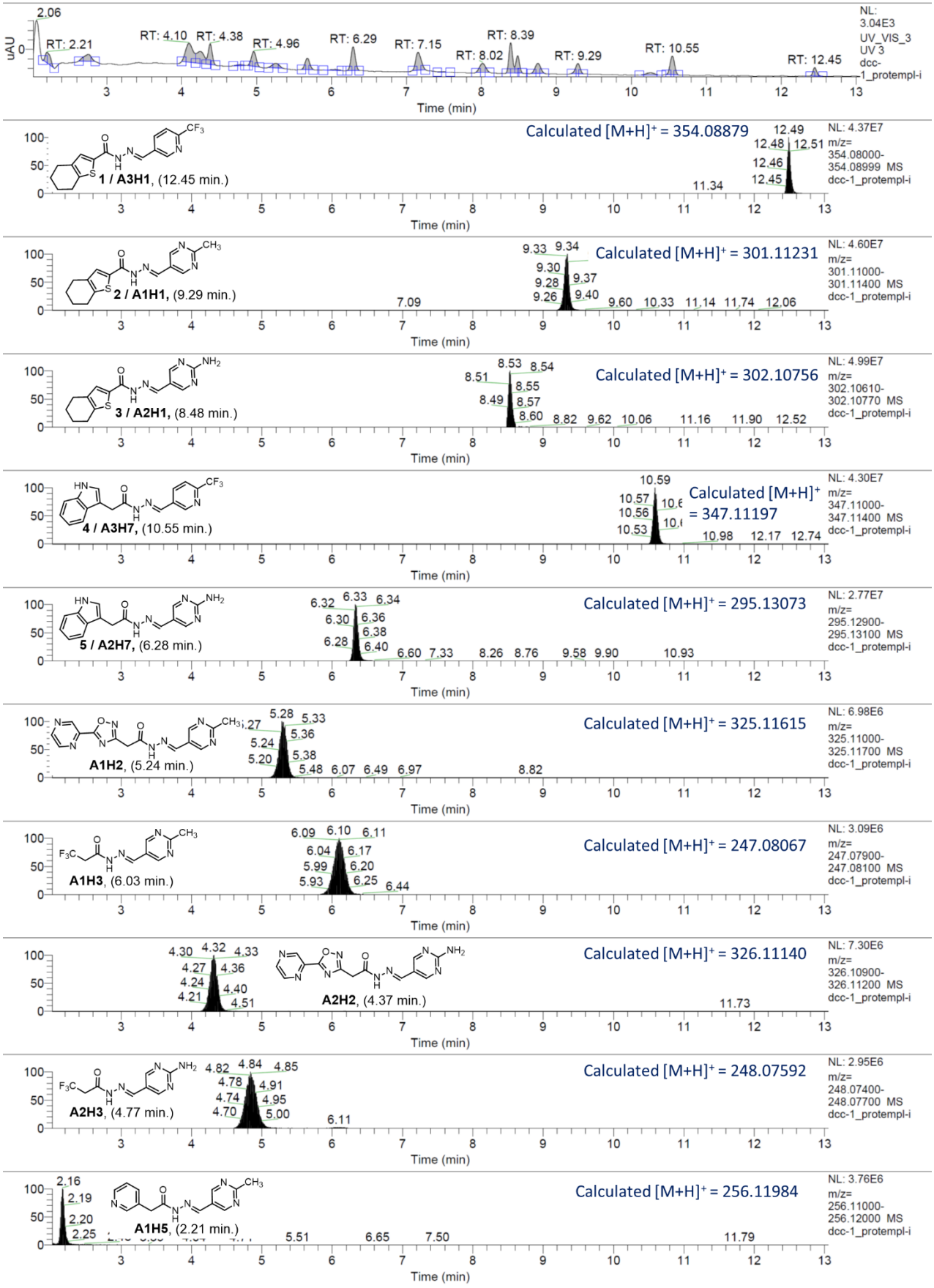

Supplementary Figure 8 d) Different acylhydrazones formed in DCC-1, their retention times, and observed mass.

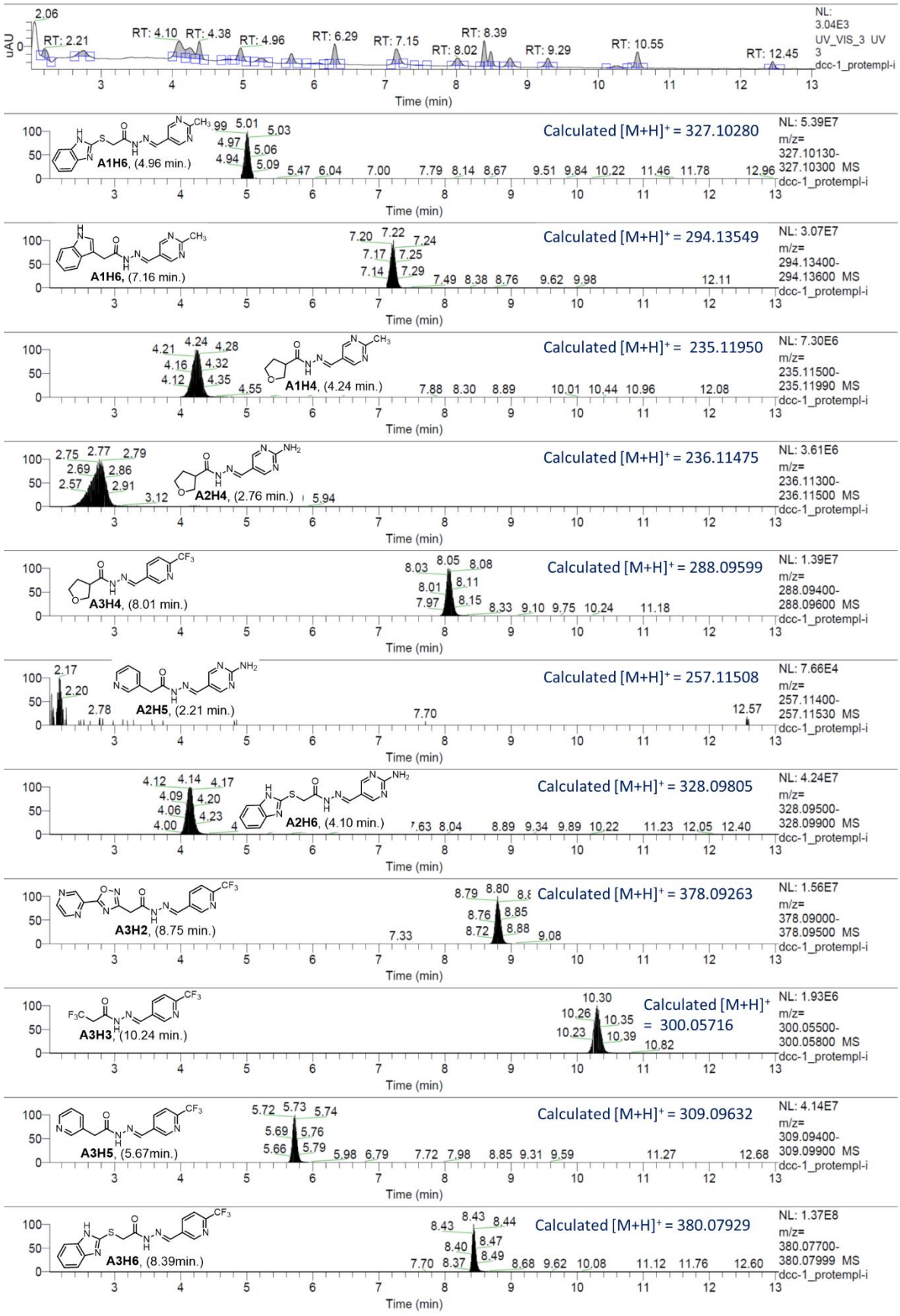

Supplementary Figure 8 e) Different acylhydrazones formed in DCC-1, their retention times, and observed mass.

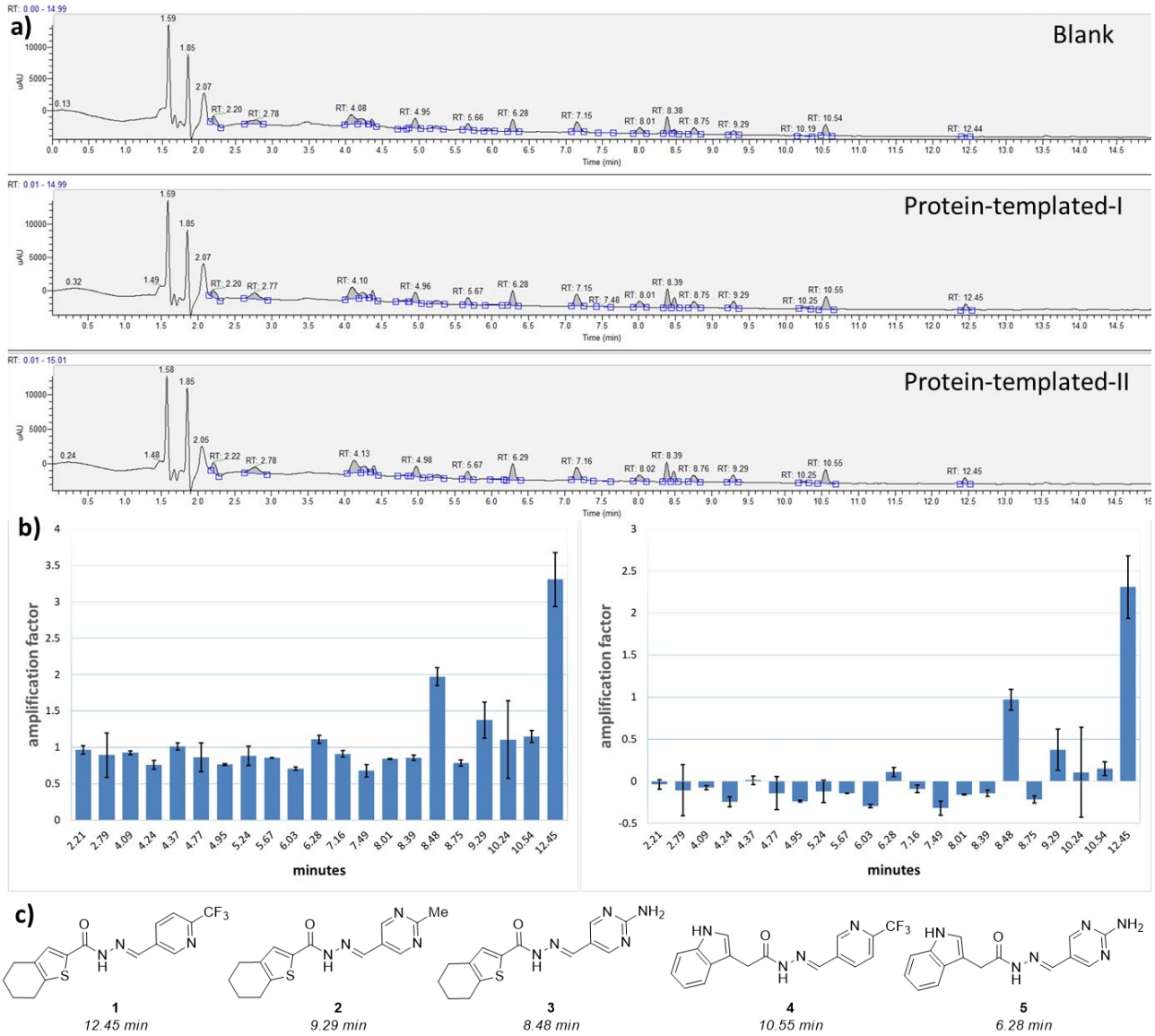

Supplementary Figure 9 a) Comparison between blank and protein-templated **DCC-1 (20 mol% protein)** at 6 h, b) amplification factor and normalized change of RPA of products, c) amplified acylhydrazone products in protein-templated DCC.

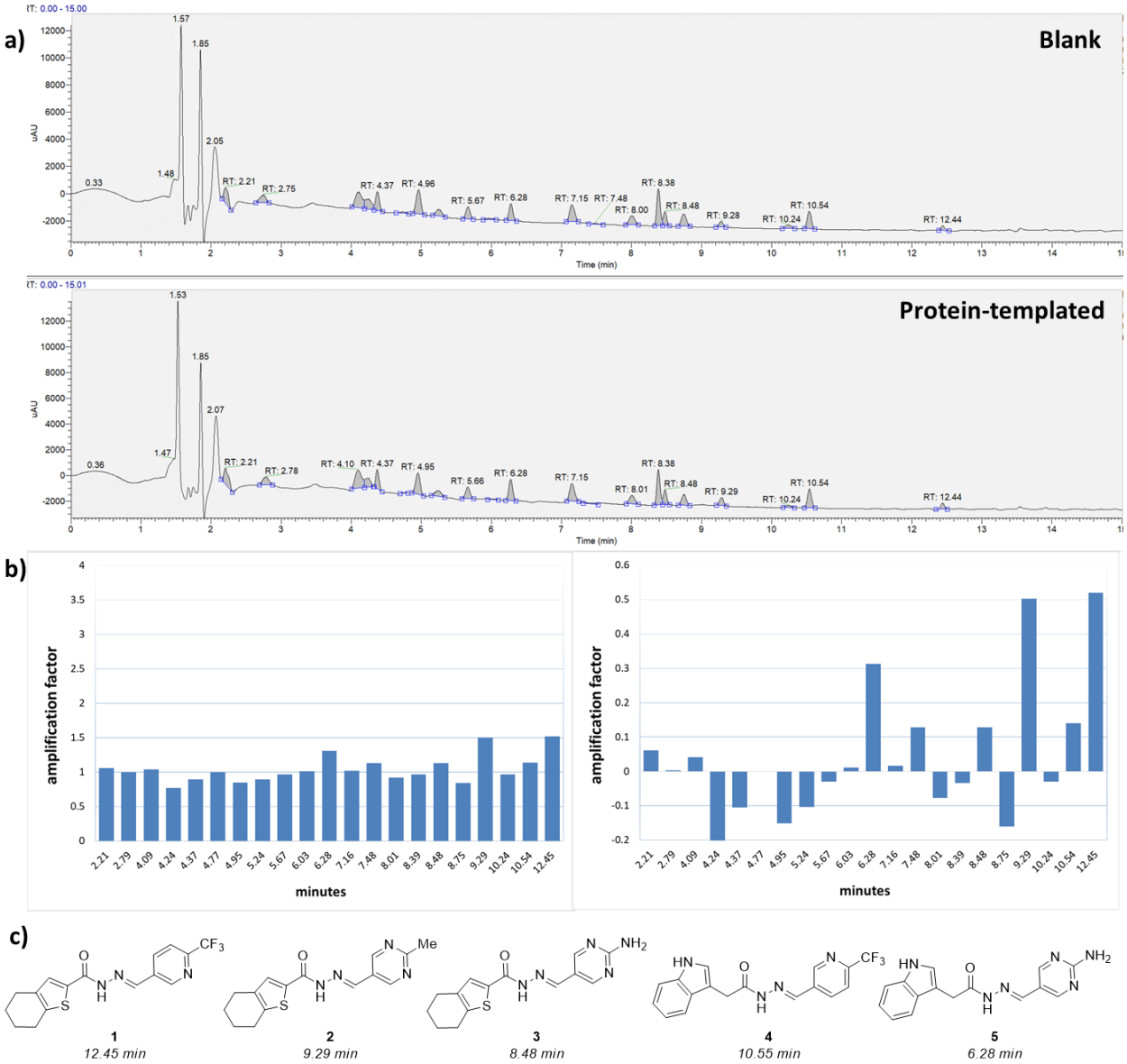

Supplementary Figure 10 a) Comparison between blank and protein-templated **DCC-1** (20 mol% protein pre-equilibrated) at 6 h, b) amplification factor and normalized change of RPA of products, c) amplified acylhydrazone products in protein-templated DCC.

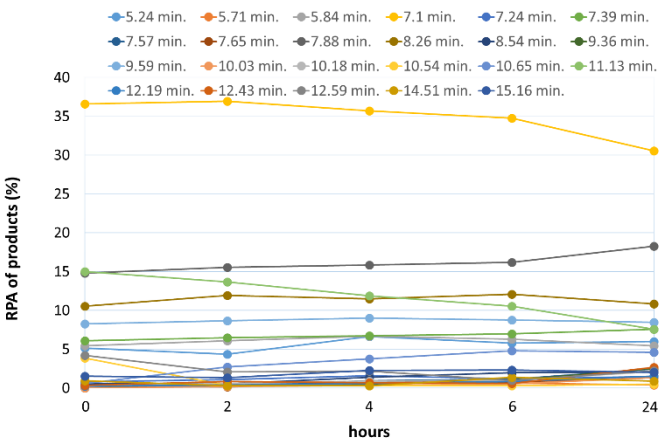

Supplementary Figure 11 Evaluation of the equilibrium state of acylhydrazone formation in blank **DCL-2** by comparing relative peak areas of products formed over time. Lines represent the formation of acylhydrazone products over time.

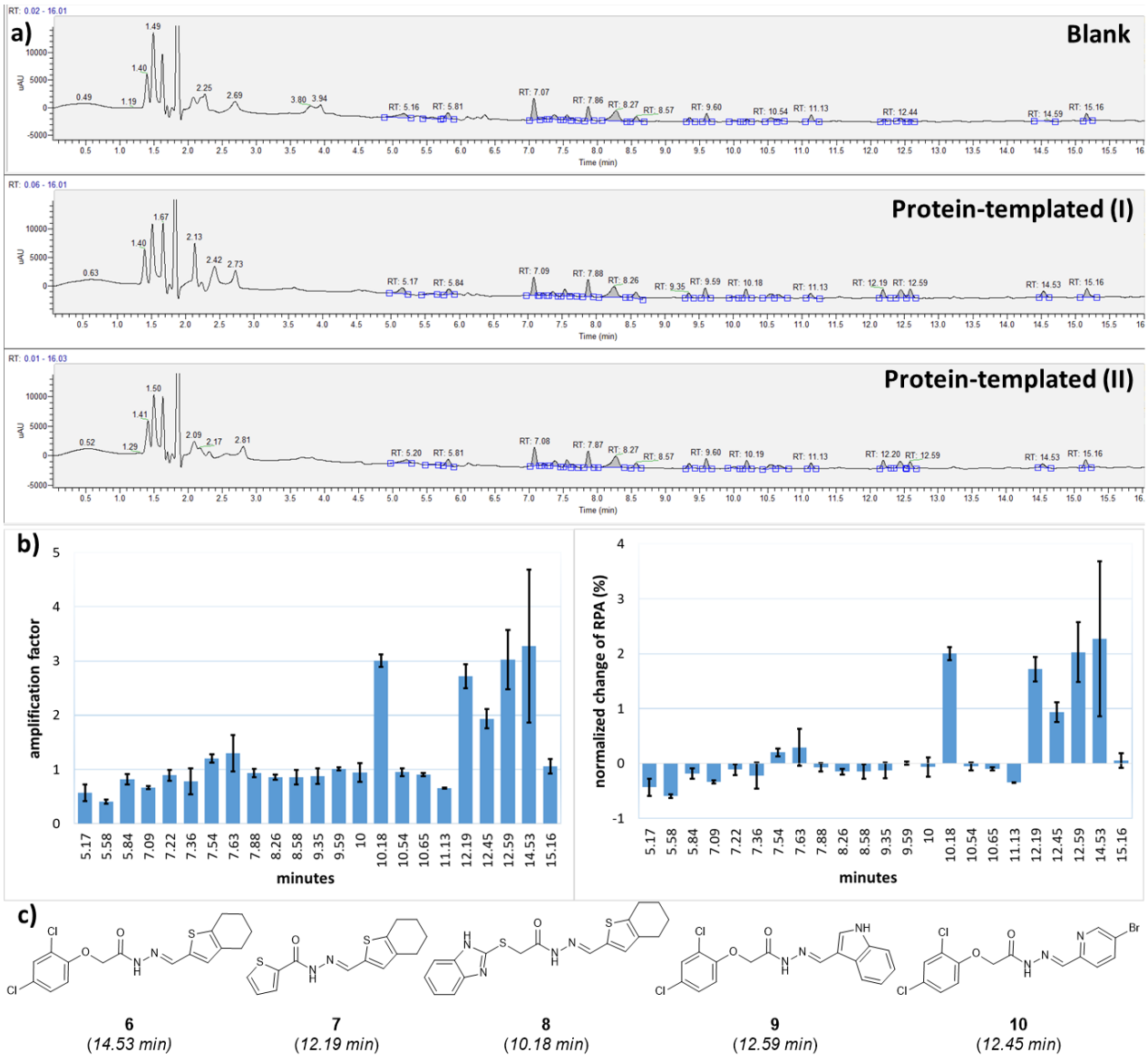

Supplementary Figure 12 a) Comparison between blank and protein-templated **DCC-2** at 24 h, b) amplification factor and normalized change of RPA of products, c) amplified acylhydrazone products in protein-templated DCC.

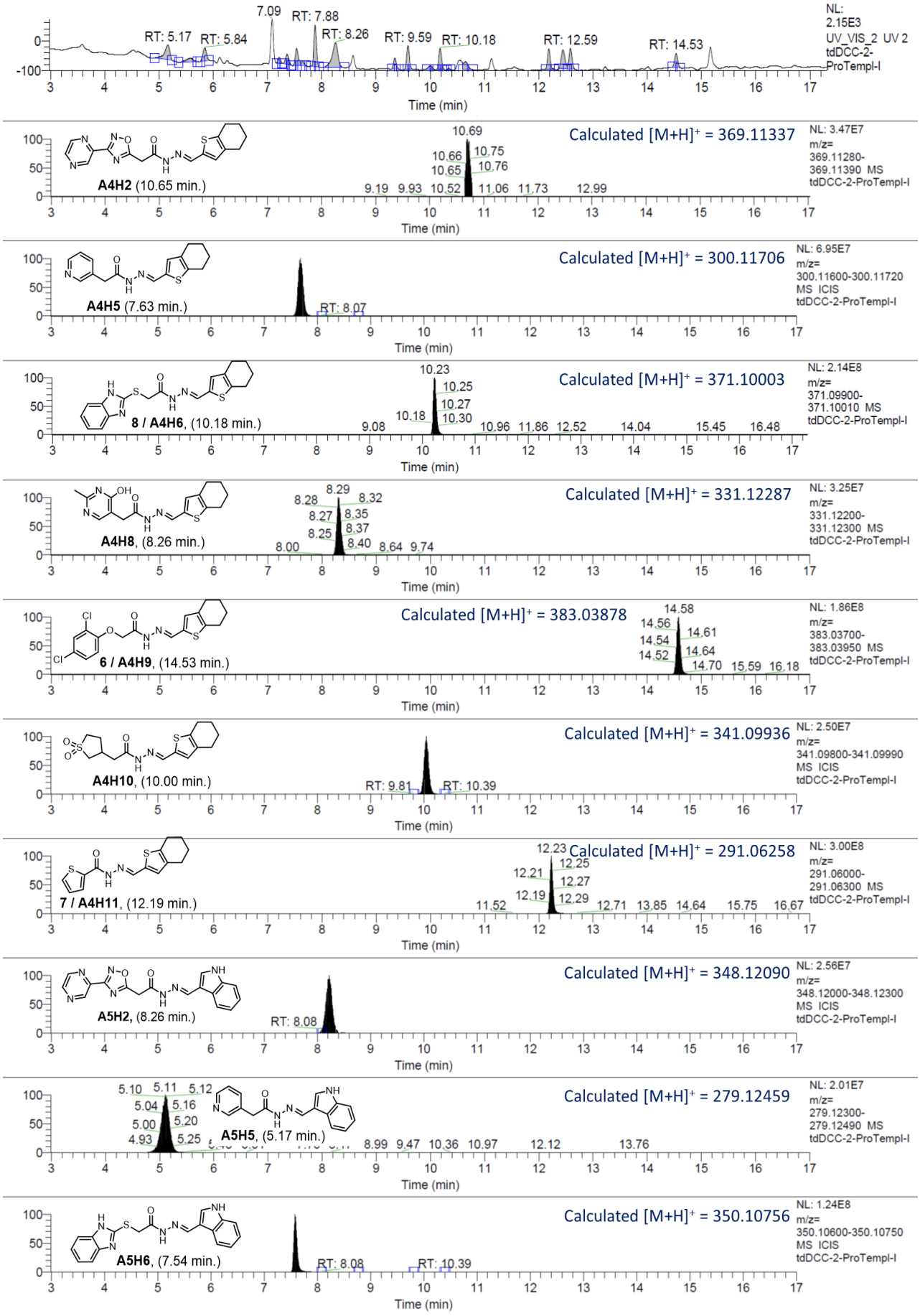

Supplementary Figure 12 d) Different acylhydrazones formed in DCC-2, their retention times, and observed mass.

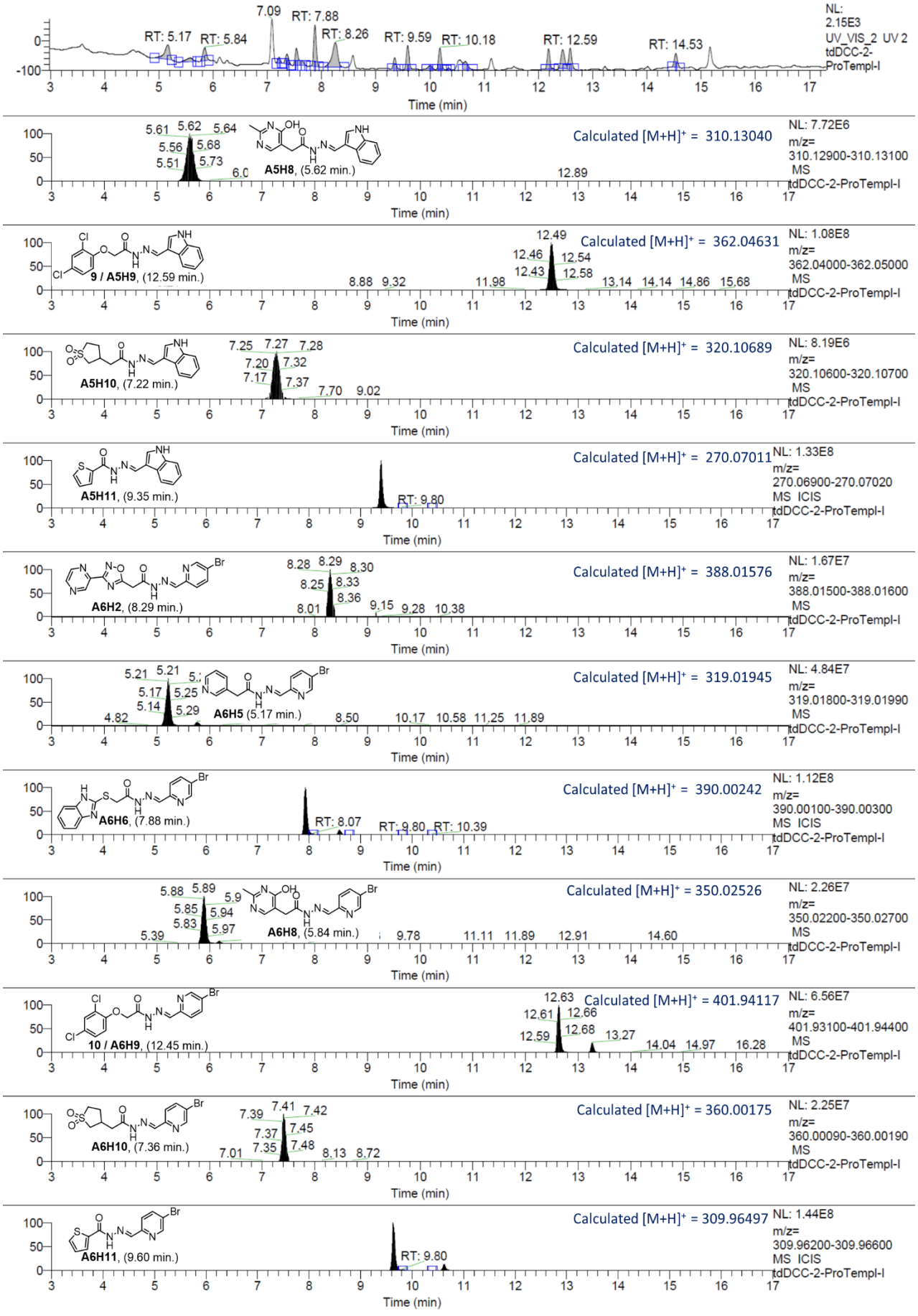

Supplementary Figure 12 e) Different acylhydrazones formed in DCC-2, their retention times, and observed mass.

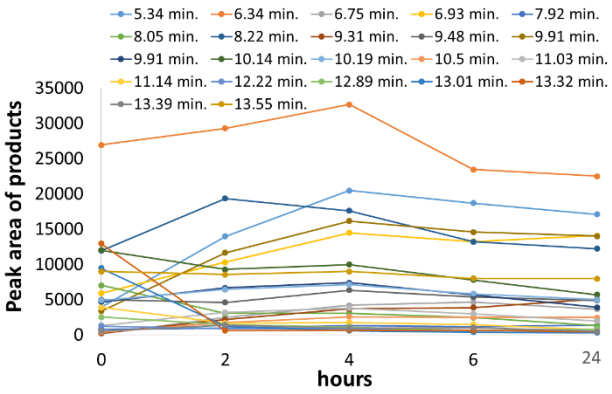

Supplementary Figure 13 Evaluation of the equilibrium state in a blank **DCL-3a** by comparing peak areas of products formed over time. Lines represent the formation of acylhydrazone products over time.

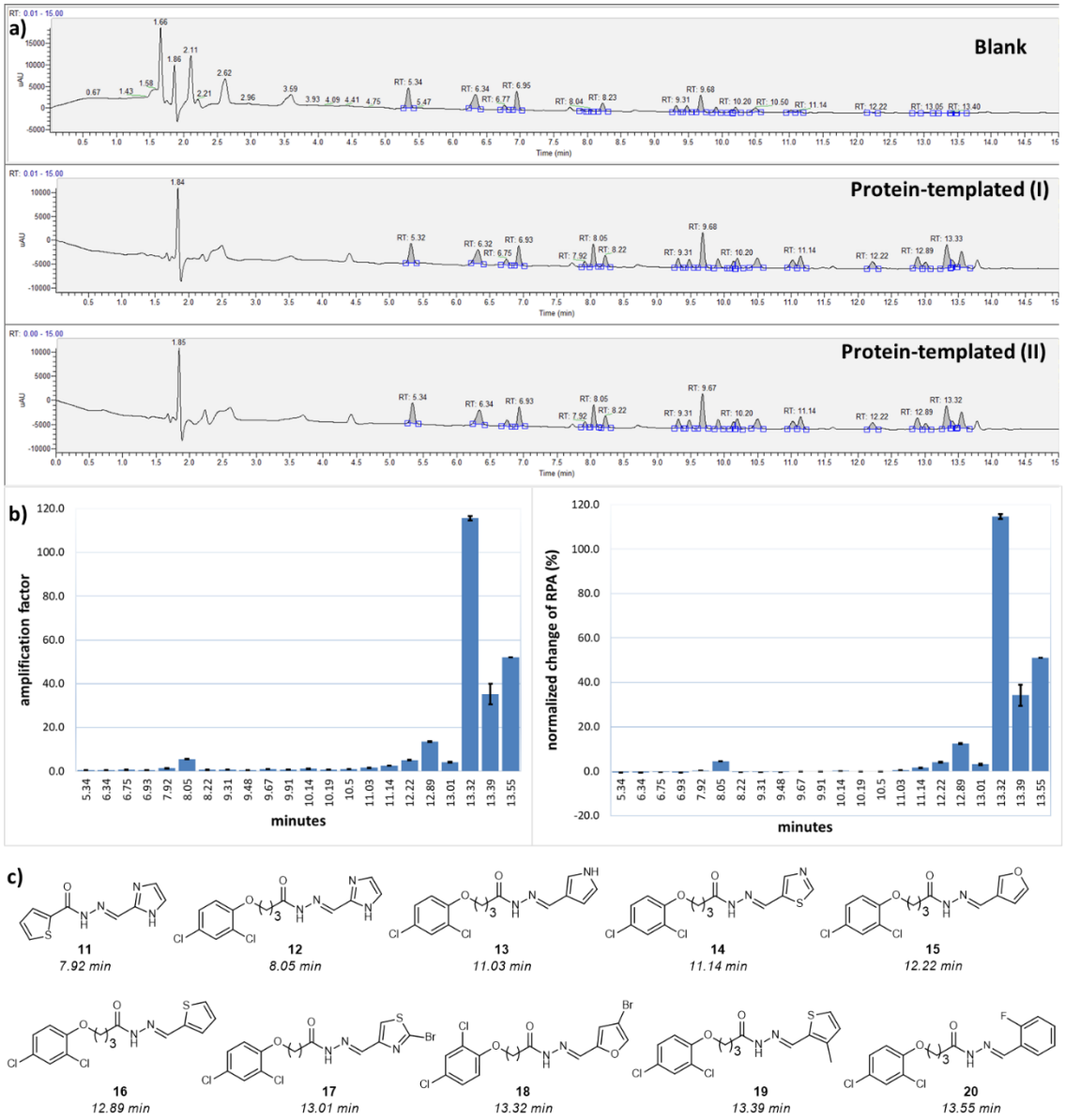

Supplementary Figure 14 a) Comparison between blank and protein-templated **DCC-3a** at 24 h, b) amplification factor and normalized change of RPA of products, c) amplified acylhydrazone products in protein-templated DCC.

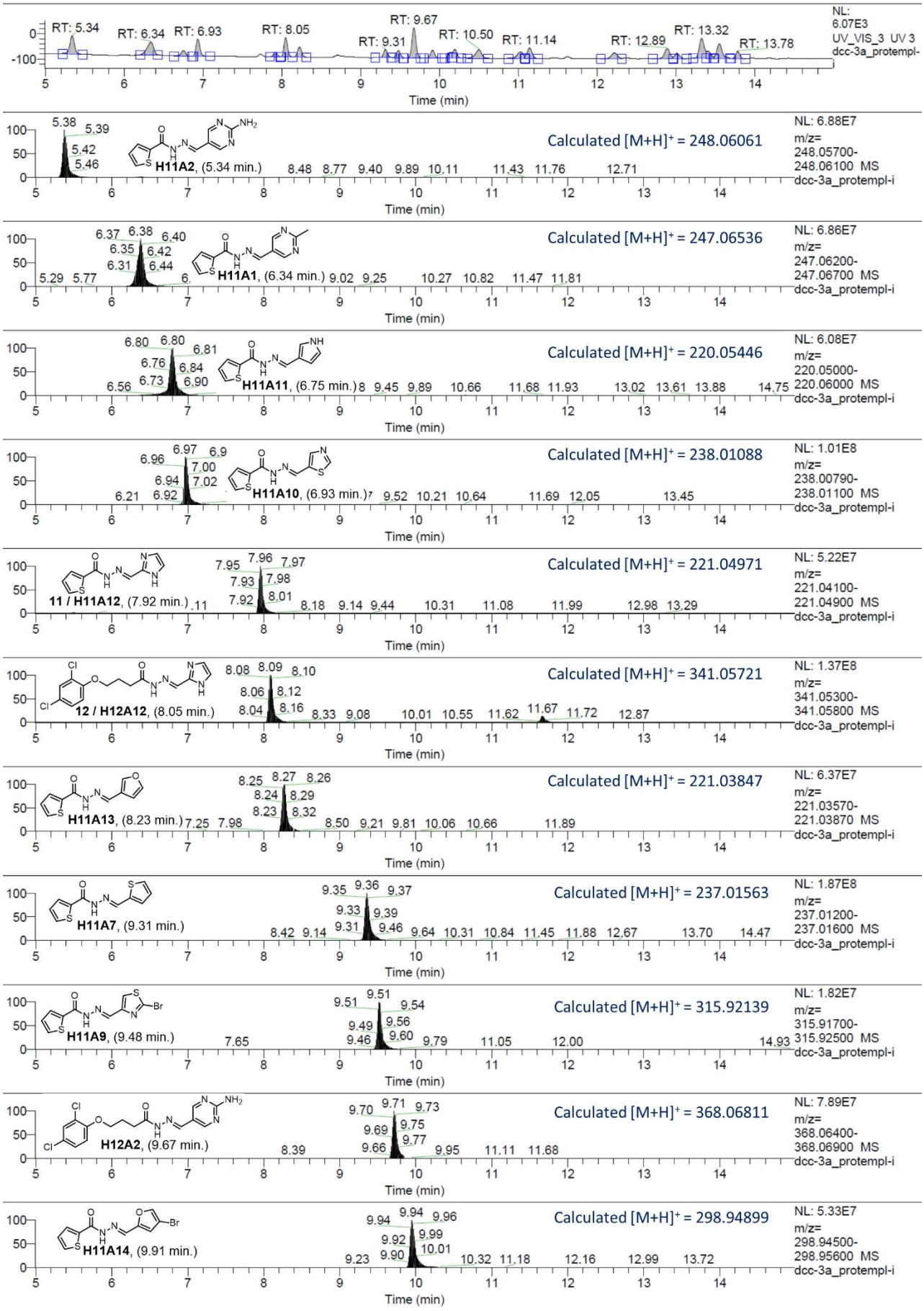

Supplementary Figure 14 d) Different acylhydrazones formed in DCC-3a, their retention times, and observed mass.

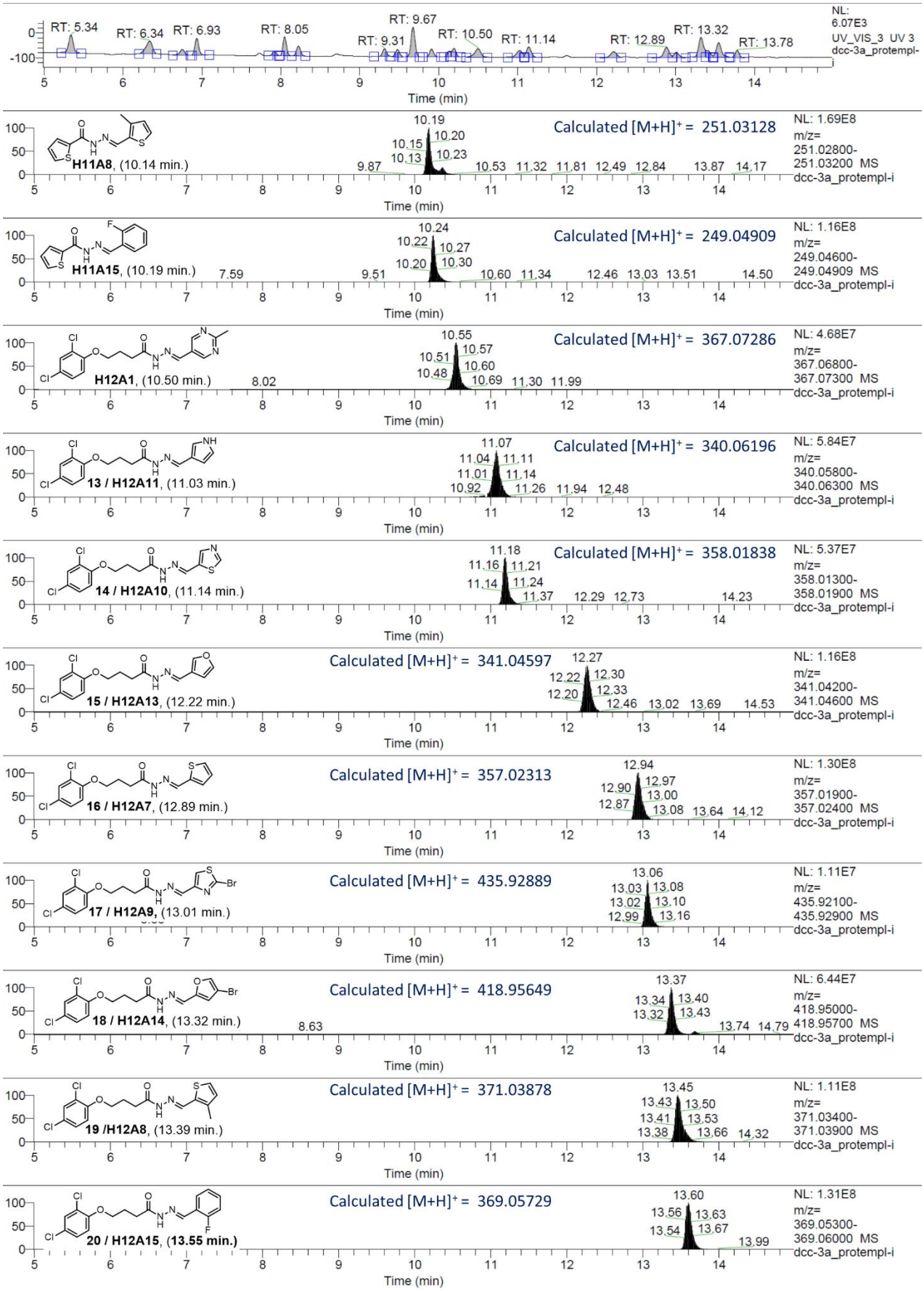

Supplementary Figure 14 e) Different acylhydrazones formed in DCC-3a, their retention times, and observed mass.

Results from DCC-3b:

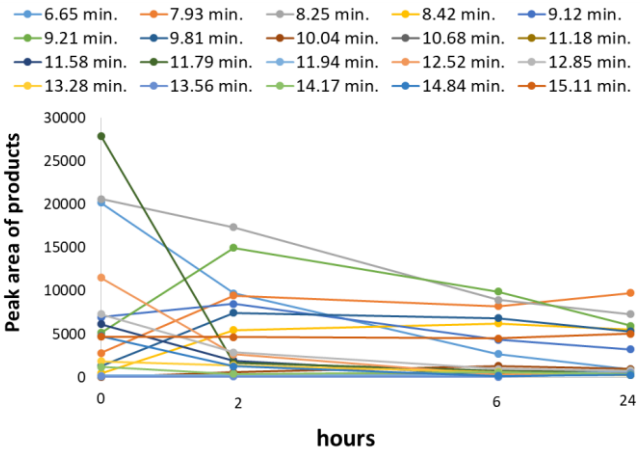

Supplementary Figure 15 Evaluation of the equilibrium state in a blank **DCL-3b** by comparing peak areas of products formed over time. Lines represent the formation of acylhydrazone products over time.

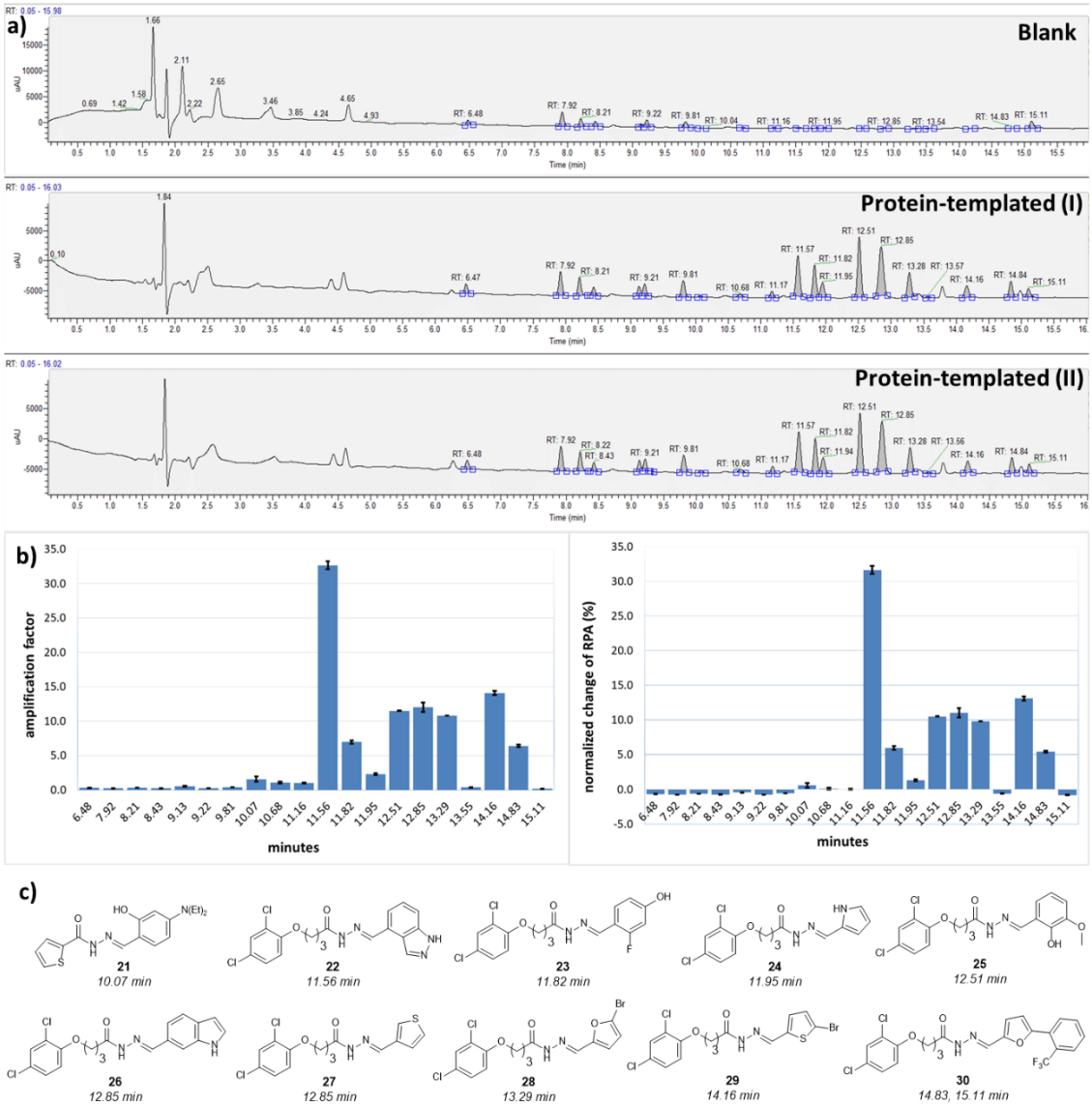

Supplementary Figure 16 a) Comparison between blank and protein-templated **DCC-3b** at 24 h, b) amplification factor and normalized change of RPA of products, c) amplified acylhydrazone products in protein-templated DCC.

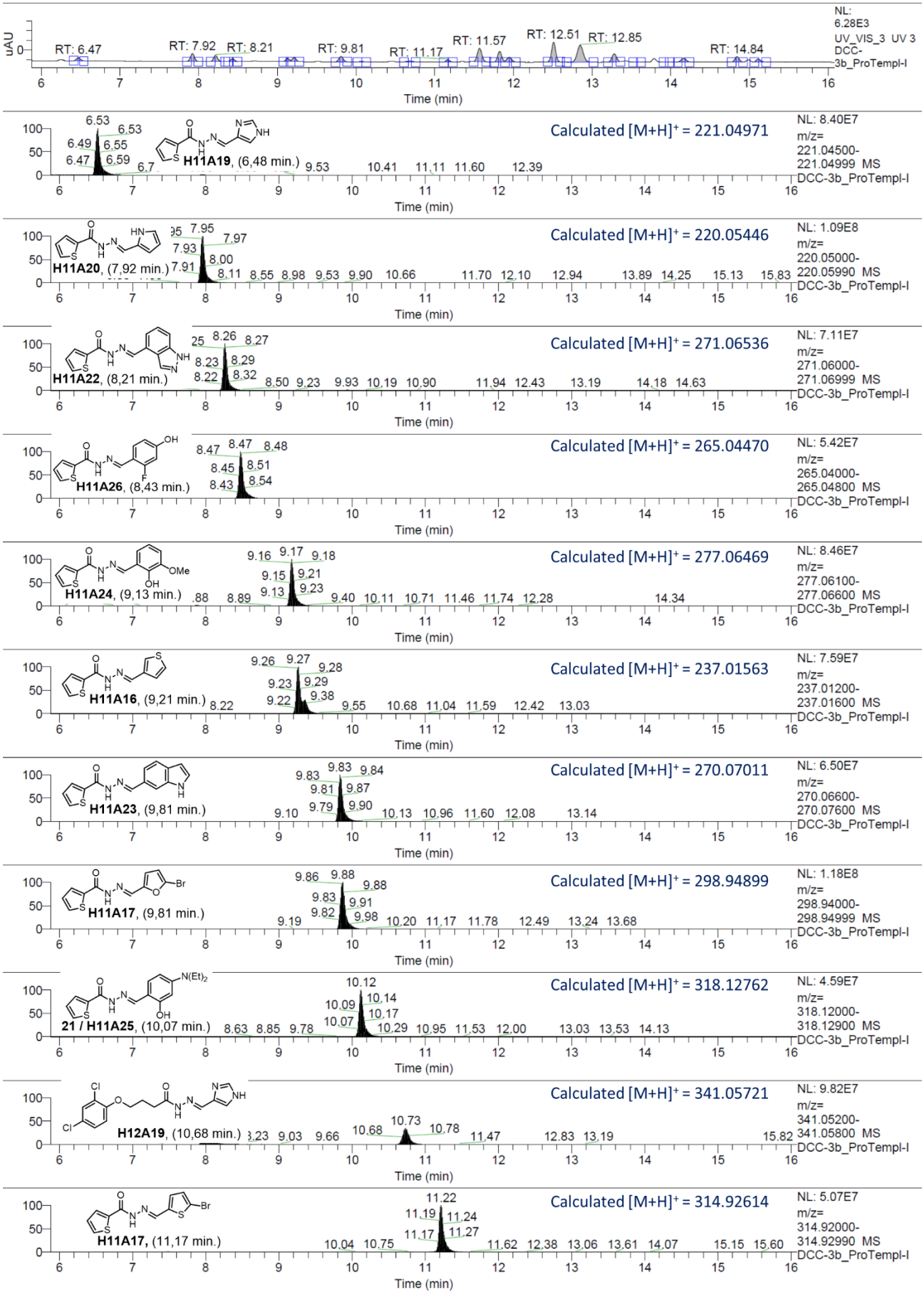

Supplementary Figure 16 d) Different acylhydrazones formed in DCC-3b, their retention times, and observed mass.

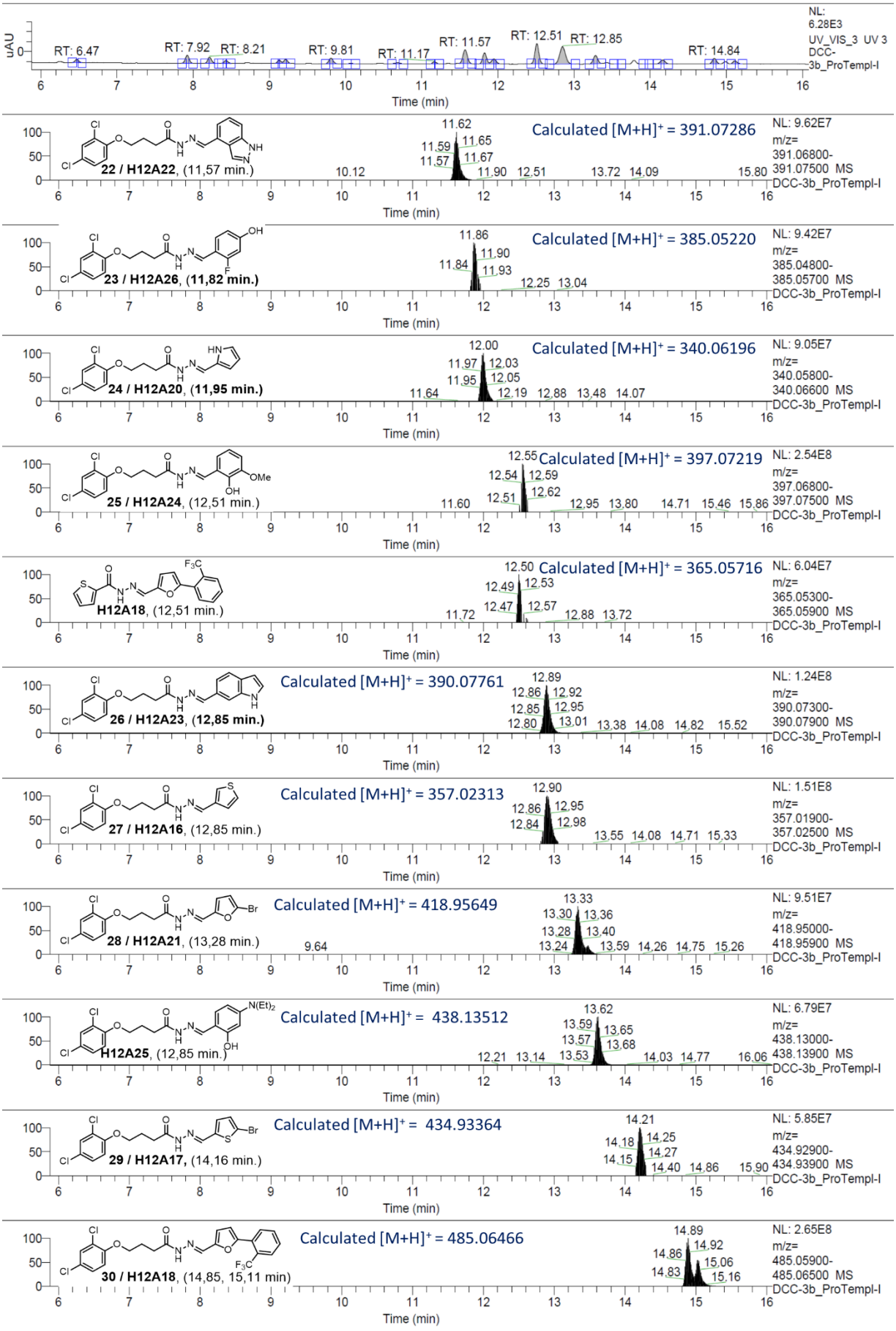

Supplementary Figure 16 e) Different acylhydrazones formed in DCC-3b, their retention times, and observed mass.

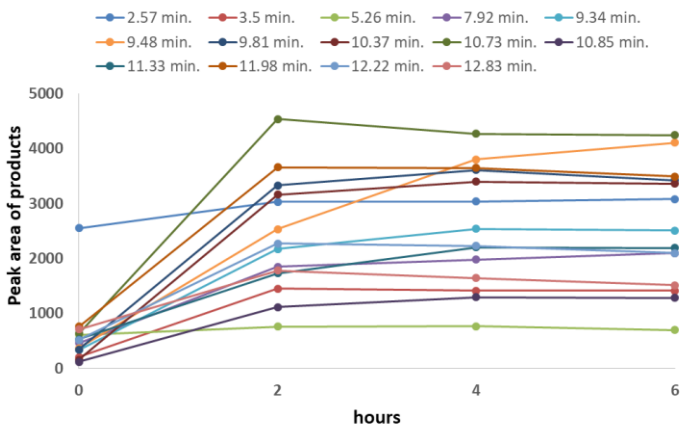

Supplementary Figure 17 Evaluation of the equilibrium state in a blank **DCL-4** by comparing peak areas of products formed over time. Lines represent the formation of acylhydrazone products over time.

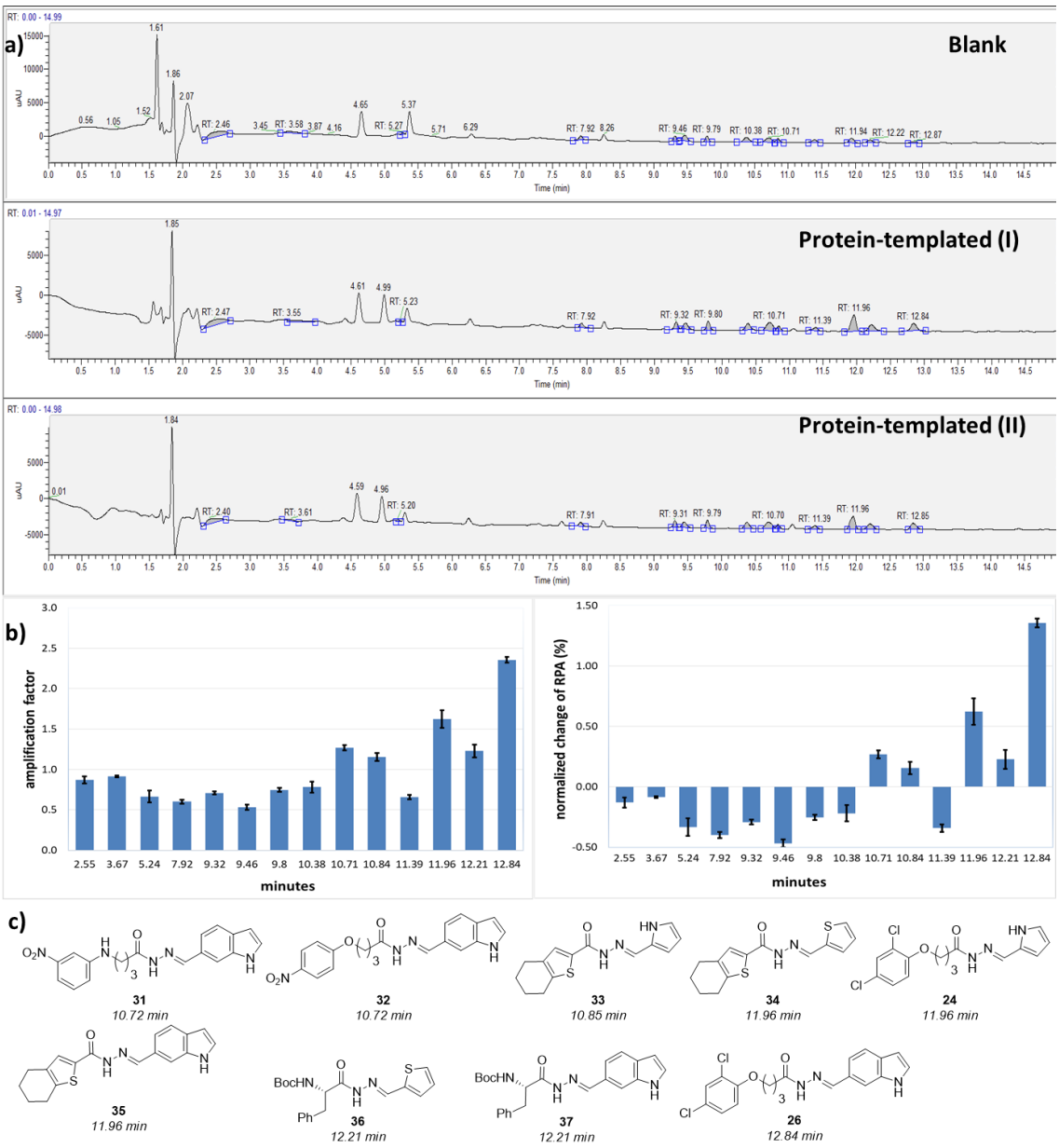

Supplementary Figure 18 a) Comparison between blank and protein-templated **DCC-4** at 6 h, b) amplified acylhydrazone products in protein-templated DCC.

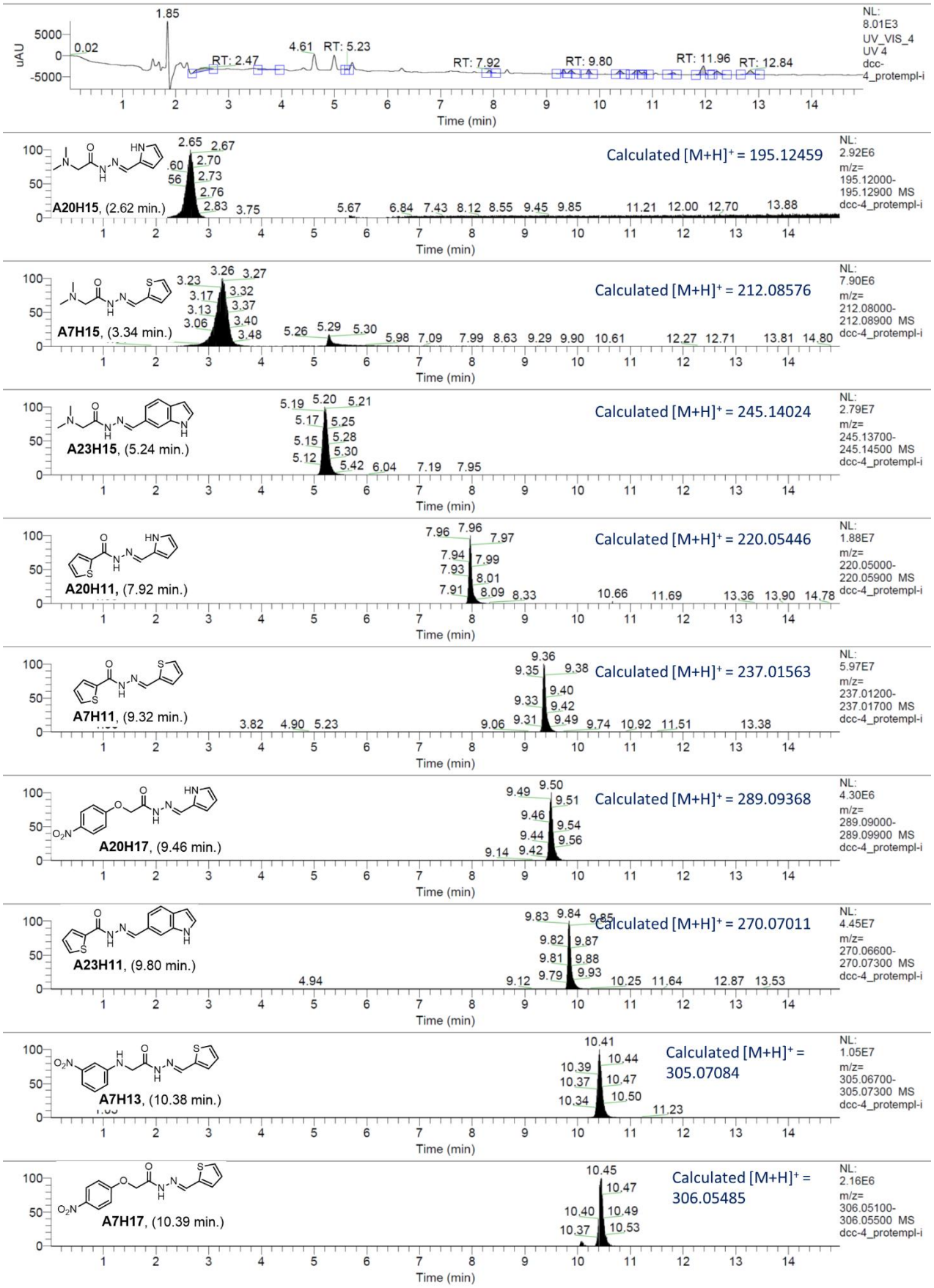

Supplementary Figure 18 e) Different acylhydrazones formed in DCC-3b, their retention times, and observed mass.

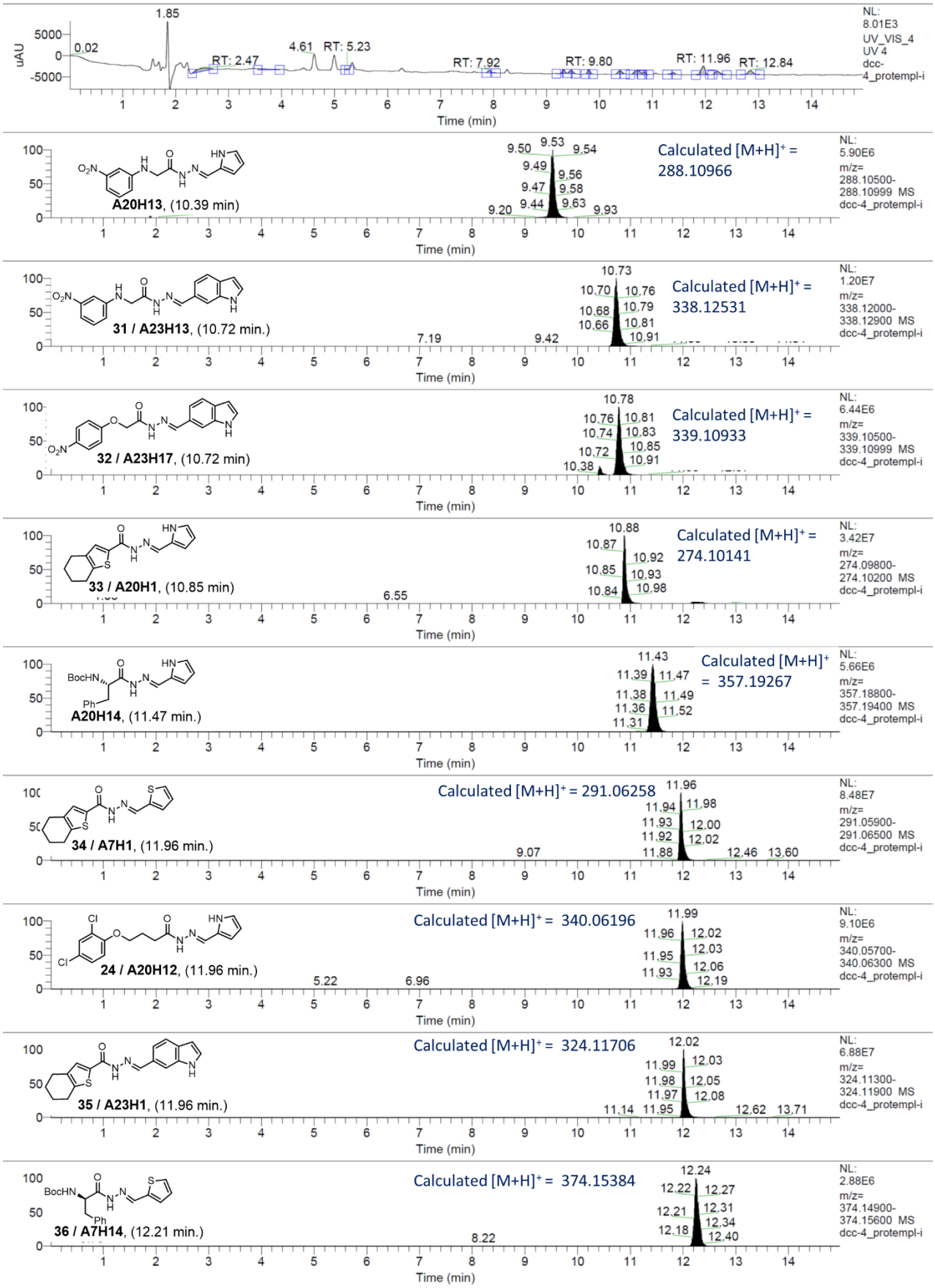

Supplementary Figure 18 f) Different acylhydrazones formed in DCC-3b, their retention times, and observed mass.

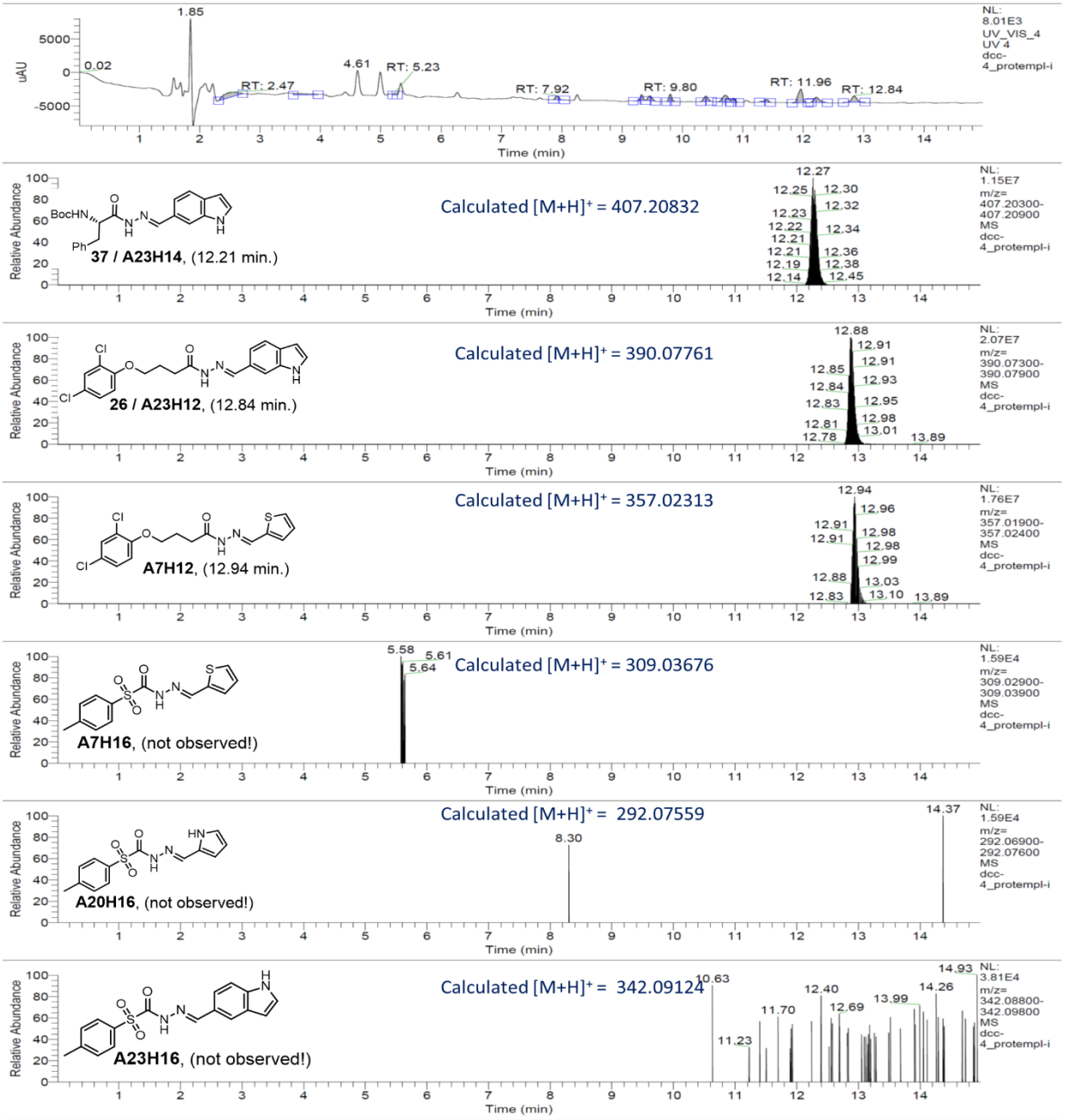

Supplementary Figure 18 g) Different acylhydrazones formed in DCC-3b, their retention times, and observed mass.

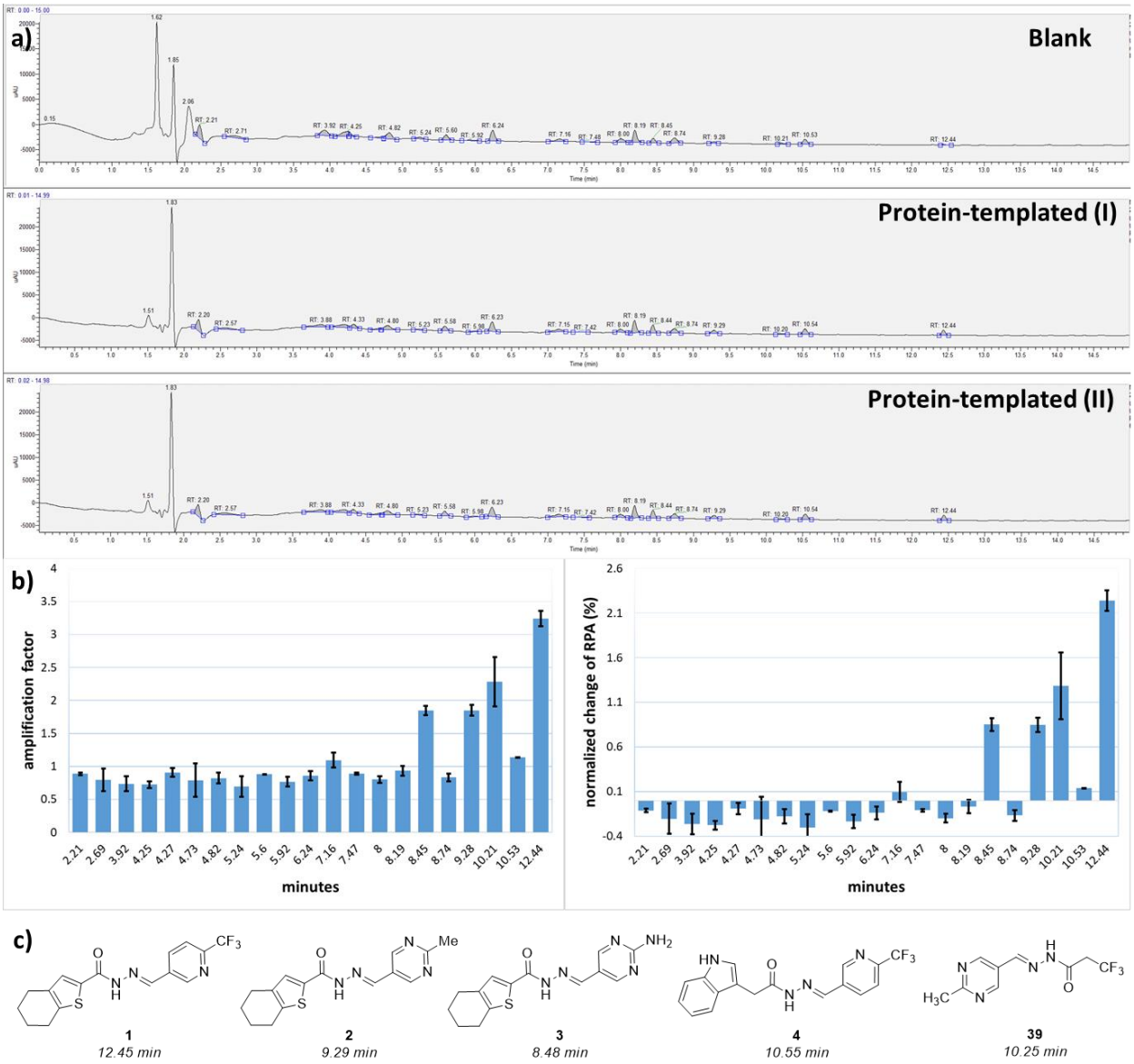

Supplementary Figure 19 a) Comparison between blank and protein-templated **DCC-5 (ThDP)** at 6 h, b) amplification factor and normalized change of RPA of products, c) amplified acylhydrazone products in protein-templated DCC.

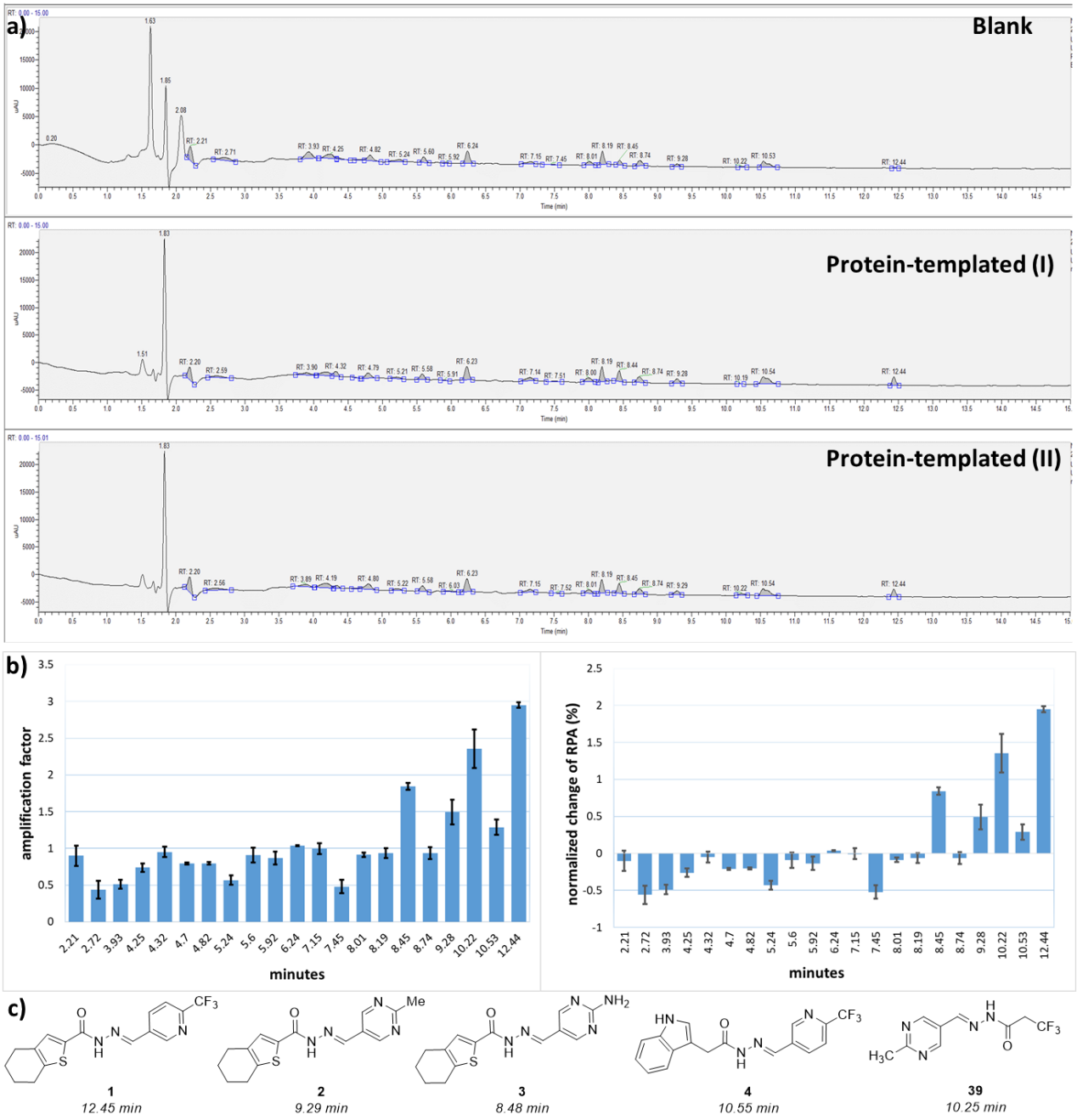

Supplementary Figure 20 a) Comparison between blank and protein-templated DCC-6 at 6 h, b) amplification factor and normalized change of RPA of products, c) amplified acylhydrazone products in protein-templated DCC.

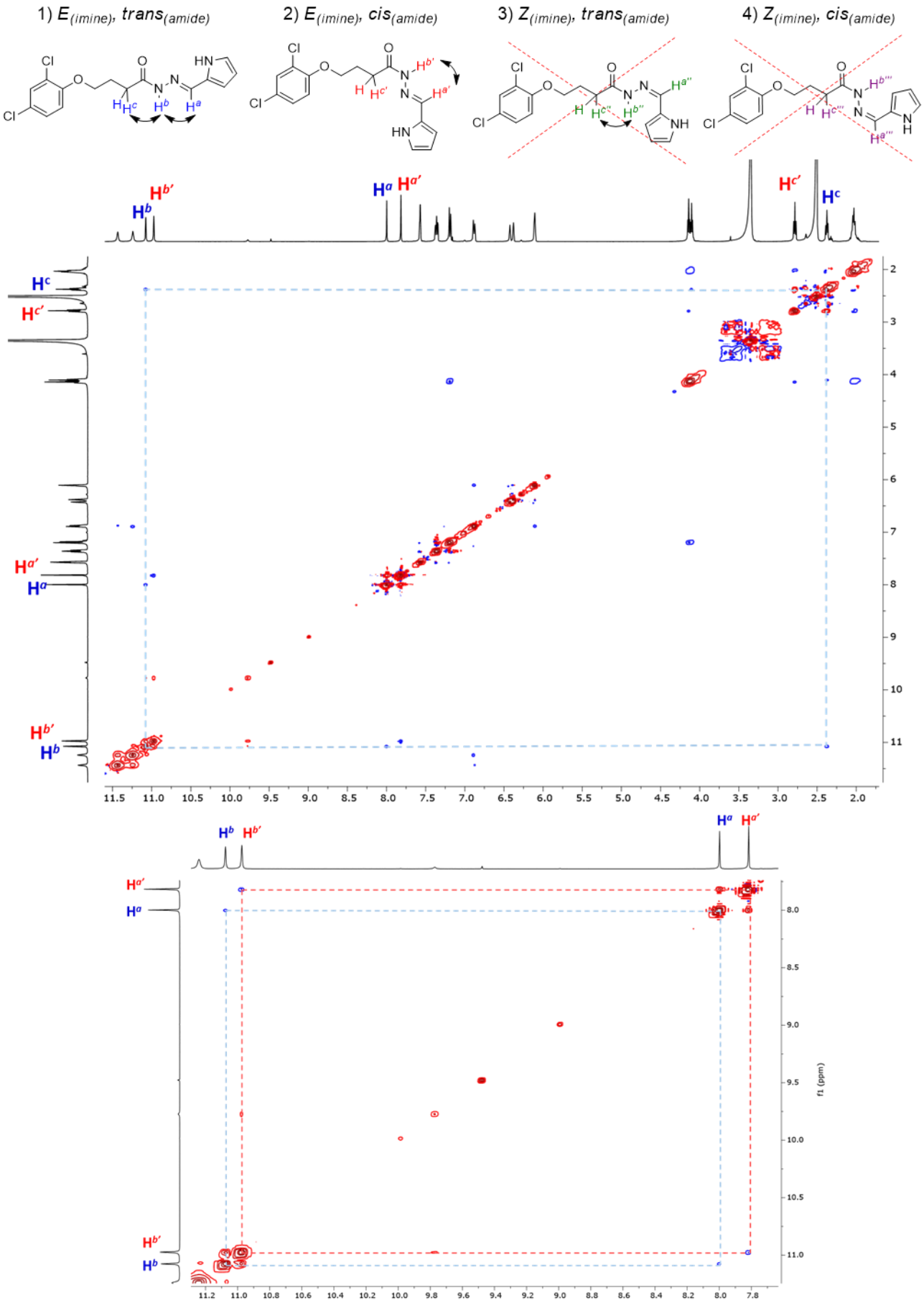

Supplementary Figure 21 NOESY NMR spectra of compound **24**.

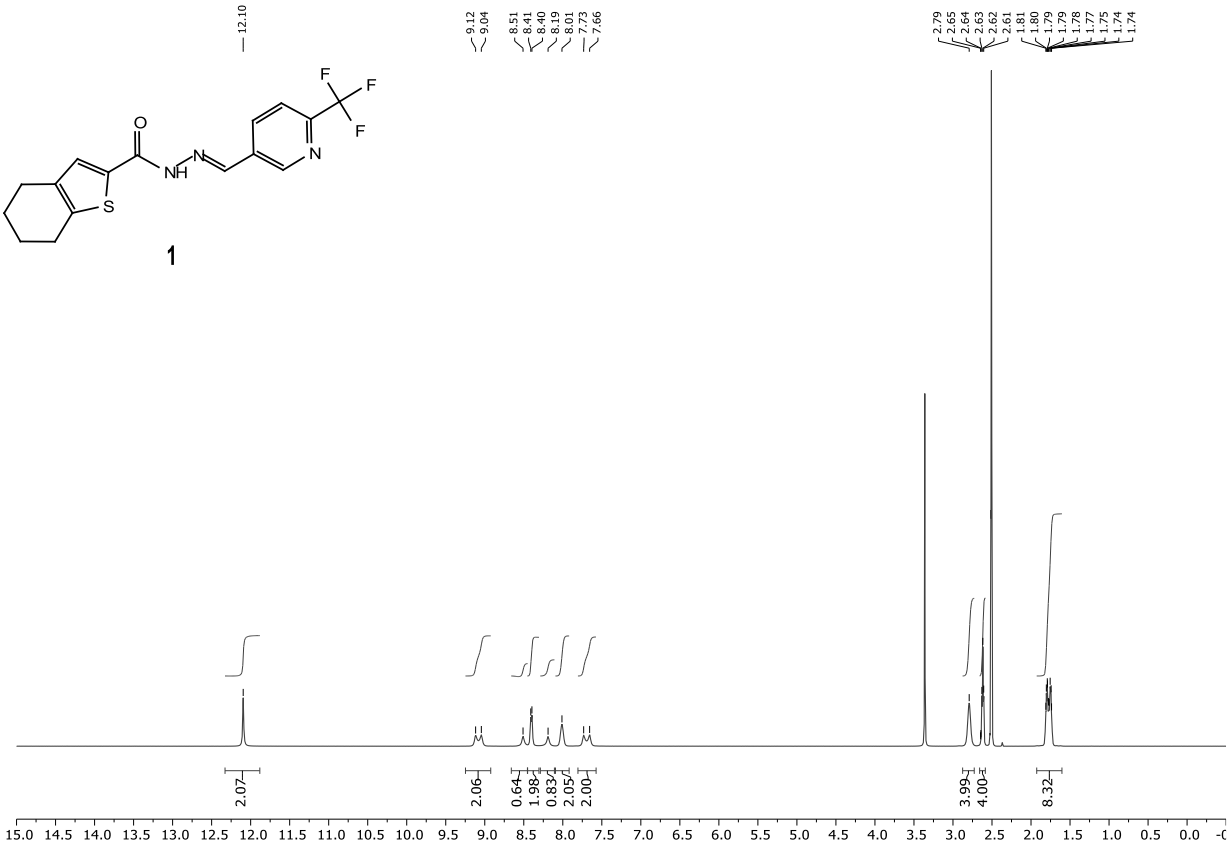

Supplementary Figure 22 ^{1}H NMR spectrum of **1.**

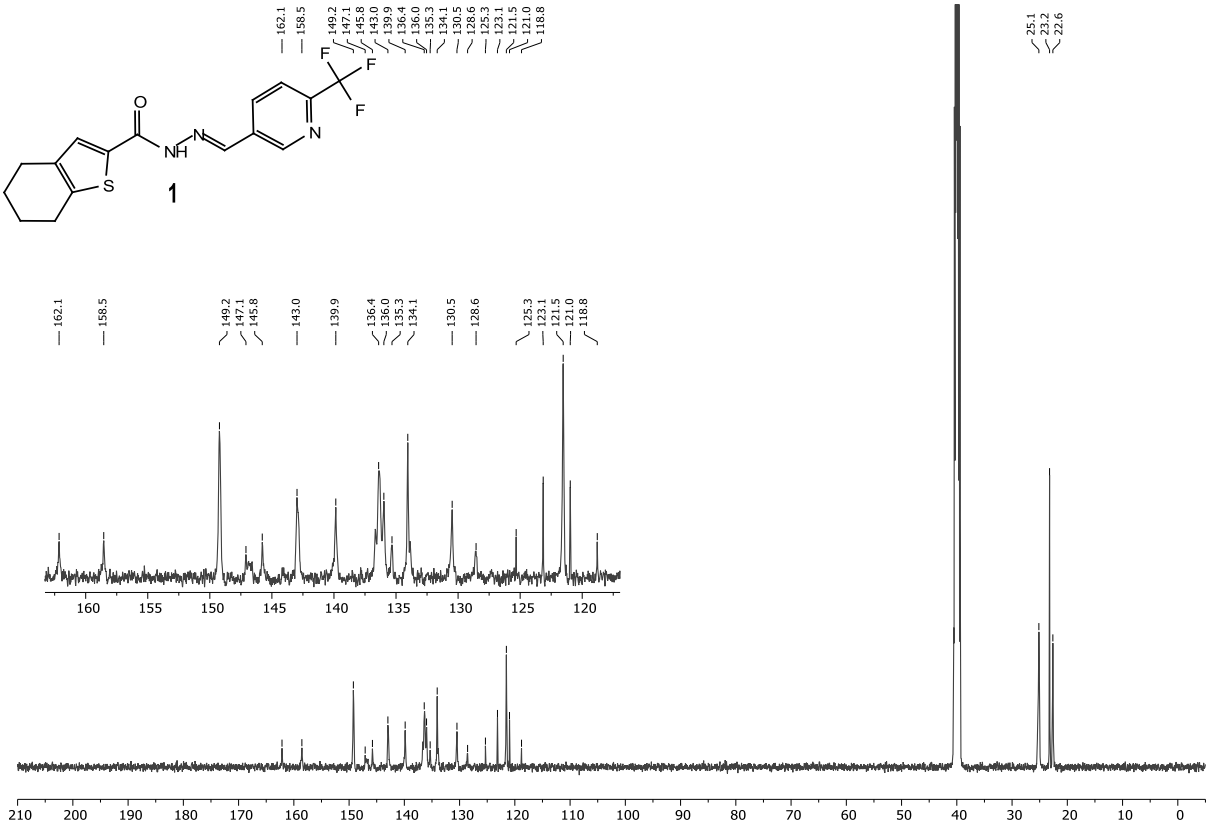

Supplementary Figure 23 ^{13}C NMR spectrum of **1.**

Supplementary Figure 24 ^{19}F NMR spectrum of **1.**

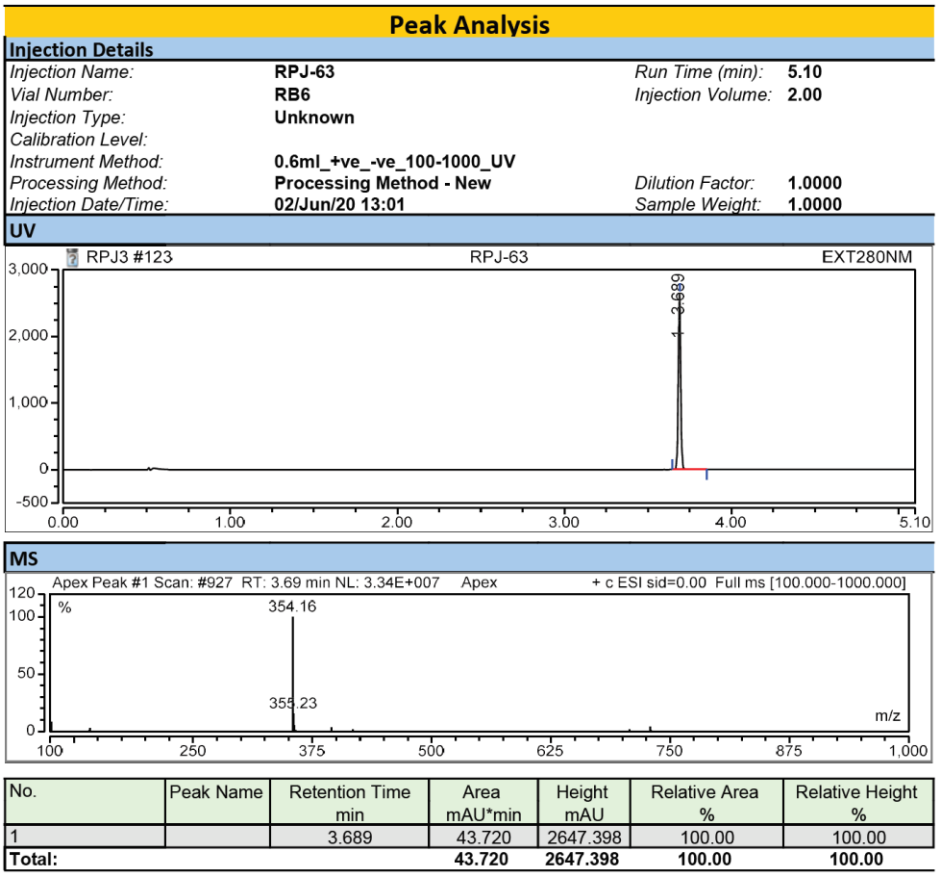

No.	Peak Name	Retention Time min	Area mAU*min	Height mAU	Relative Area %	Relative Height %
1		3.689	43.720	2647.398	100.00	100.00
Total:			**43.720**	**2647.398**	**100.00**	**100.00**

Supplementary Figure 25 HPLC purity analysis of **1.**

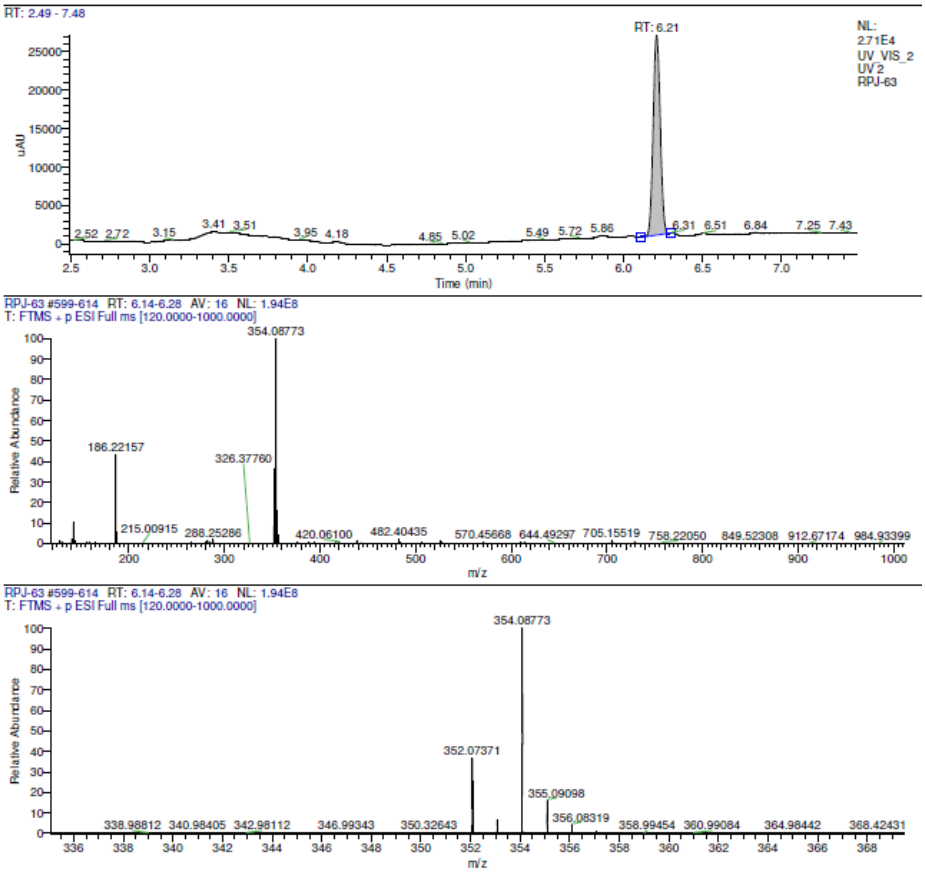

Supplementary Figure 26 HRMS of **1.**

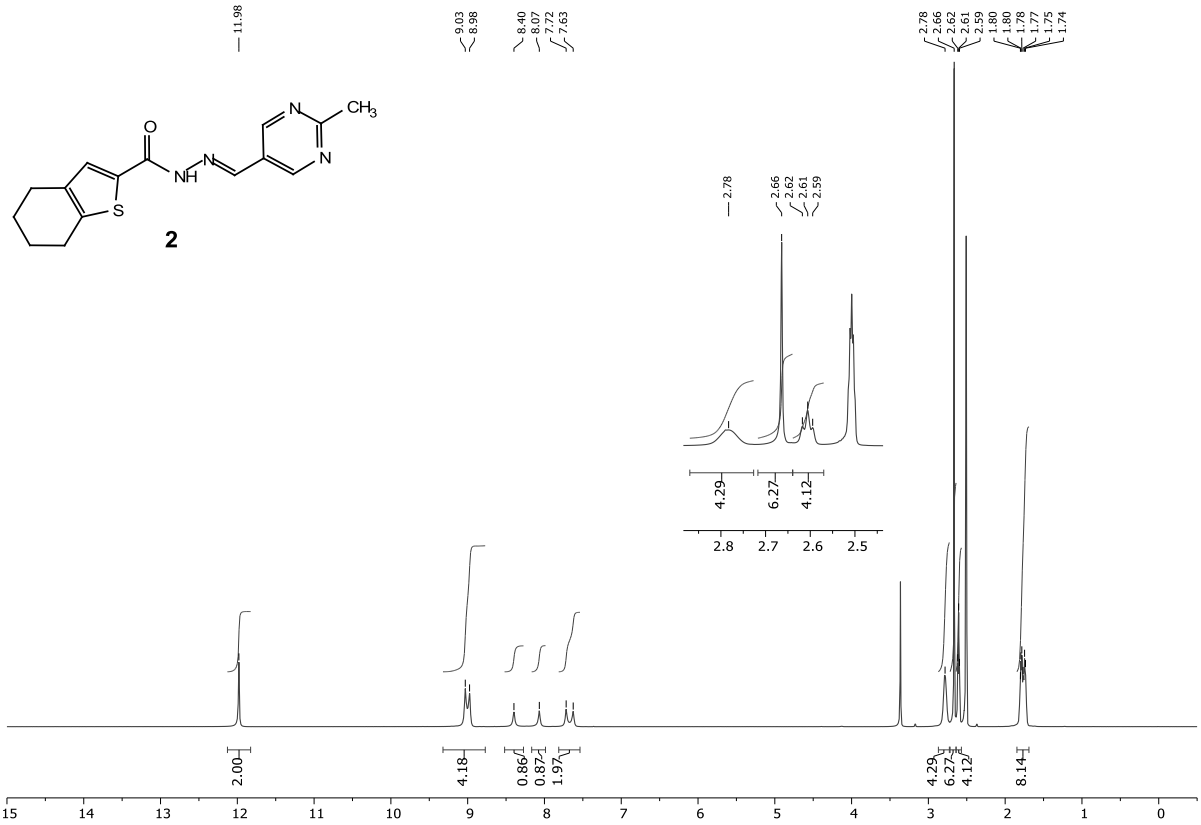

Supplementary Figure 27 ^{1}H NMR spectrum of **2.**

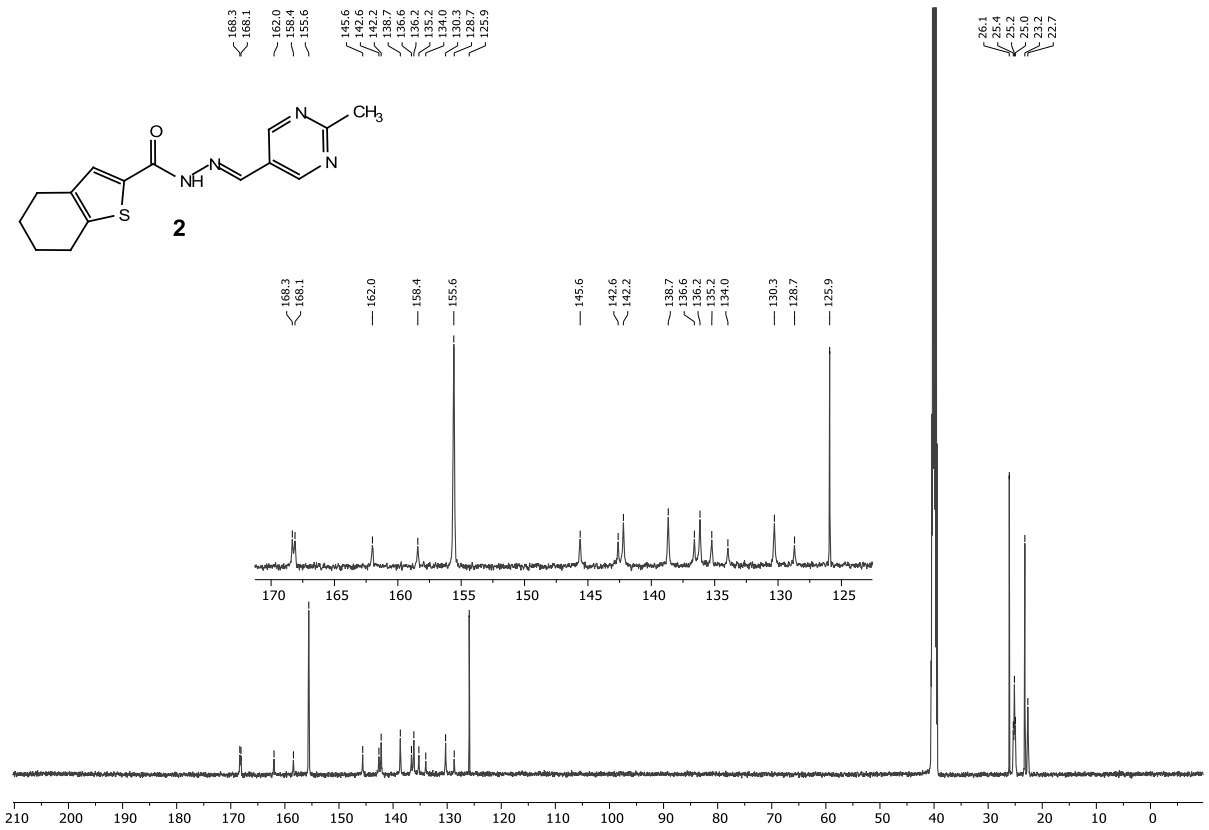

Supplementary Figure 28 ^{13}C NMR spectrum of **2.**

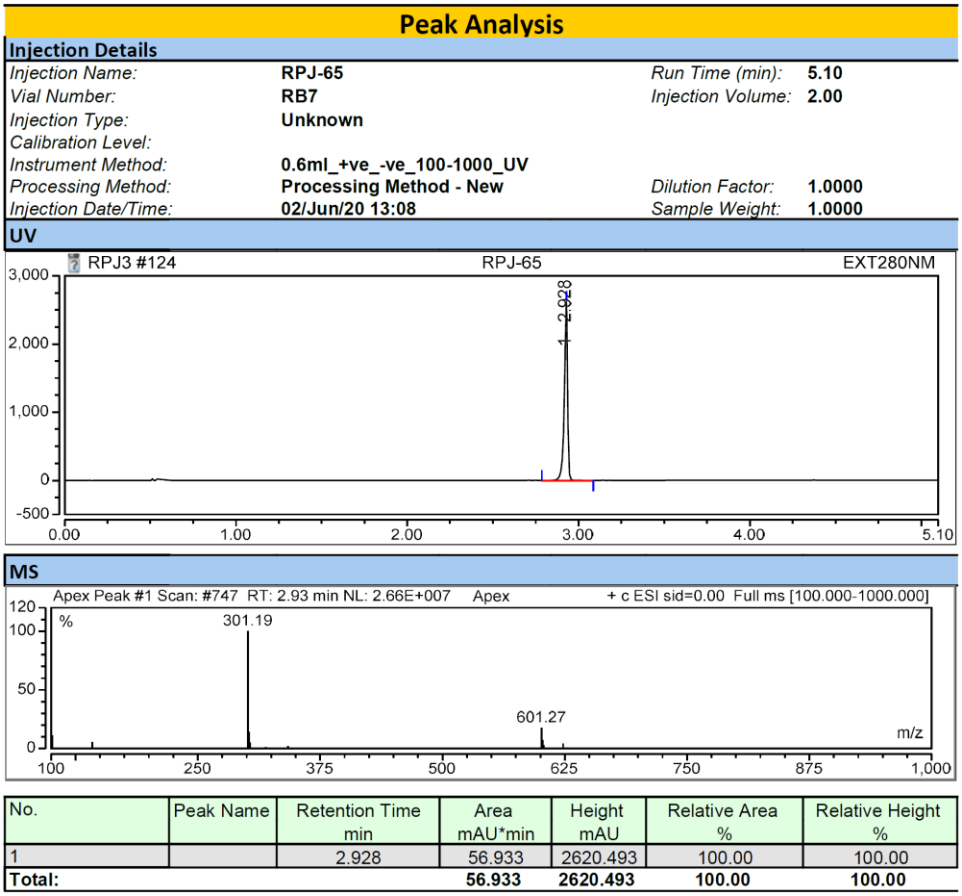

No.	Peak Name	Retention Time min	Area mAU*min	Height mAU	Relative Area %	Relative Height %
1		2.928	56.933	2620.493	100.00	100.00
Total:			**56.933**	**2620.493**	**100.00**	**100.00**

Supplementary Figure 29 HPLC purity analysis of **2.**

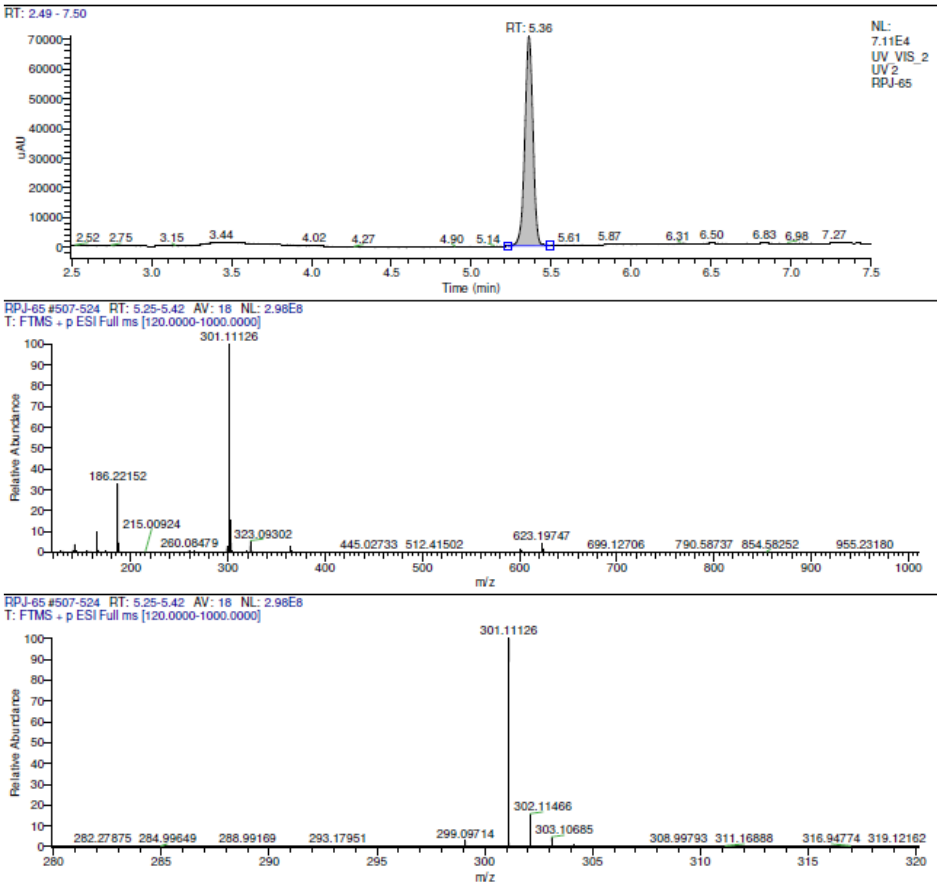

Supplementary Figure 30 HRMS of **2.**

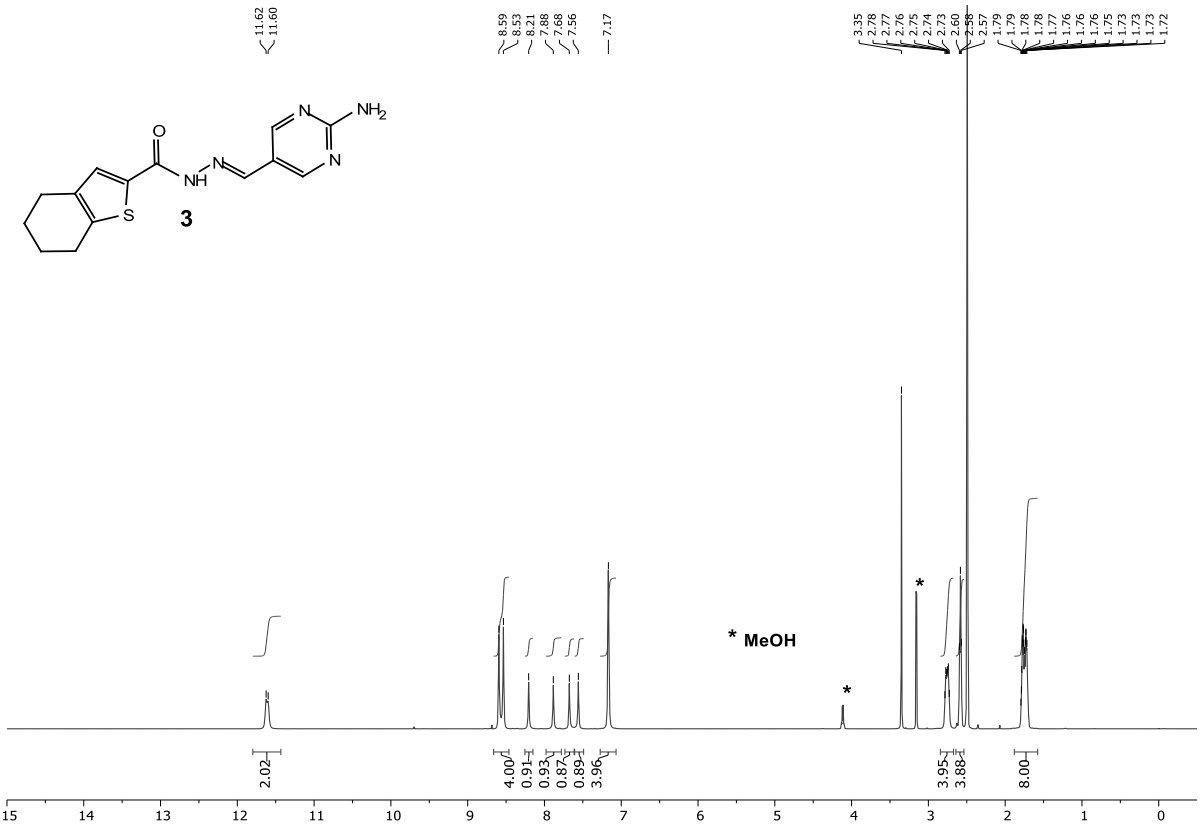

Supplementary Figure 31 ^{1}H NMR spectrum of **3.**

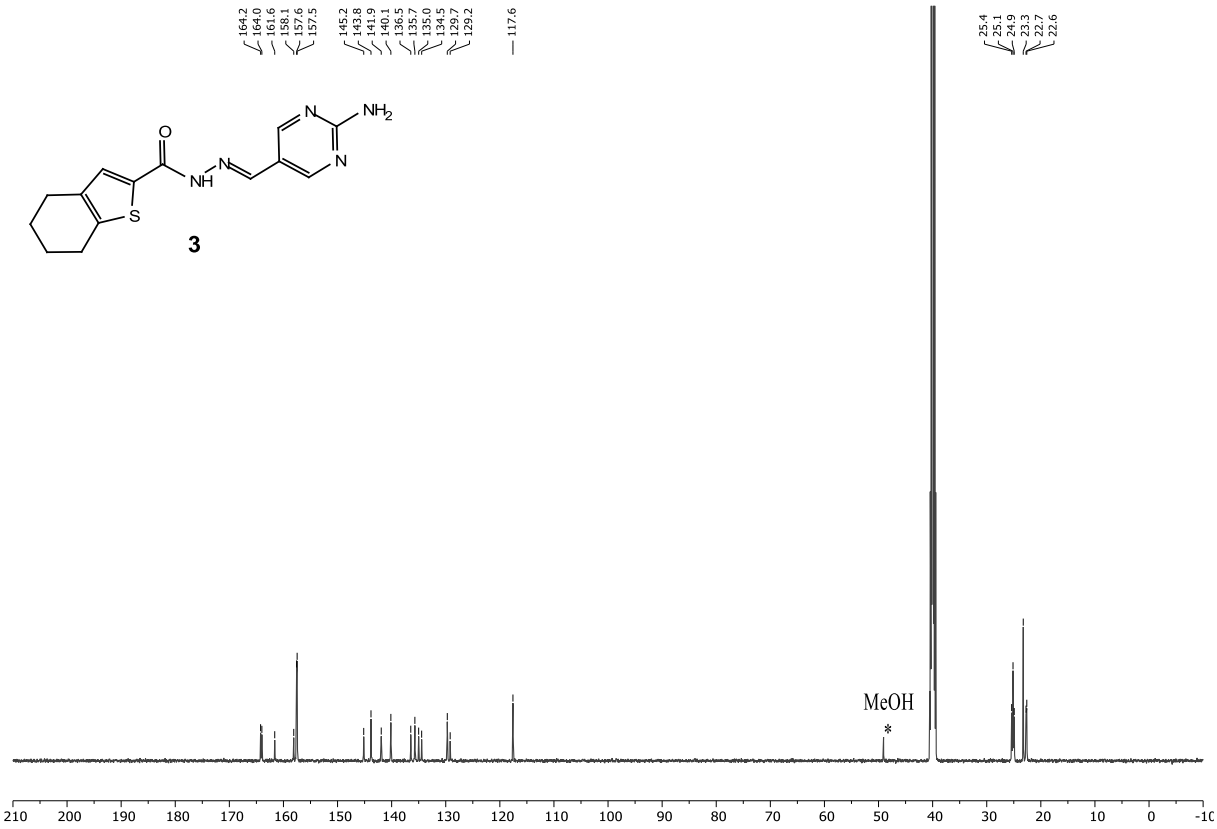

Supplementary Figure 32 ^{13}C NMR spectrum of **3.**

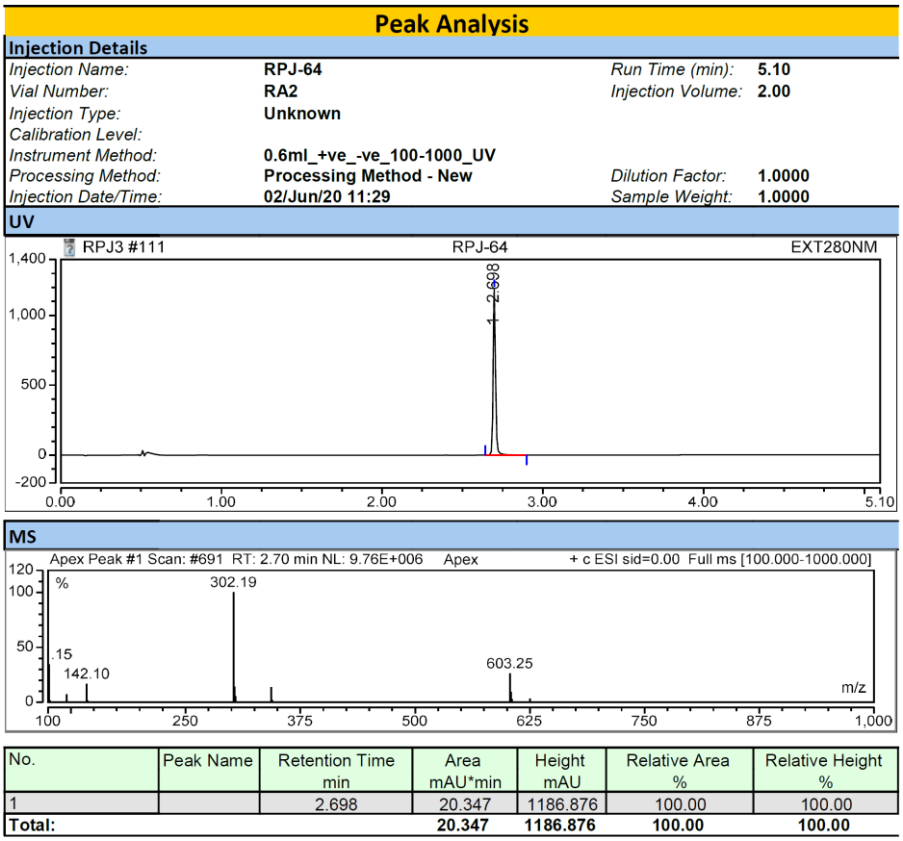

No.	Peak Name	Retention Time min	Area mAU*min	Height mAU	Relative Area %	Relative Height %
1		2.698	20.347	1186.876	100.00	100.00
Total:			**20.347**	**1186.876**	**100.00**	**100.00**

Supplementary Figure 33 HPLC purity analysis of **3.**

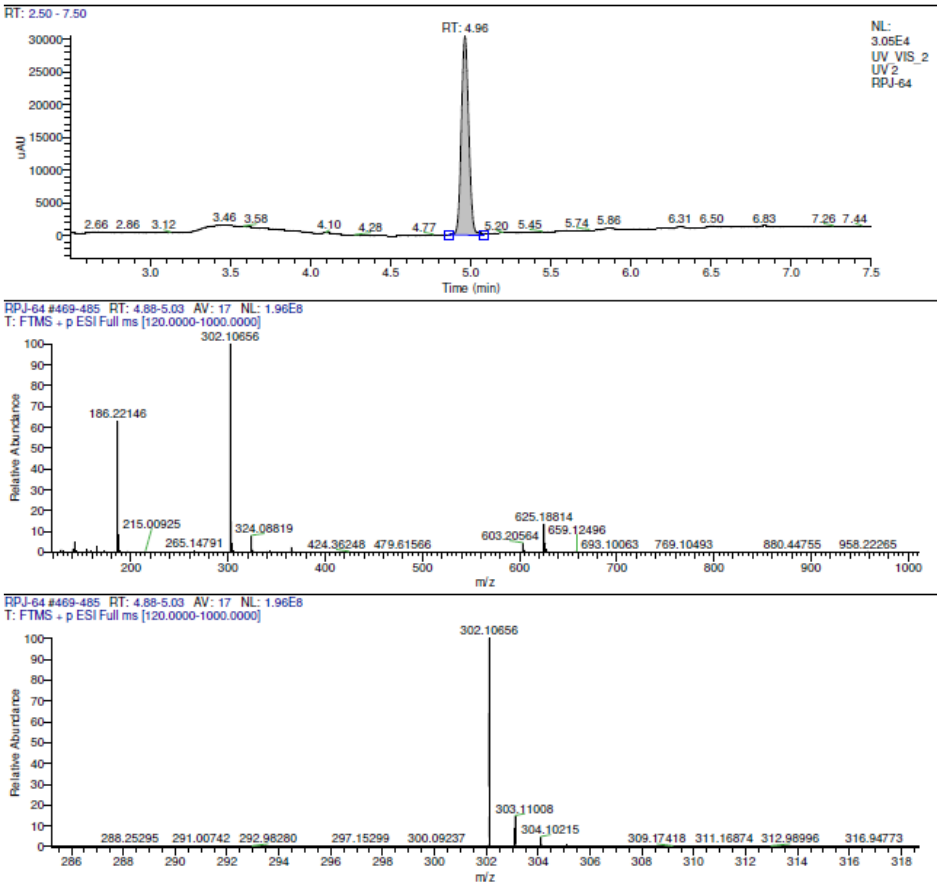

Supplementary Figure 34 HRMS of **3.**

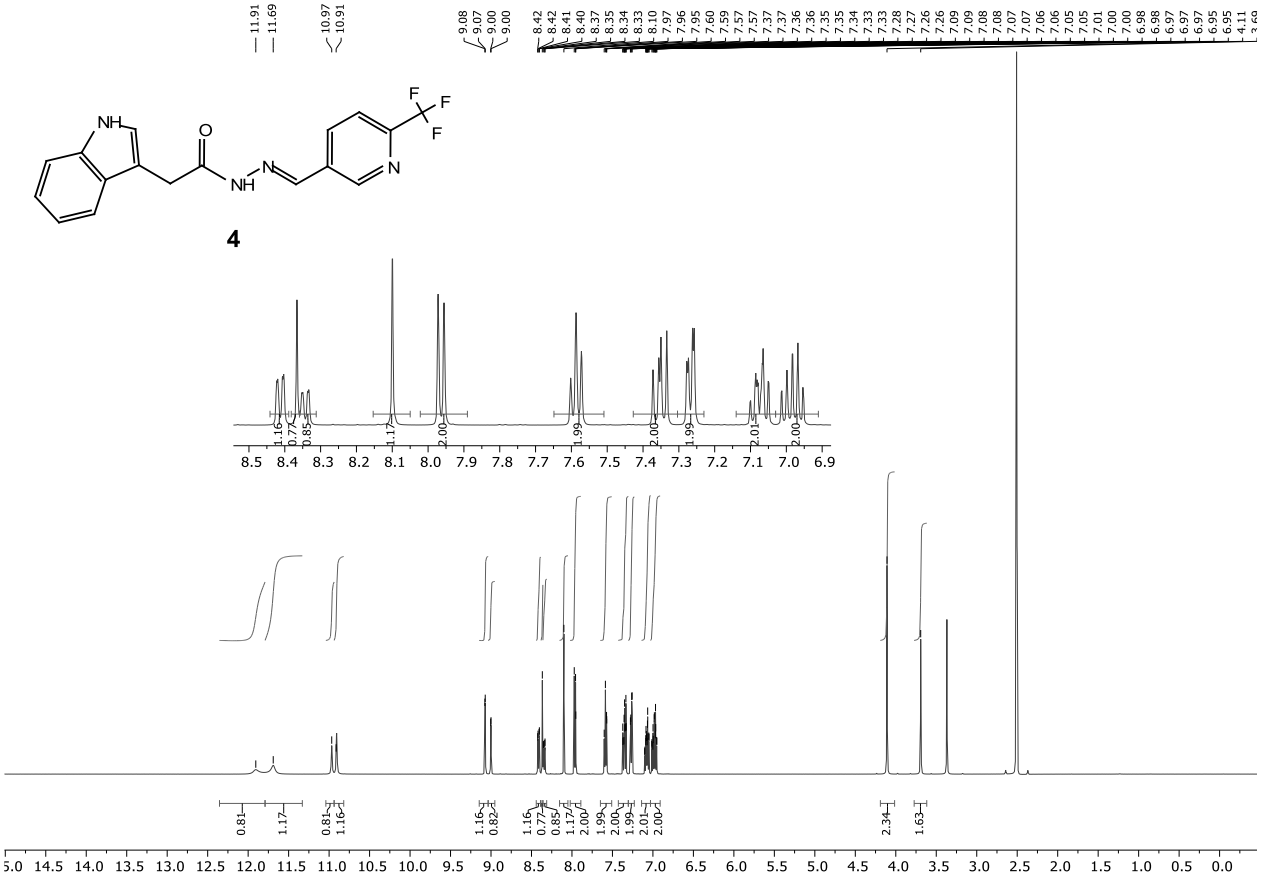

Supplementary Figure 35 ^{1}H NMR spectrum of **4.**

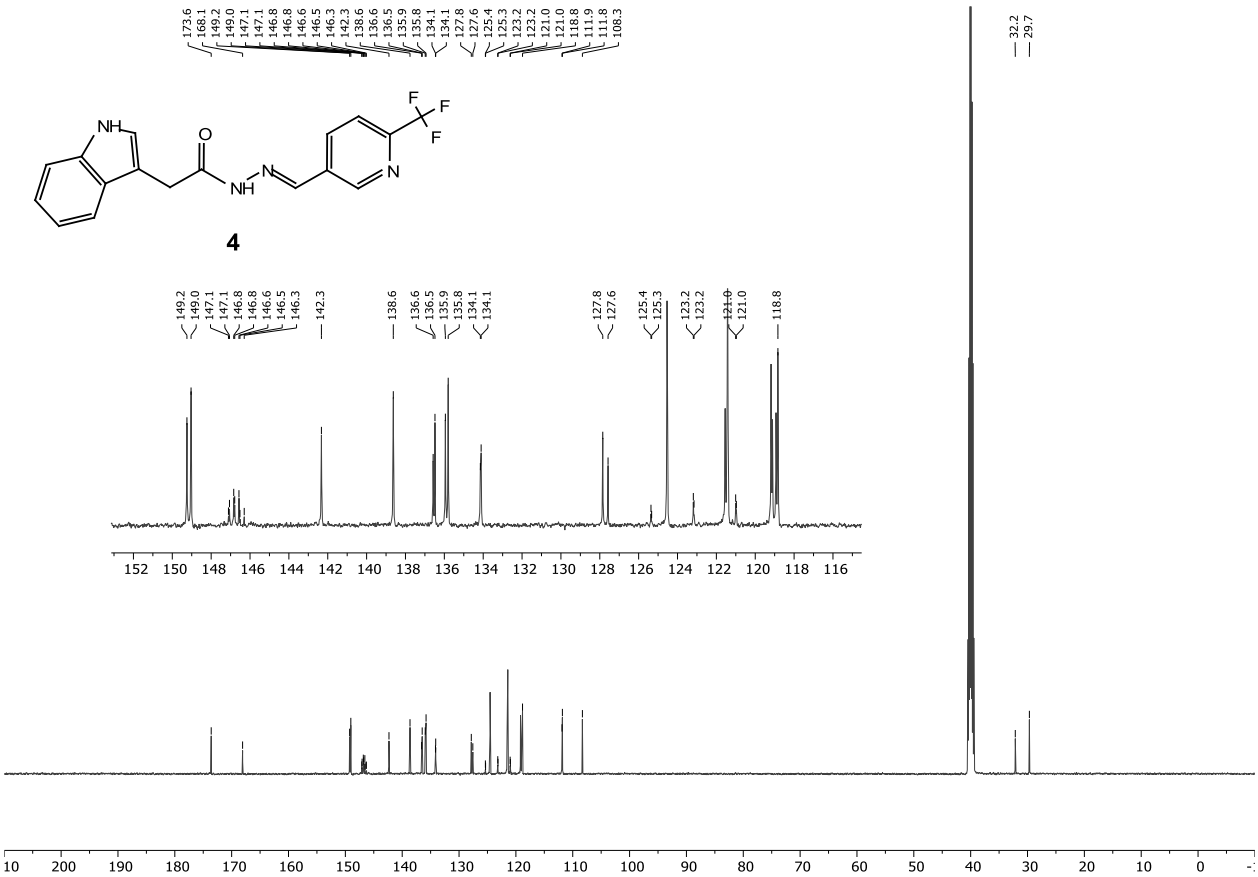

Supplementary Figure 36 ^{13}C NMR spectrum of **4.**

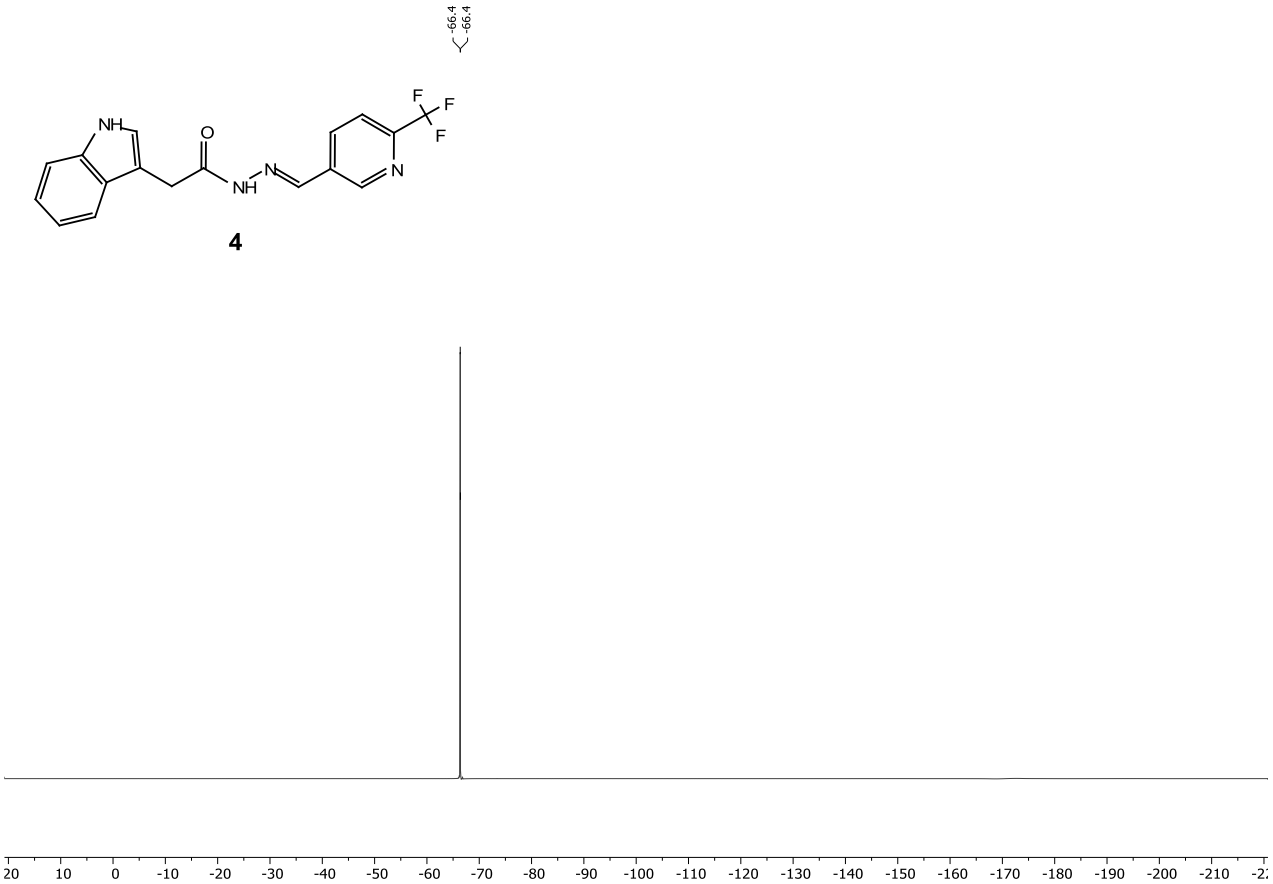

Supplementary Figure 37 ^{19}F NMR spectrum of **4.**

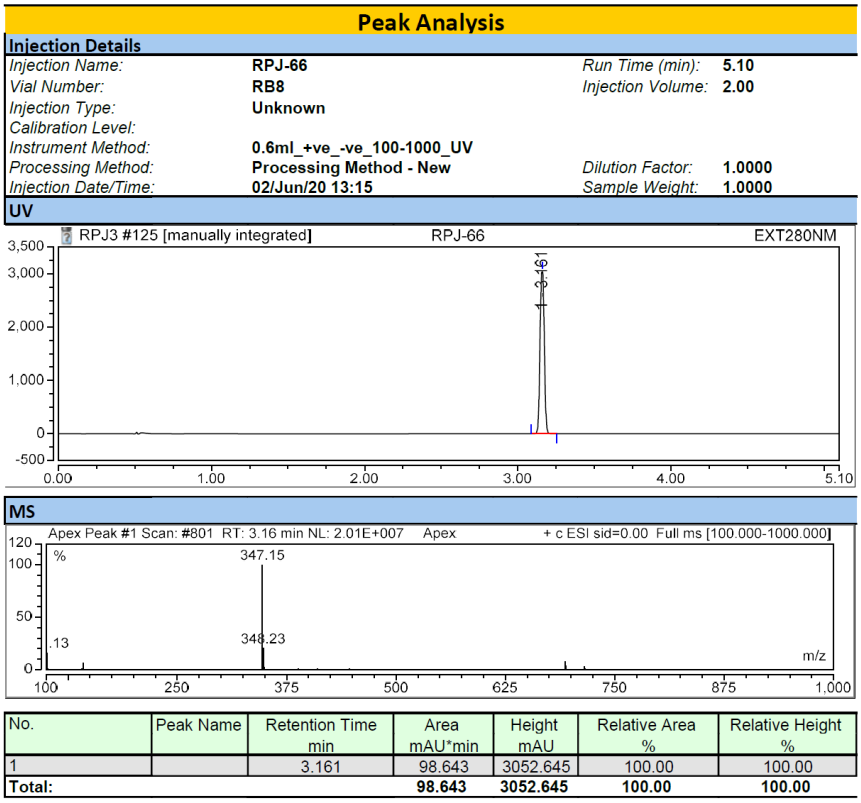

No.	Peak Name	Retention Time min	Area mAU*min	Height mAU	Relative Area %	Relative Height %
1		3.161	98.643	3052.645	100.00	100.00
Total:			**98.643**	**3052.645**	**100.00**	**100.00**

Supplementary Figure 38 HPLC purity analysis of **4.**

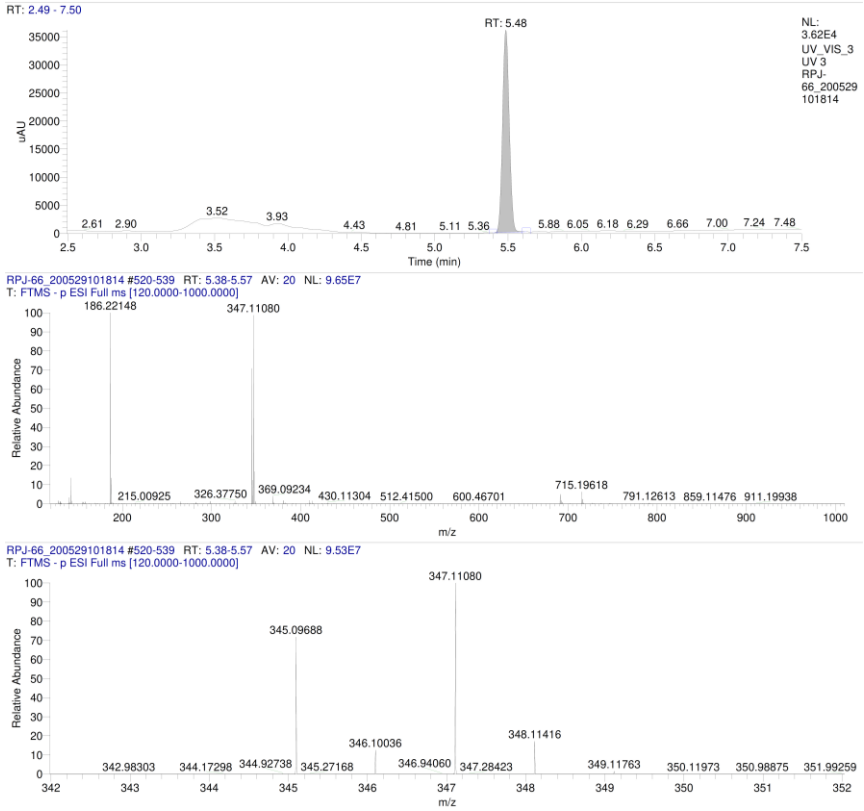

Supplementary Figure 39 HRMS of **4.**

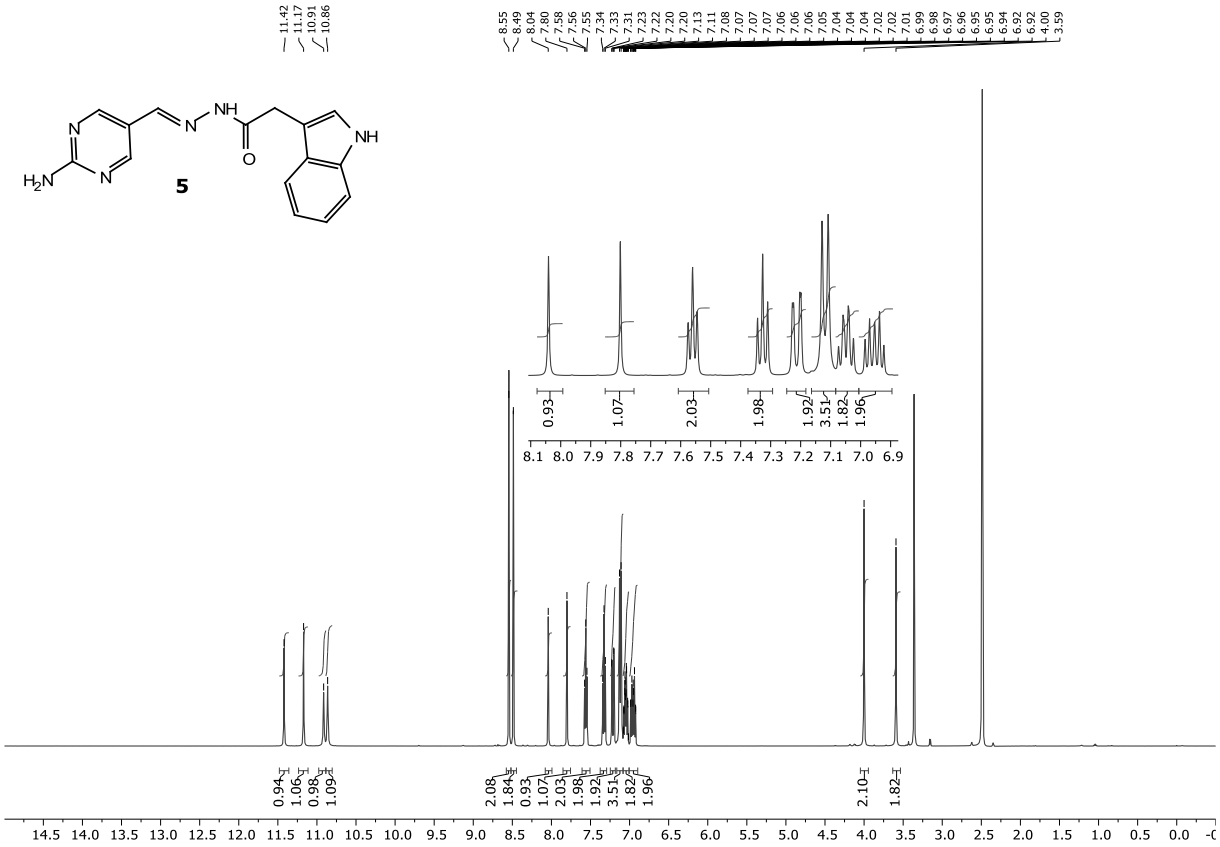

Supplementary Figure 40 ^{1}H NMR spectrum of **5.**

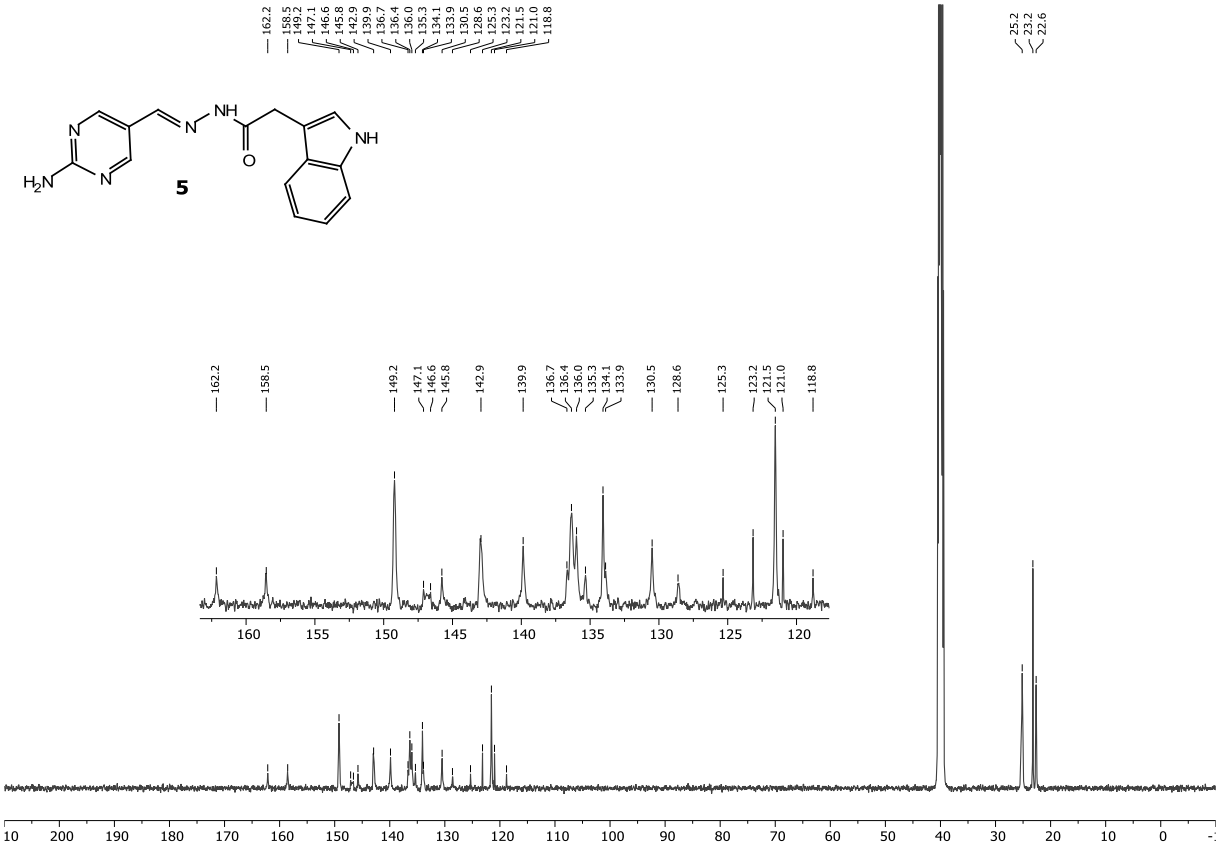

Supplementary Figure 41 ^{13}C NMR spectrum of **5.**

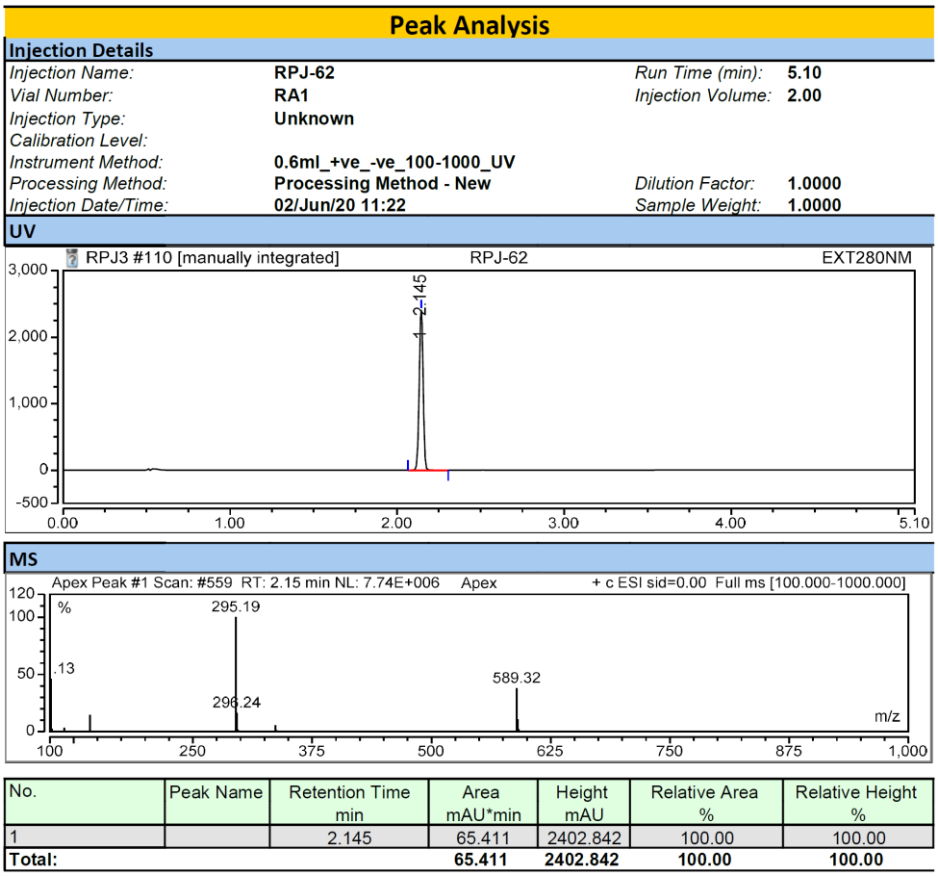

No.	Peak Name	Retention Time min	Area mAU*min	Height mAU	Relative Area %	Relative Height %
1		2.145	65.411	2402.842	100.00	100.00
Total:			**65.411**	**2402.842**	**100.00**	**100.00**

Supplementary Figure 42 HPLC purity analysis of **5.**

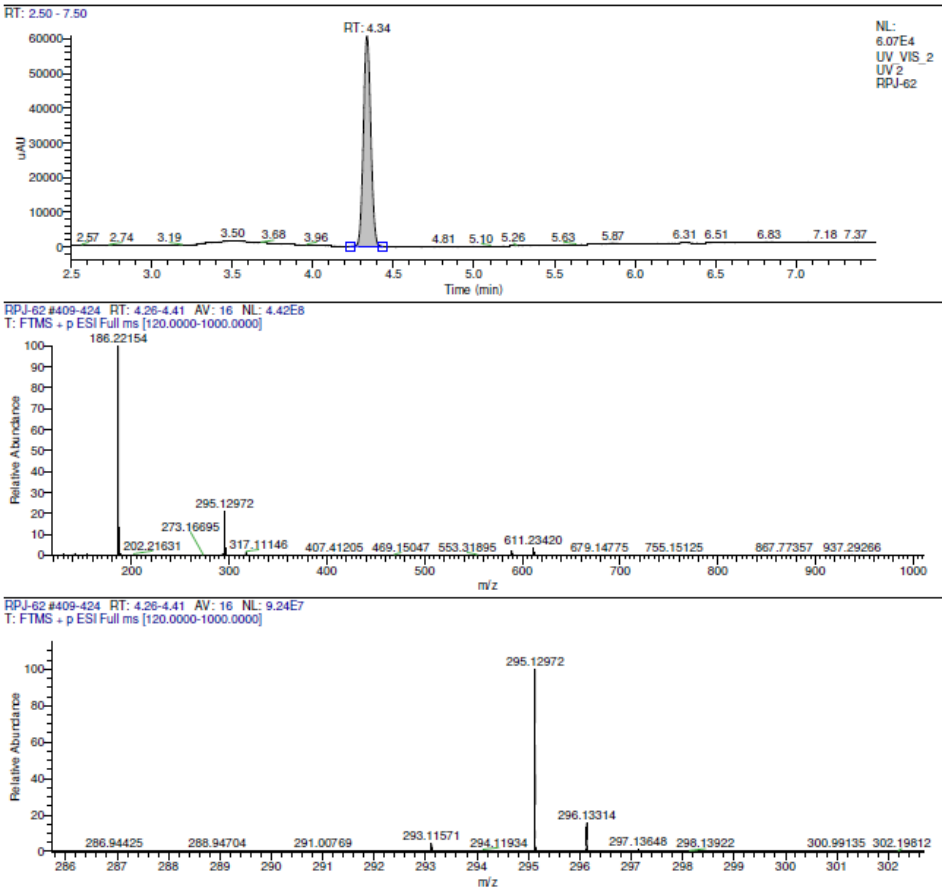

Supplementary Figure 43 HRMS of **5.**

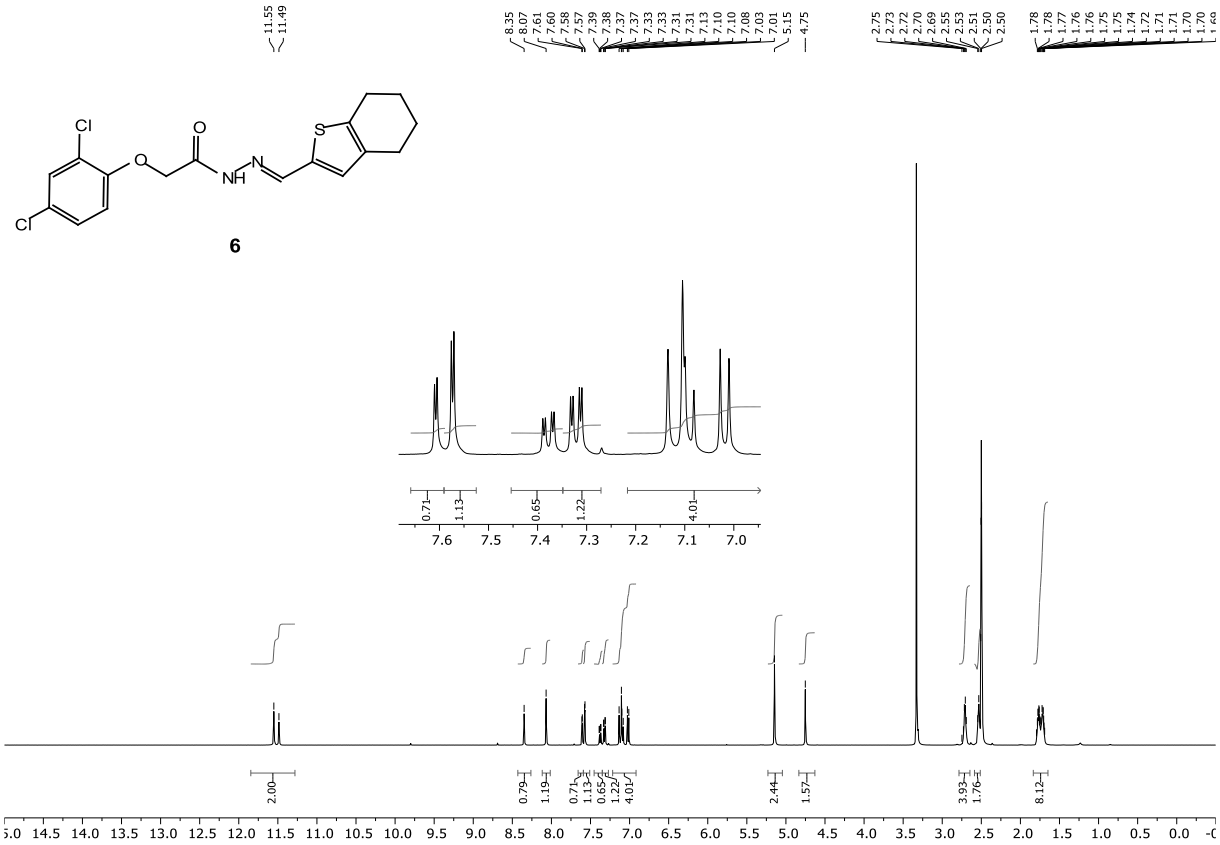

Supplementary Figure 44 ^{1}H NMR spectrum of **6.**

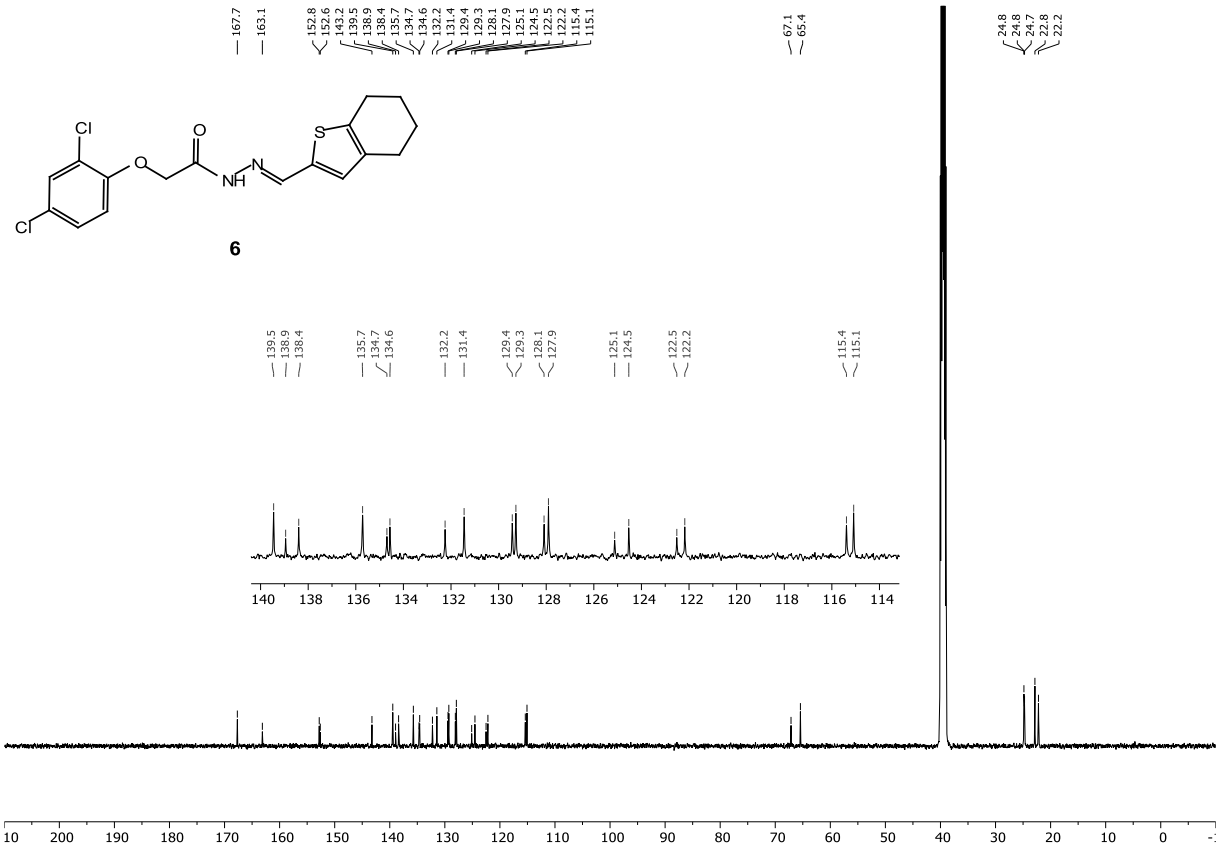

Supplementary Figure 45 ^{13}C NMR spectrum of **6.**

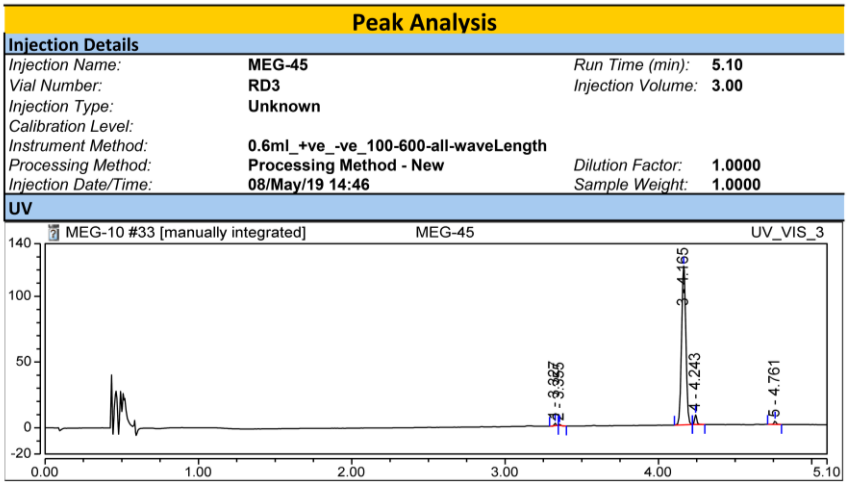

No.	Peak Name	Retention Time min	Area mAU*min	Height mAU	Relative Area %	Relative Height %
1		3.327	0.020	1.938	0.50	1.45
2		3.355	0.008	0.878	0.19	0.66
3		4.165	3.882	120.809	95.49	90.44
4		4.243	0.115	7.303	2.83	5.47
5		4.761	0.040	2.654	0.99	1.99
Total:			**4.066**	**133.583**	**100.00**	**100.00**

Supplementary Figure 46 HPLC purity analysis of **6.**

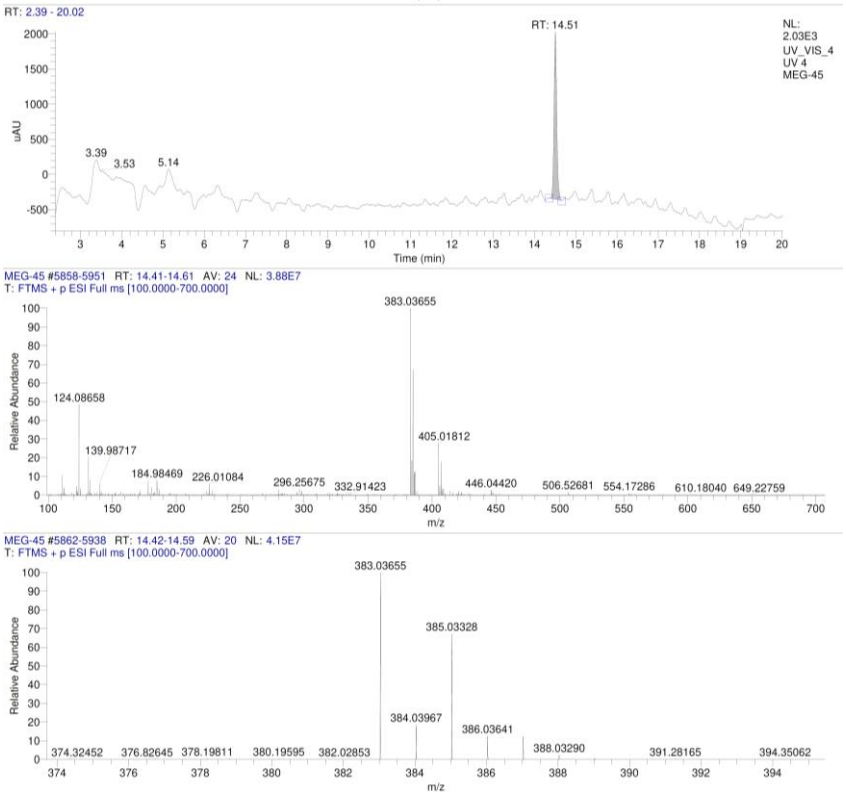

Supplementary Figure 47 HRMS of **6.**

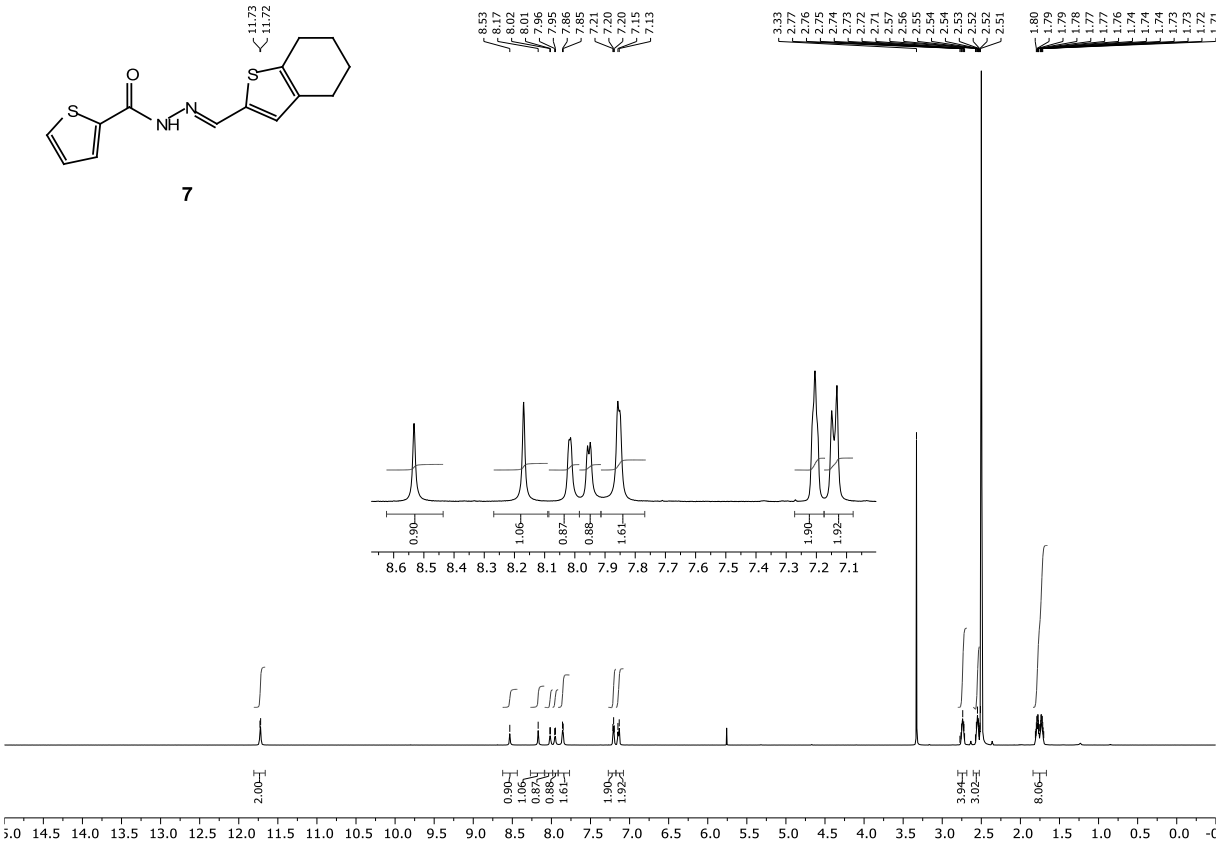

Supplementary Figure 48 ^{1}H NMR spectrum of **7.**

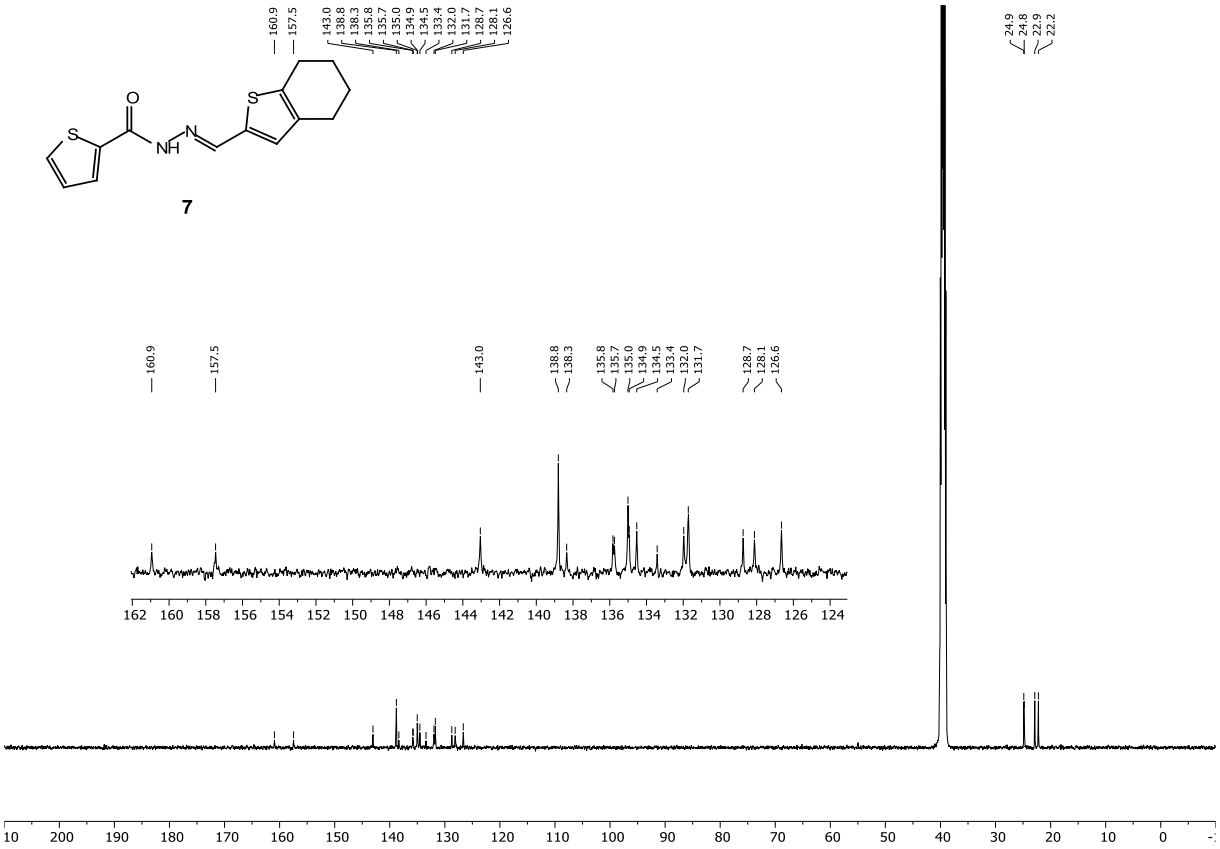

Supplementary Figure 49 ^{13}C NMR spectrum of **7.**

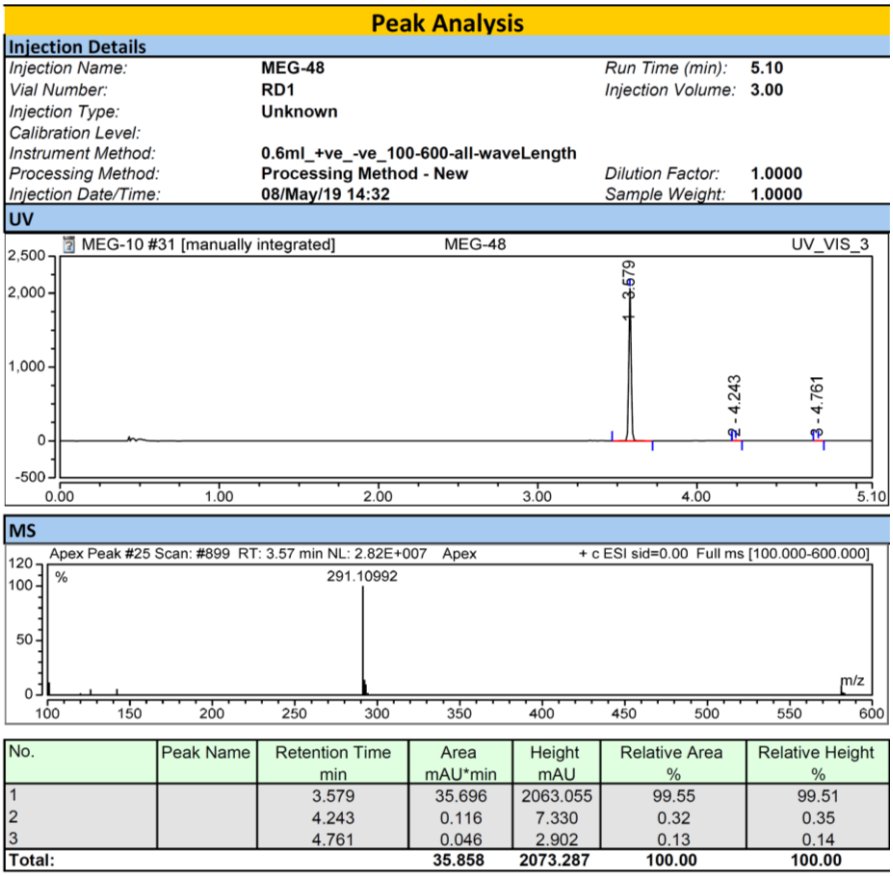

No.	Peak Name	Retention Time min	Area mAU*min	Height mAU	Relative Area %	Relative Height %
1		3.579	35.696	2063.055	99.55	99.51
2		4.243	0.116	7.330	0.32	0.35
3		4.761	0.046	2.902	0.13	0.14
Total:			**35.858**	**2073.287**	**100.00**	**100.00**

Supplementary Figure 50 HPLC purity analysis of **7**.

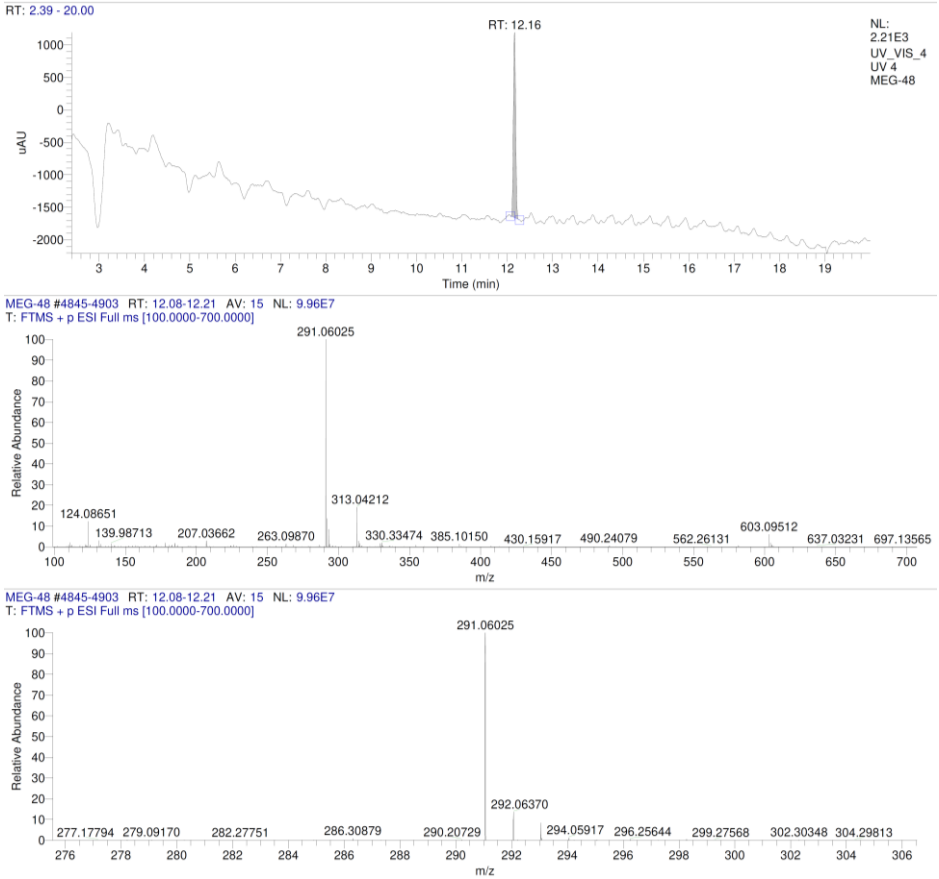

Supplementary Figure 51 HRMS of **7.**

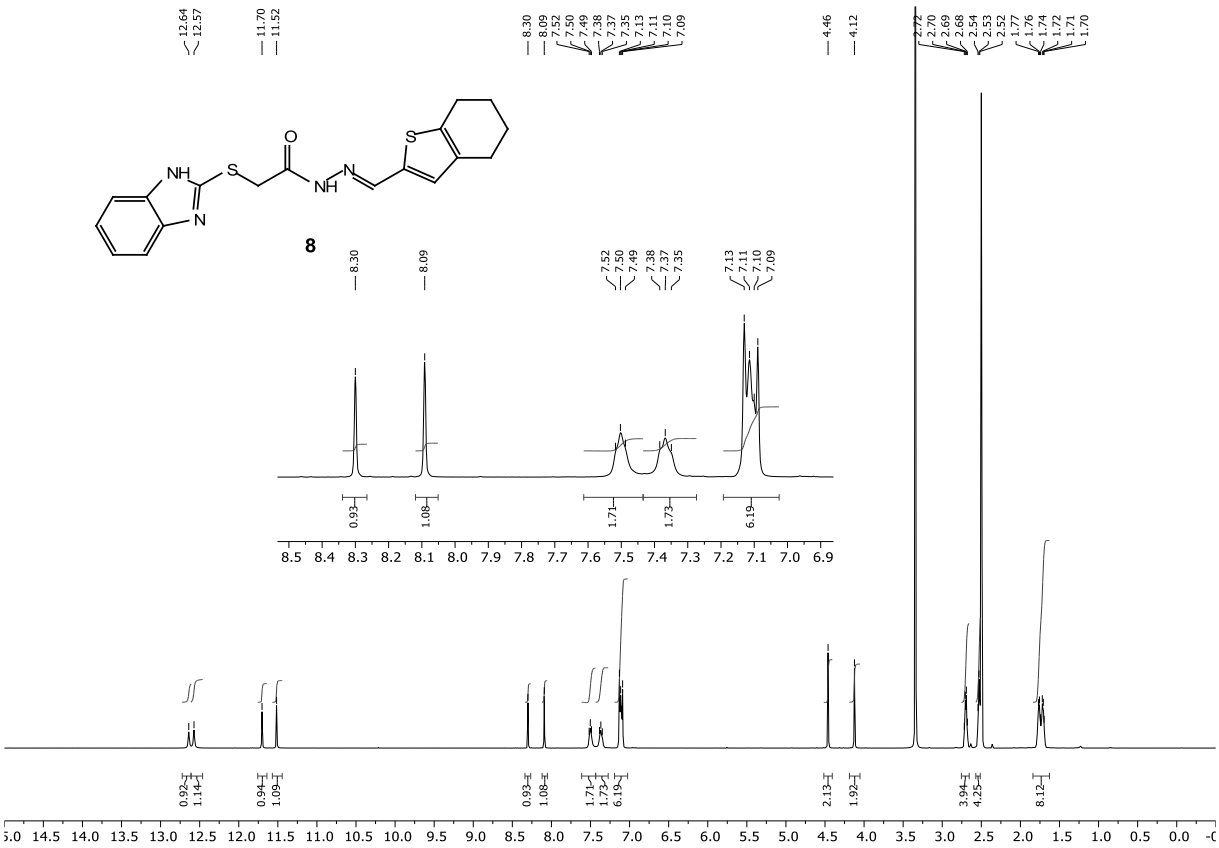

Supplementary Figure 52 ^{1}H NMR spectrum of **8.**

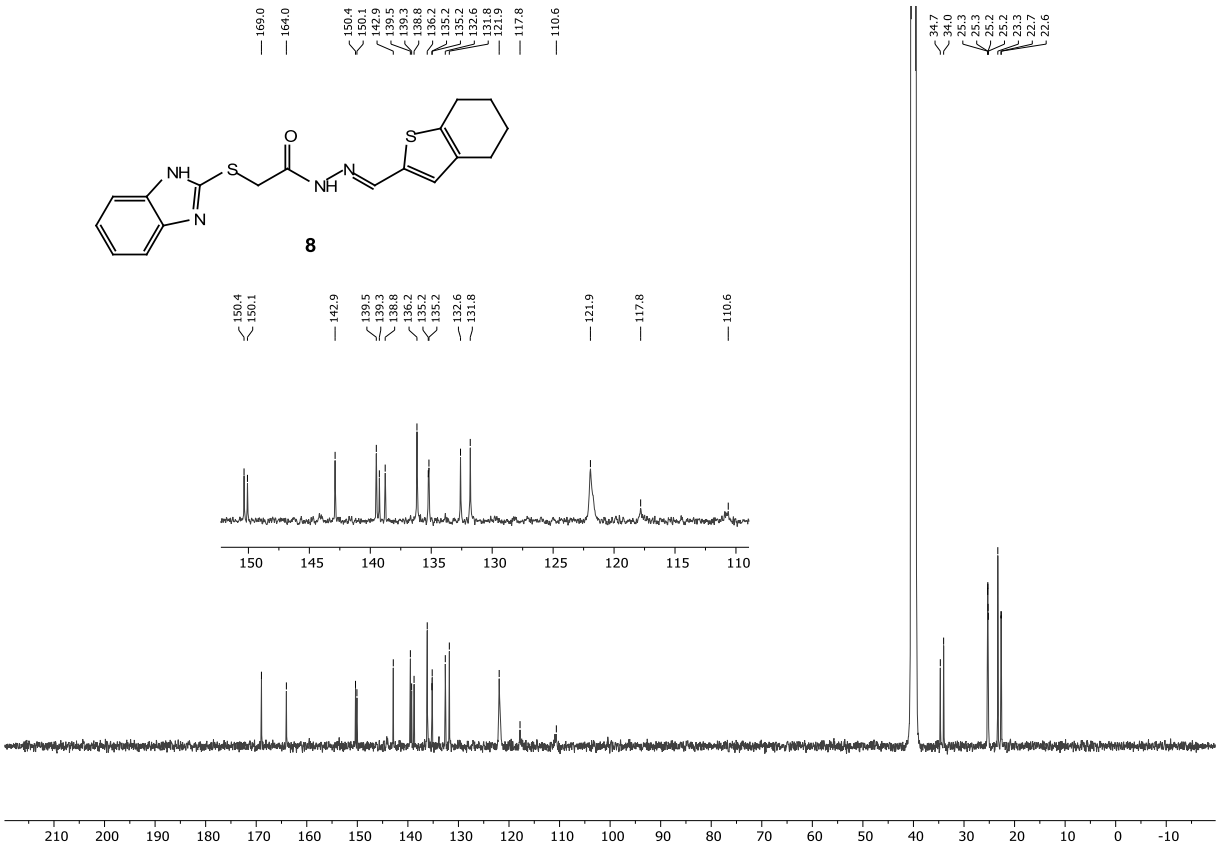

Supplementary Figure 53 ^{13}C NMR spectrum of **8.**

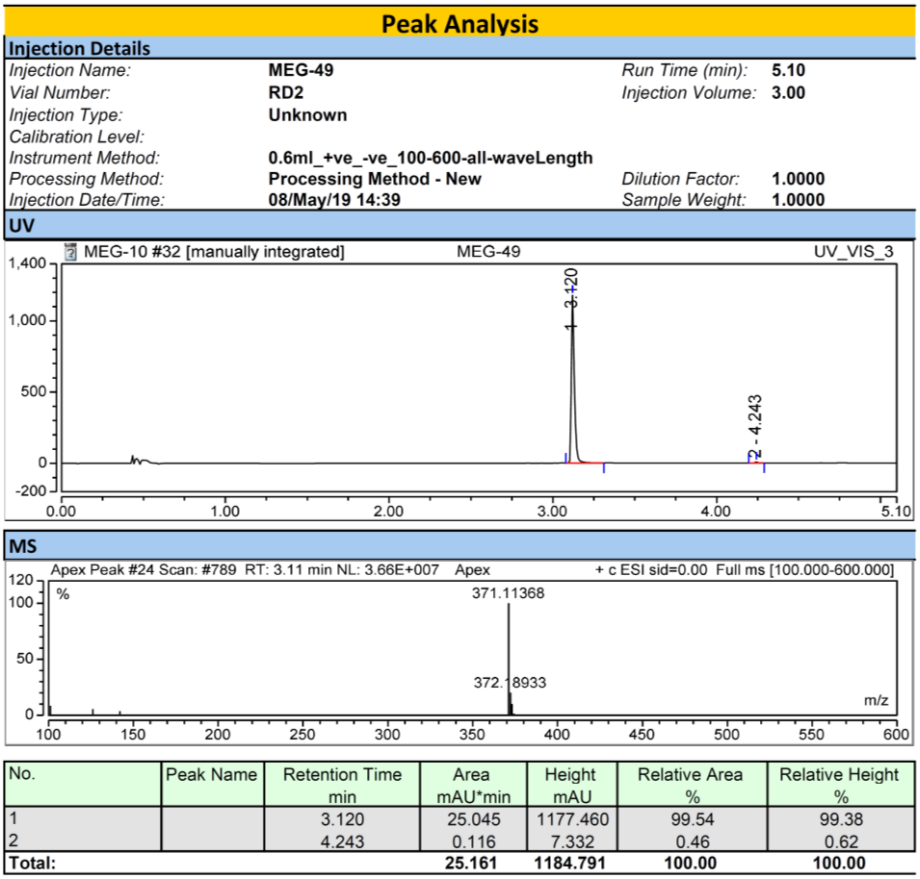

No.	Peak Name	Retention Time min	Area mAU*min	Height mAU	Relative Area %	Relative Height %
1		3.120	25.045	1177.460	99.54	99.38
2		4.243	0.116	7.332	0.46	0.62
Total:			**25.161**	**1184.791**	**100.00**	**100.00**

Supplementary Figure 54 HPLC purity analysis of **8.**

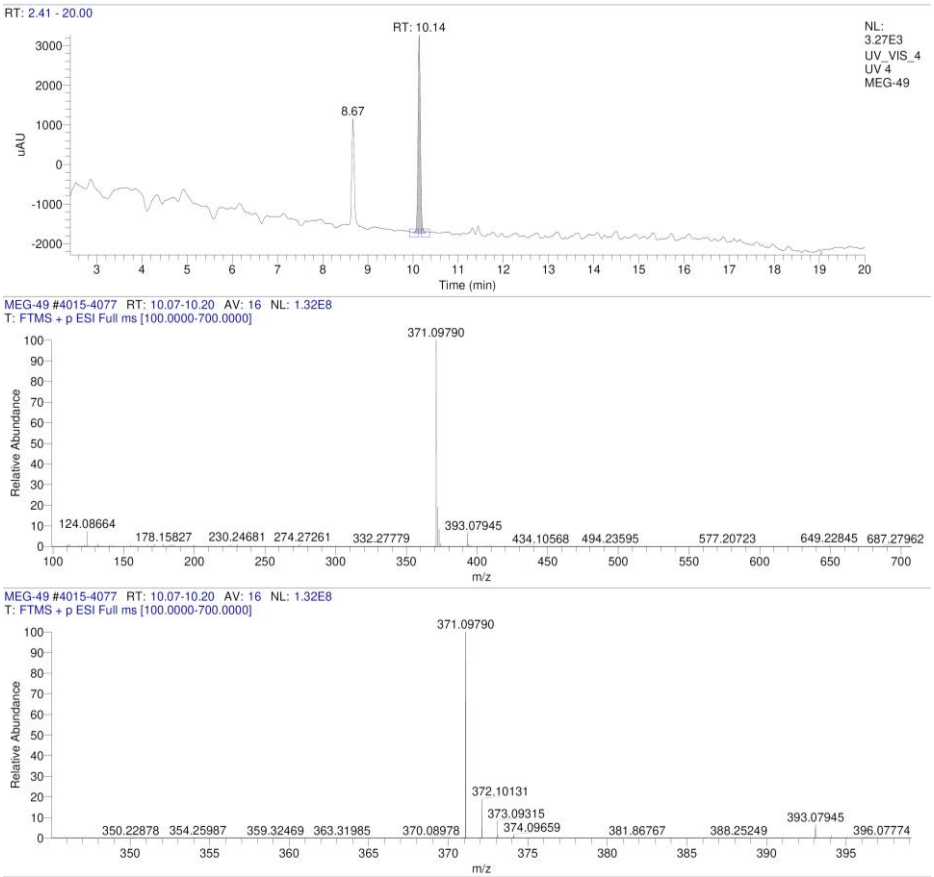

Supplementary Figure 55 HRMS of **8.**

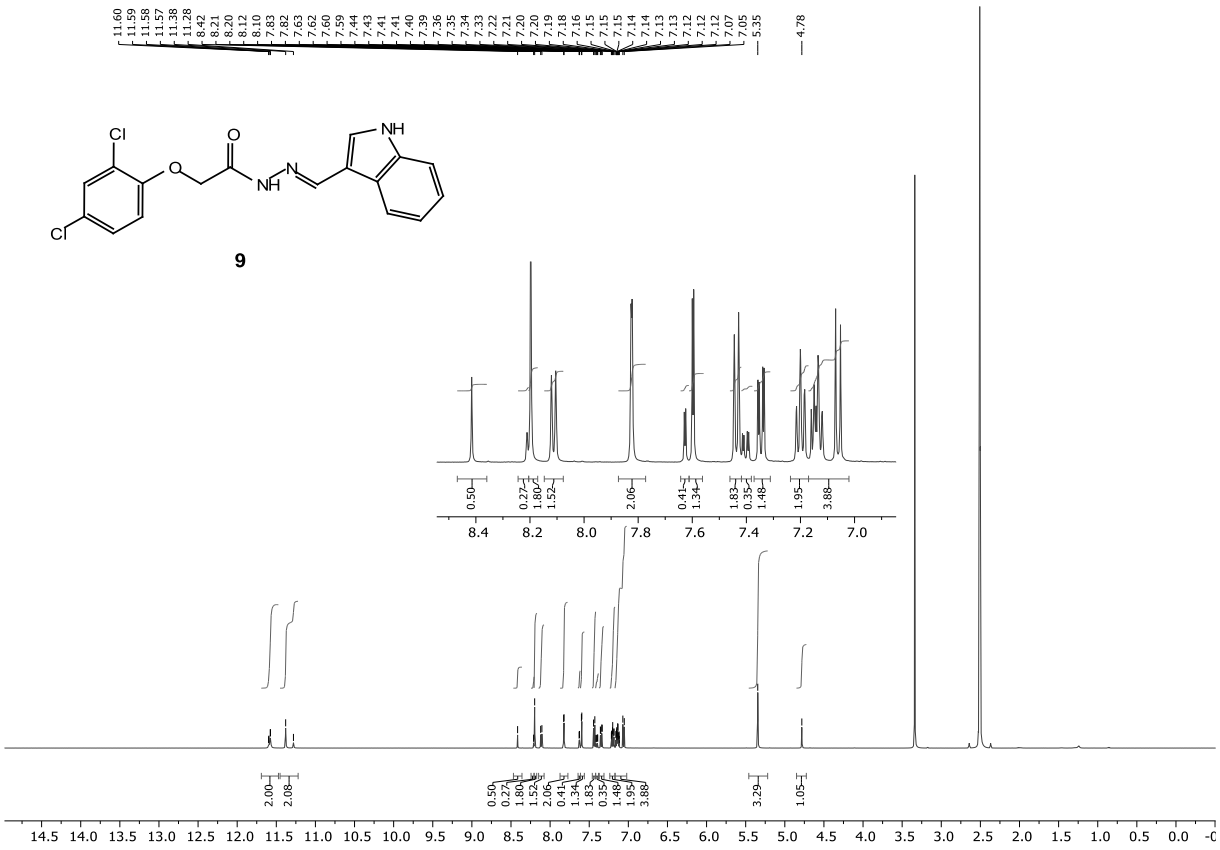

Supplementary Figure 56 ^{1}H NMR spectrum of **9.**

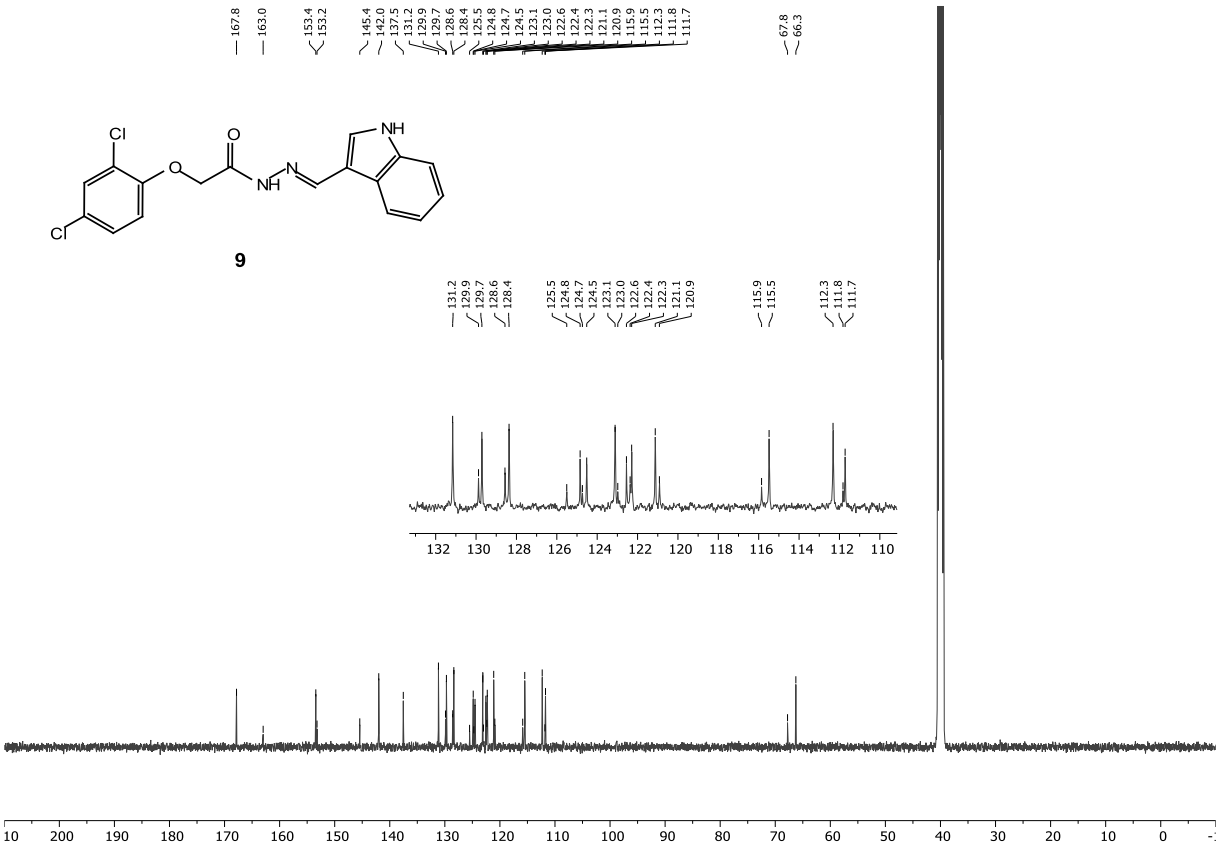

Supplementary Figure 57 ^{13}C NMR spectrum of **9.**

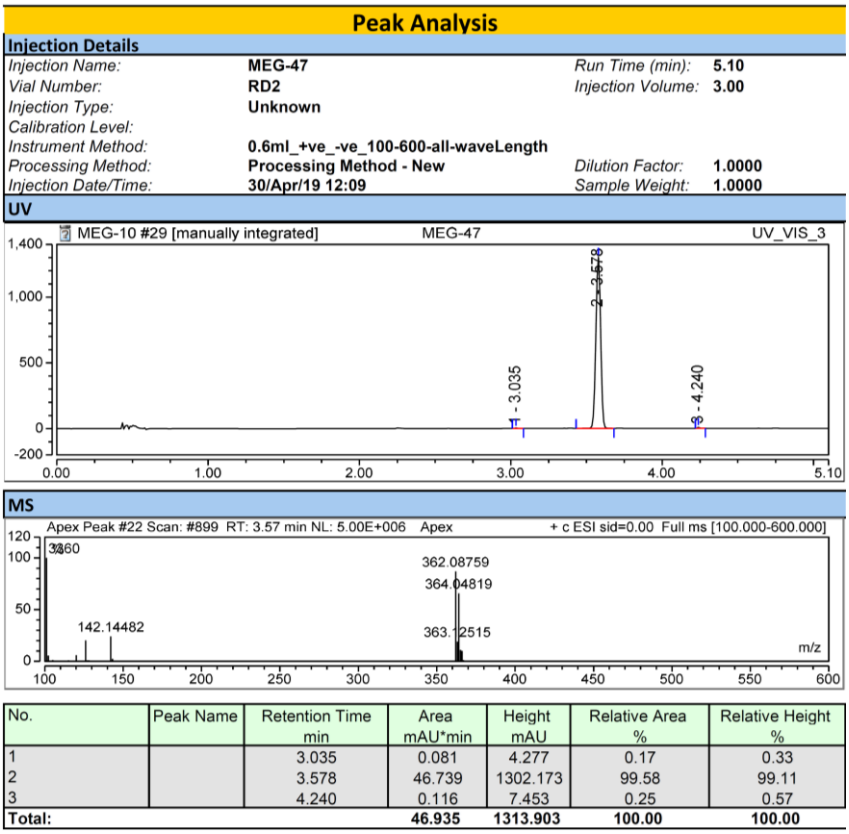

No.	Peak Name	Retention Time min	Area mAU*min	Height mAU	Relative Area %	Relative Height %
1		3.035	0.081	4.277	0.17	0.33
2		3.578	46.739	1302.173	99.58	99.11
3		4.240	0.116	7.453	0.25	0.57
Total:			**46.935**	**1313.903**	**100.00**	**100.00**

Supplementary Figure 58 HPLC purity analysis of **9.**

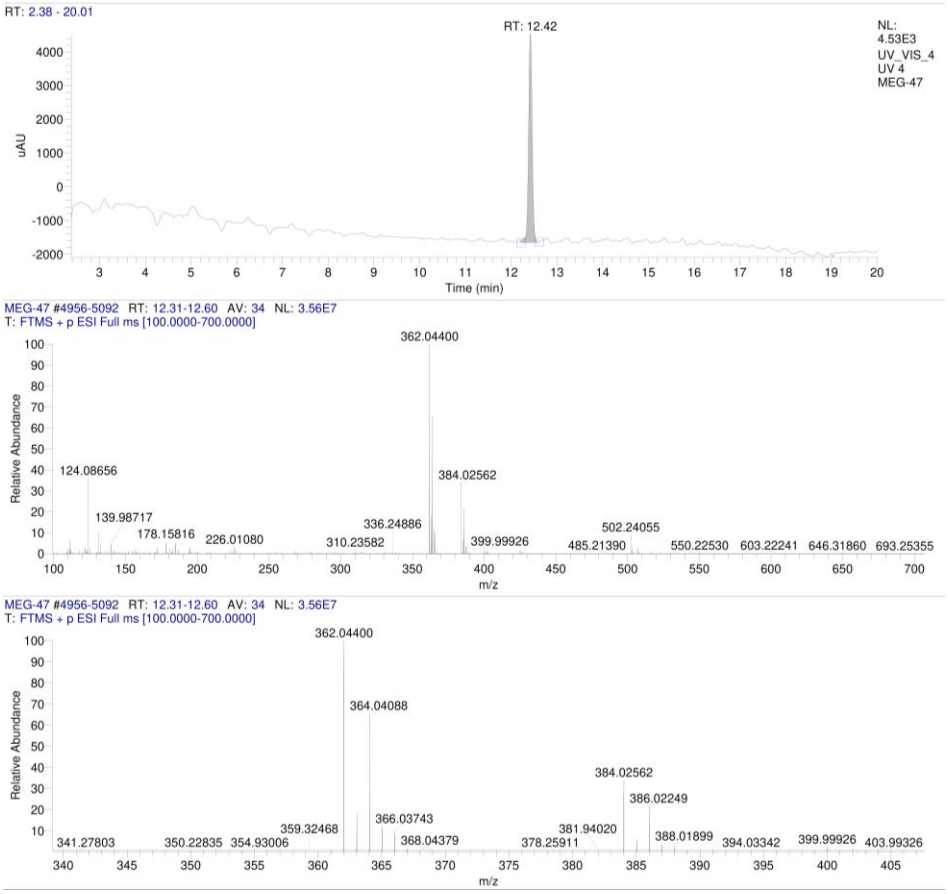

Supplementary Figure 59 HRMS of **9.**

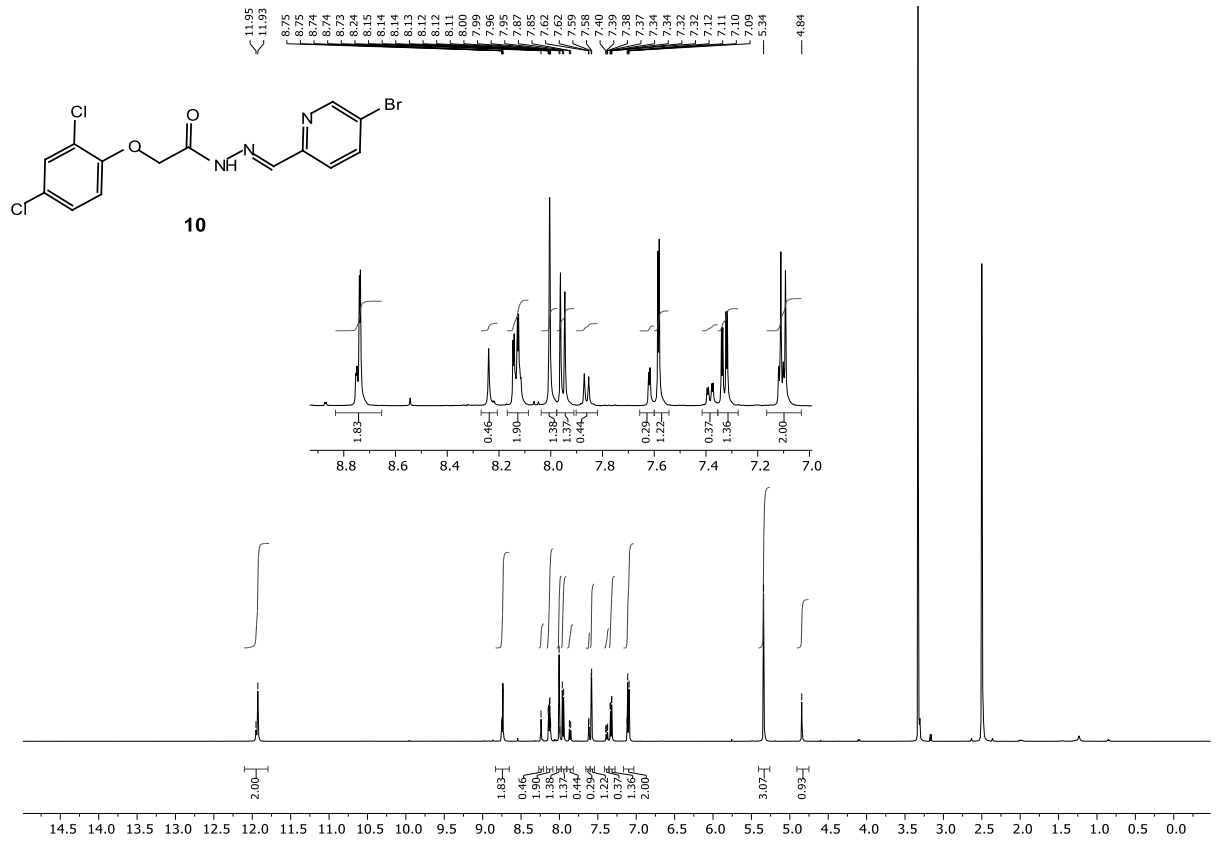

Supplementary Figure 60 ^{1}H NMR spectrum of **10.**

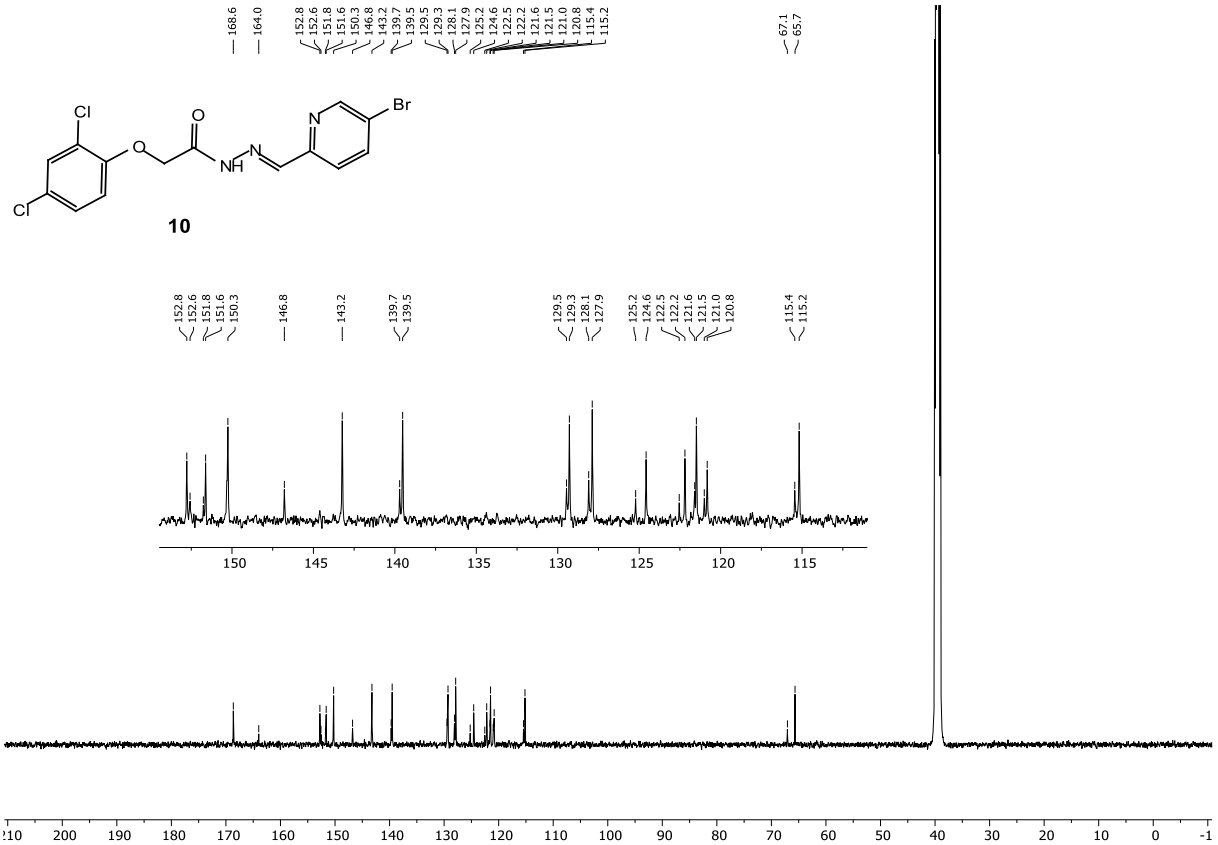

Supplementary Figure 61 ^{13}C NMR spectrum of **10.**

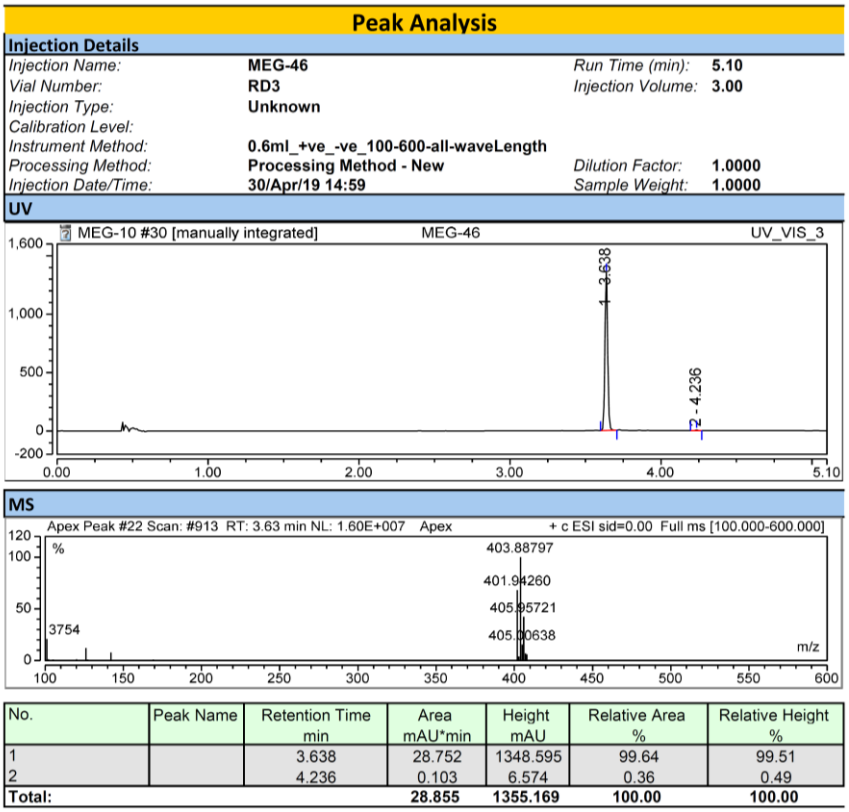

No.	Peak Name	Retention Time min	Area mAU*min	Height mAU	Relative Area %	Relative Height %
1		3.638	28.752	1348.595	99.64	99.51
2		4.236	0.103	6.574	0.36	0.49
Total:			**28.855**	**1355.169**	**100.00**	**100.00**

Supplementary Figure 62 HPLC purity analysis of **10.**

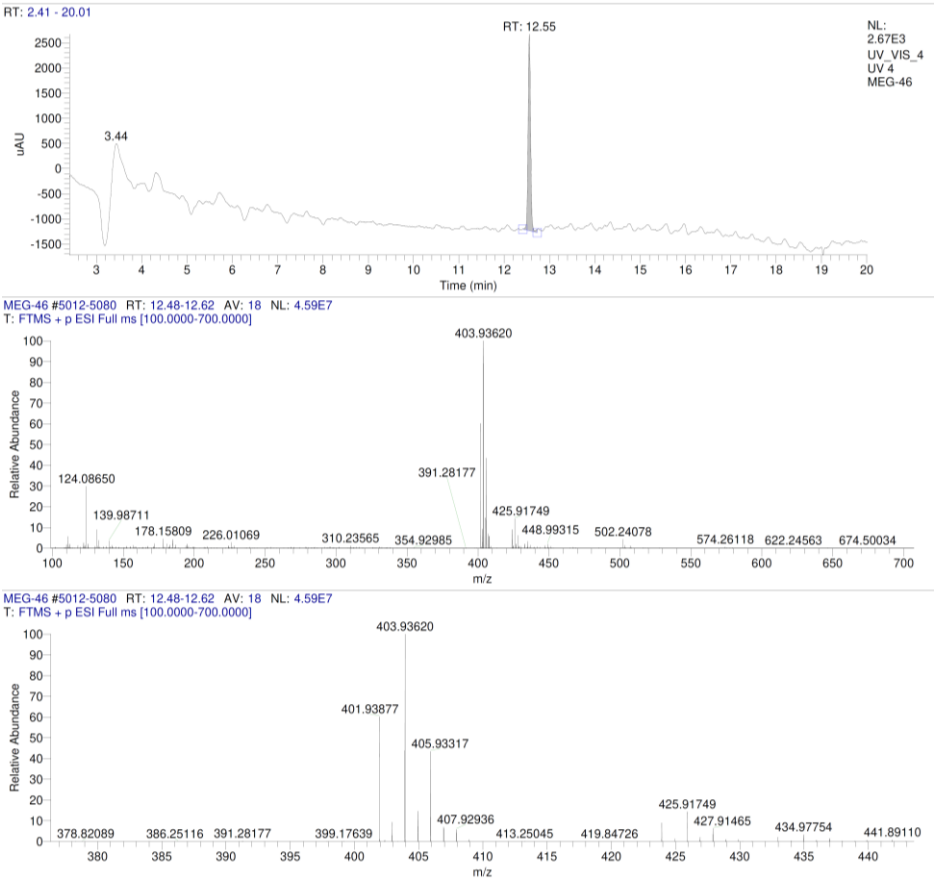

Supplementary Figure 63 HRMS of **10.**

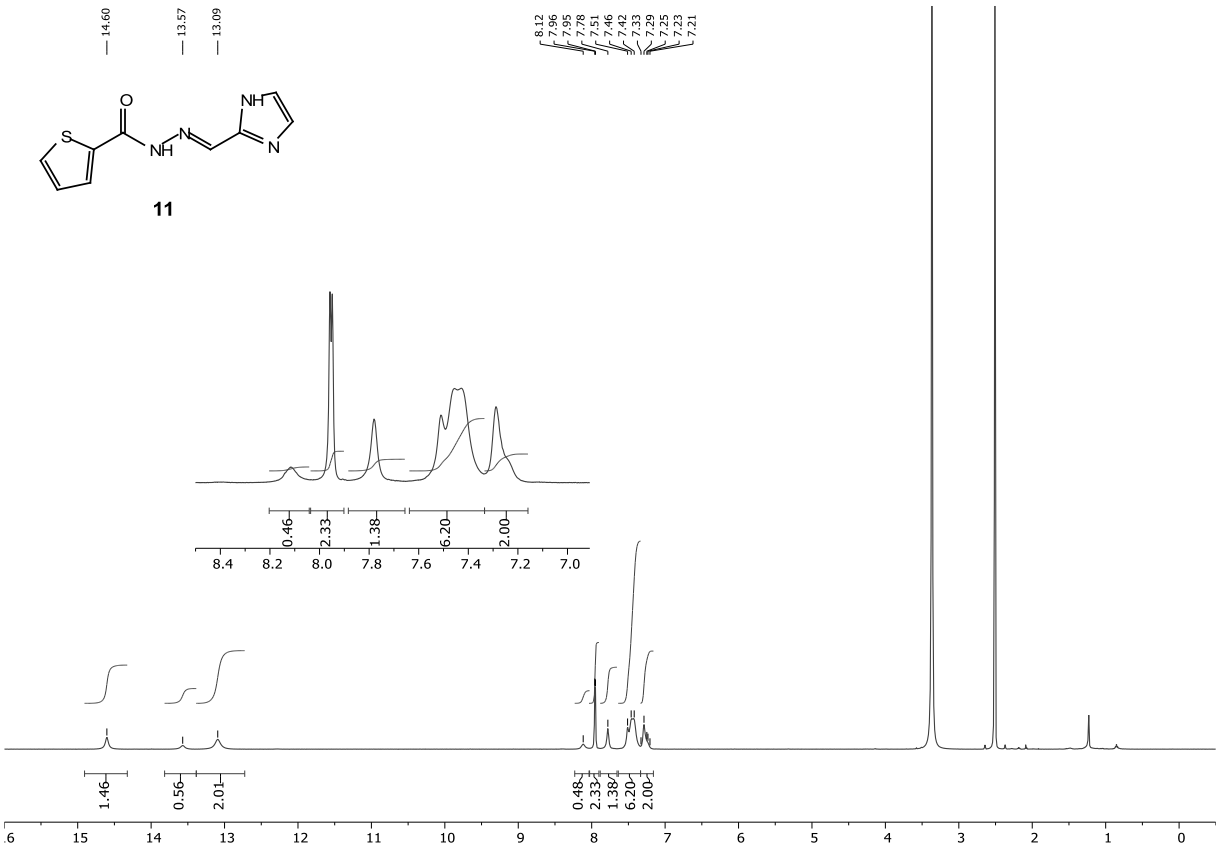

Supplementary Figure 64 ^{1}H NMR spectrum of **11.**

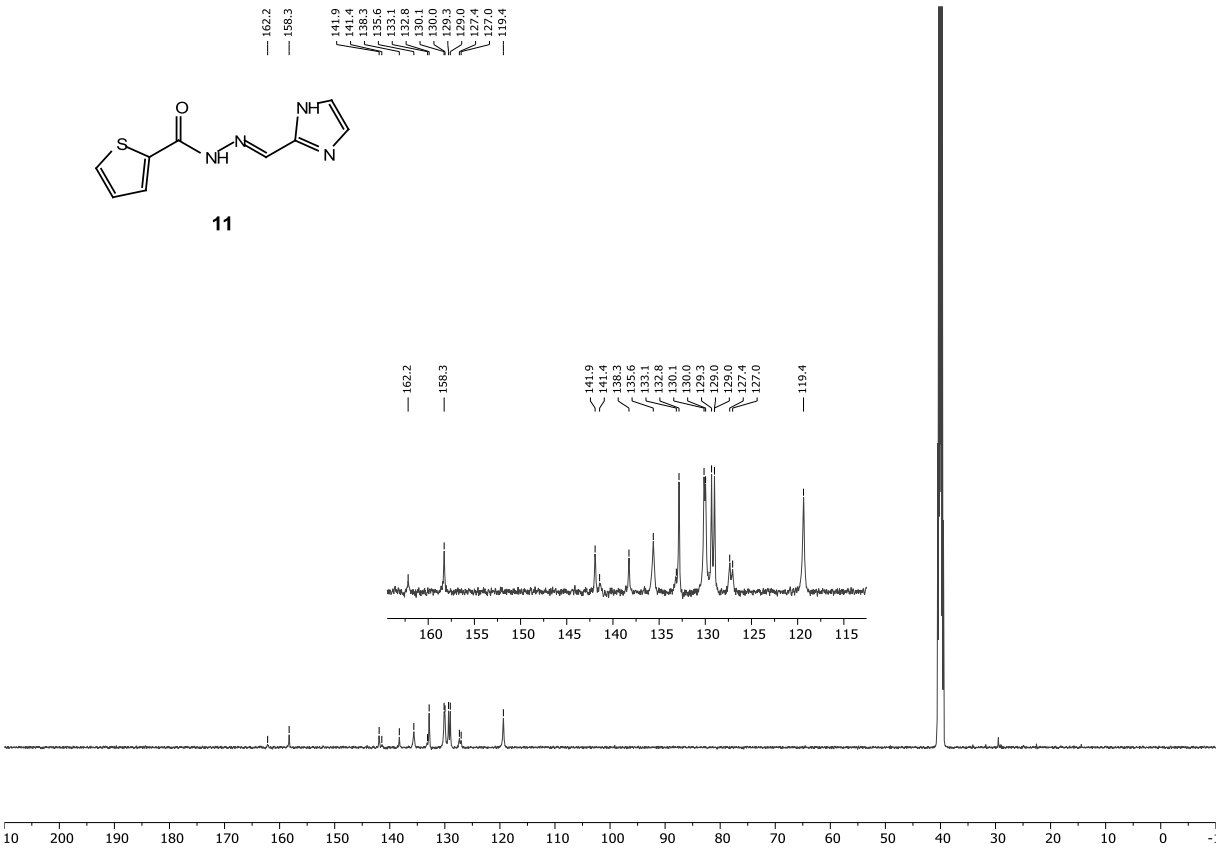

Supplementary Figure 65 ^{13}C NMR spectrum of **11.**

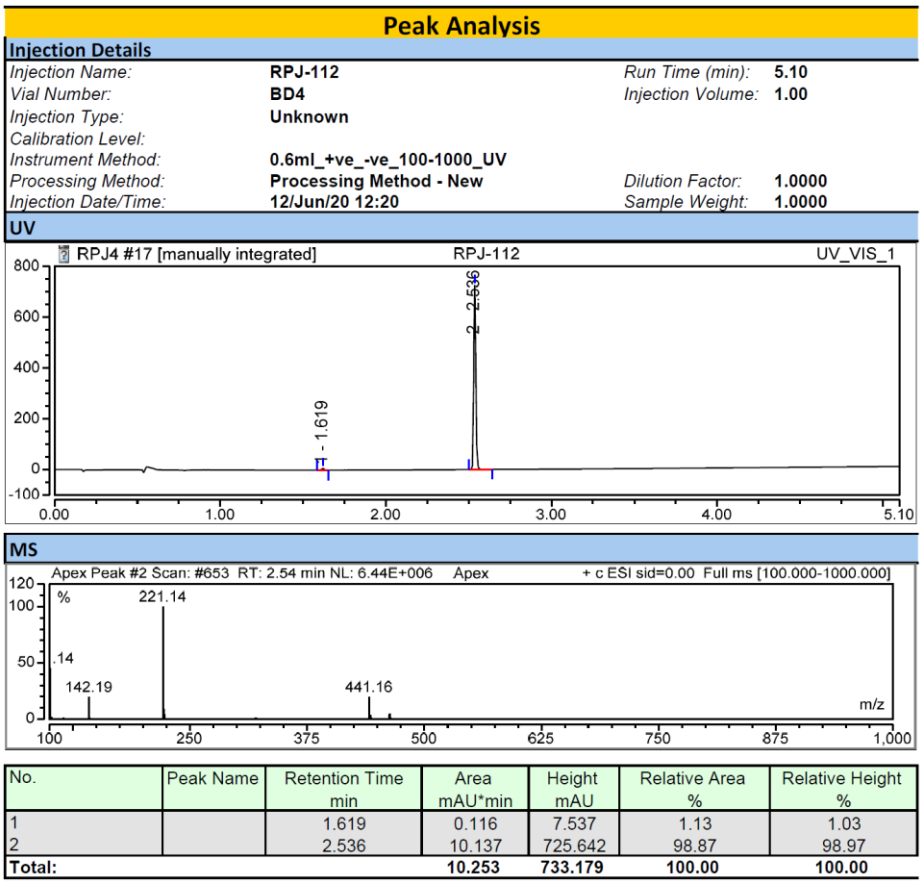

No.	Peak Name	Retention Time min	Area mAU*min	Height mAU	Relative Area %	Relative Height %
1		1.619	0.116	7.537	1.13	1.03
2		2.536	10.137	725.642	98.87	98.97
Total:			**10.253**	**733.179**	**100.00**	**100.00**

Supplementary Figure 66 HPLC purity analysis of **11.**

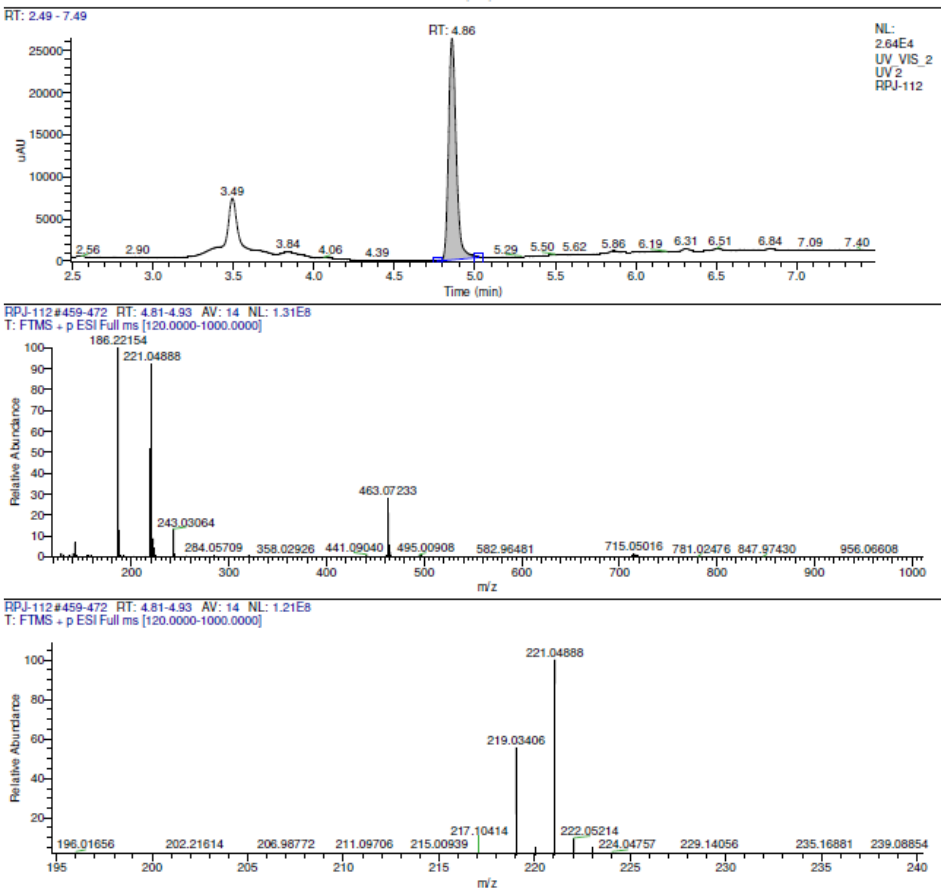

Supplementary Figure 67 HRMS of **11.**

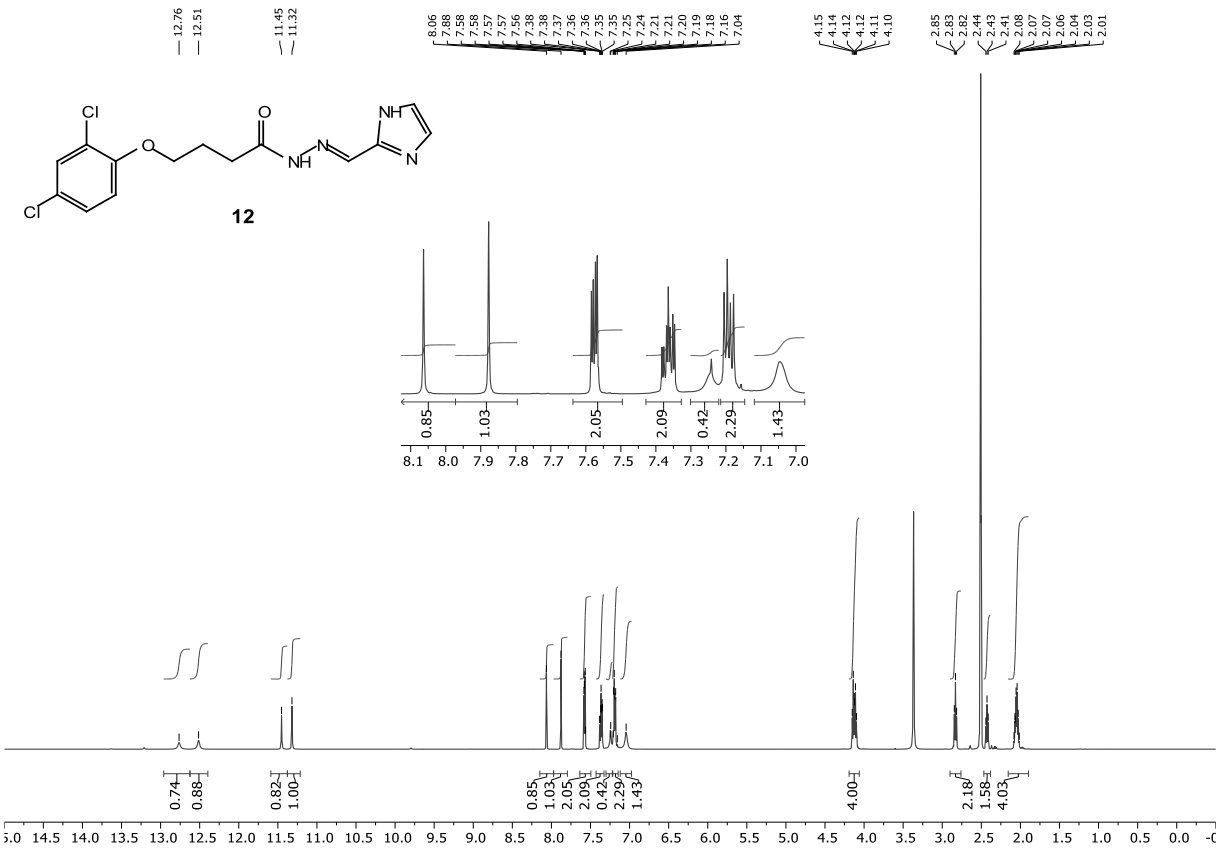

Supplementary Figure 68 ^{1}H NMR spectrum of **12.**

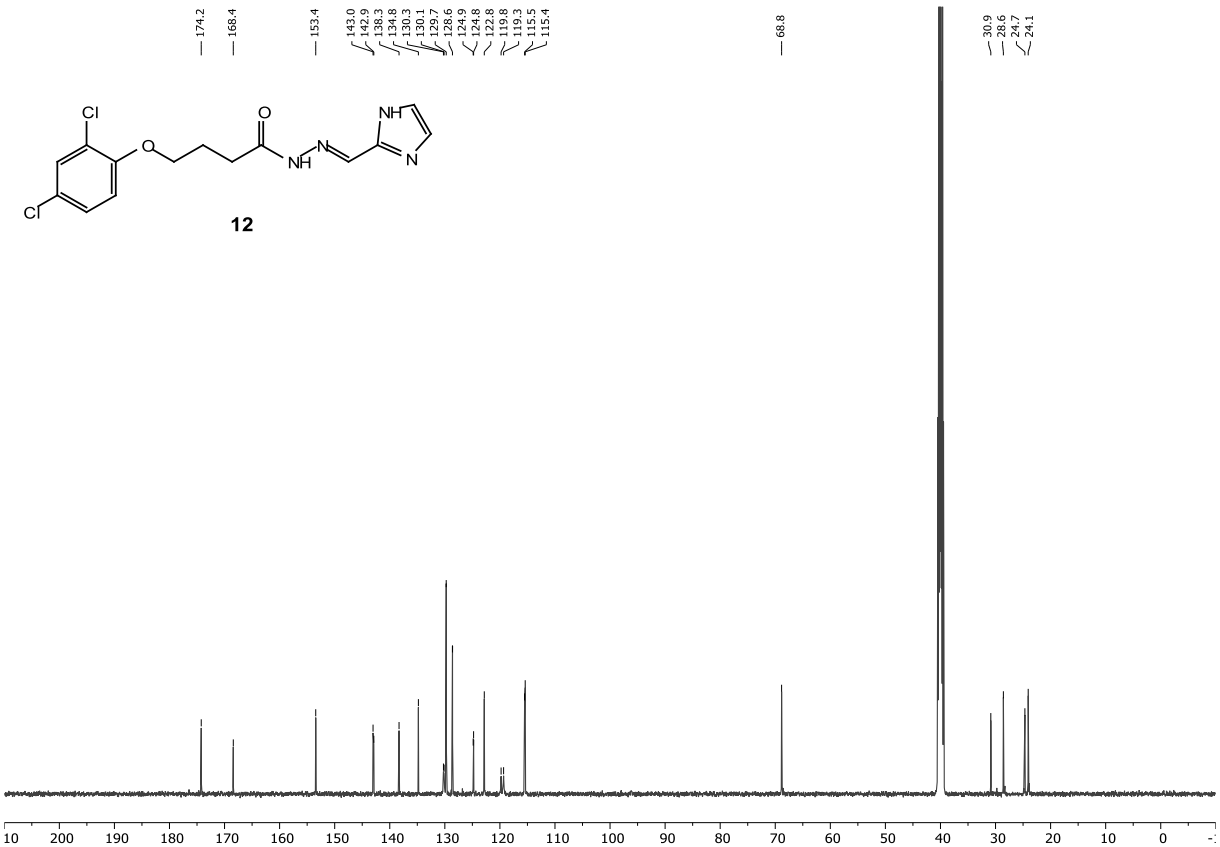

Supplementary Figure 69 ^{13}C NMR spectrum of **12.**

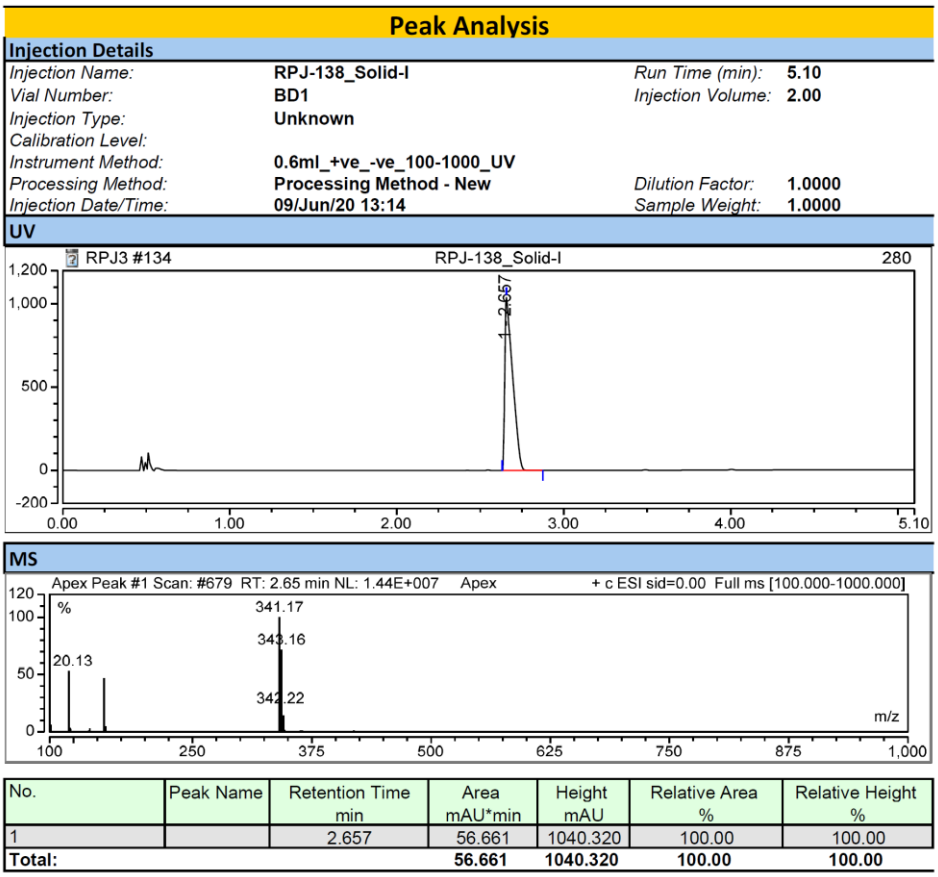

No.	Peak Name	Retention Time min	Area mAU*min	Height mAU	Relative Area %	Relative Height %
1		2.657	56.661	1040.320	100.00	100.00
Total:			**56.661**	**1040.320**	**100.00**	**100.00**

Supplementary Figure 70HPLC purity analysis of **12.**

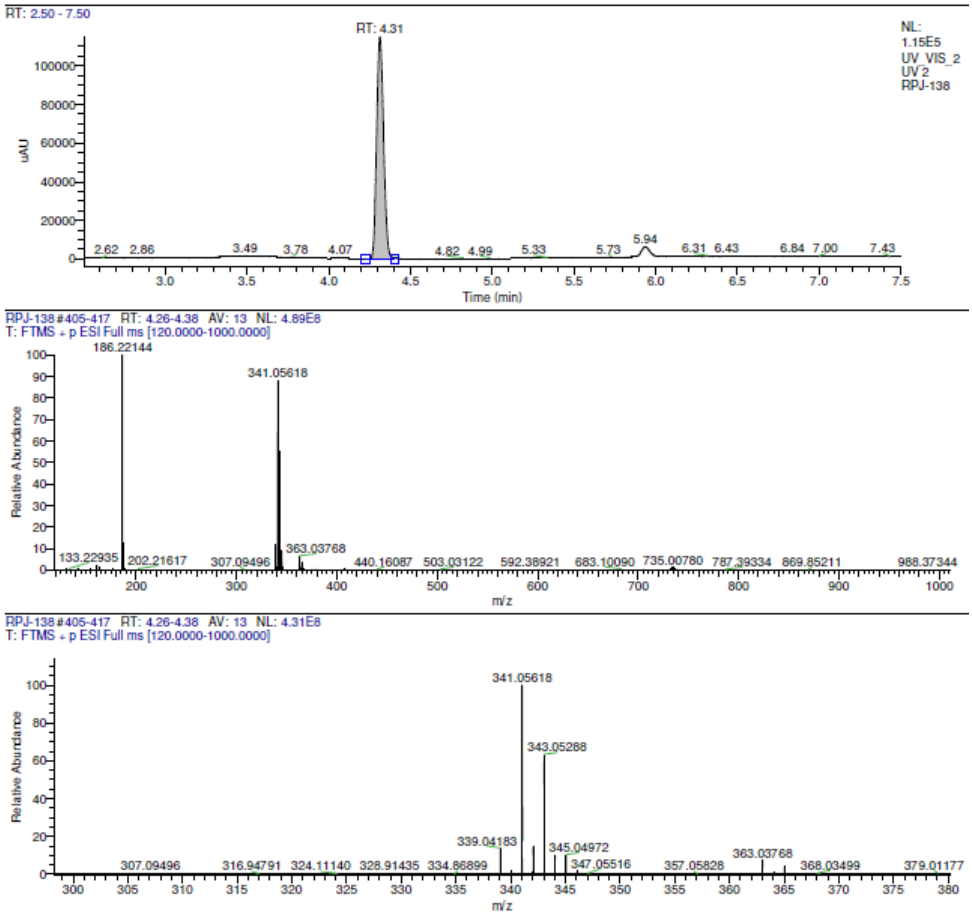

Supplementary Figure 71 HRMS of **12.**

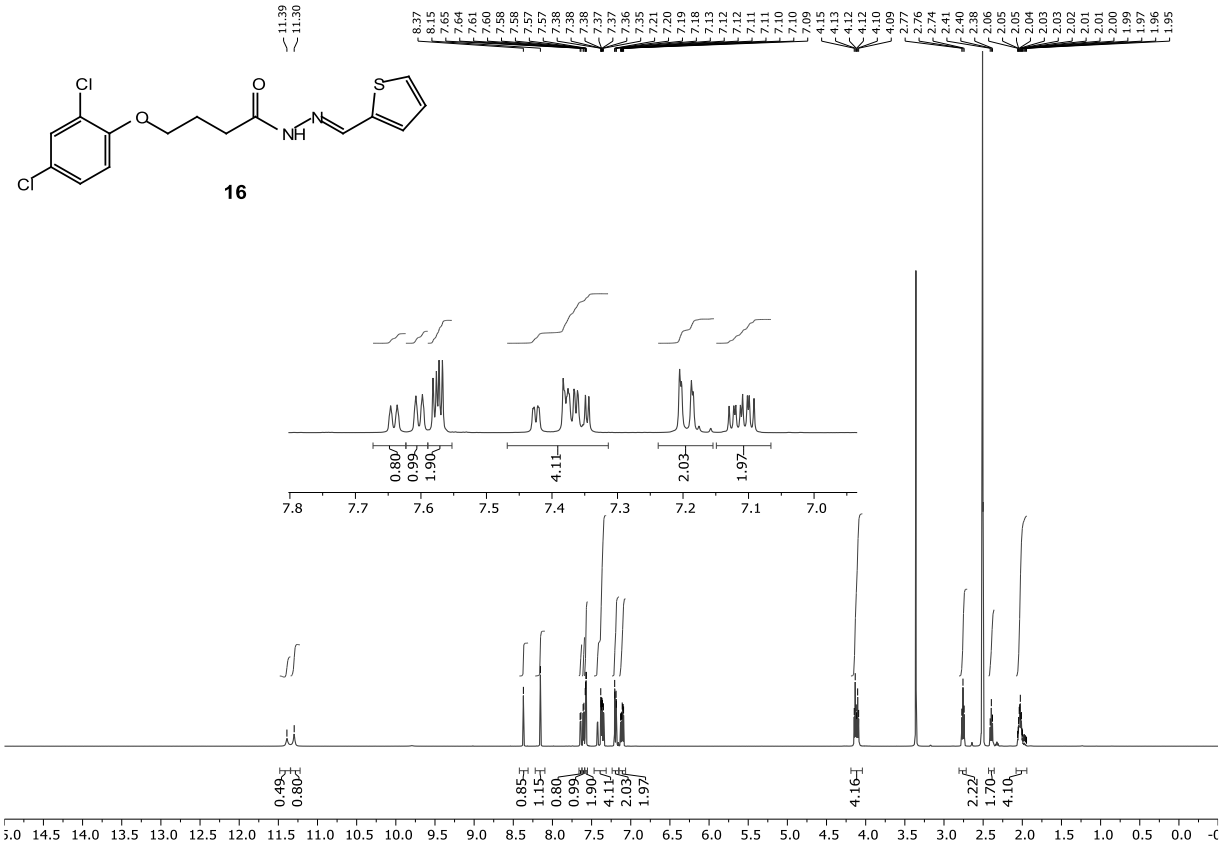

Supplementary Figure 72 ^{1}H NMR spectrum of **16.**

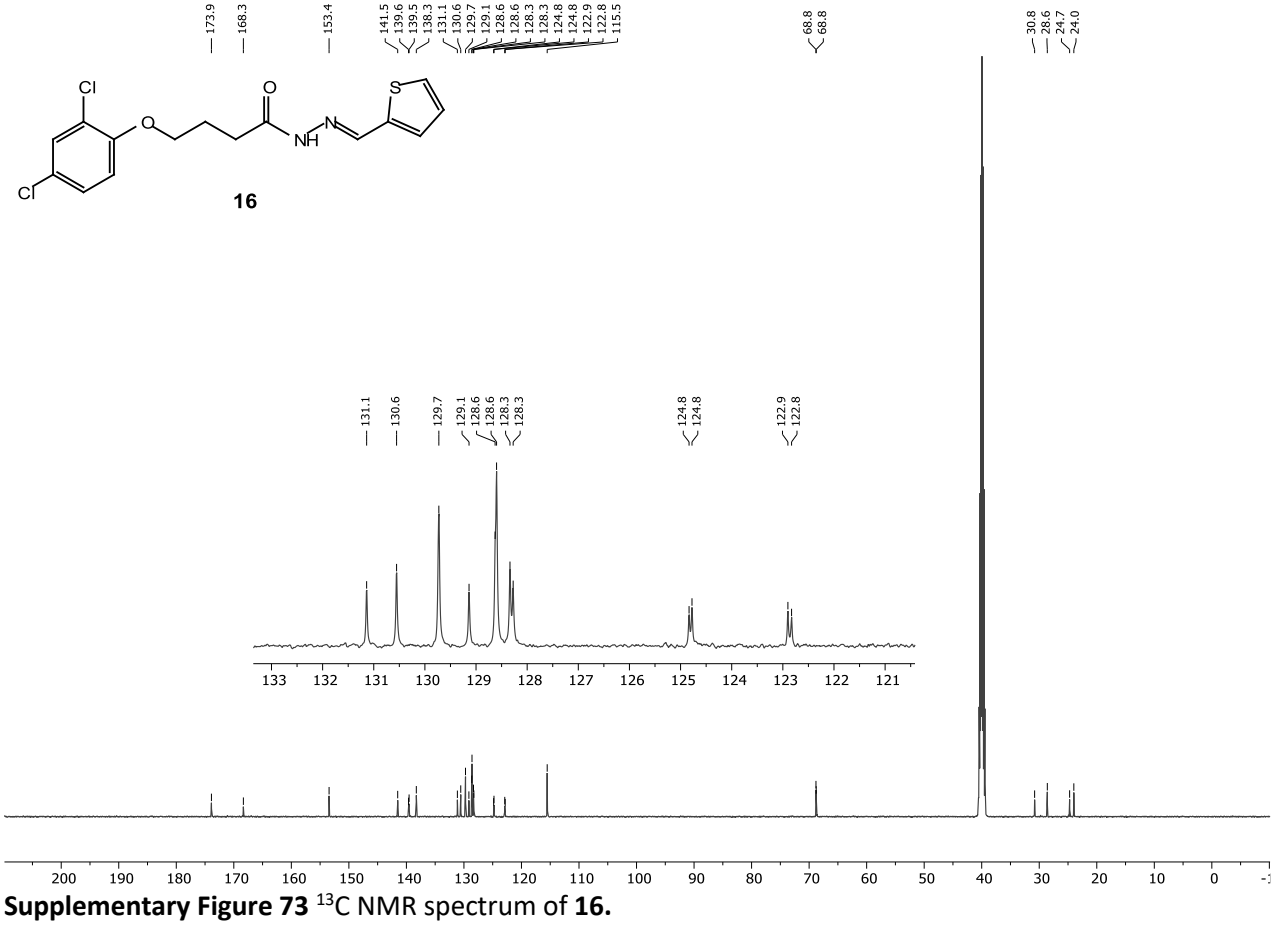

Supplementary Figure 73 ^{13}C NMR spectrum of **16.**

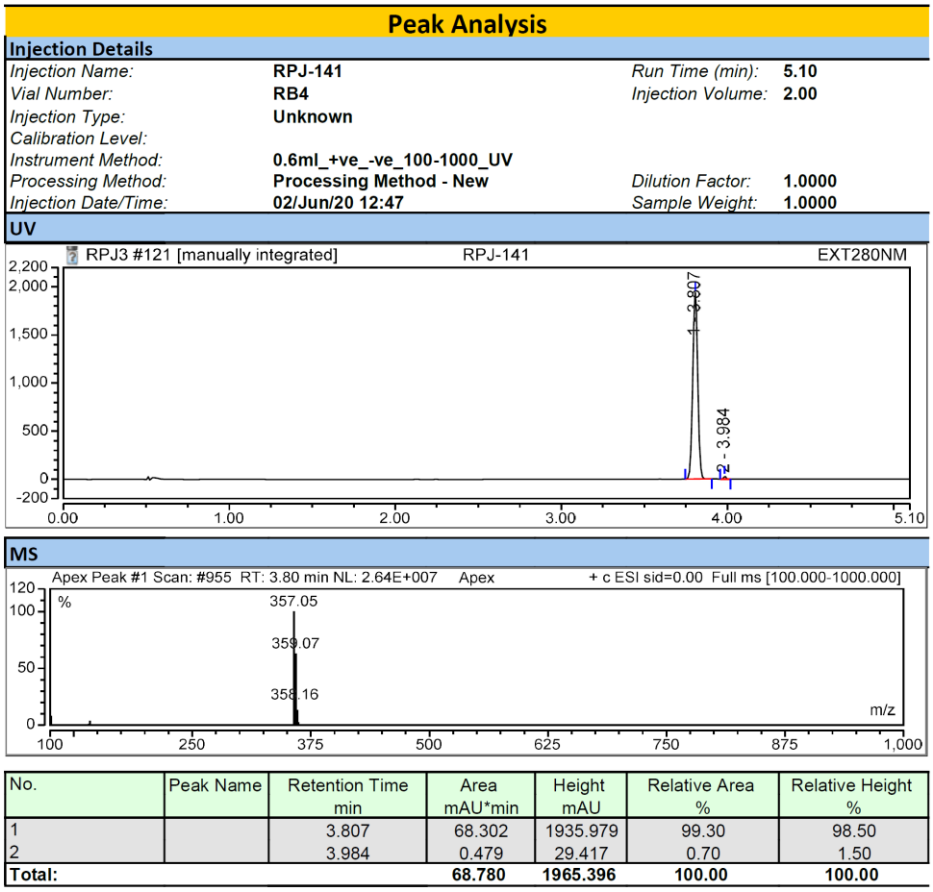

No.	Peak Name	Retention Time min	Area mAU*min	Height mAU	Relative Area %	Relative Height %
1		3.807	68.302	1935.979	99.30	98.50
2		3.984	0.479	29.417	0.70	1.50
Total:			**68.780**	**1965.396**	**100.00**	**100.00**

Supplementary Figure 74 HPLC purity analysis of **16.**

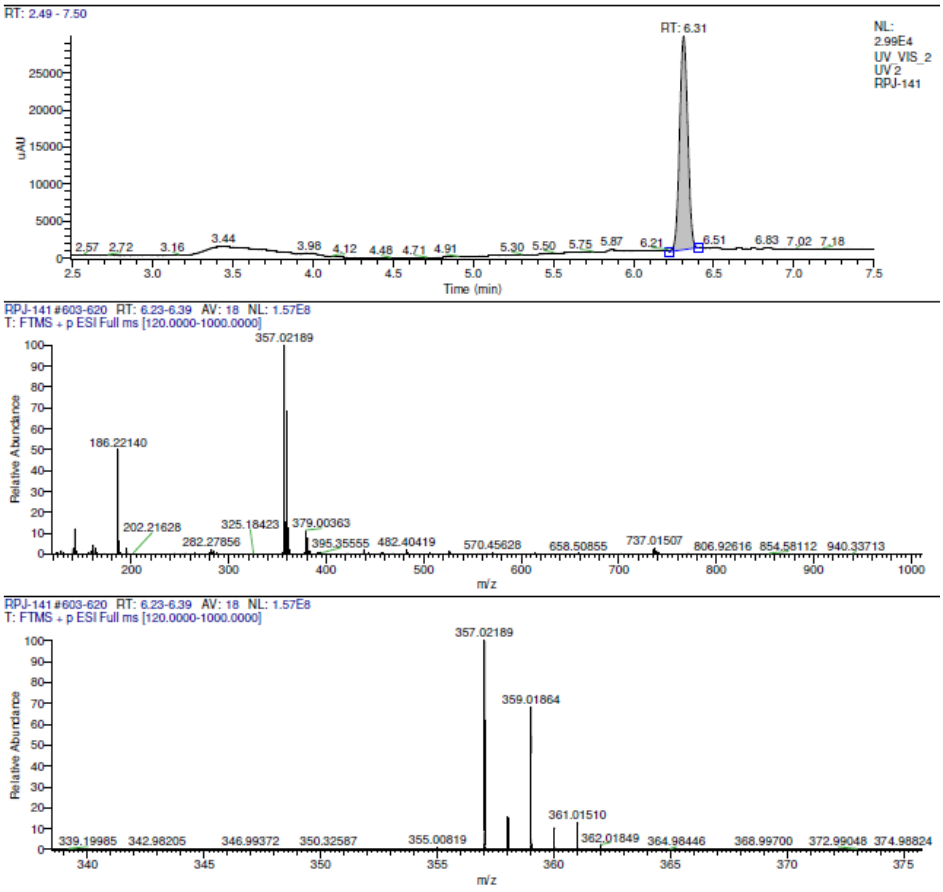

Supplementary Figure 75 HRMS of **16.**

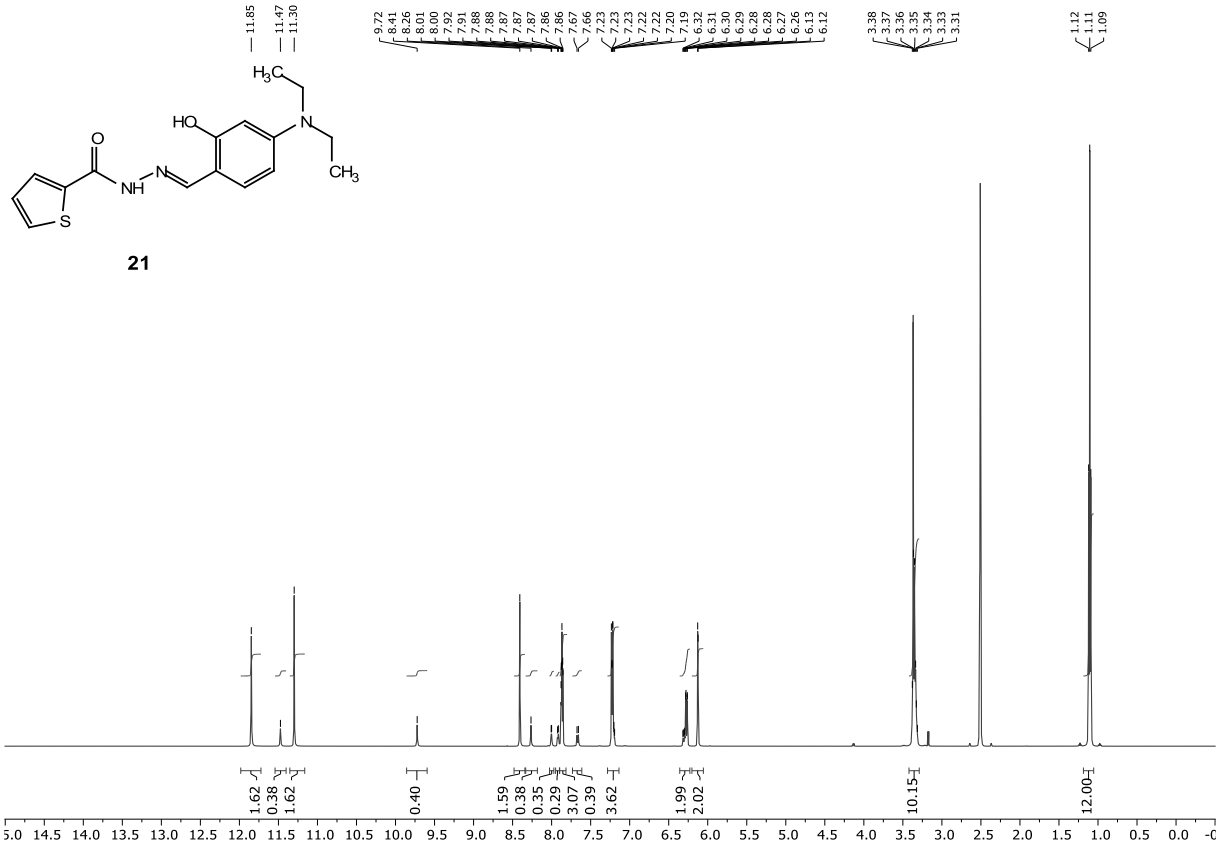

Supplementary Figure 76 ^{1}H NMR spectrum of **21.**

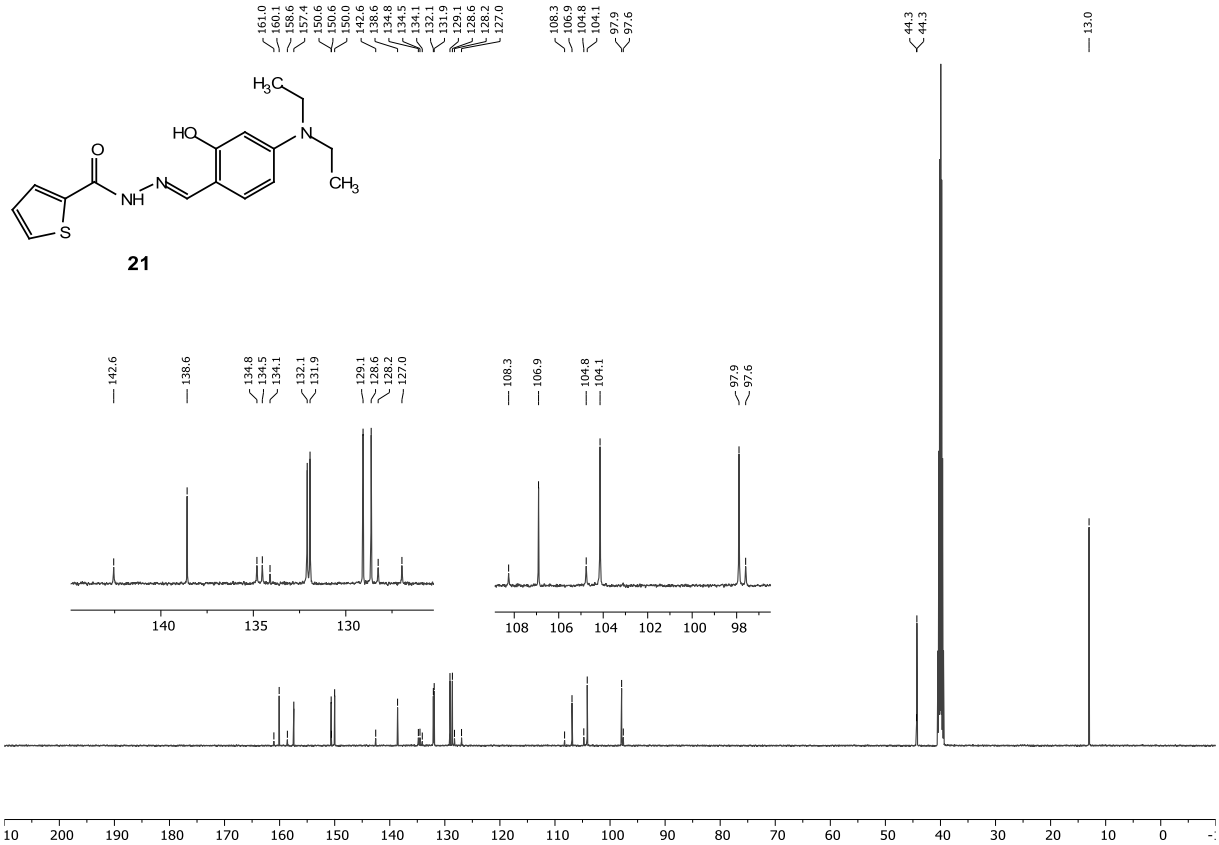

Supplementary Figure 77 ^{13}C NMR spectrum of **21.**

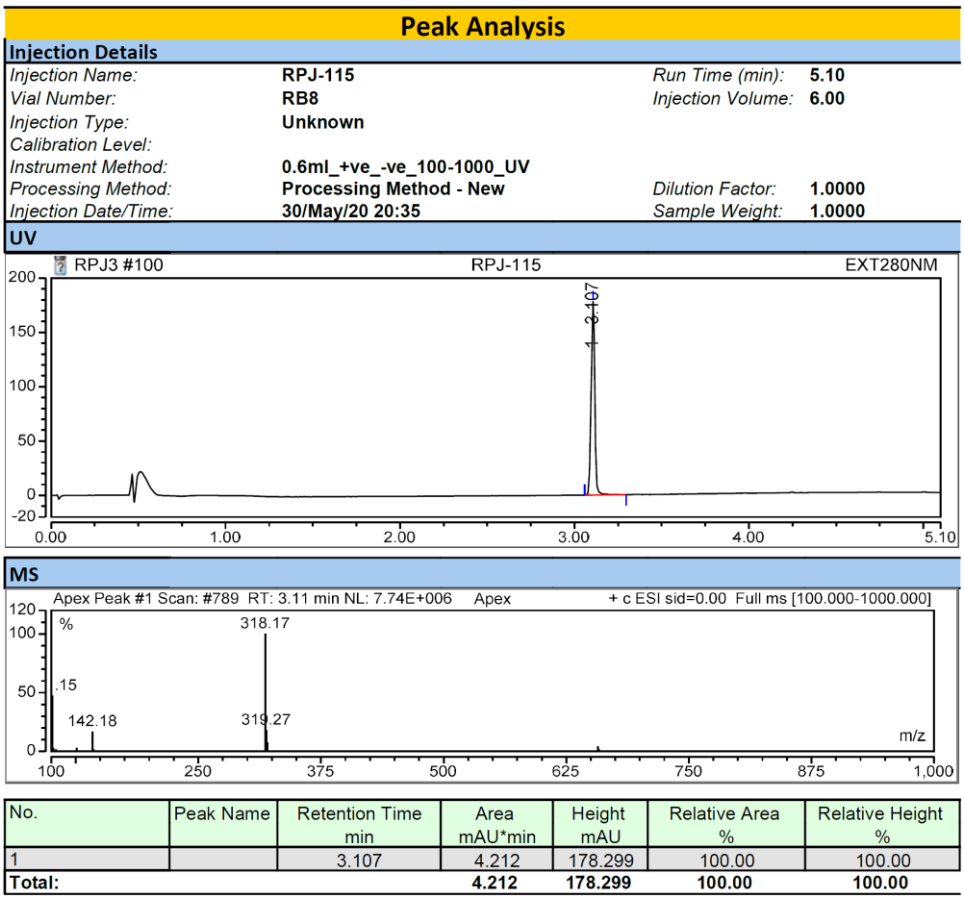

No.	Peak Name	Retention Time min	Area mAU*min	Height mAU	Relative Area %	Relative Height %
1		3.107	4.212	178.299	100.00	100.00
Total:			**4.212**	**178.299**	**100.00**	**100.00**

Supplementary Figure 78 HPLC purity analysis of **21.**

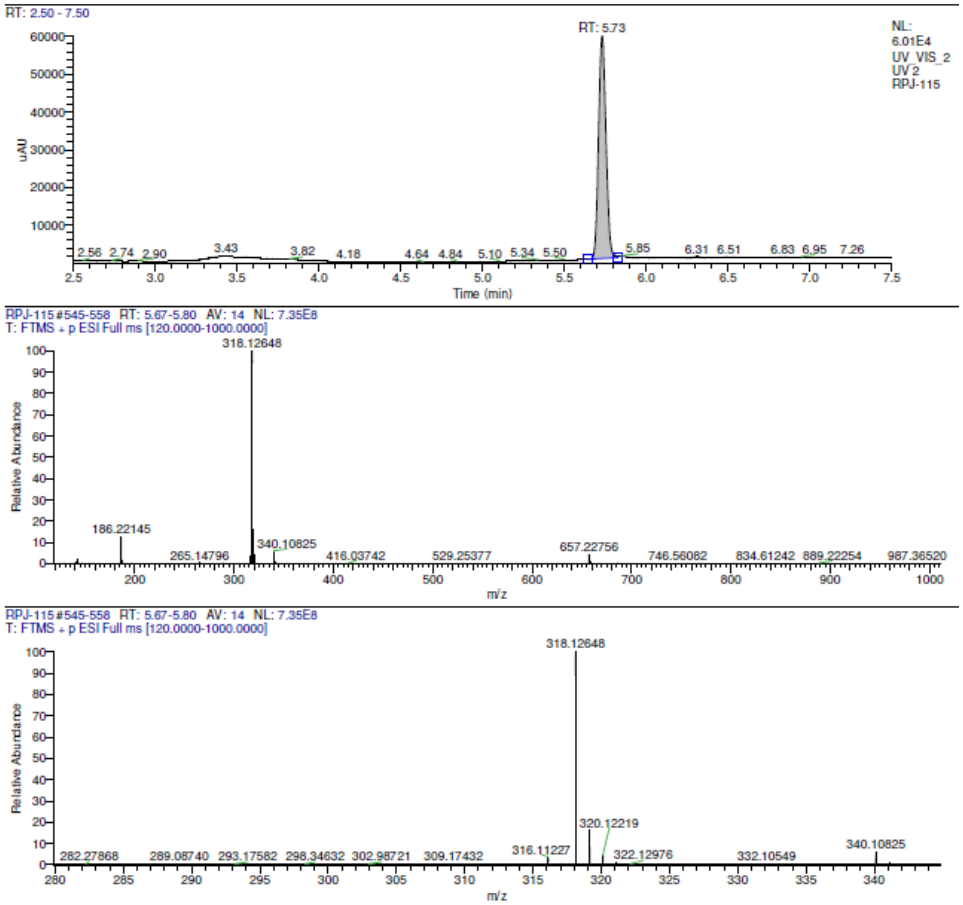

Supplementary Figure 79 HRMS of **21.**

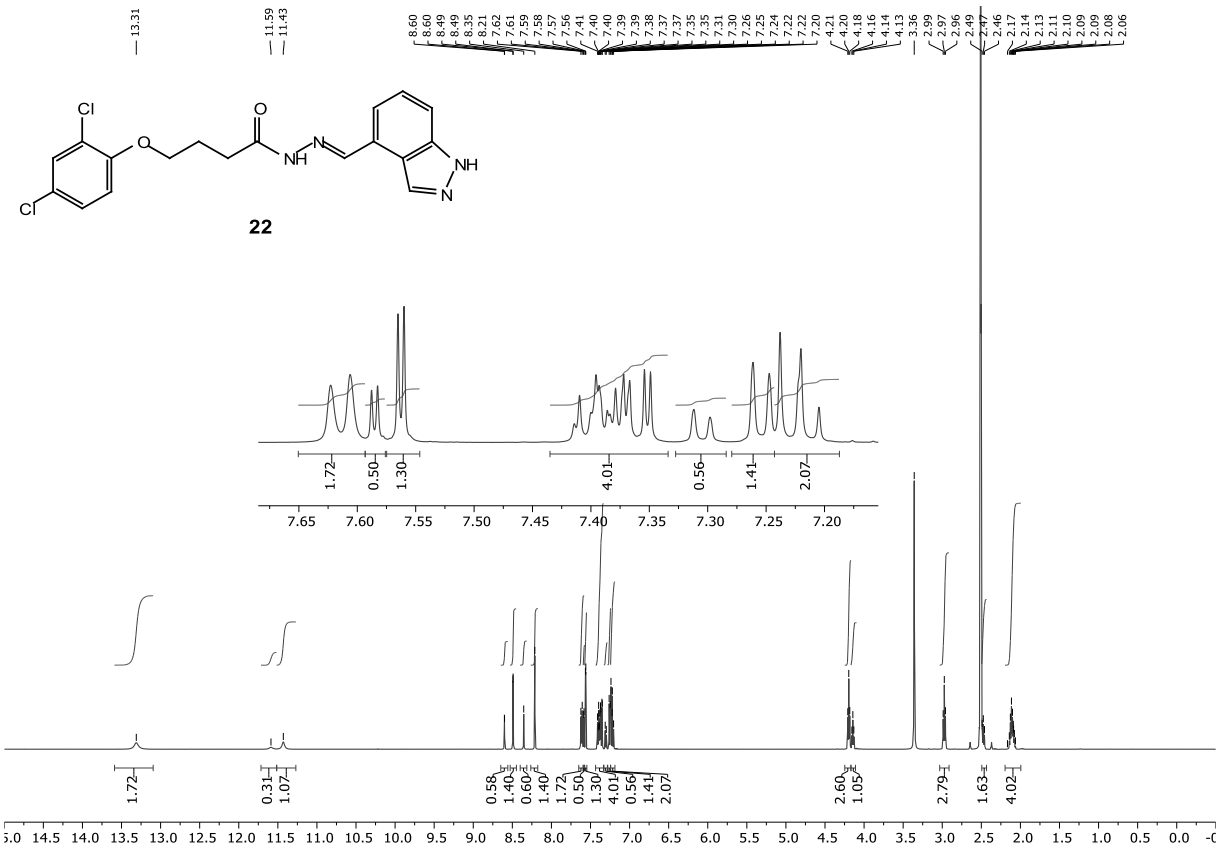

Supplementary Figure 80 ^{1}H NMR spectrum of **22.**

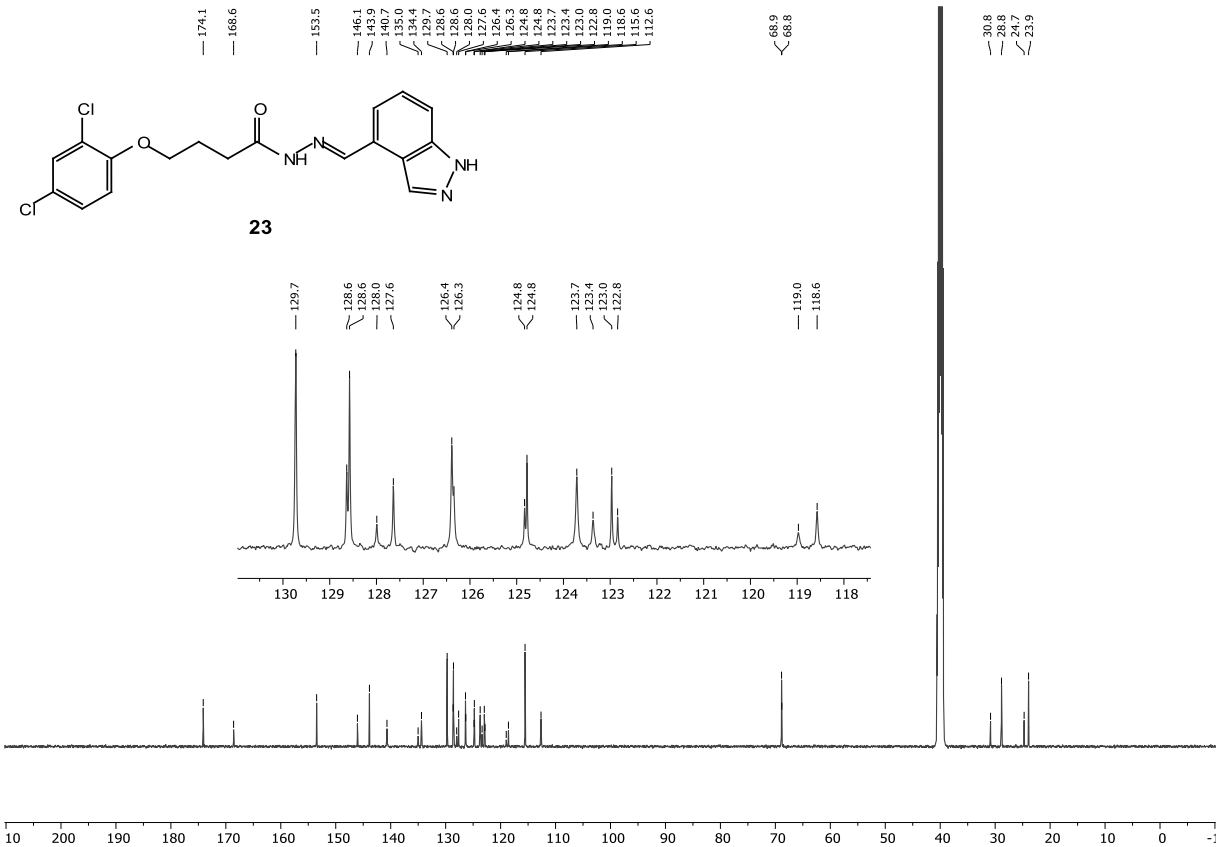

Supplementary Figure 81 ^{13}C NMR spectrum of **22.**

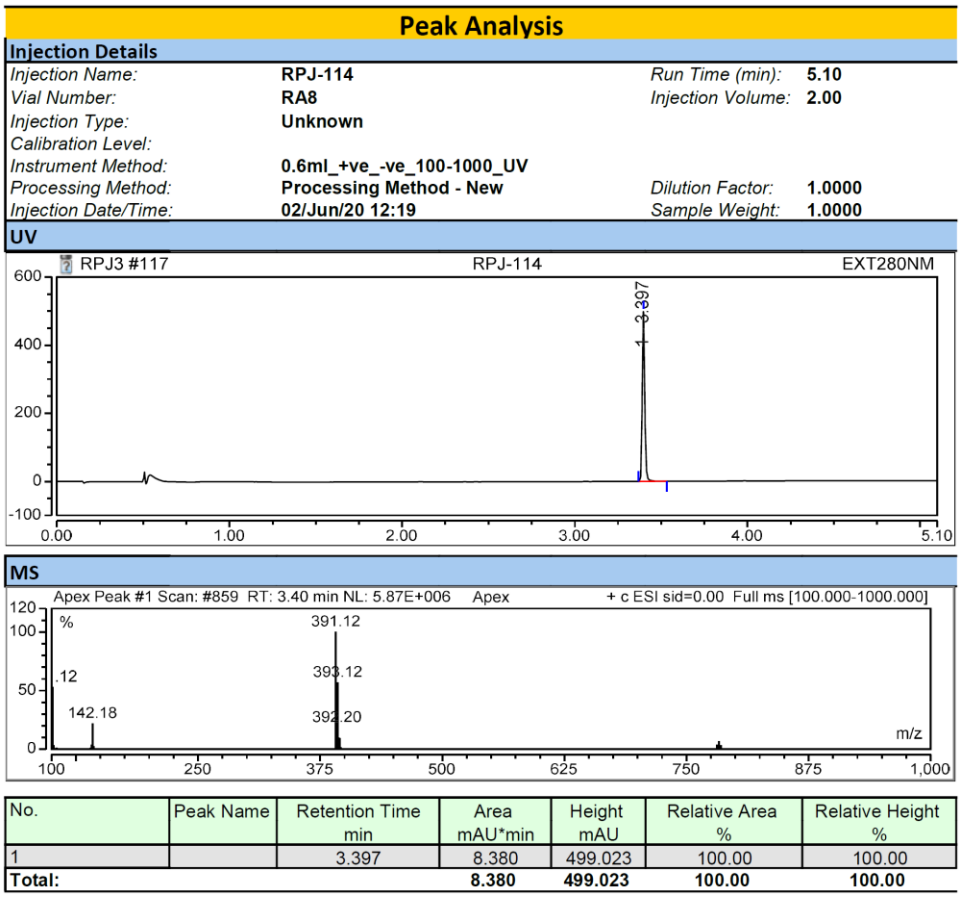

No.	Peak Name	Retention Time min	Area mAU*min	Height mAU	Relative Area %	Relative Height %
1		3.397	8.380	499.023	100.00	100.00
Total:			**8.380**	**499.023**	**100.00**	**100.00**

Supplementary Figure 82 HPLC purity analysis of **22.**

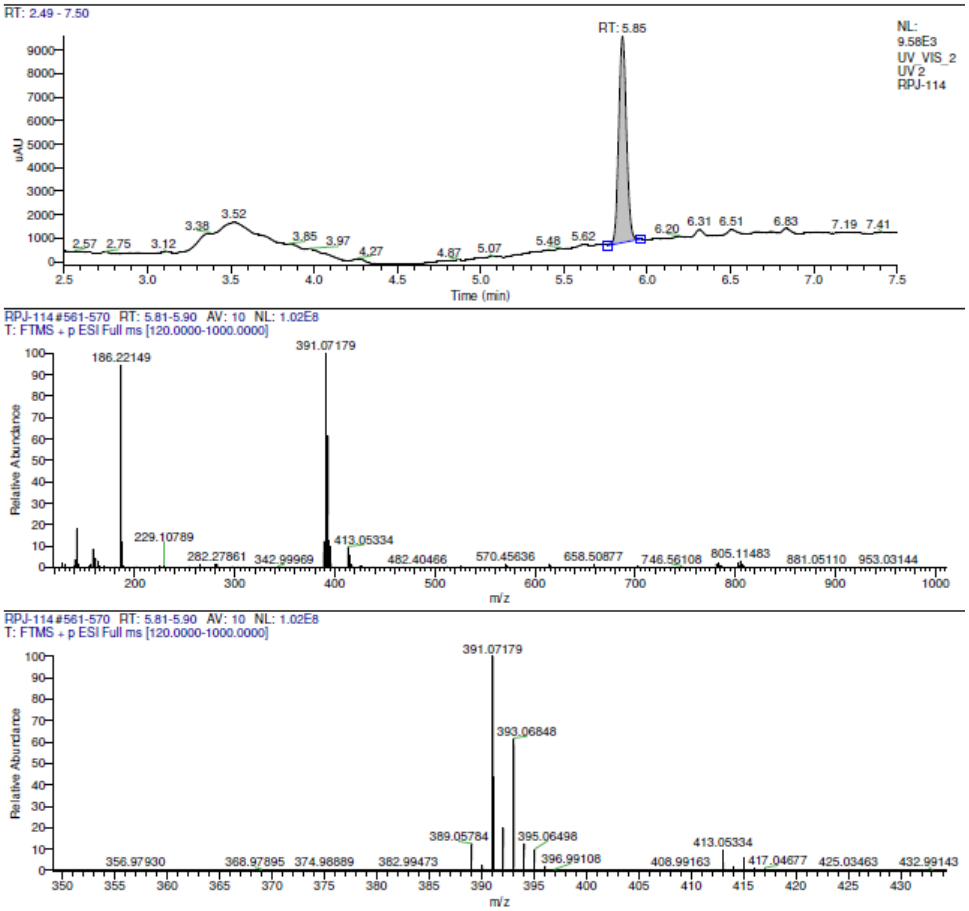

Supplementary Figure 83 HRMS of **22.**

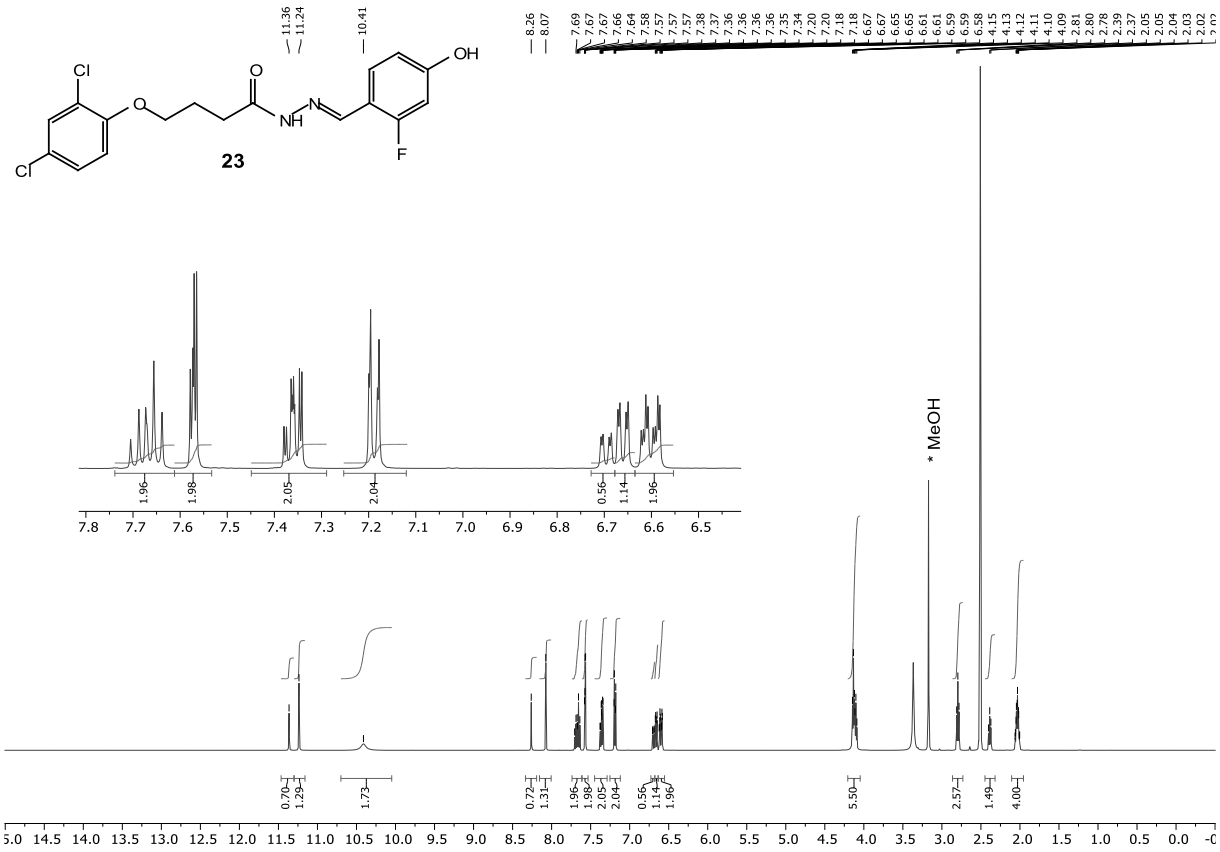

Supplementary Figure 84 ^{1}H NMR spectrum of **23.**

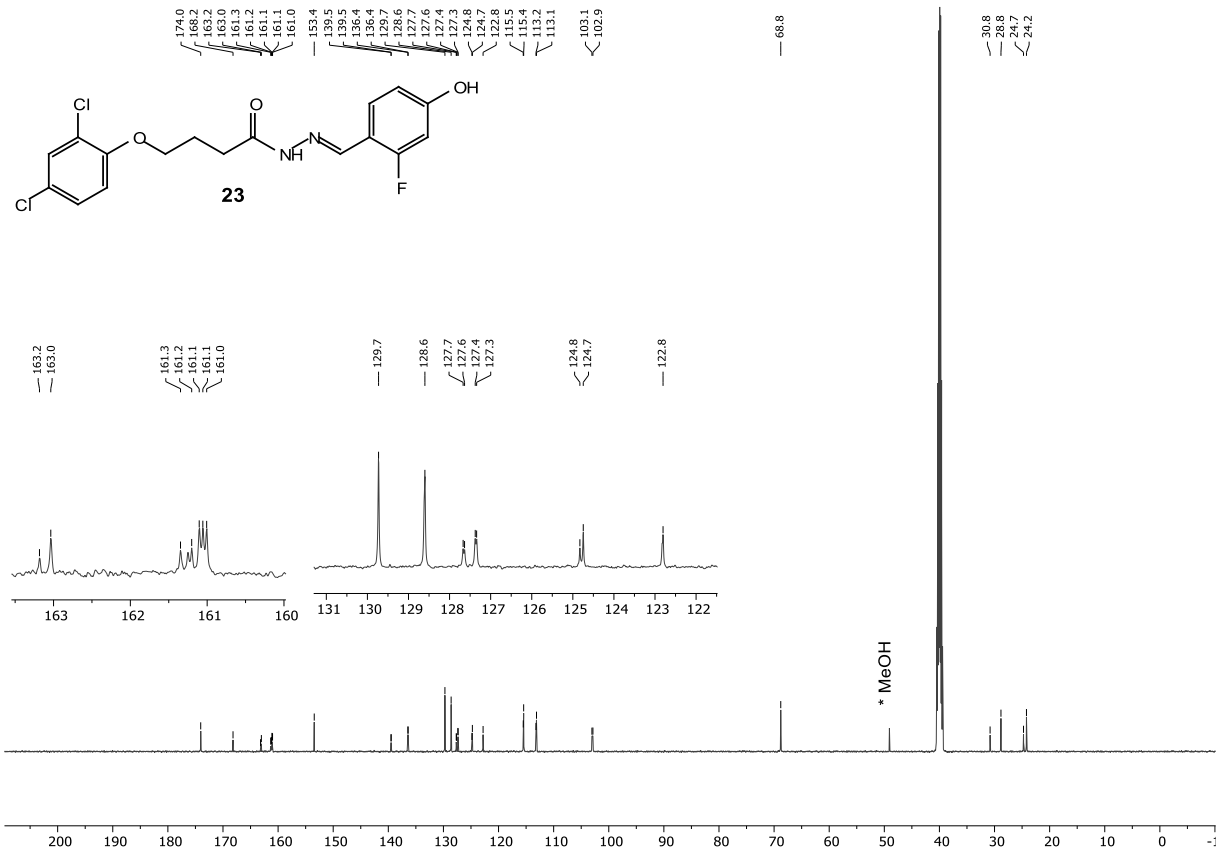

Supplementary Figure 85 ^{13}C NMR spectrum of **23.**

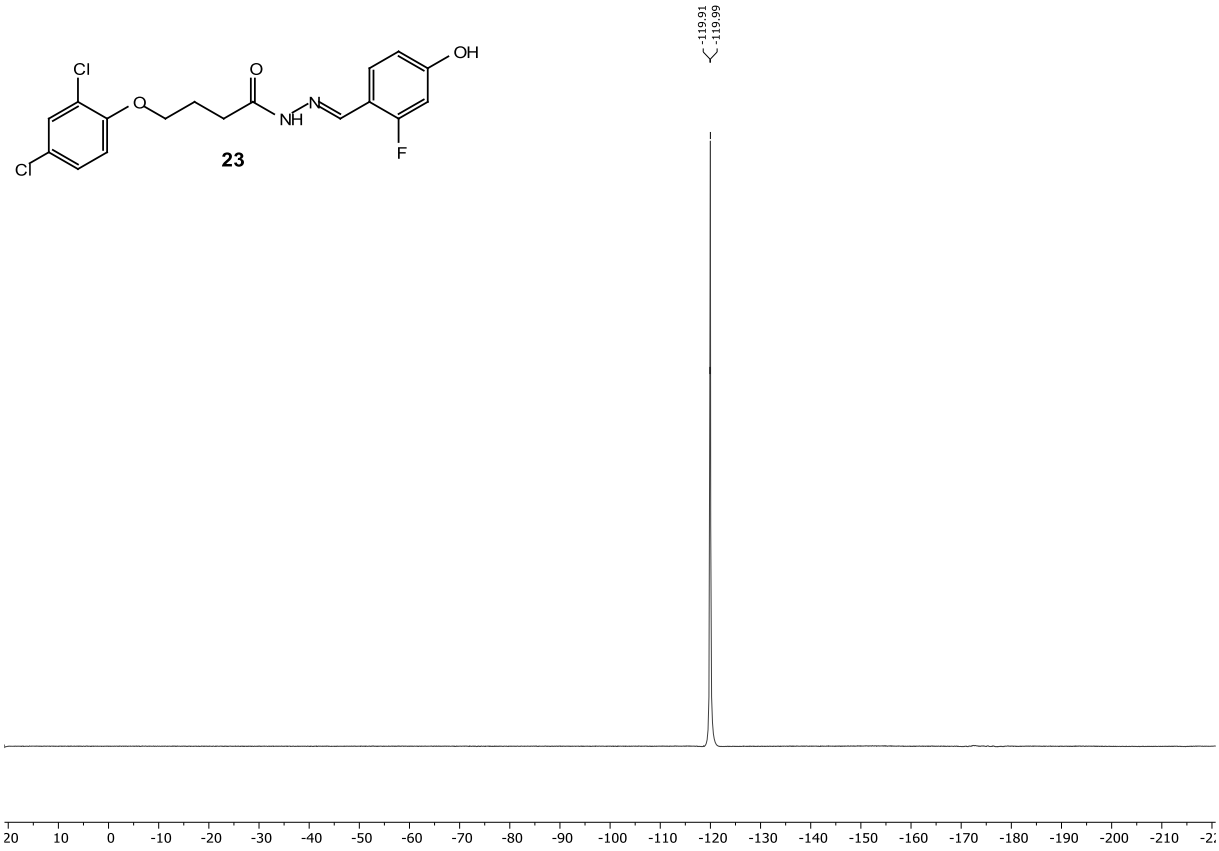

Supplementary Figure 86 ^{19}F NMR spectrum of **23.**

Peak Analysis

Injection Details			
Injection Name:	**RPJ-132**	*Run Time (min):*	**5.10**
Vial Number:	**RC6**	*Injection Volume:*	**6.00**
Injection Type:	**Unknown**		
Calibration Level:			
Instrument Method:	**0.6ml_+ve_-ve_100-1000_UV**		
Processing Method:	**Processing Method - New**	*Dilution Factor:*	**1.0000**
Injection Date/Time:	**30/May/20 21:18**	*Sample Weight:*	**1.0000**

UV

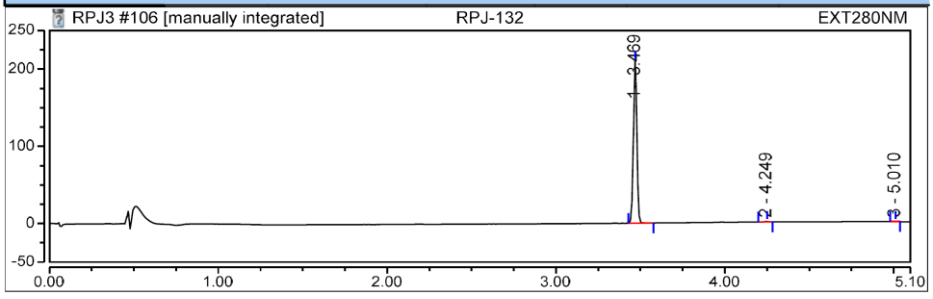

MS

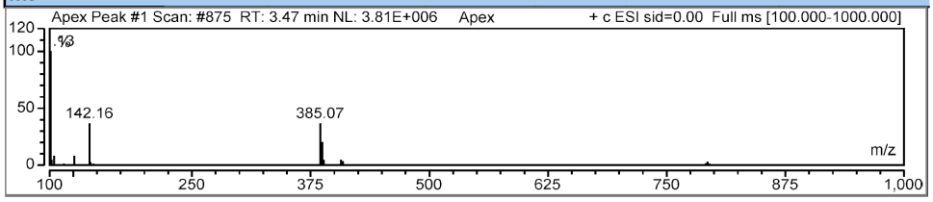

No.	Peak Name	Retention Time min	Area mAU*min	Height mAU	Relative Area %	Relative Height %
1		3.469	5.029	209.891	99.52	99.37
2		4.249	0.016	0.848	0.31	0.40
3		5.010	0.009	0.472	0.17	0.22
Total:			**5.053**	**211.212**	**100.00**	**100.00**

Supplementary Figure 87 HPLC purity analysis of **23.**

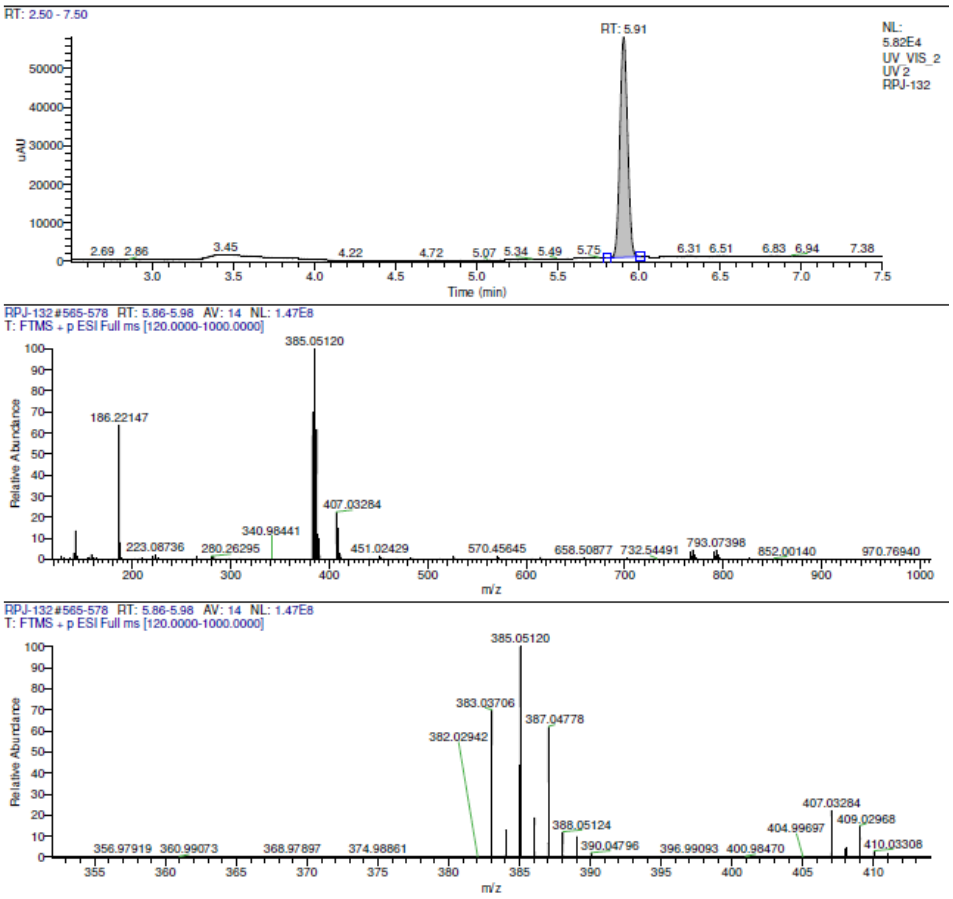

Supplementary Figure 88 HRMS of **23.**

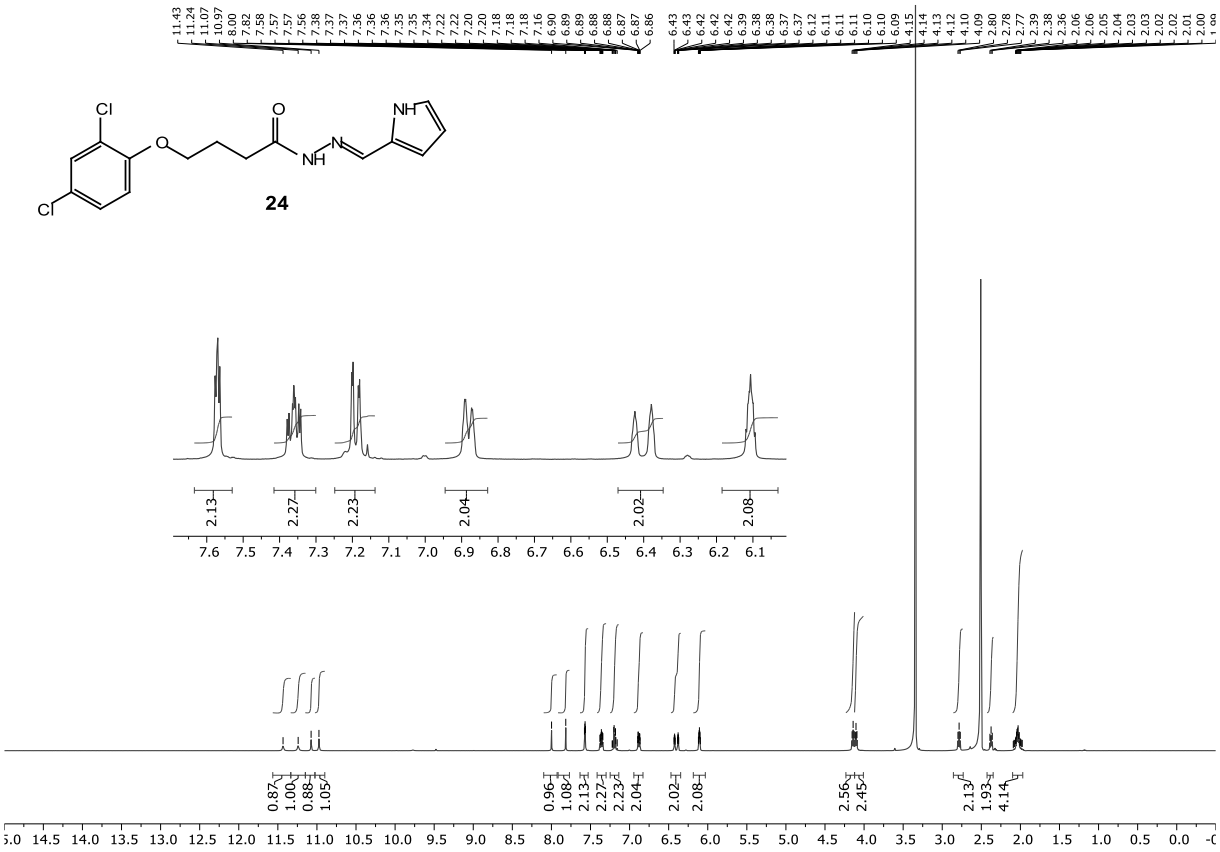

Supplementary Figure 89 ^{1}H NMR spectrum of **24.**

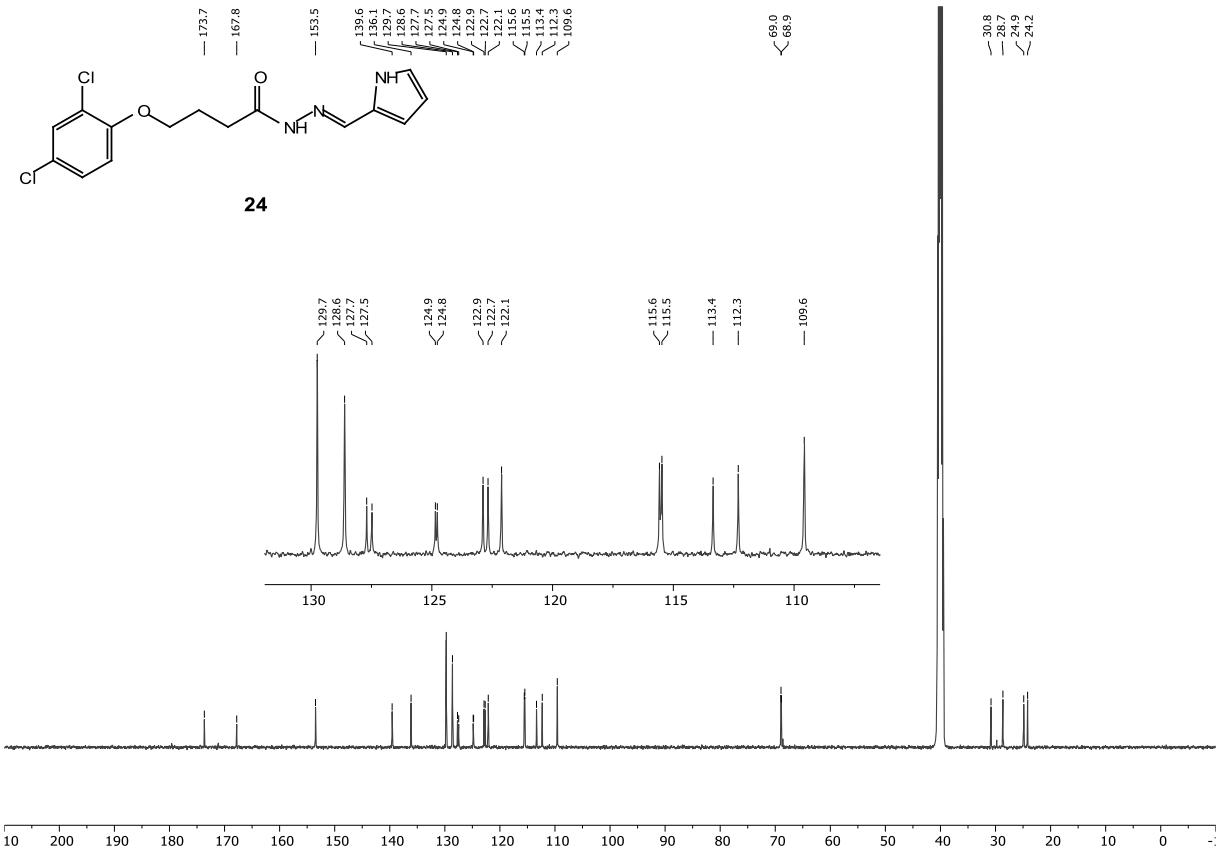

Supplementary Figure 90 ^{13}C NMR spectrum of **24.**

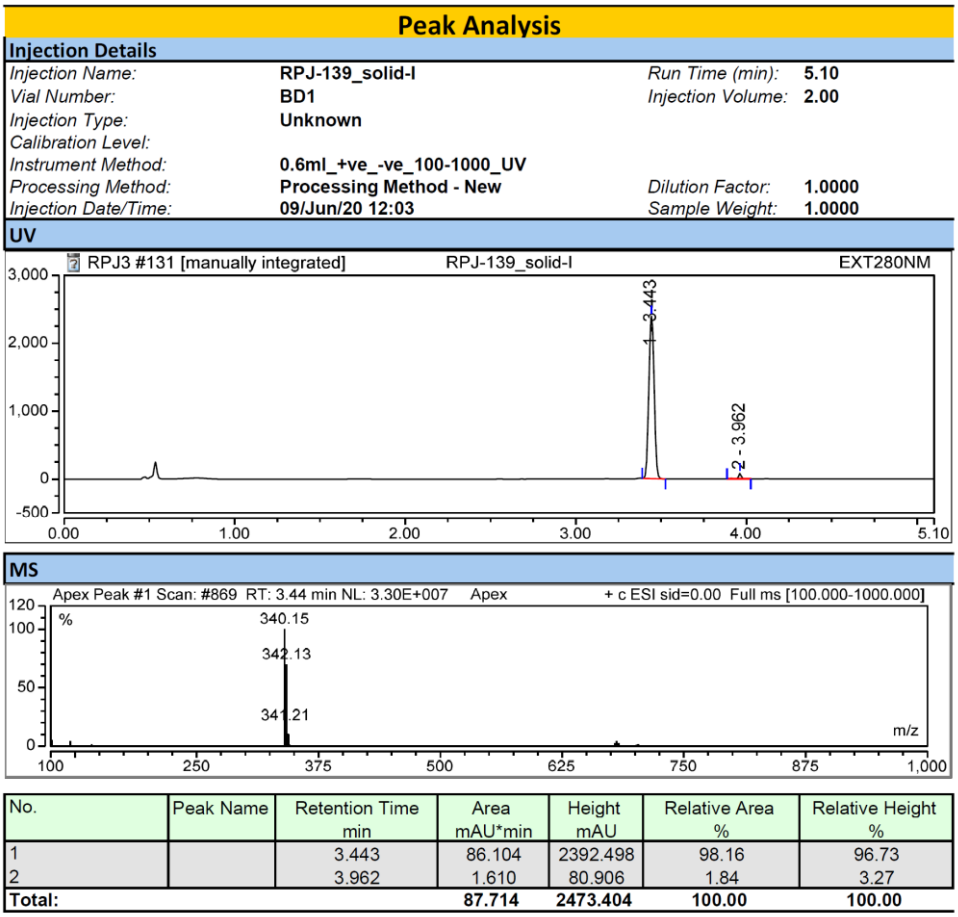

No.	Peak Name	Retention Time min	Area mAU*min	Height mAU	Relative Area %	Relative Height %
1		3.443	86.104	2392.498	98.16	96.73
2		3.962	1.610	80.906	1.84	3.27
Total:			**87.714**	**2473.404**	**100.00**	**100.00**

Supplementary Figure 91 HPLC purity analysis of **24.**

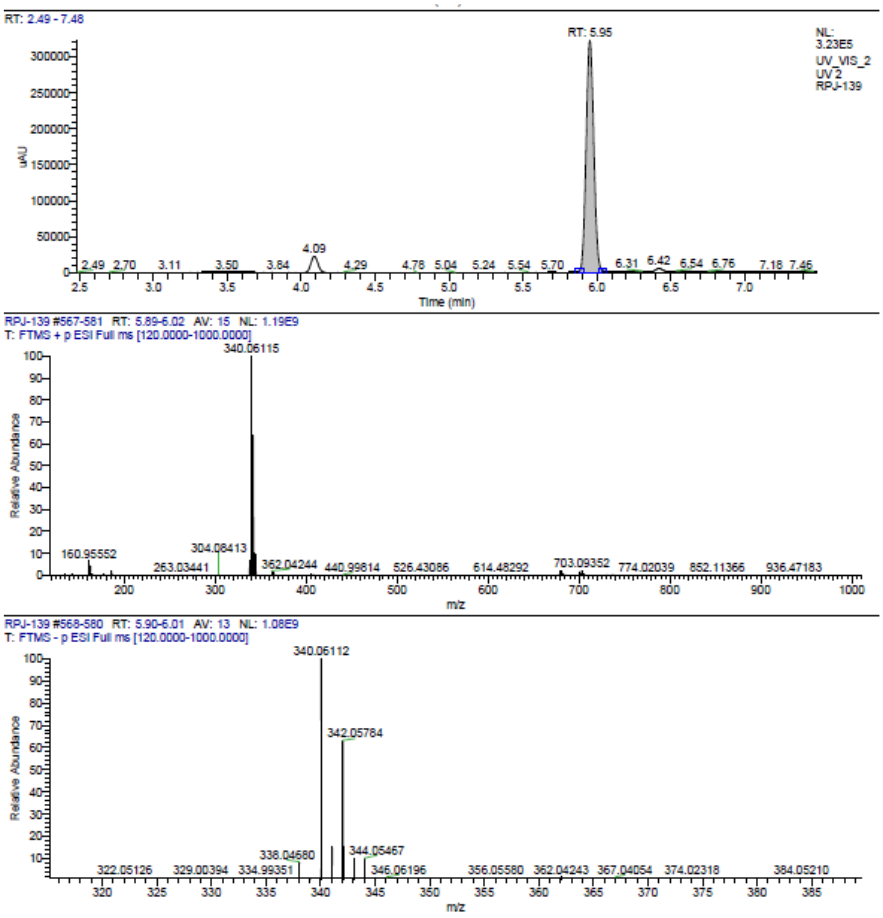

Supplementary Figure 92 HRMS of **24.**

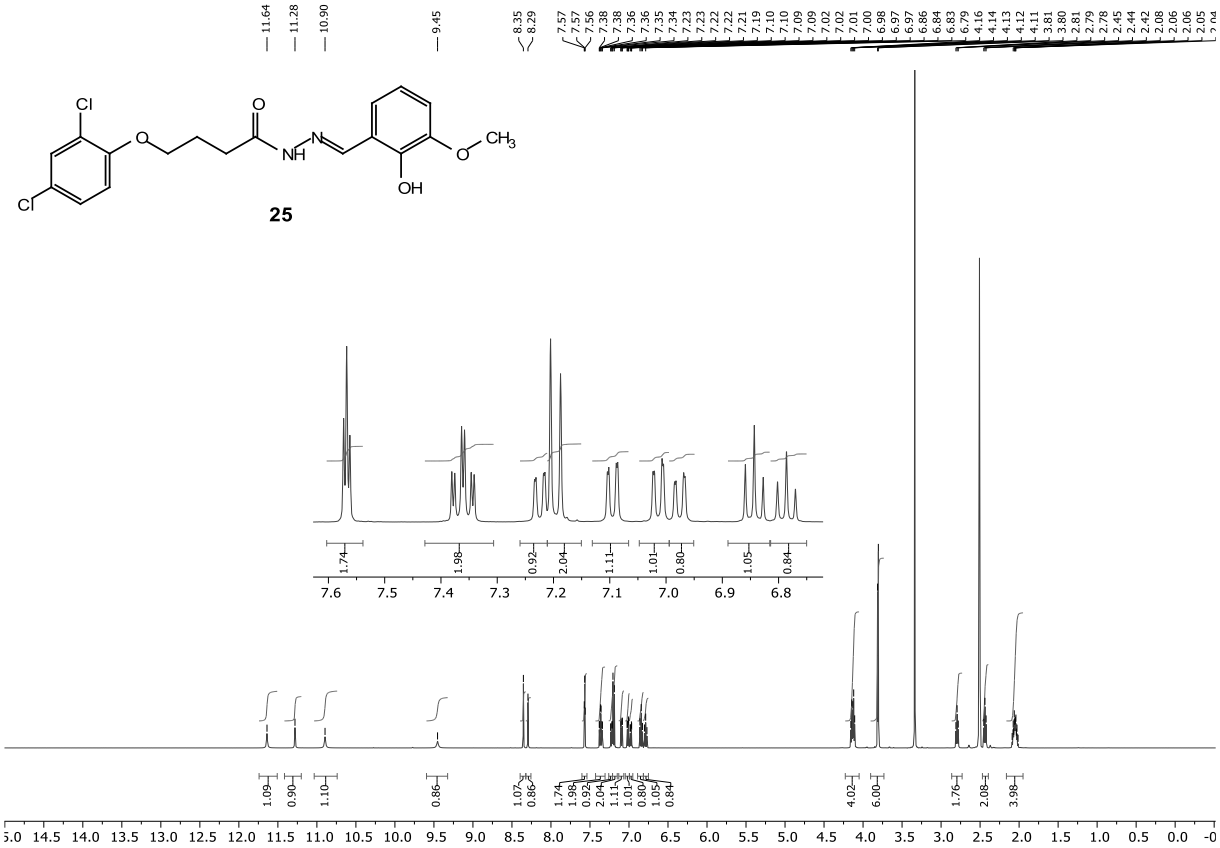

Supplementary Figure 93 ^{1}H NMR spectrum of **25.**

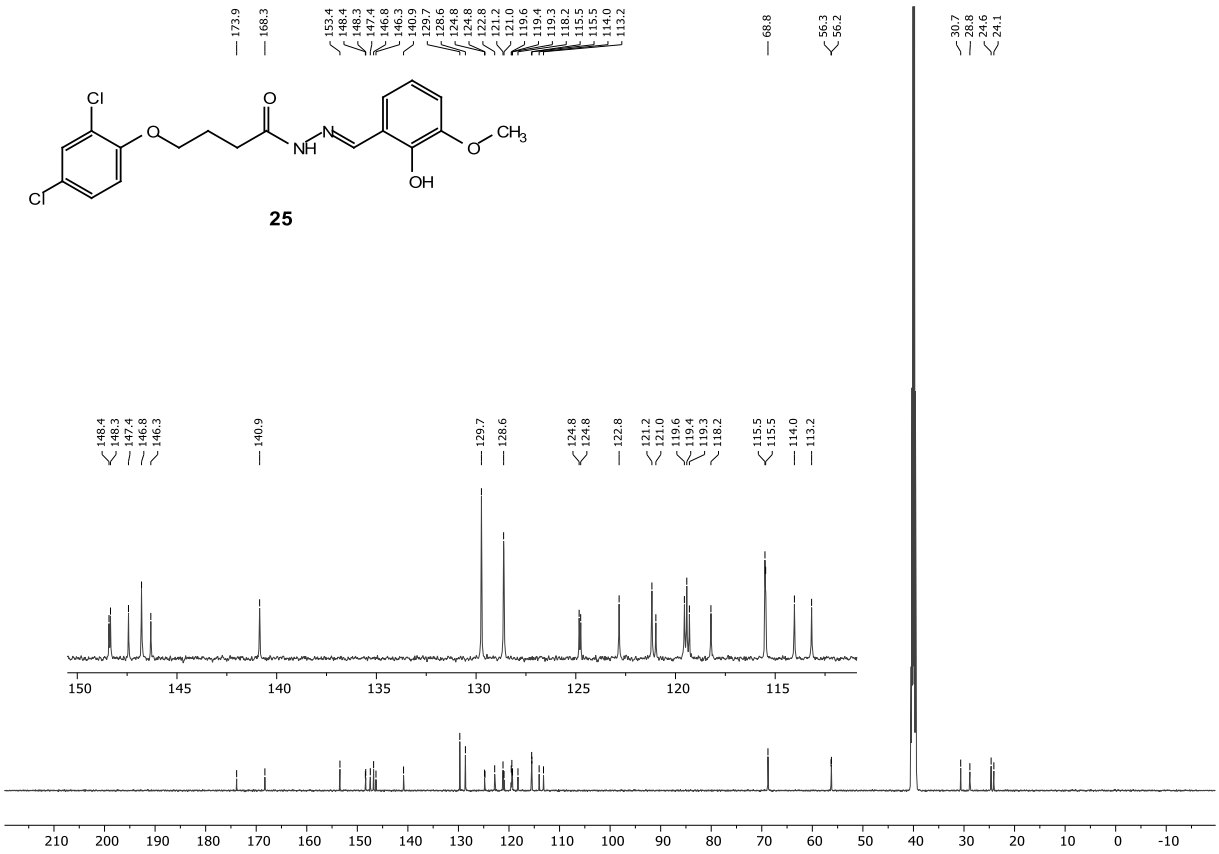

Supplementary Figure 94 ^{13}C NMR spectrum of **25.**

Peak Analysis

Injection Details

Injection Name:	**RPJ-131**	*Run Time (min):*	**5.10**
Vial Number:	**RC5**	*Injection Volume:*	**6.00**
Injection Type:	**Unknown**		
Calibration Level:			
Instrument Method:	**0.6ml_+ve_-ve_100-1000_UV**		
Processing Method:	**Processing Method - New**	*Dilution Factor:*	**1.0000**
Injection Date/Time:	**30/May/20 21:11**	*Sample Weight:*	**1.0000**

UV

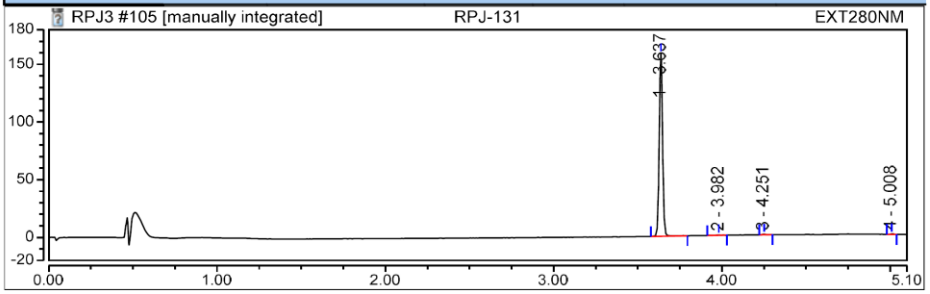

MS

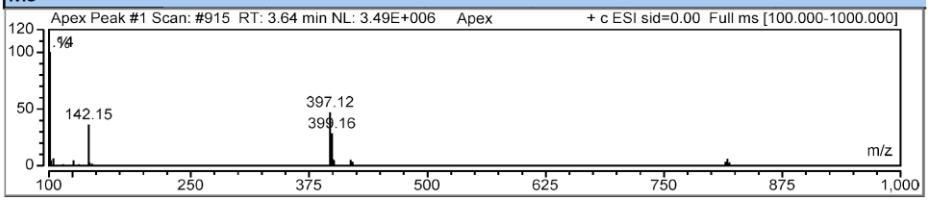

No.	Peak Name	Retention Time min	Area mAU*min	Height mAU	Relative Area %	Relative Height %
1		3.637	3.596	158.304	99.19	99.15
2		3.982	0.011	0.315	0.29	0.20
3		4.251	0.009	0.572	0.25	0.36
4		5.008	0.010	0.467	0.26	0.29
Total:			**3.625**	**159.658**	**100.00**	**100.00**

Supplementary Figure 95 HPLC purity analysis of **25.**

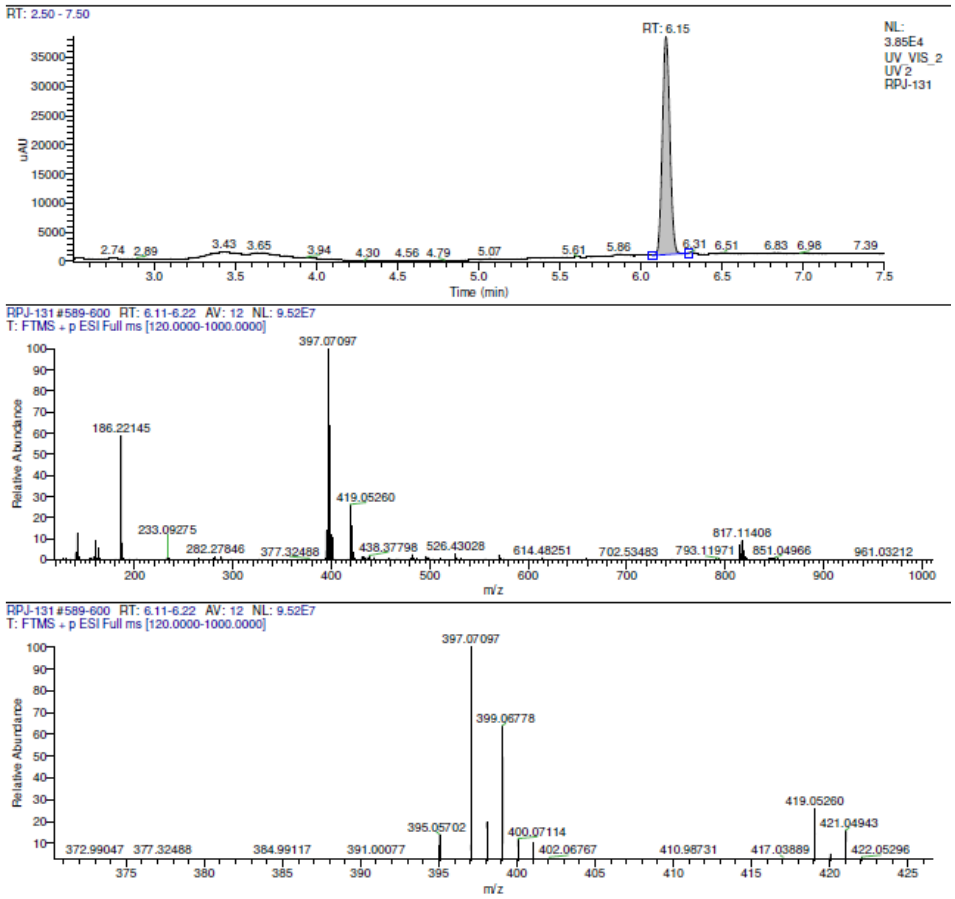

Supplementary Figure 96 HRMS of **25.**

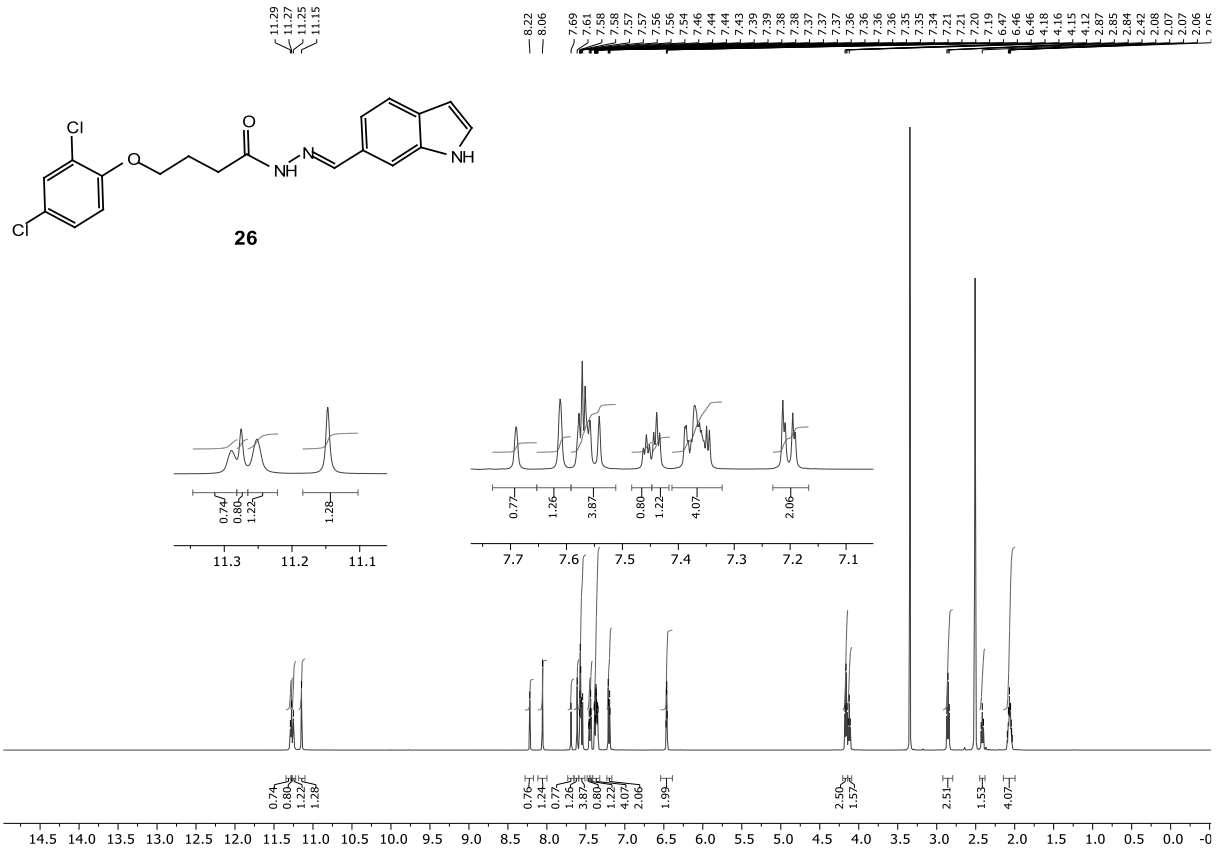

Supplementary Figure 97 ^{1}H NMR spectrum of **26.**

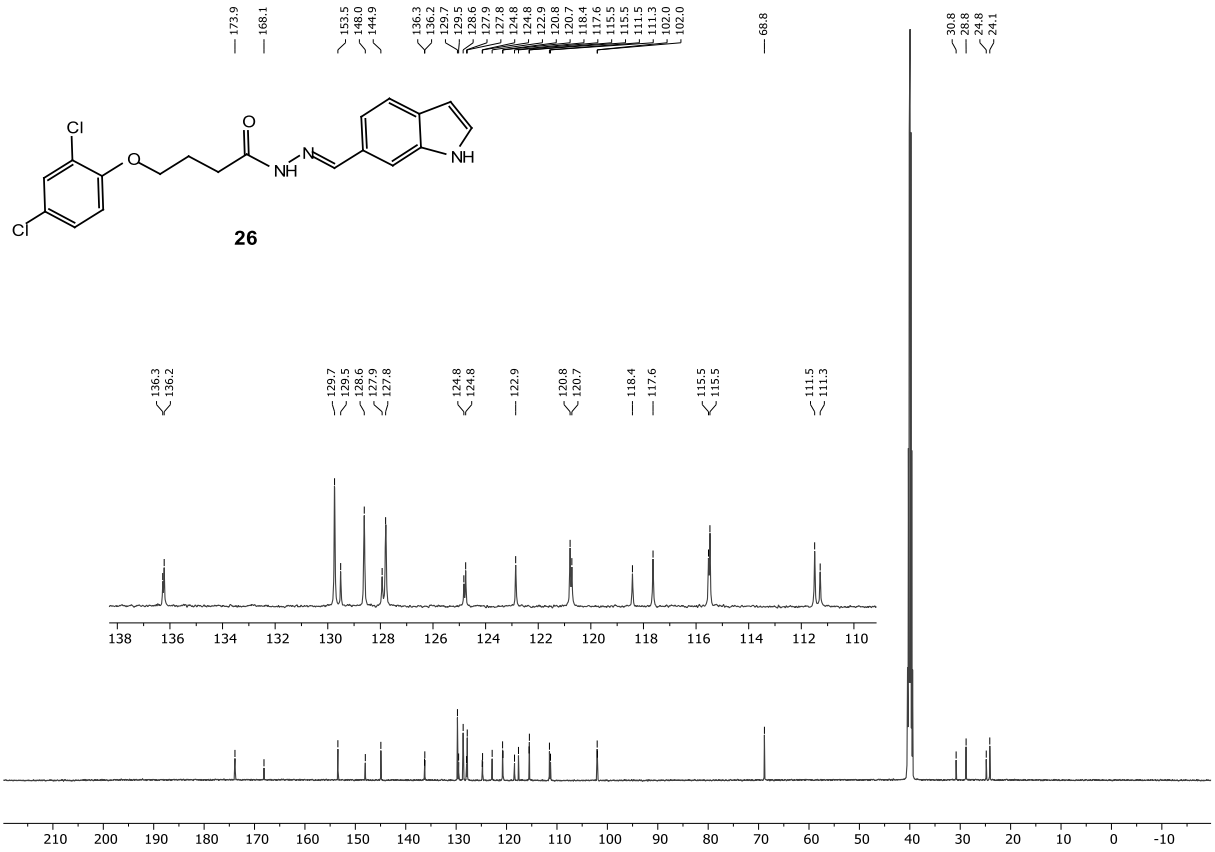

Supplementary Figure 98 ^{13}C NMR spectrum of **26.**

Peak Analysis

Injection Details

Injection Name:	**RPJ-130**	*Run Time (min):*	**5.10**
Vial Number:	**RB1**	*Injection Volume:*	**2.00**
Injection Type:	**Unknown**		
Calibration Level:			
Instrument Method:	**0.6ml_+ve_-ve_100-1000_UV**		
Processing Method:	**Processing Method - New**	*Dilution Factor:*	**1.0000**
Injection Date/Time:	**02/Jun/20 12:26**	*Sample Weight:*	**1.0000**

UV

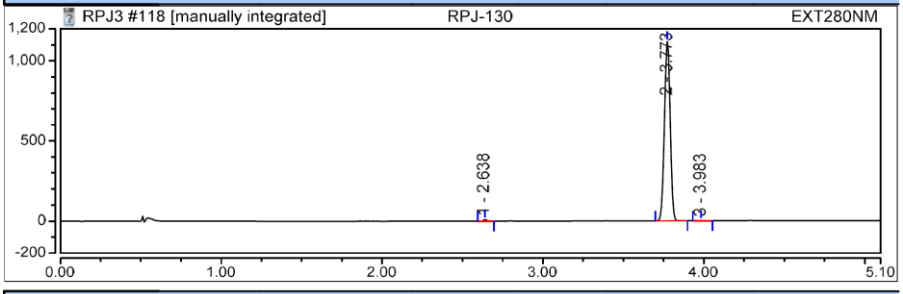

MS

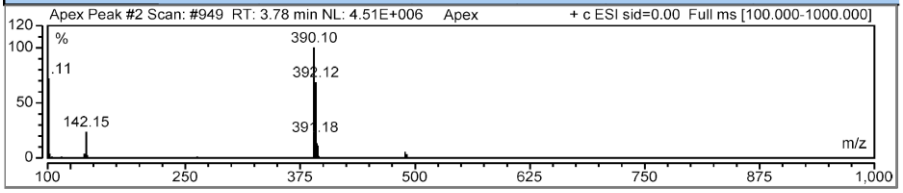

No.	Peak Name	Retention Time min	Area mAU*min	Height mAU	Relative Area %	Relative Height %
1		2.638	0.234	9.281	0.51	0.82
2		3.773	45.787	1120.564	99.34	98.92
3		3.983	0.068	2.994	0.15	0.26
Total:			**46.089**	**1132.838**	**100.00**	**100.00**

Supplementary Figure 99 HPLC purity analysis of **26.**

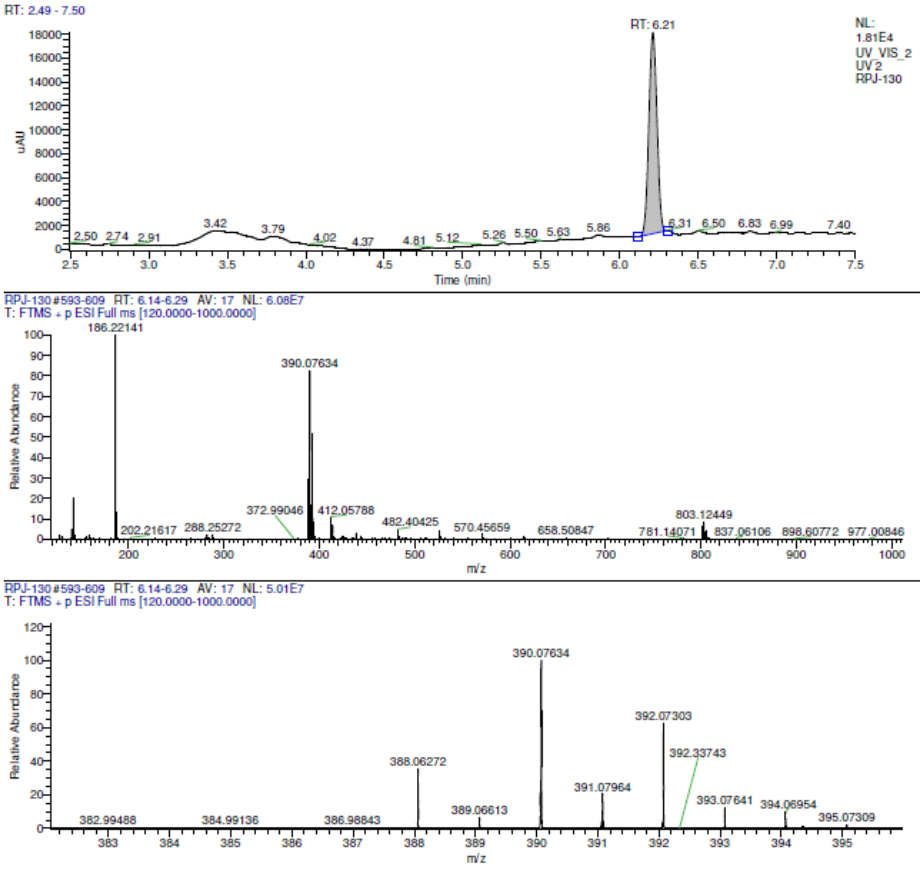

Supplementary Figure 100 HRMS of **26.**

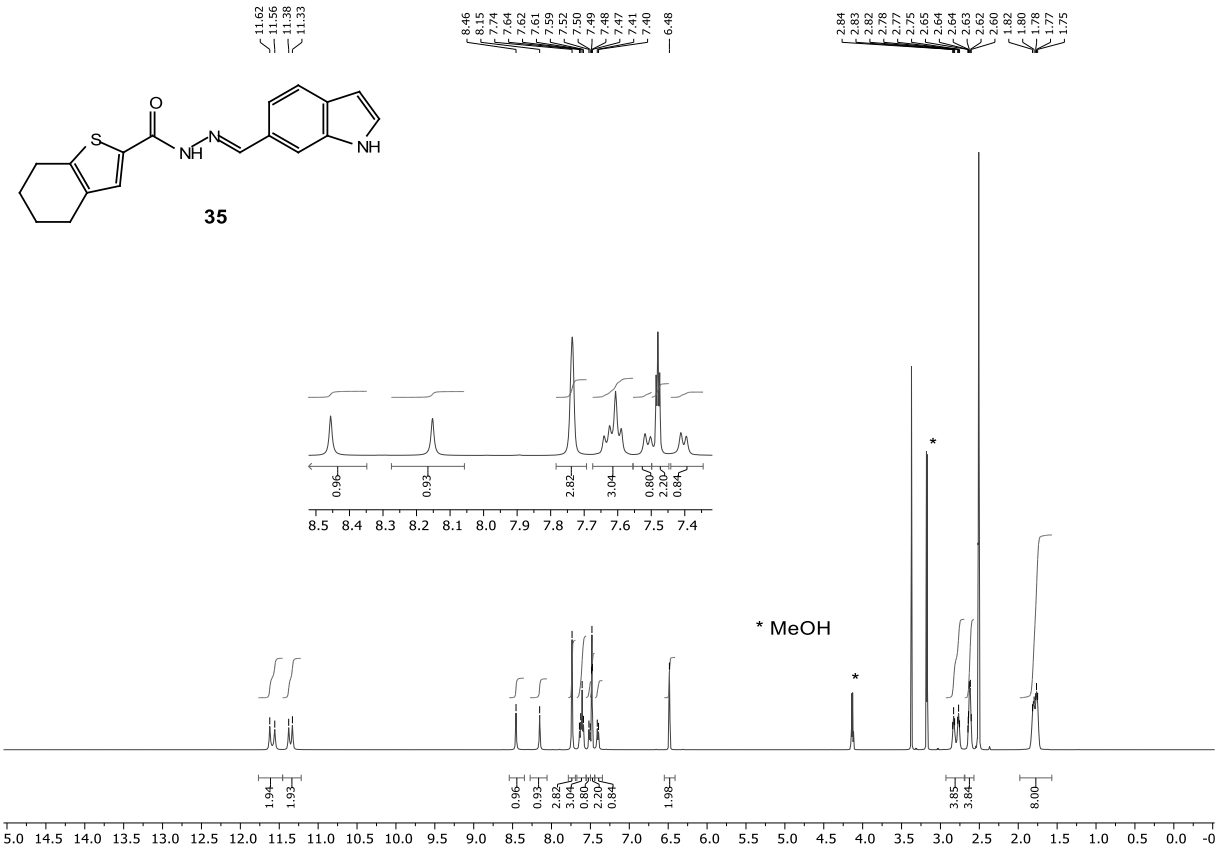

Supplementary Figure 101 ^{1}H NMR spectrum of **35.**

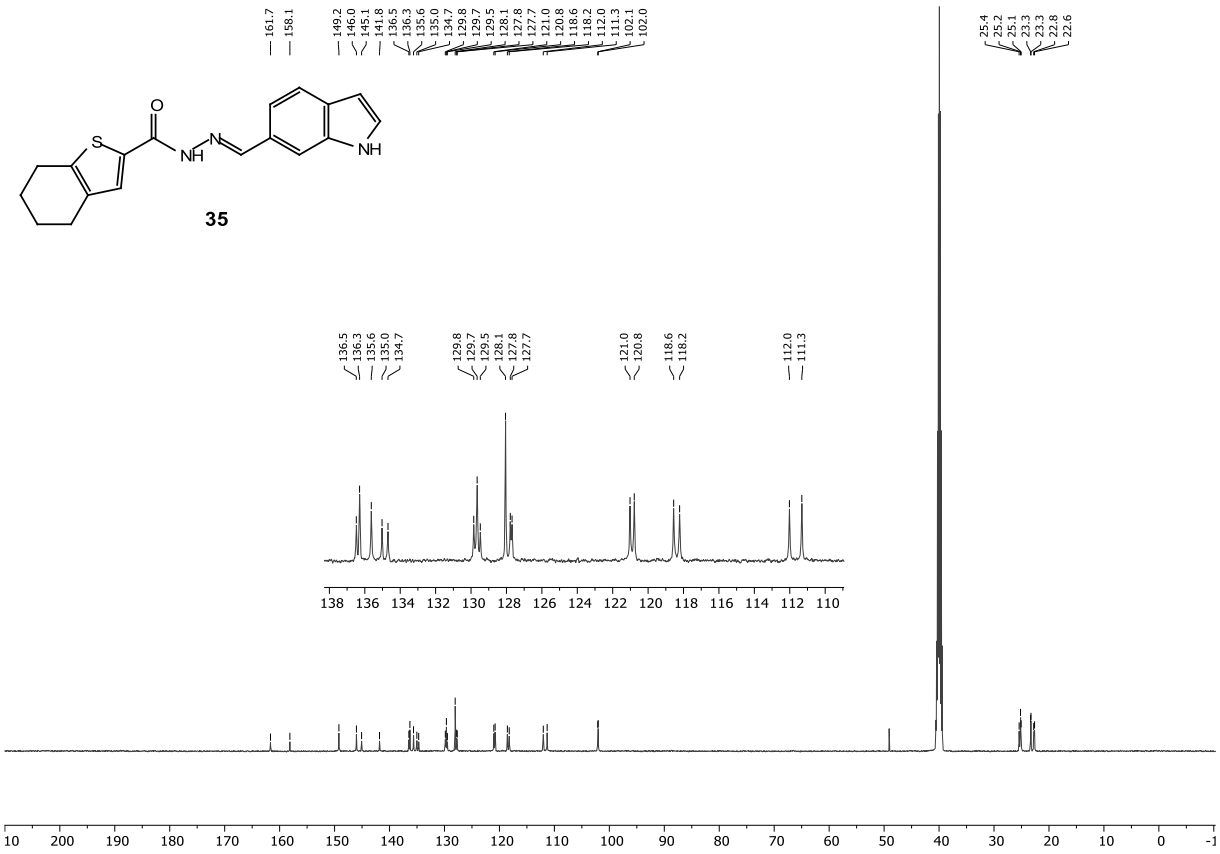

Supplementary Figure 102 ^{13}C NMR spectrum of **35.**

Peak Analysis

Injection Details

Injection Name:	**RPJ-110**	*Run Time (min):*	**5.10**
Vial Number:	**RB3**	*Injection Volume:*	**6.00**
Injection Type:	**Unknown**		
Calibration Level:			
Instrument Method:	**0.6ml_+ve_-ve_100-1000_UV**		
Processing Method:	**Processing Method - New**	*Dilution Factor:*	**1.0000**
Injection Date/Time:	**30/May/20 20:00**	*Sample Weight:*	**1.0000**

UV

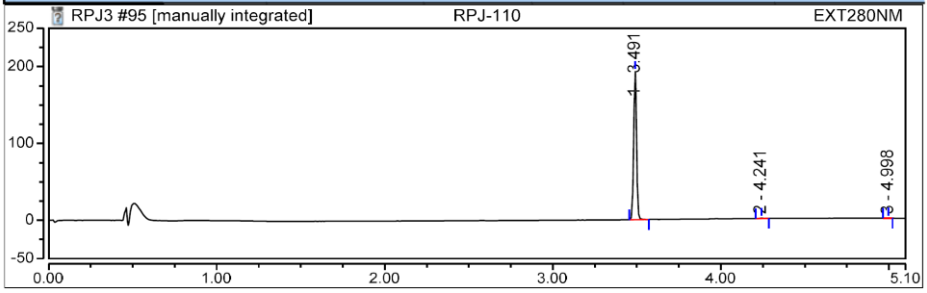

MS

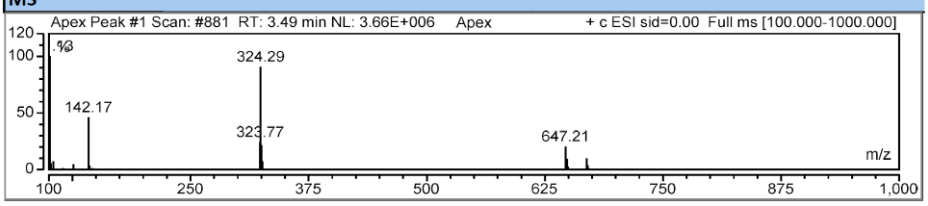

No.	Peak Name	Retention Time min	Area mAU*min	Height mAU	Relative Area %	Relative Height %
1		3.491	3.781	193.105	99.54	99.45
2		4.241	0.010	0.625	0.26	0.32
3		4.998	0.008	0.441	0.20	0.23
Total:			**3.798**	**194.171**	**100.00**	**100.00**

Supplementary Figure 103 HPLC purity analysis of **35.**

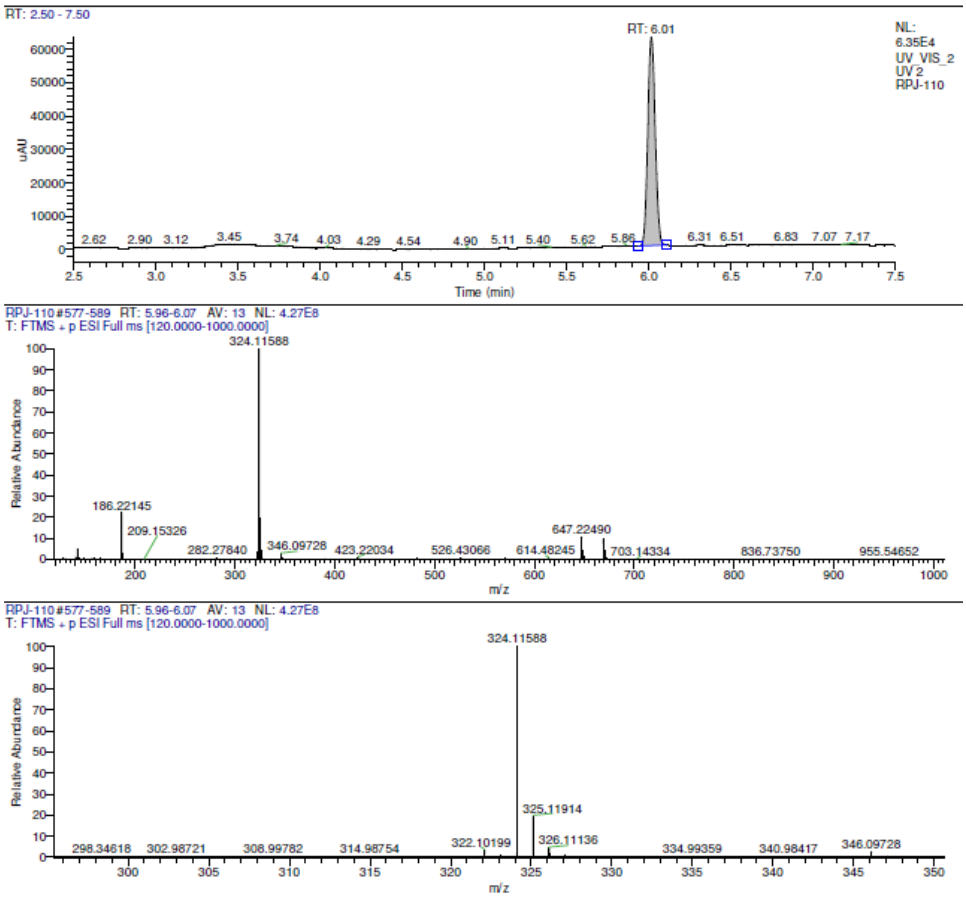

Supplementary Figure 104 HRMS of **35.**

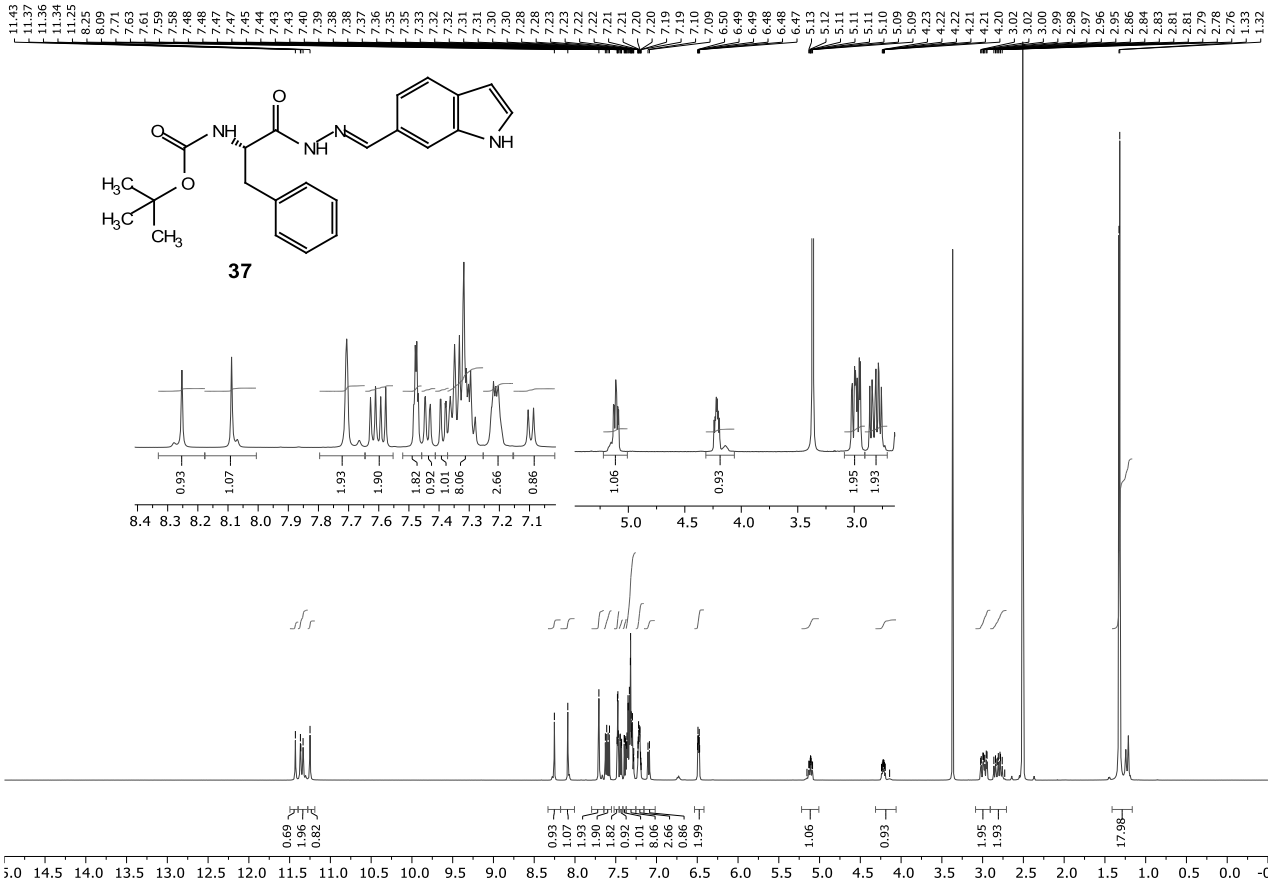

Supplementary Figure 105 ^{1}H NMR spectrum of **37.**

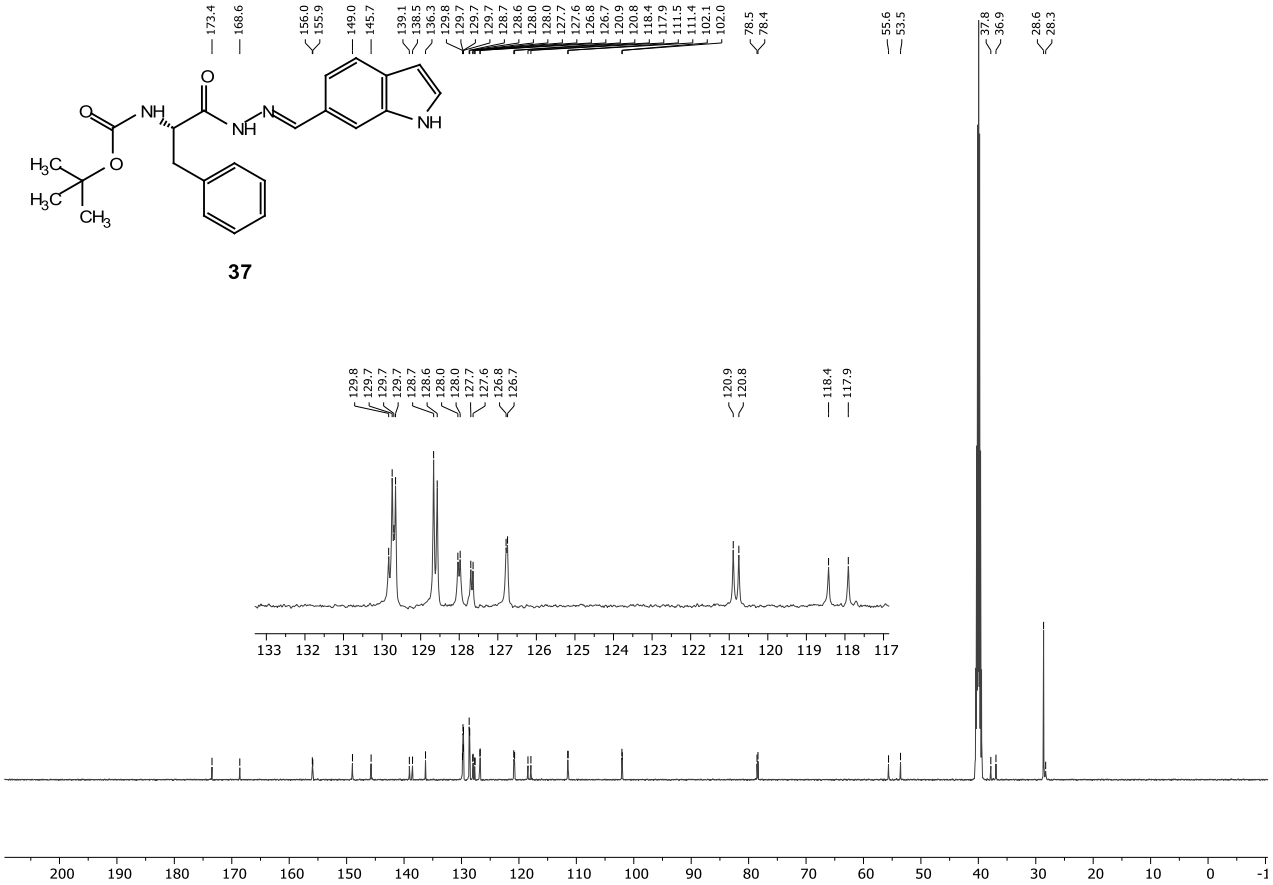

Supplementary Figure 106 ^{13}C NMR spectrum of **37.**

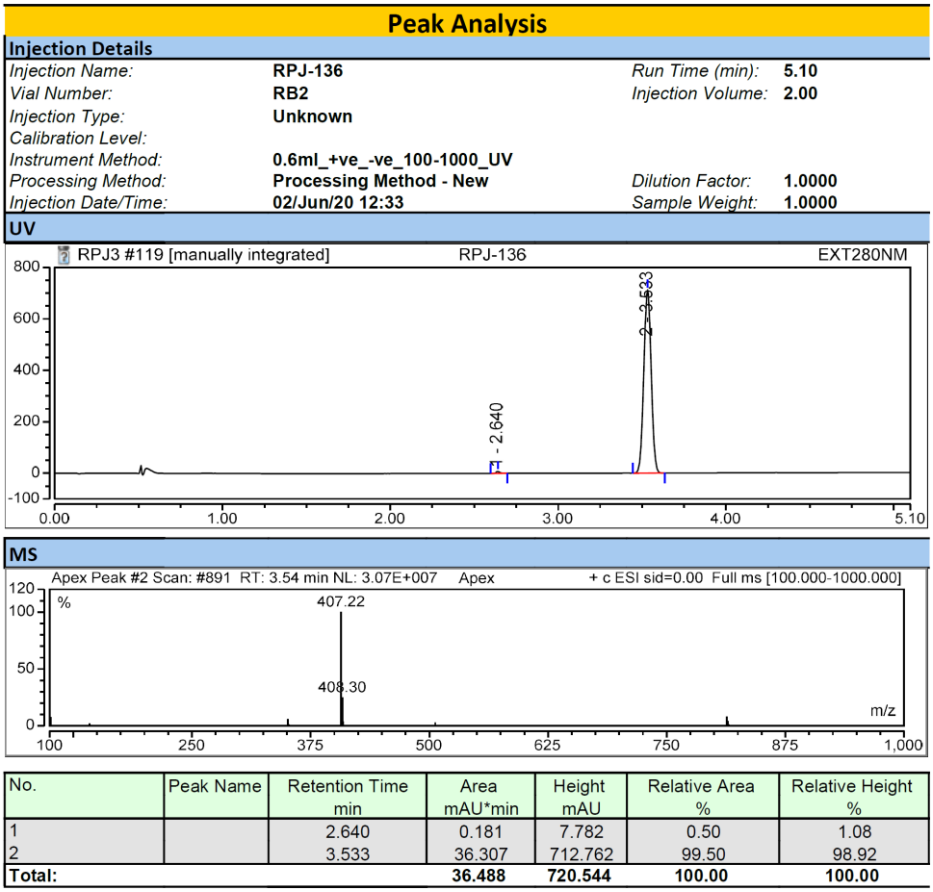

No.	Peak Name	Retention Time min	Area mAU*min	Height mAU	Relative Area %	Relative Height %
1		2.640	0.181	7.782	0.50	1.08
2		3.533	36.307	712.762	99.50	98.92
Total:			**36.488**	**720.544**	**100.00**	**100.00**

Supplementary Figure 107 HPLC purity analysis of **37.**

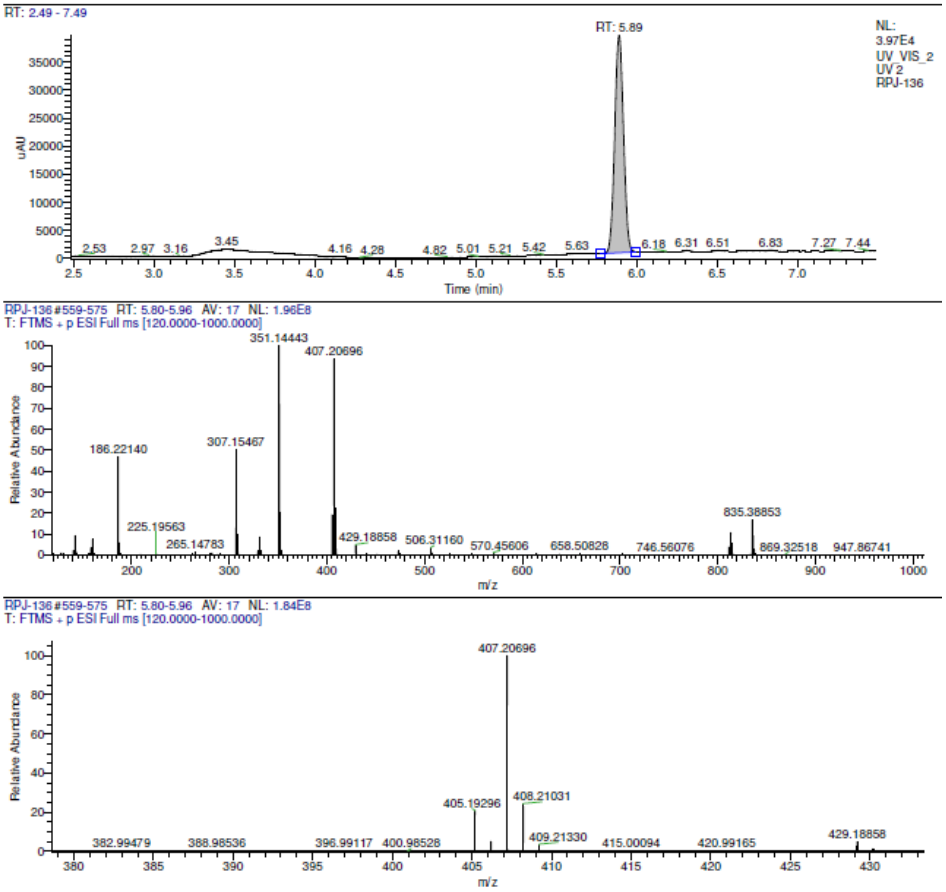

Supplementary Figure 108 HRMS of **37.**

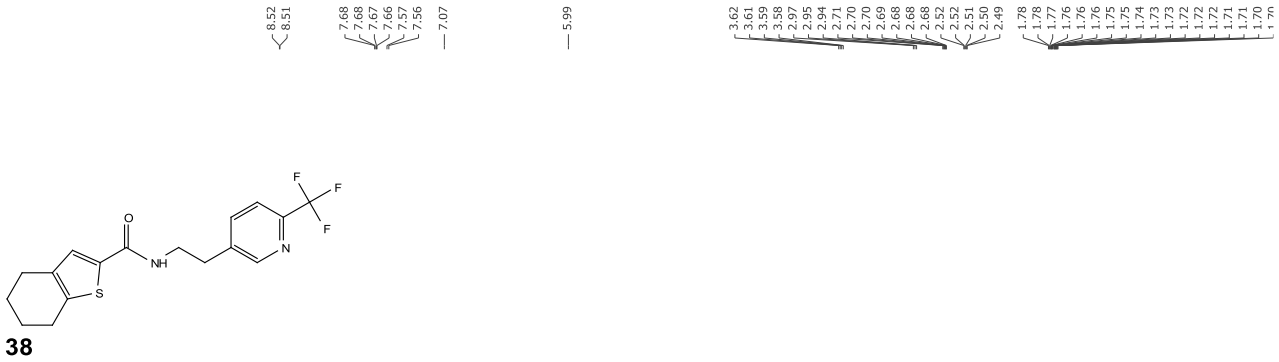

38

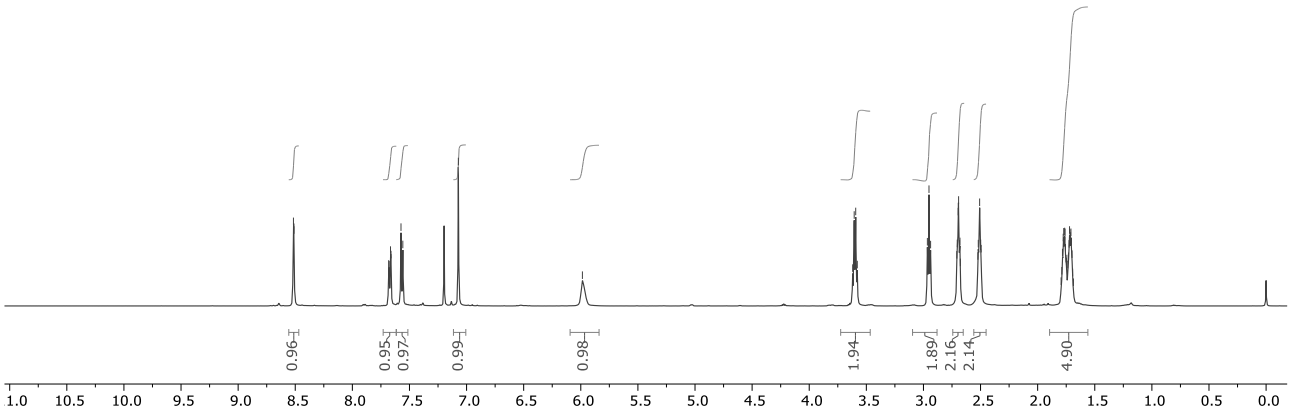

Supplementary Figure 109 ^{1}H NMR spectrum of **38.**

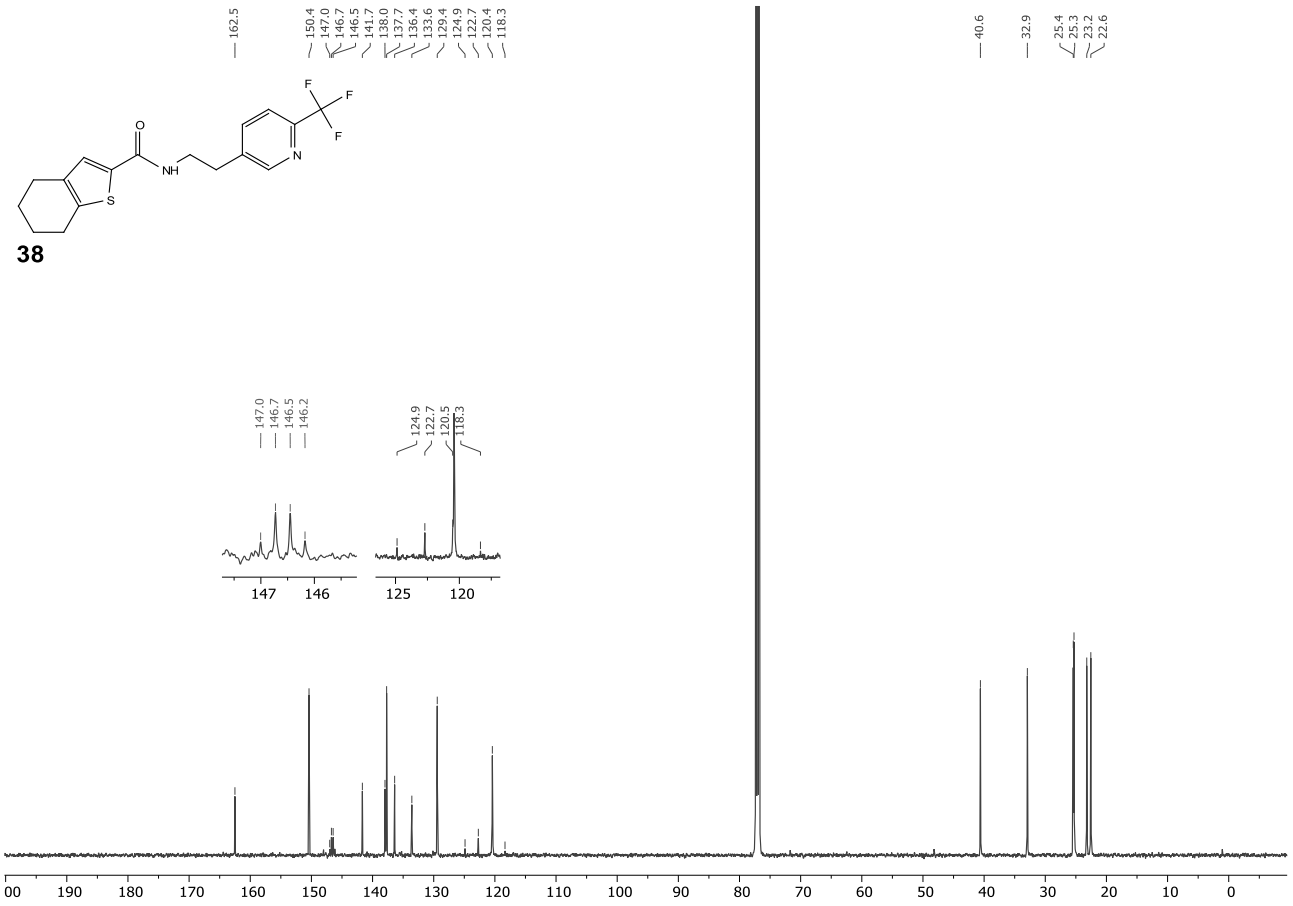

Supplementary Figure 110 ^{13}C NMR spectrum of **38.**

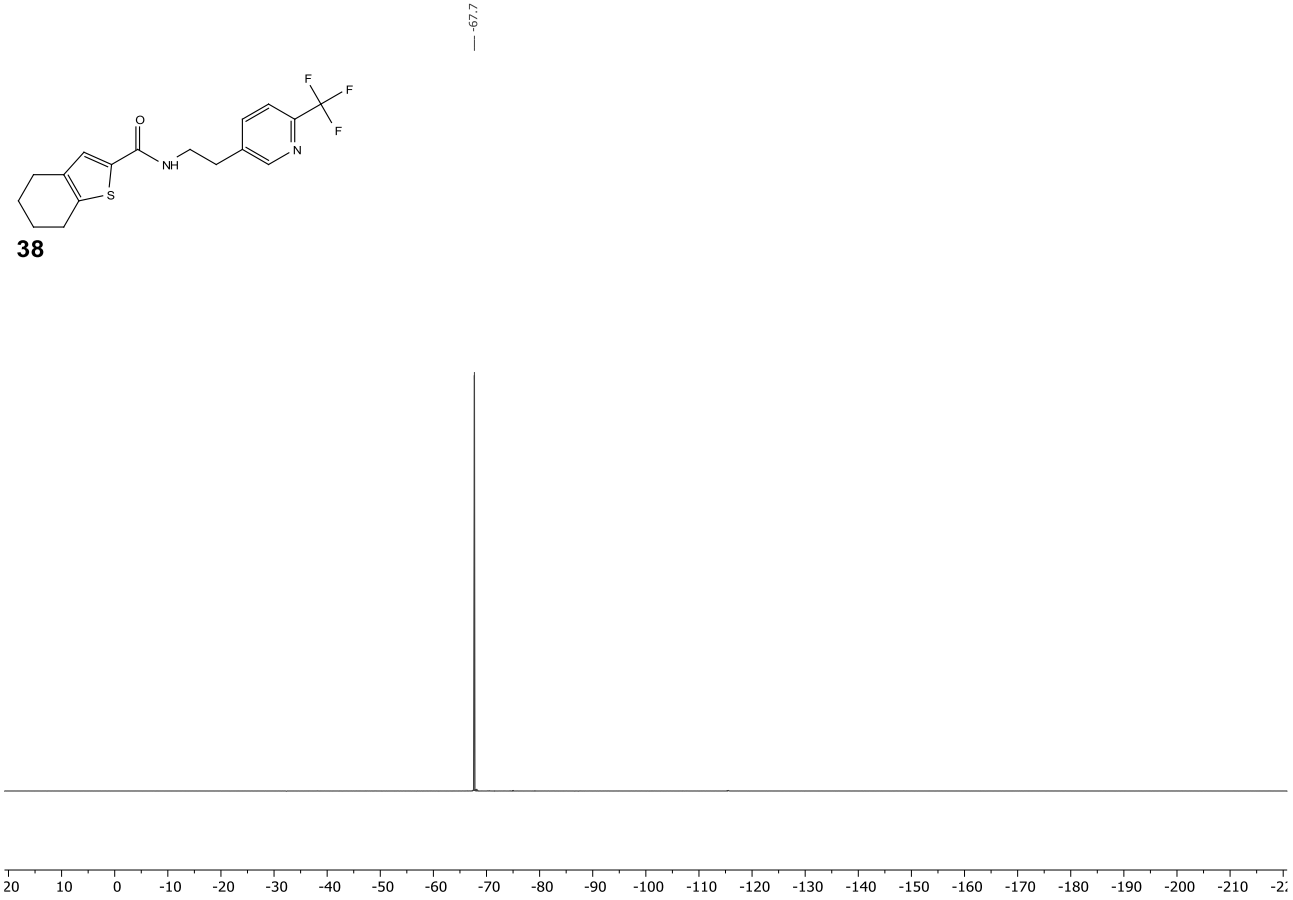

Supplementary Figure 111 ^{19}F NMR spectrum of **38.**

Peak Analysis

Injection Details

Injection Name:	**RPJ221-purity**	*Run Time (min):*	**5.10**
Vial Number:	**BD2**	*Injection Volume:*	**2.00**
Injection Type:	**Unknown**		
Calibration Level:			
Instrument Method:	**0.6ml_+ve_-ve_100-1000_UV**		
Processing Method:	**Processing Method - New**	*Dilution Factor:*	**1.0000**
Injection Date/Time:	**08/Mar/21 12:01**	*Sample Weight:*	**1.0000**

UV

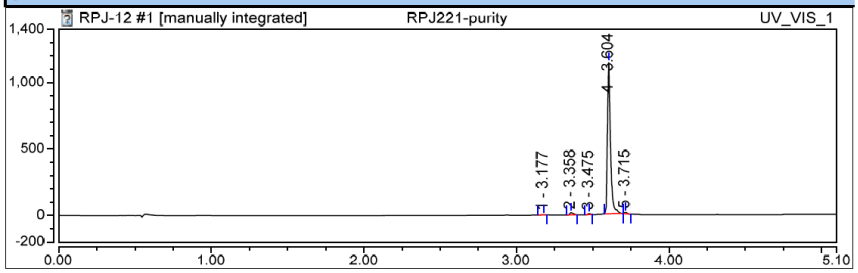

MS

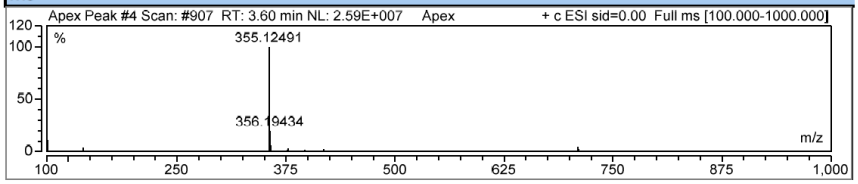

No.	Peak Name	Retention Time min	Area mAU*min	Height mAU	Relative Area %	Relative Height %
1		3.177	0.086	4.142	0.32	0.35
2		3.358	0.415	17.232	1.54	1.46
3		3.475	0.154	8.891	0.57	0.75
4		3.604	26.041	1138.851	96.76	96.50
5		3.715	0.217	11.032	0.81	0.93
Total:			**26.913**	**1180.149**	**100.00**	**100.00**

Supplementary Figure 112 HPLC purity analysis of **38**.

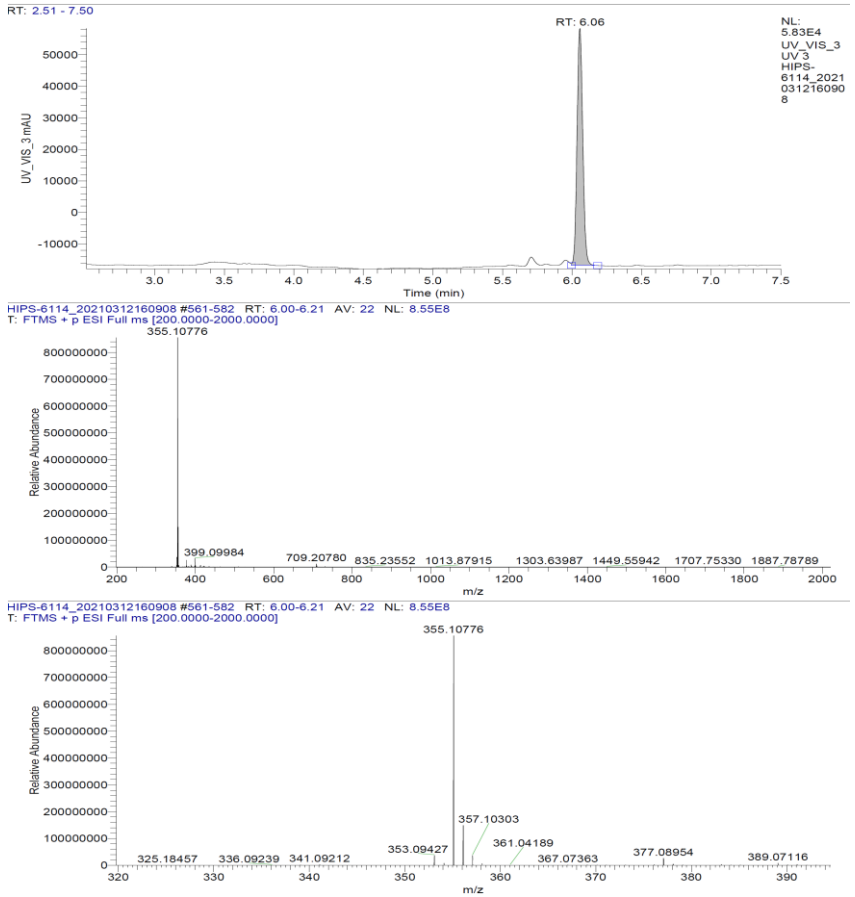

Supplementary Figure 113 HRMS of **38**.

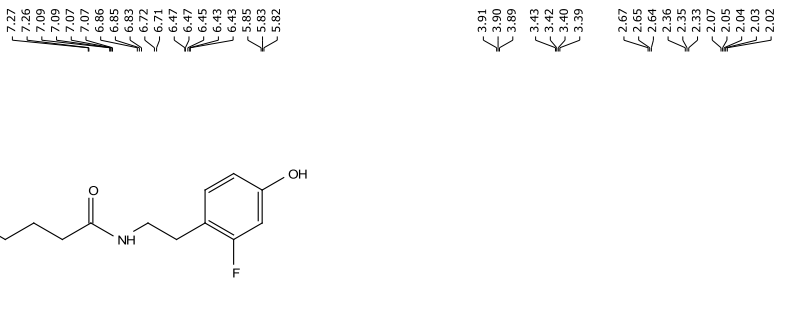

Supplementary Figure 114 ^{1}H NMR spectrum of **39.**

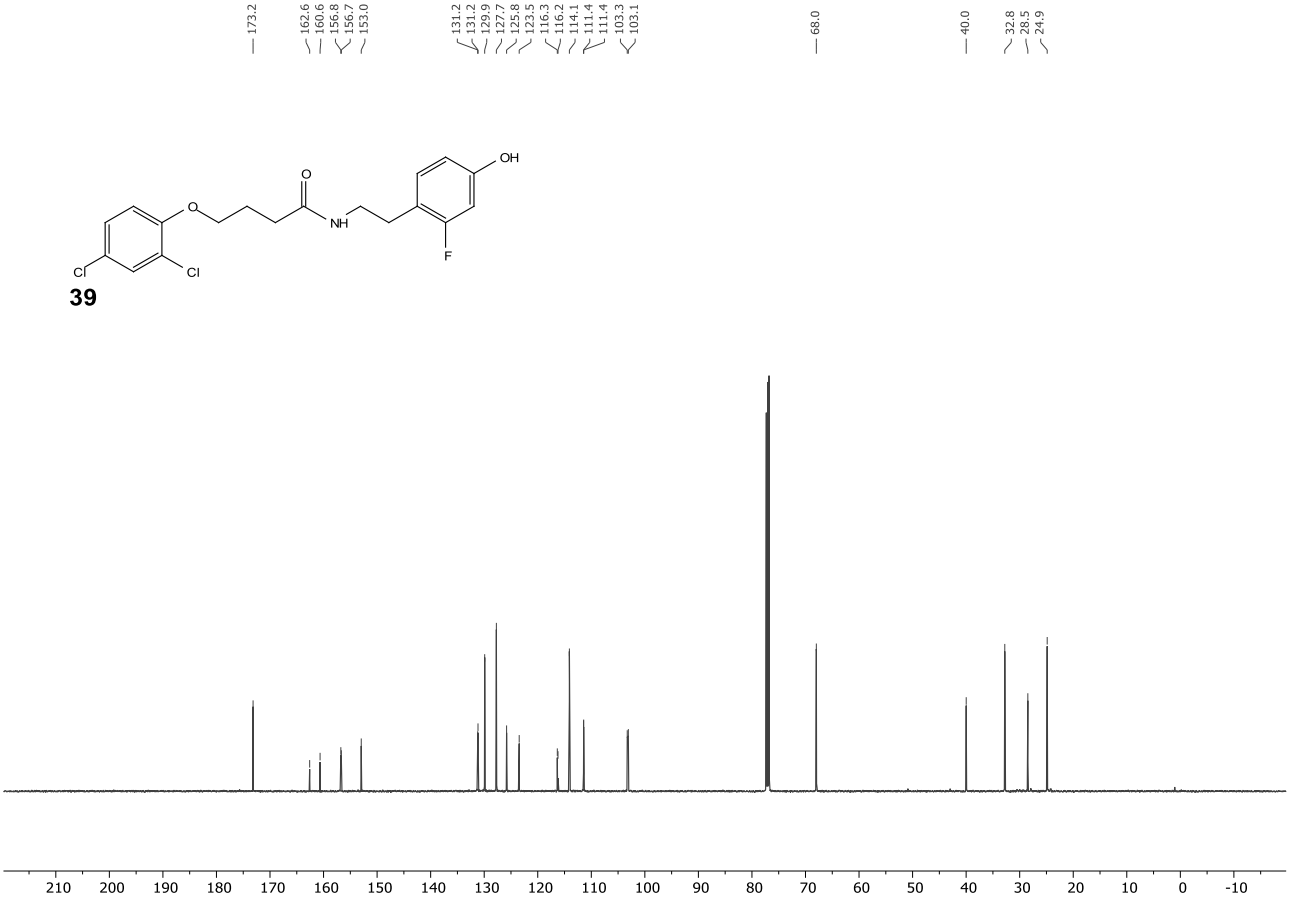

Supplementary Figure 115 ^{13}C NMR spectrum of **39.**

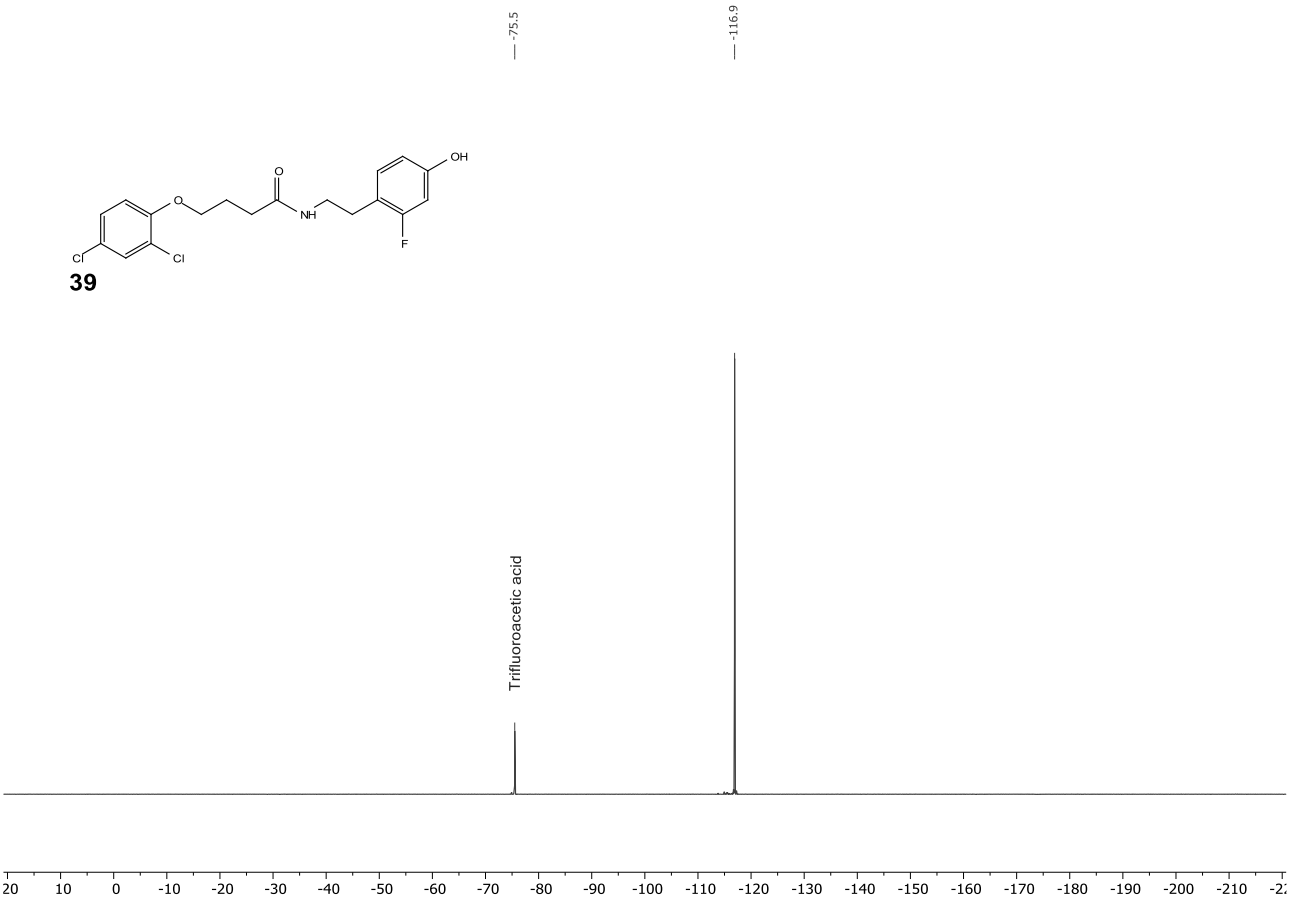

39

Supplementary Figure 116 ^{19}F NMR spectrum of **39.**

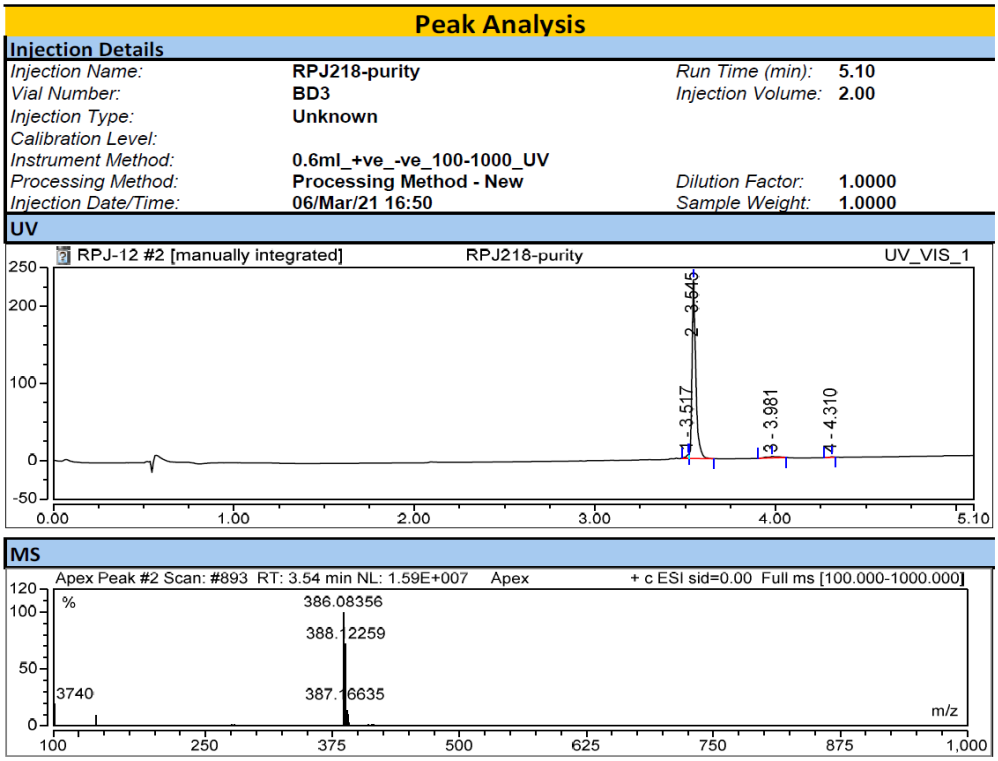

No.	Peak Name	Retention Time min	Area mAU*min	Height mAU	Relative Area %	Relative Height %
1		3.517	0.084	4.917	1.44	2.05
2		3.545	5.541	232.264	95.77	96.77
3		3.981	0.146	1.779	2.52	0.74
4		4.310	0.016	1.048	0.27	0.44
Total:			**5.786**	**240.008**	**100.00**	**100.00**

Supplementary Figure 117 HPLC purity analysis of **39**.

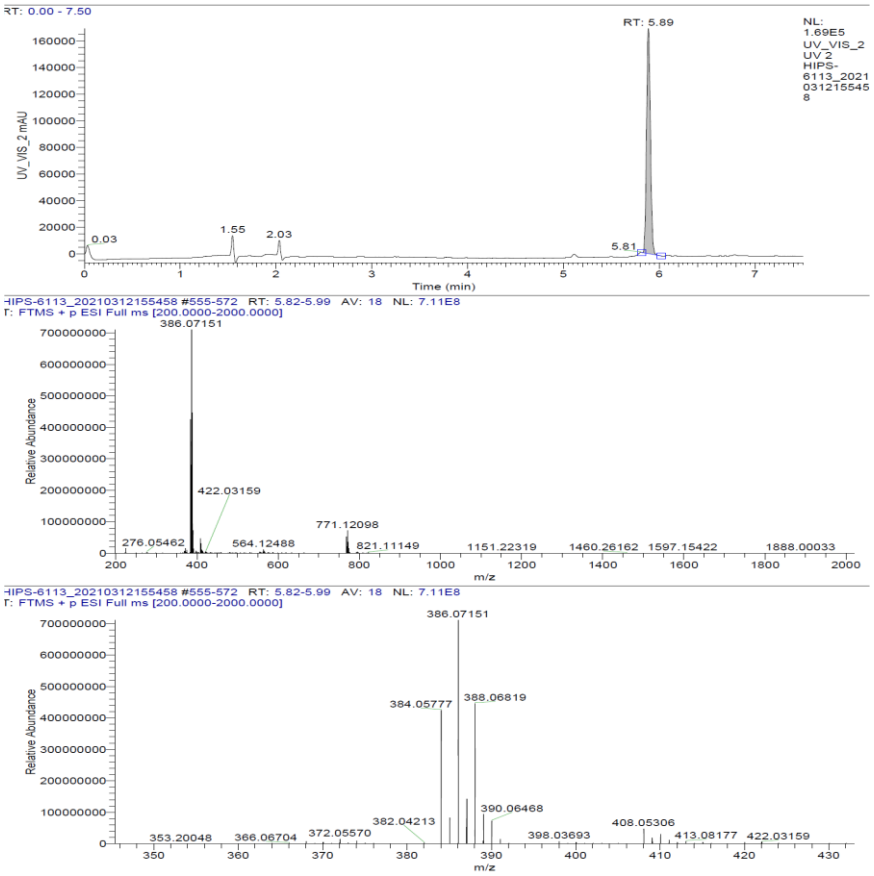

Supplementary Figure 118 HRMS of **39**.

40

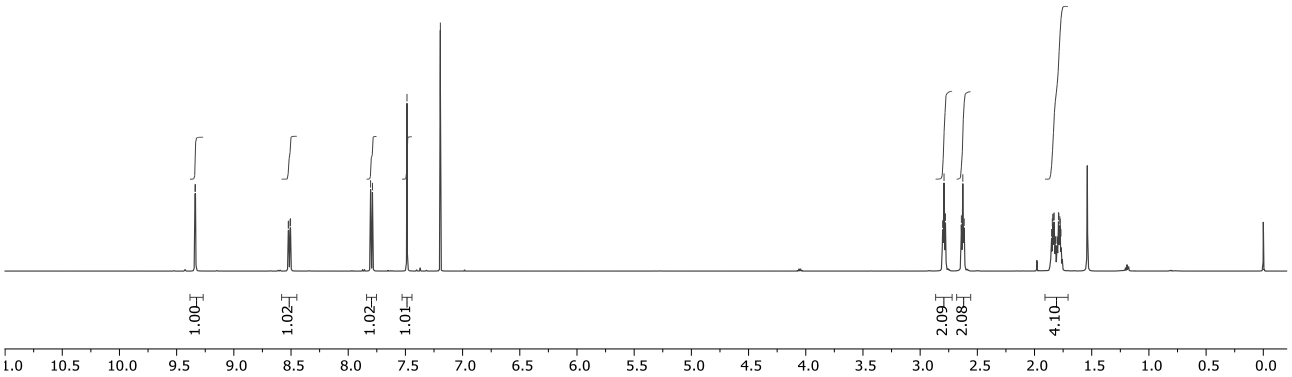

Supplementary Figure 119 ^{1}H NMR spectrum of **40.**

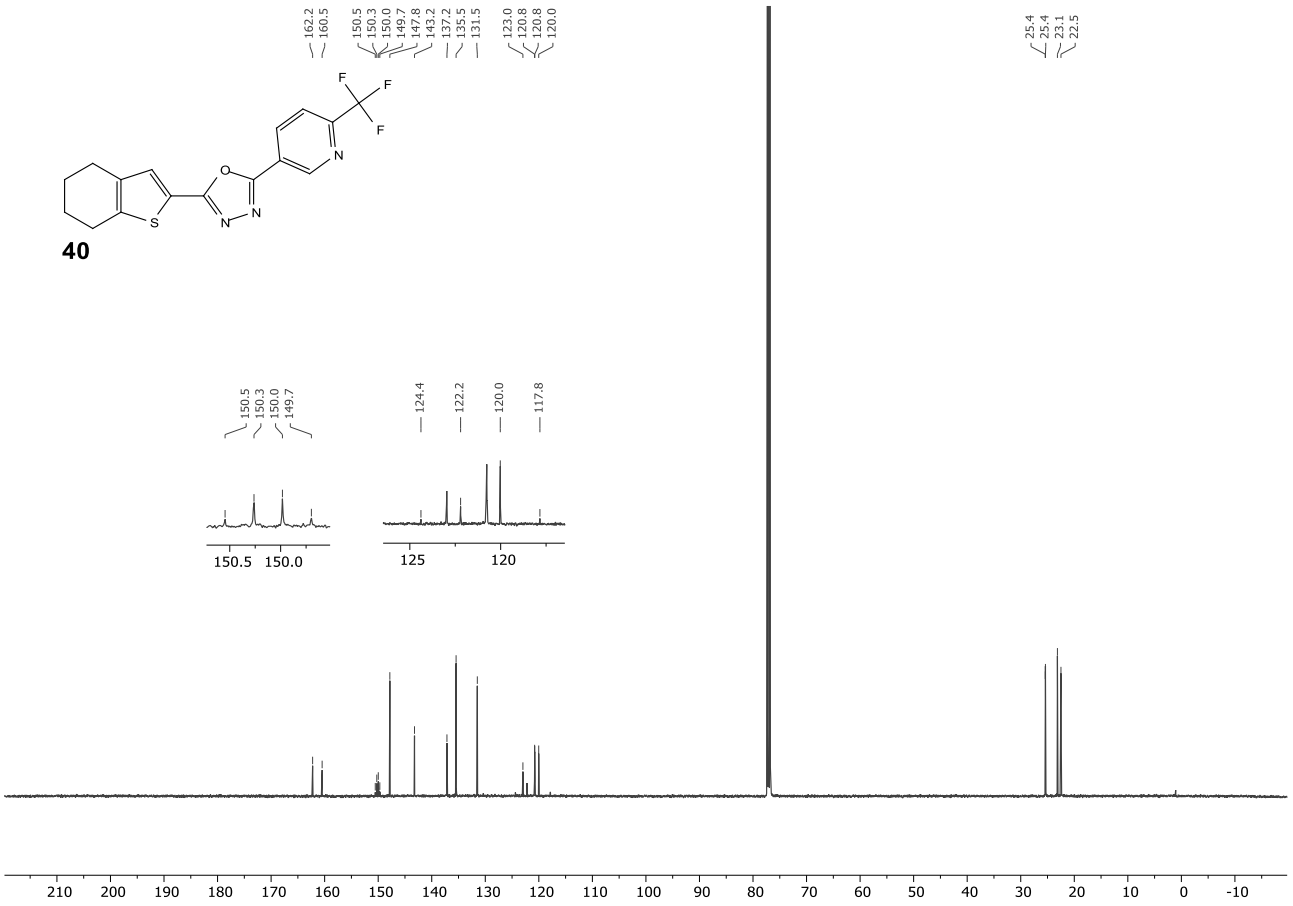

Supplementary Figure 120 ^{13}C NMR spectrum of **40.**

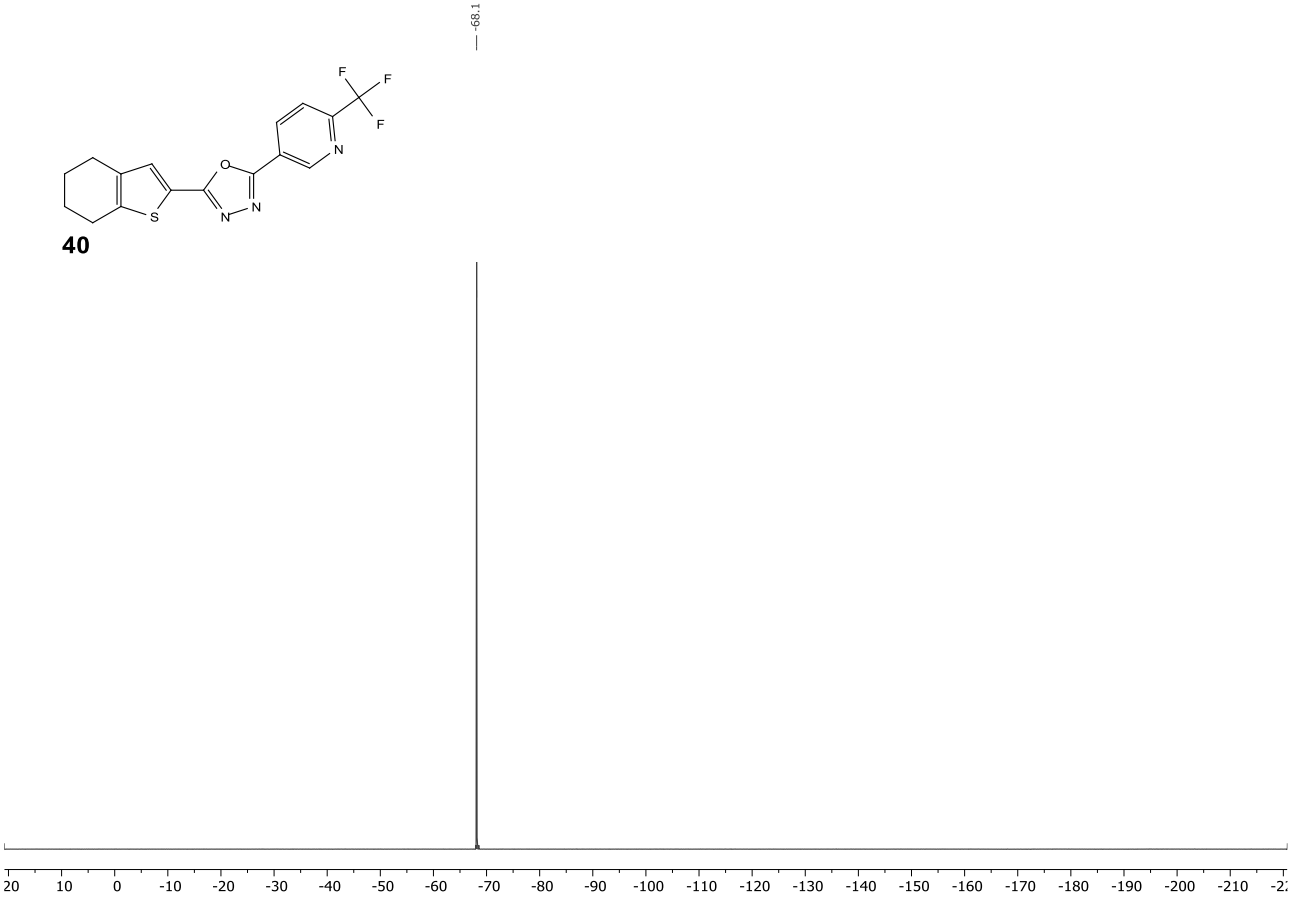

Supplementary Figure 121 ^{19}F NMR spectrum of **40.**

Peak Analysis

Injection Details

Injection Name:	**RPJ-223-Purity**	*Run Time (min):*	**5.10**
Vial Number:	**BD1**	*Injection Volume:*	**2.00**
Injection Type:	**Unknown**		
Calibration Level:			
Instrument Method:	**0.6ml_+ve_-ve_100-1000_UV**		
Processing Method:	**Processing Method - New**	*Dilution Factor:*	**1.0000**
Injection Date/Time:	**10/Mar/21 17:37**	*Sample Weight:*	**1.0000**

UV

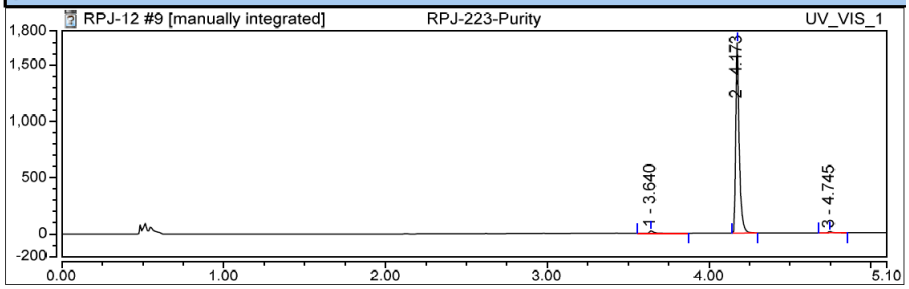

MS

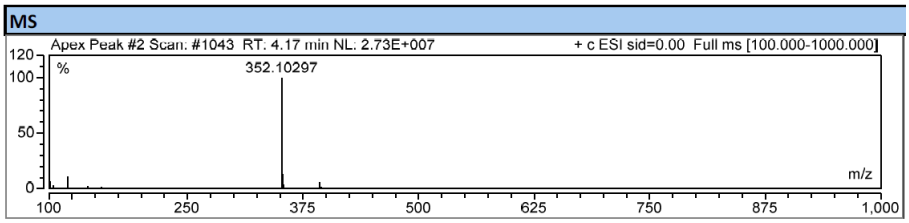

No.	Peak Name	Retention Time min	Area mAU*min	Height mAU	Relative Area %	Relative Height %
1		3.640	0.743	23.123	1.75	1.34
2		4.173	41.540	1687.233	97.51	97.94
3		4.745	0.319	12.303	0.75	0.71
Total:			**42.603**	**1722.660**	**100.00**	**100.00**

Supplementary Figure 122 HPLC purity analysis of **40**.

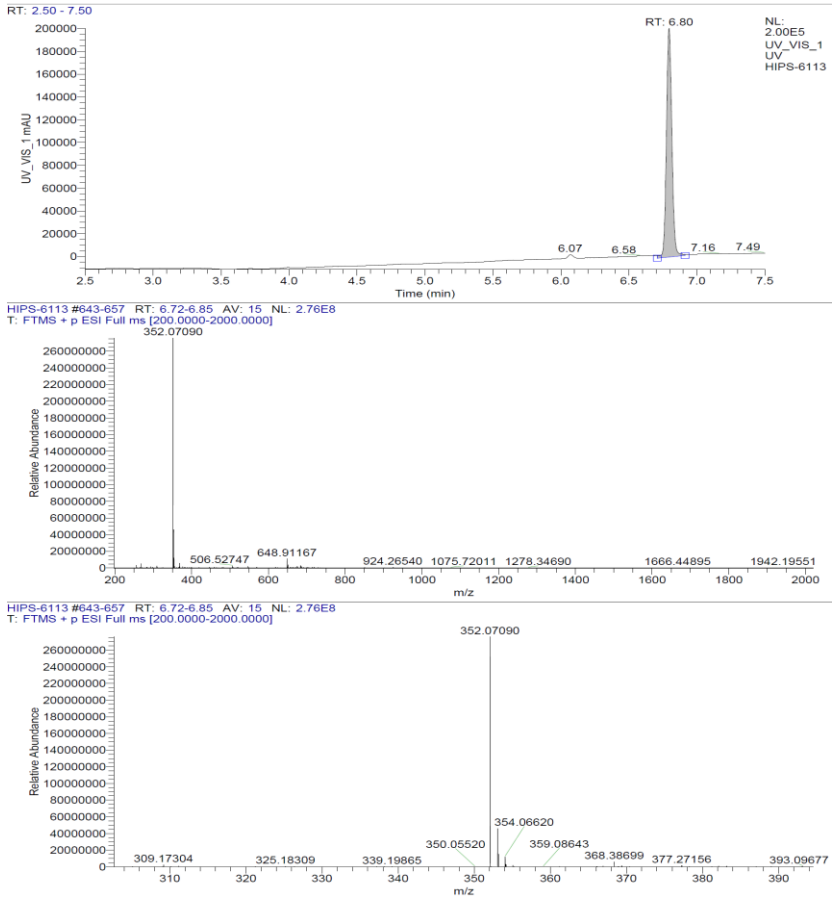

Supplementary Figure 123 HRMS of **40**.

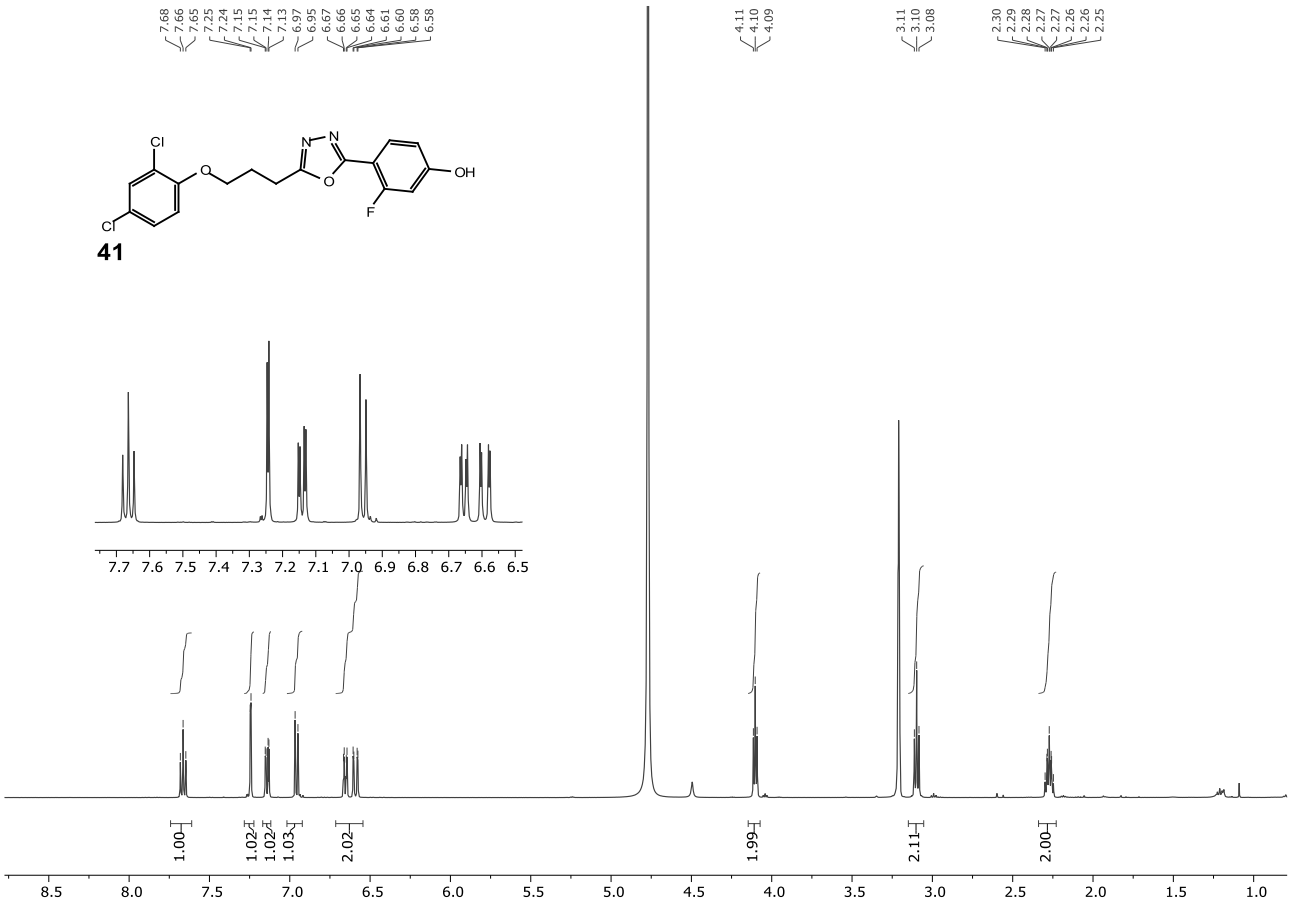

Supplementary Figure 124 ^{1}H NMR spectrum of **41**.

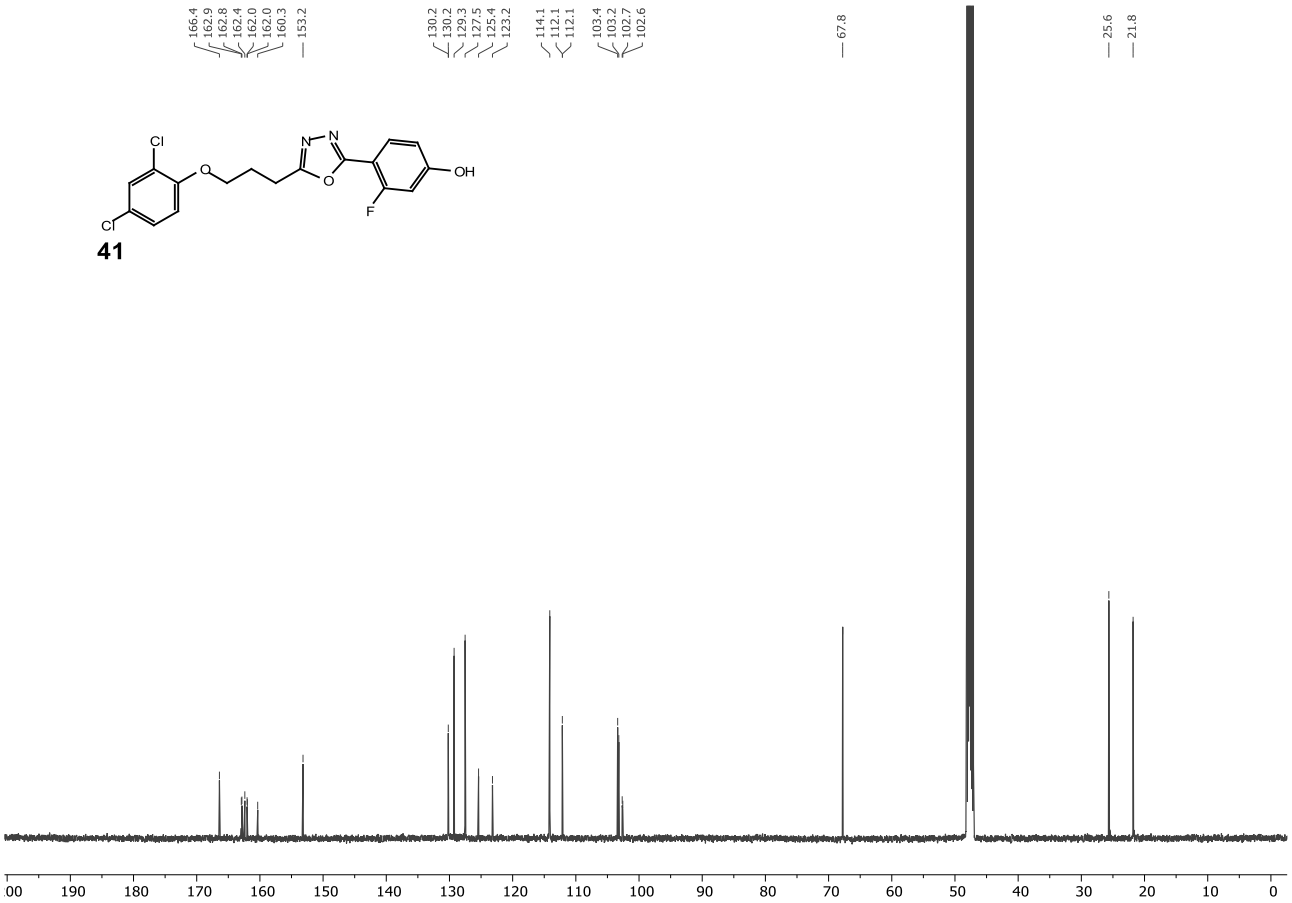

Supplementary Figure 125 ^{13}C NMR spectrum of **41**.

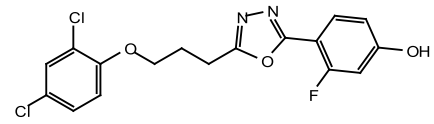

41

Supplementary Figure 126 ^{19}F NMR spectrum of **41.**

Name	PJN-31-purity
position	BD1
inj. vol.	2.00
time	16/Sep/2020 07:44
instr. method	0.6ml_+ve_-ve_100-600-all-waveLength
proc. method	Processing Method - New

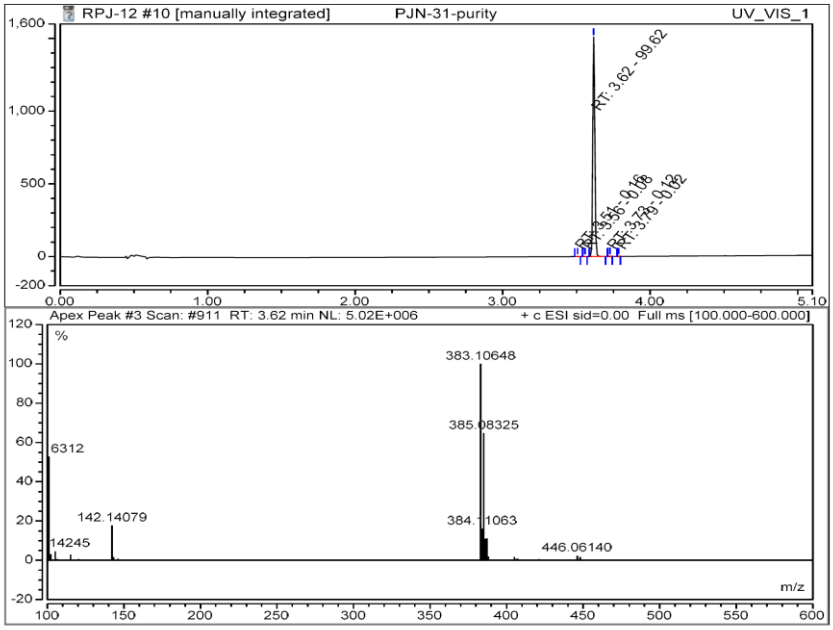

No.	Peak Name	Ret. Time min	Area mAU*min	Height mAU	Rel. Area %	Rel. Height %	Amount n.a.
1		3.508	0.036	1.770	0.16	0.12	n.a.
2		3.557	0.019	1.347	0.08	0.09	n.a.
3		3.617	22.933	1510.529	99.62	99.64	n.a.
4		3.726	0.028	1.931	0.12	0.13	n.a.
5		3.786	0.004	0.337	0.02	0.02	n.a.
Total:			**23.020**	**1515.914**	**100.00**	**100.00**	

Supplementary Figure 127 HPLC purity analysis of **41**.

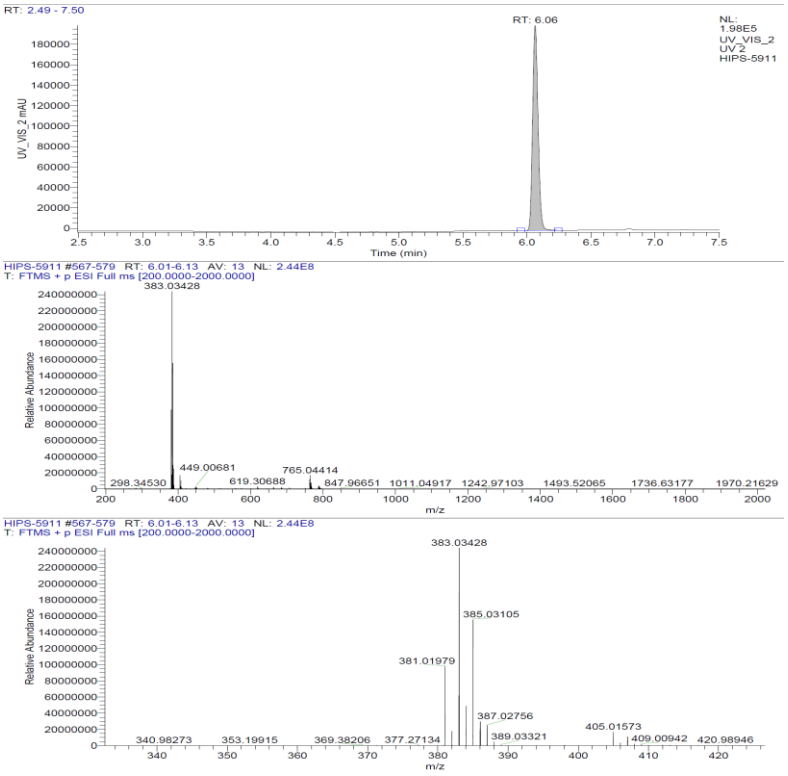

Supplementary Figure 128 HRMS of **41**.

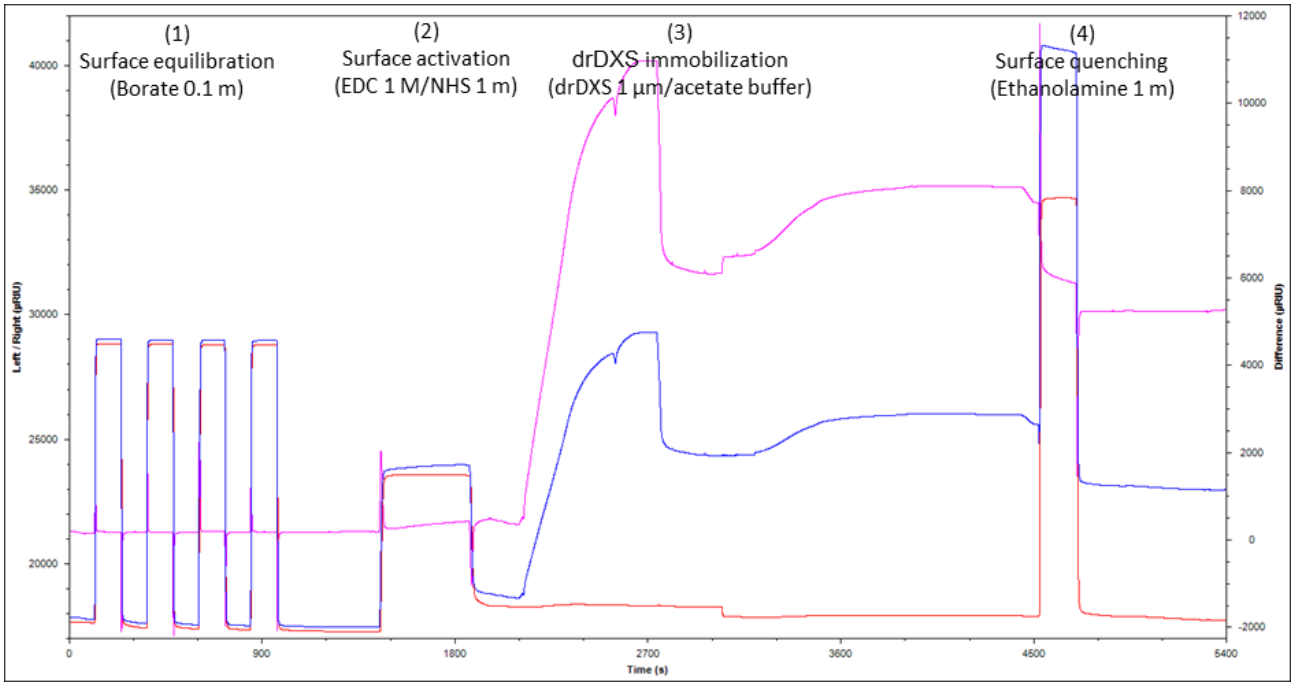

Supplementary Figure 129 Sensorgram of the immobilization procedure for drDXPS on CMD500M sensor chip: (1) Four injections of cleaning solution, (2) activation solution, (3) drDXPS, and (4) quenching solution. The blue, red, and magenta curves represent the left (active) channel, right (reference) channel, and the difference, respectively.

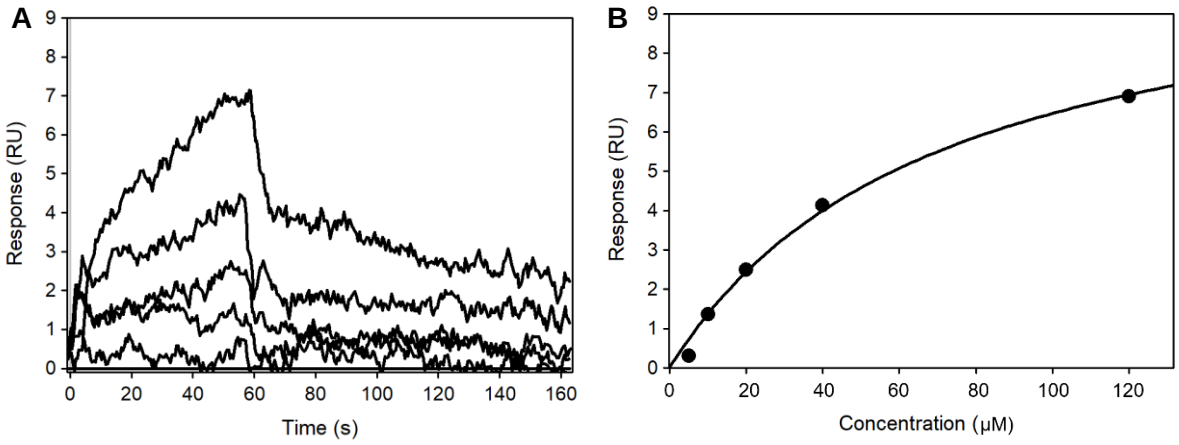

Supplementary Figure 130 (A) Overlay of sensorgrams of **1** injected at concentrations 5−120 μM over an immobilized drDXPS; (B) Fitting of responses at equilibrium according to 1:1 Langmuir binding model (K_D: 70 ± 5 μM).

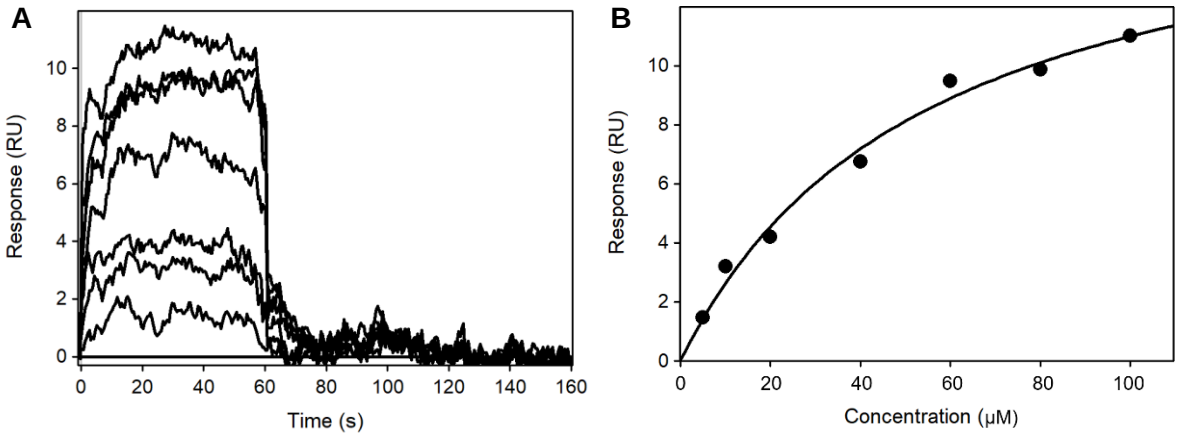

Supplementary Figure 131 (A) Overlay of sensorgrams of **2** injected at concentrations 5−100 μM over an immobilized drDXPS; (B) Fitting of responses at equilibrium according to 1:1 Langmuir binding model (K_D: 55 ± 5 μM).

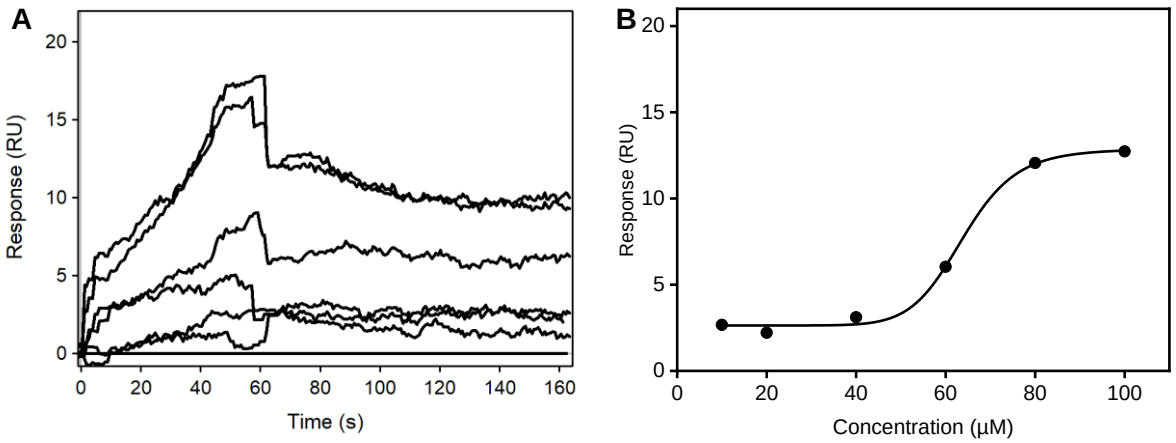

Supplementary Figure 132 (A) Overlay of sensorgrams of **3** injected at concentrations 10−100 μM over an immobilized drDXPS; (B) Fitting of responses at equilibrium according to Hill equation (K_D: 64 ± 2 μM).

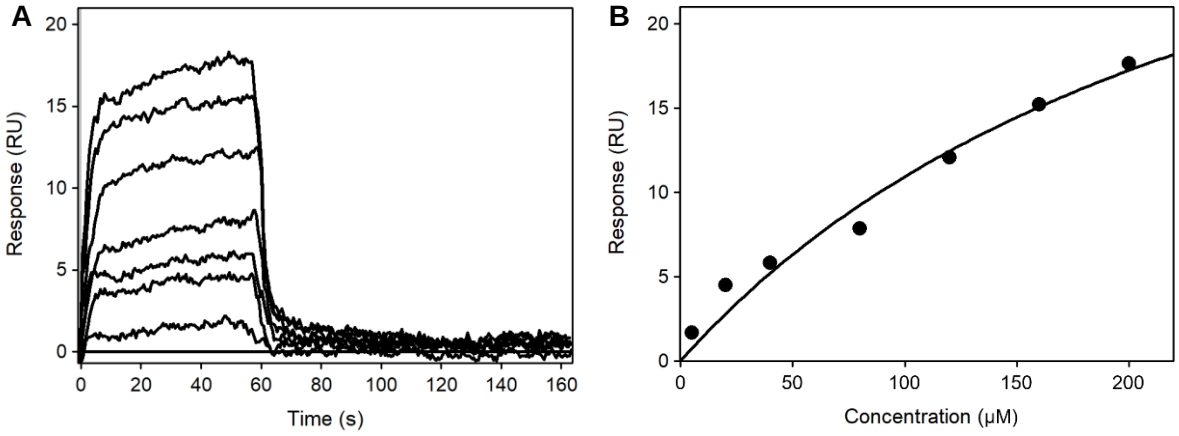

Supplementary Figure 133. (A) Overlay of sensorgrams of **5** injected at concentrations 5−200 μM over an immobilized drDXPS; (B) Fitting of responses at equilibrium according to 1:1 Langmuir binding model (K_D: 270 ± 40 μM).

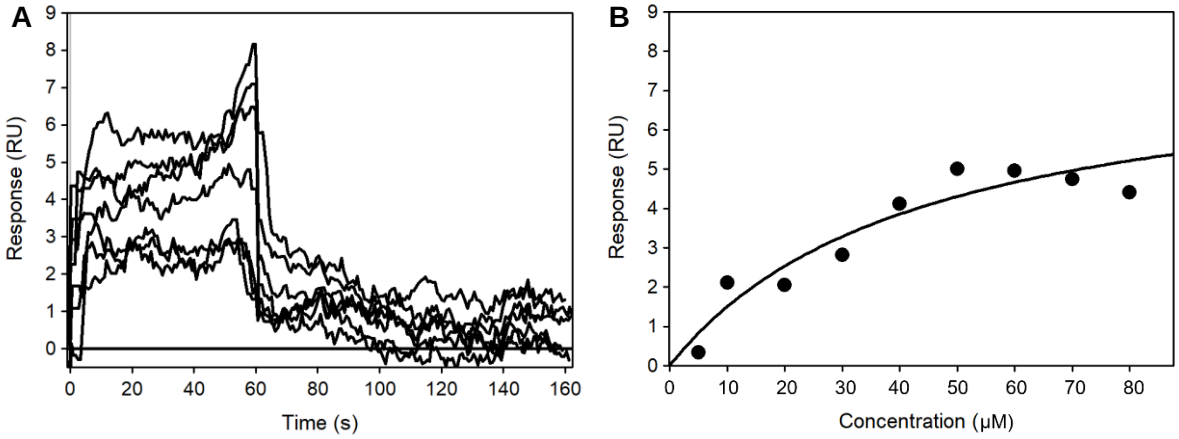

Supplementary Figure 134 (A) Overlay of sensorgrams of **7** injected at concentrations 5−80 μM over an immobilized drDXPS; (B) Fitting of responses at equilibrium according to 1:1 Langmuir binding model (K_D: 40 ± 10 μM).

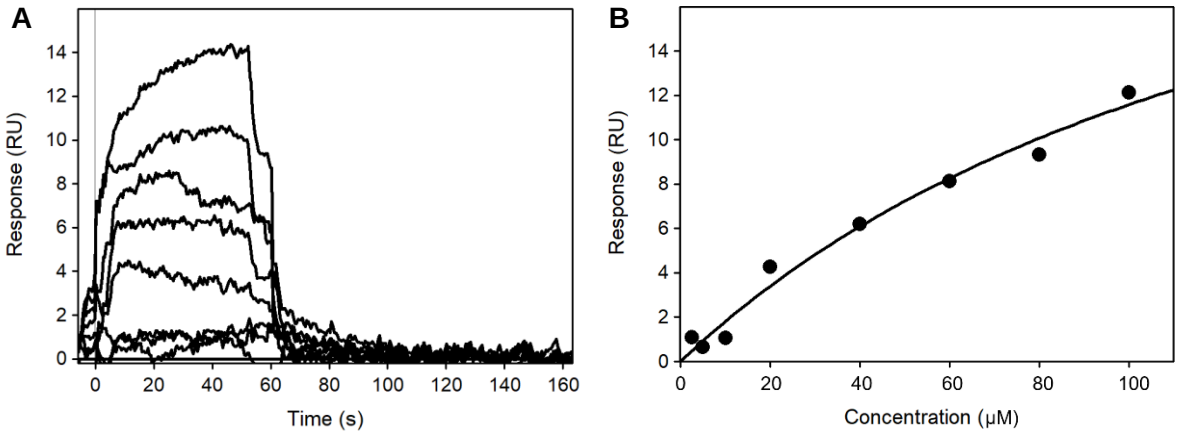

Supplementary Figure 135 (A) Overlay of sensorgrams of **9** injected at concentrations 2.5−80 μM over an immobilized drDXPS; (B) Fitting of responses at equilibrium according to 1:1 Langmuir binding model (K_D: 150 ± 30 μM).

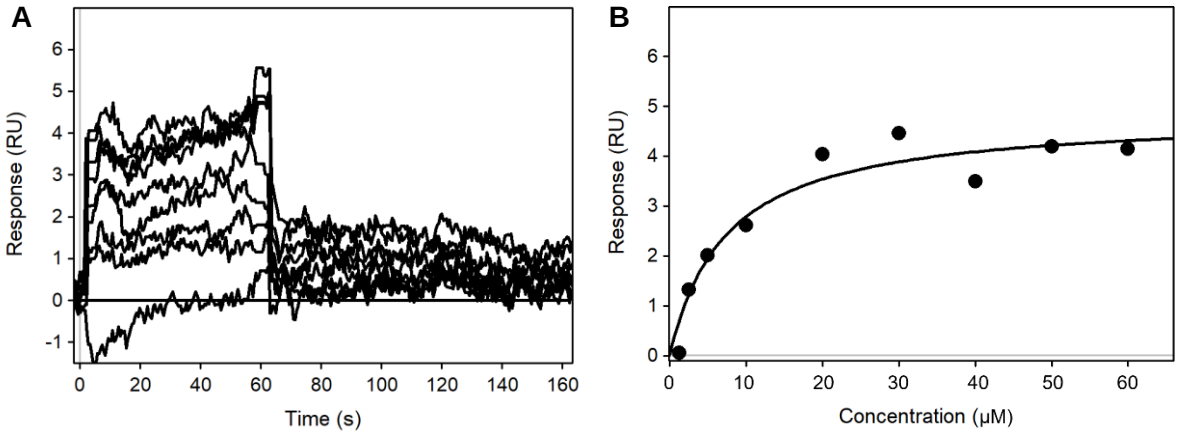

Supplementary Figure 136 (A) Overlay of sensorgrams of **10** injected at concentrations 2.5−60 μM over an immobilized drDXPS; (B) Fitting of responses at equilibrium according to 1:1 Langmuir binding model (K_D: 7 ± 1 μM).

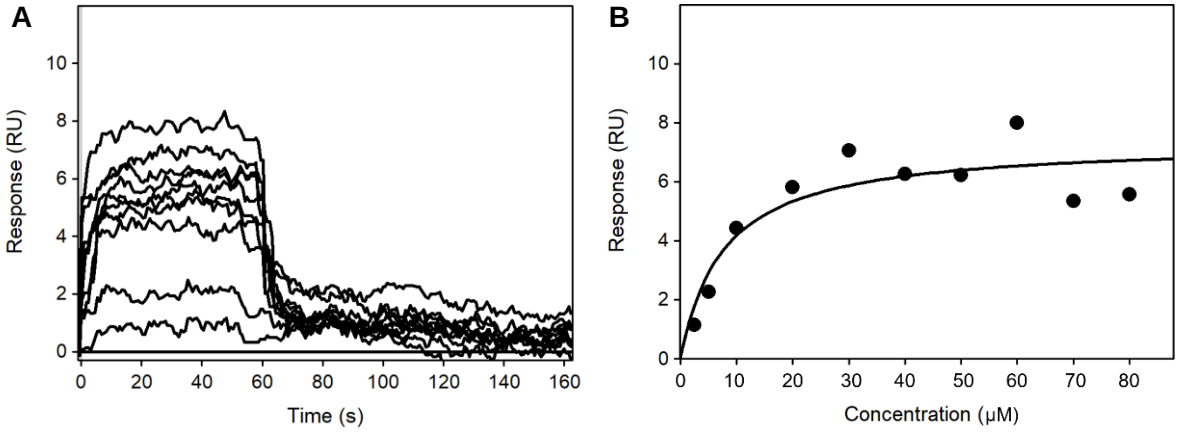

Supplementary Figure 137 (A) Overlay of sensorgrams of **11** injected at concentrations 2.5−80 μM over an immobilized drDXPS; (B) Fitting of responses at equilibrium according to 1:1 Langmuir binding model (K_D: 8 ± 2 μM).

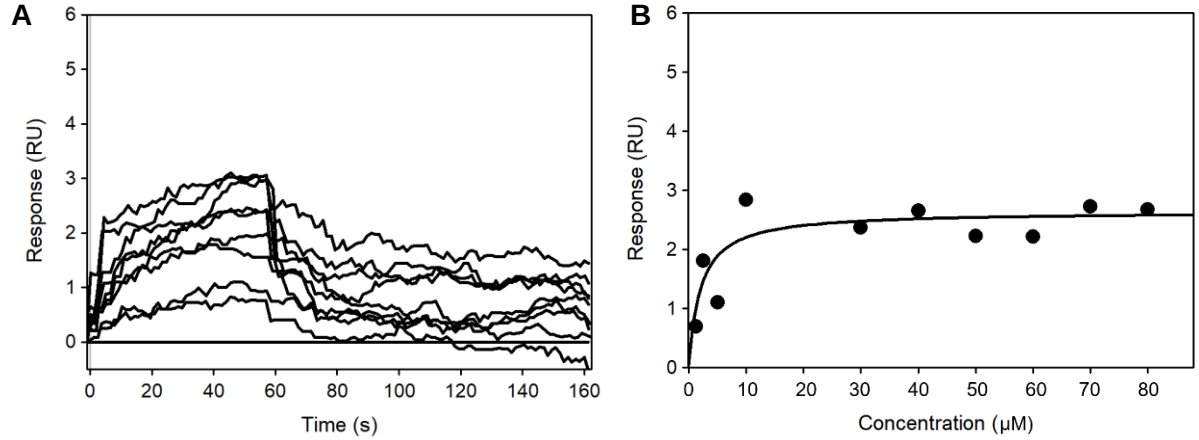

Supplementary Figure 138 (A) Overlay of sensorgrams of **12** injected at concentrations 1.25−80 μM over an immobilized drDXPS; (B) Fitting of responses at equilibrium according to 1:1 Langmuir binding model (K_D: 2 ± 1 μM).

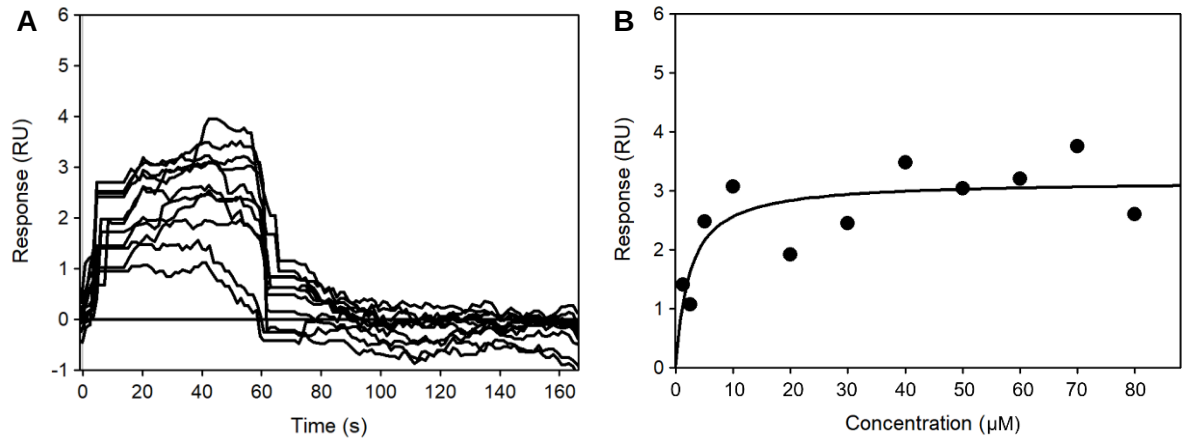

Supplementary Figure 139 (A) Overlay of sensorgrams of **21** injected at concentrations 1.25–80 μM over an immobilized drDXPS; (B) Fitting of responses at equilibrium according to 1:1 Langmuir binding model (K_D: 3 ± 1 μM).

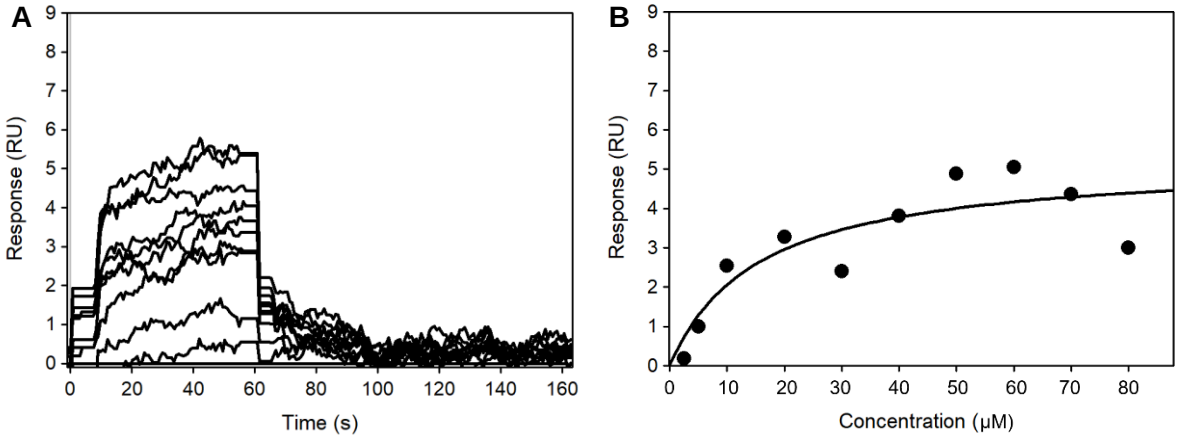

Supplementary Figure 140 (A) Overlay of sensorgrams of **22** injected at concentrations 1.25–80 μM over an immobilized drDXPS; (B) Fitting of responses at equilibrium according to 1:1 Langmuir binding model (K_D: 15 ± 3 μM).

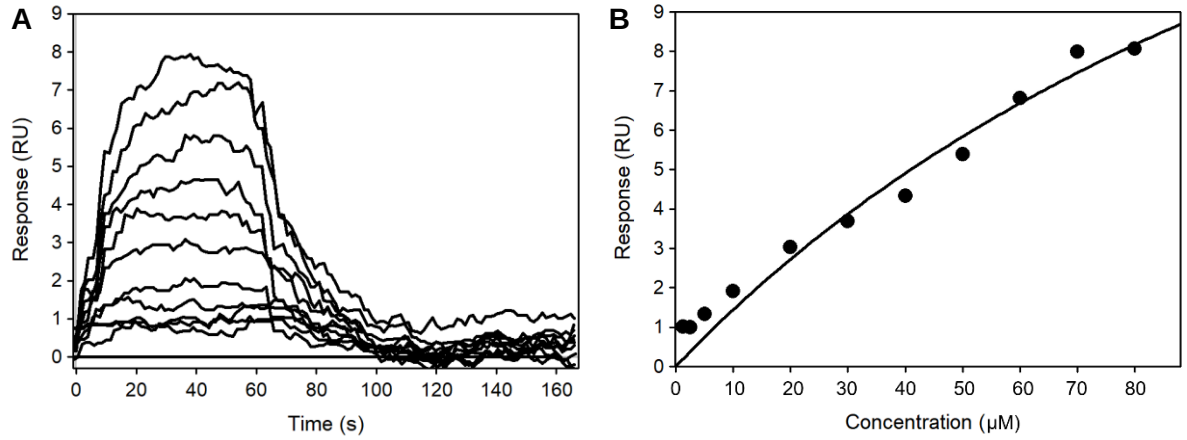

Supplementary Figure 141 (A) Overlay of sensorgrams of **23** injected at concentrations 1.25–80 μM over an immobilized drDXPS; (B) Fitting of responses at equilibrium according to 1:1 Langmuir binding model (K_D: 160 ± 50 μM).

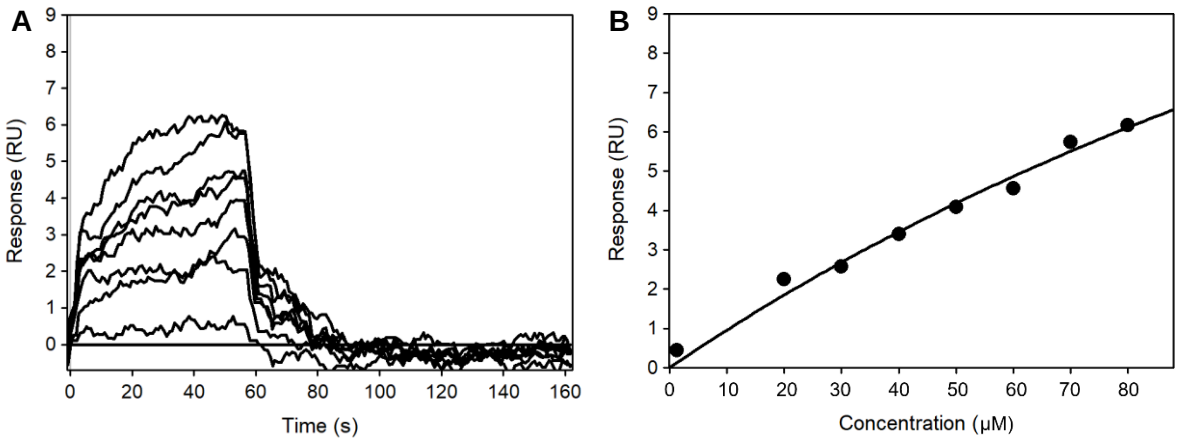

Supplementary Figure 142 (A) Overlay of sensorgrams of **24** injected at concentrations 1.25–80 μM over an immobilized drDXPS; (B) Fitting of responses at equilibrium according to 1:1 Langmuir binding model (K_D: 260 ± 80 μM).

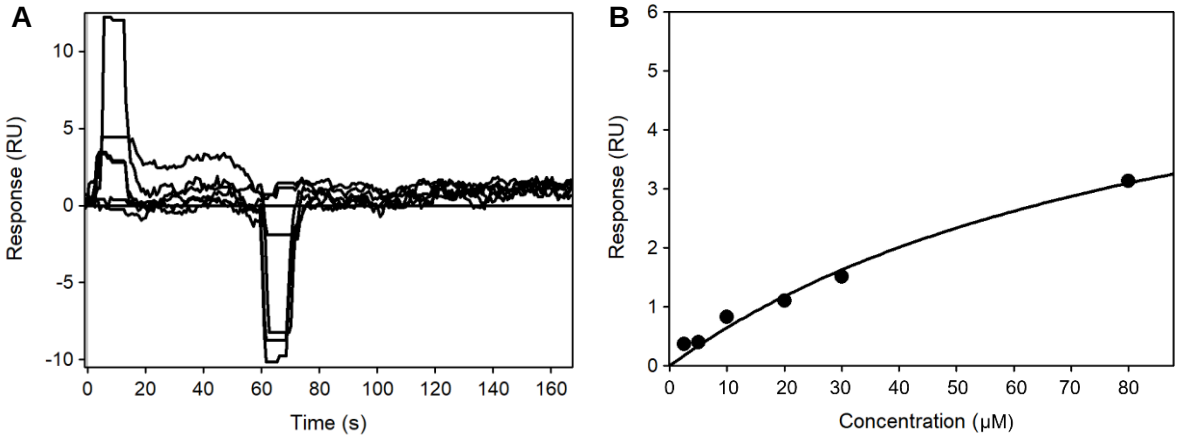

Supplementary Figure 143 (A) Overlay of sensorgrams of **25** injected at concentrations 1.25–80 μM over an immobilized drDXPS; (B) Fitting of responses at equilibrium according to 1:1 Langmuir binding model (K_D: 90 ± 20 μM).

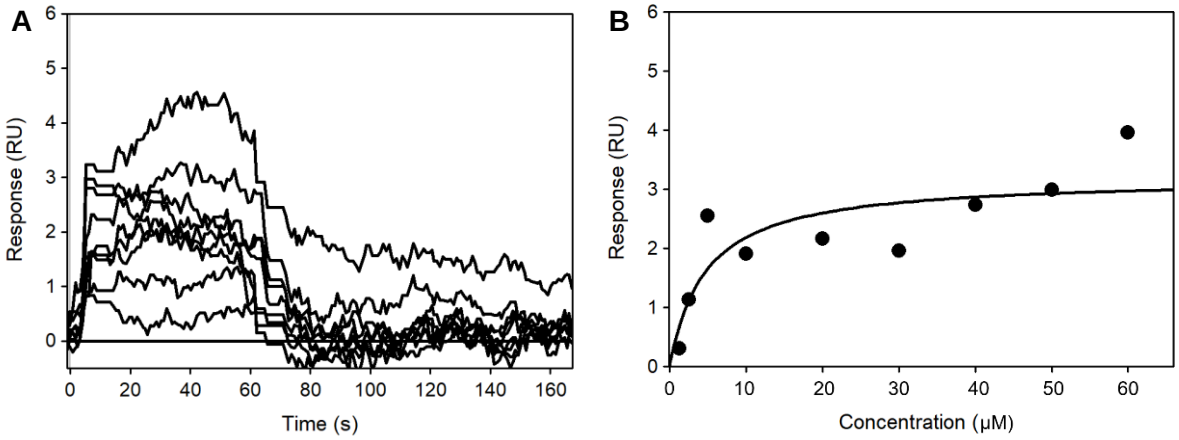

Supplementary Figure 144 (A) Overlay of sensorgrams of **26** injected at concentrations 1.25–60 μM over an immobilized drDXPS; (B) Fitting of responses at equilibrium according to 1:1 Langmuir binding model (K_D: 5 ± 2 μM).

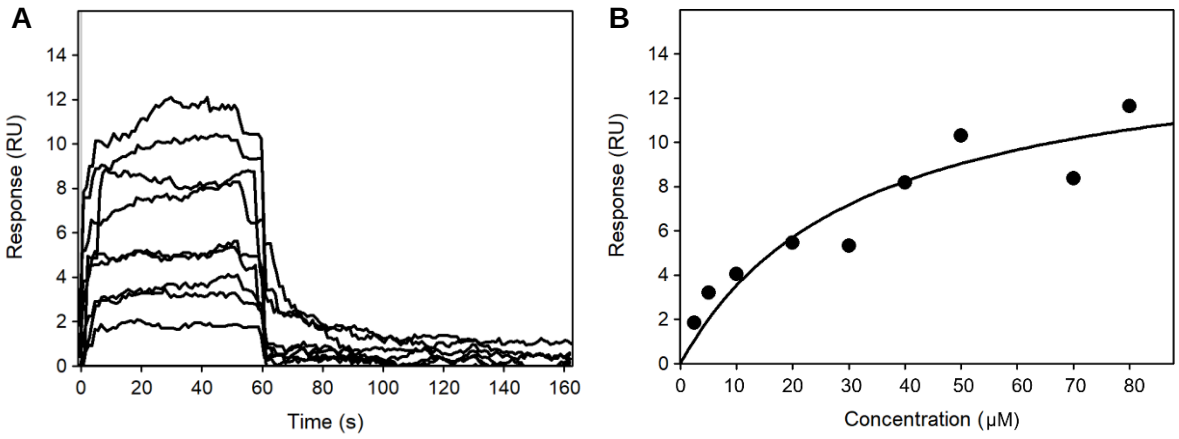

Supplementary Figure 145 (A) Overlay of sensorgrams of **35** injected at concentrations 2.5−80 μM over an immobilized drDXPS; (B) Fitting of responses at equilibrium according to 1:1 Langmuir binding model (K_D: 32 ± 8 μM).

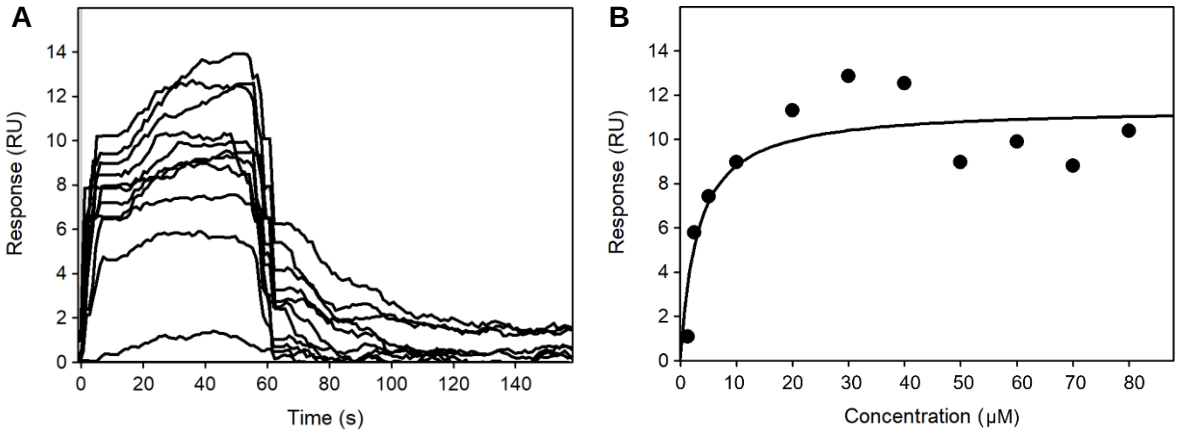

Supplementary Figure 146 (A) Overlay of sensorgrams of **37** injected at concentrations 1.25−80 μM over an immobilized drDXPS; (B) Fitting of responses at equilibrium according to 1:1 Langmuir binding model (K_D: 3 ± 1 μM).

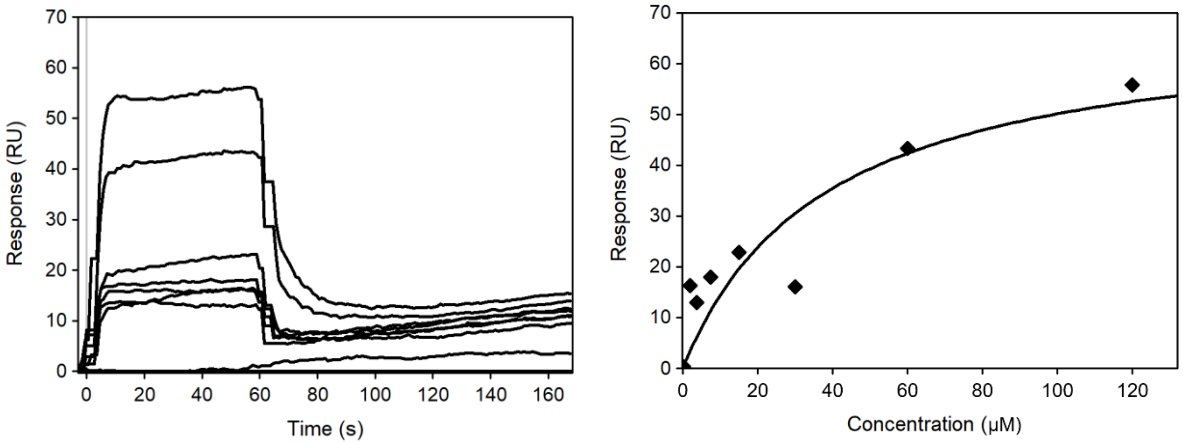

Supplementary Figure 147 (A) Overlay of sensorgrams of **38** injected at concentrations 0.2−120 μM over an immobilized drDXS; (B) Fitting of responses at equilibrium according to 1:1 Langmuir binding model (K_D: 40 ± 10 μM).

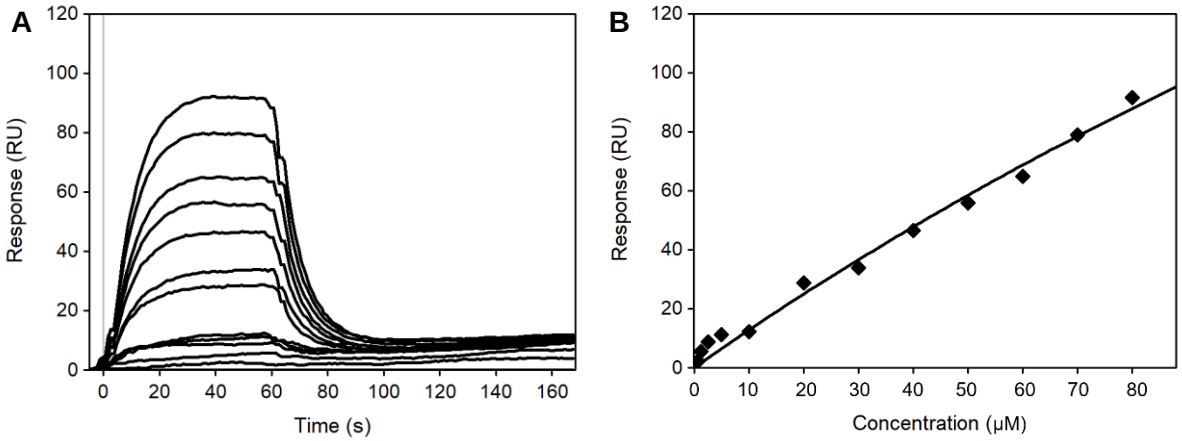

Supplementary Figure 148 (A) Overlay of sensorgrams of **39** injected at concentrations 0.6−80 μM over an immobilized drDXS; (B) Fitting of responses at equilibrium according to 1:1 Langmuir binding model (K_D: 290 ± 30 μM).

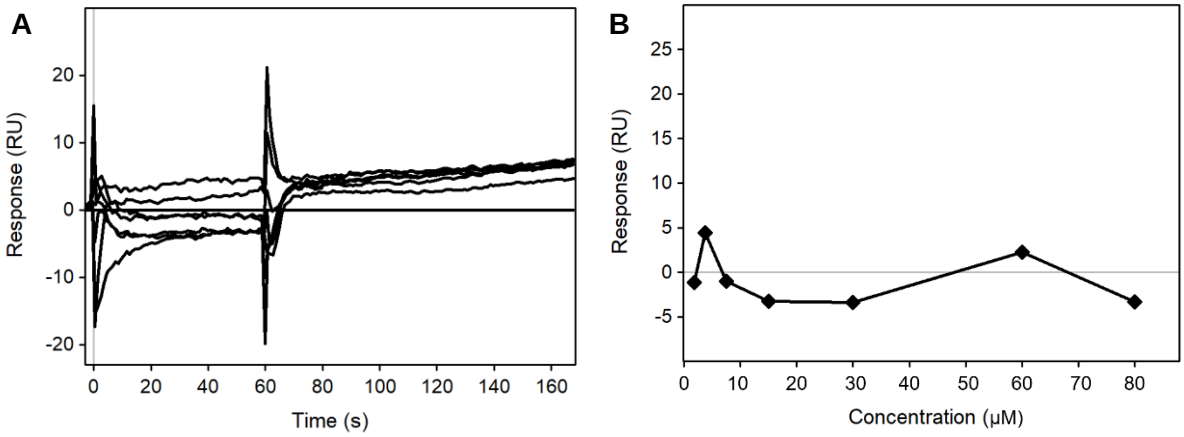

Supplementary Figure 149 (A) Overlay of sensorgrams of **40** injected at concentrations 1.9−80 μM over an immobilized drDXS; (B) Responses at equilibrium are concentration-independent and could not be fitted to Langmuir nor Hill binding model, indicating no significant binding.

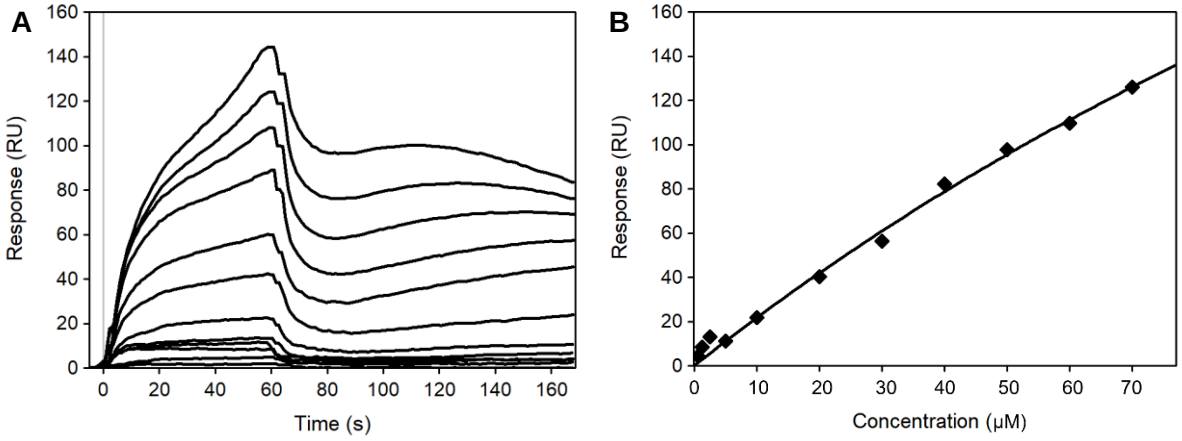

Supplementary Figure 150 (A) Overlay of sensorgrams of **41** injected at concentrations 0.6−70 μM over an immobilized drDXS; (B) Fitting of responses at equilibrium according to 1:1 Langmuir binding model (K_D: 290 ± 40 μM).

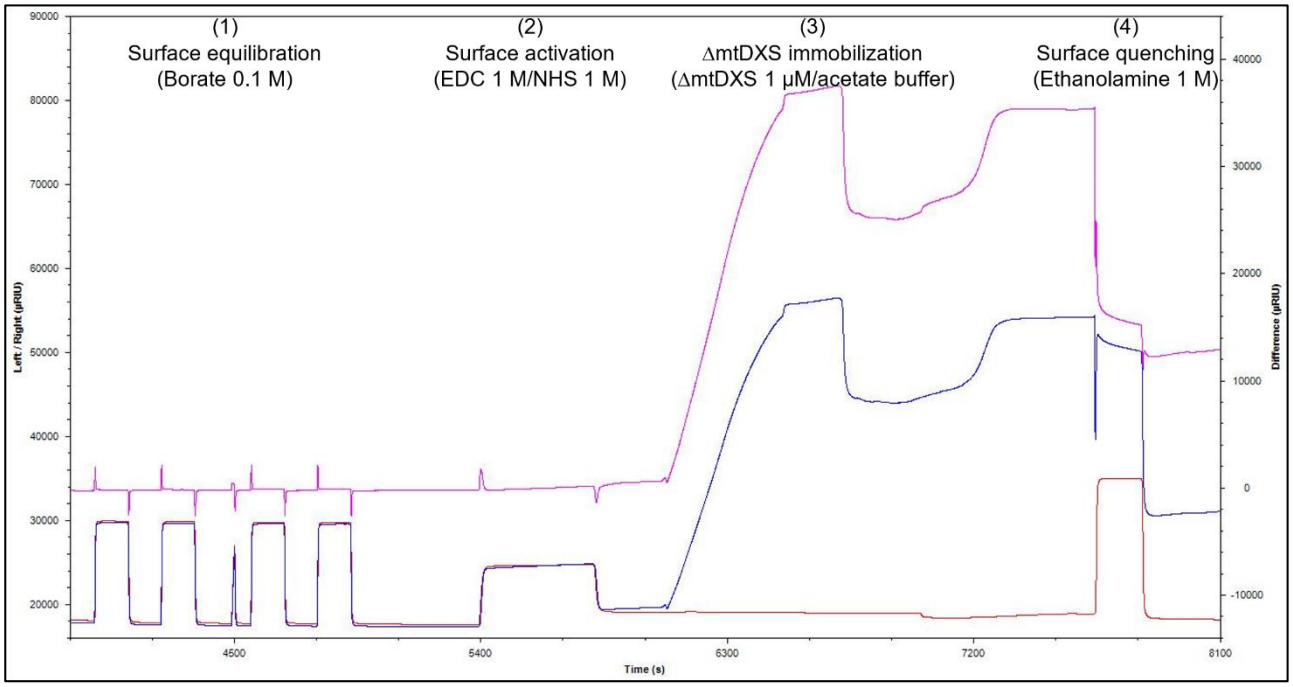

Supplementary Figure 151 Sensorgram of the immobilization procedure for ΔmtDXPS on CMD500M sensor chip: (1) Four injections of cleaning solution, (2) activation solution, (3) ΔmtDXPS, and (4) quenching solution. The blue, red, and magenta curves represent the left (active) channel, right (reference) channel, and the difference, respectively.

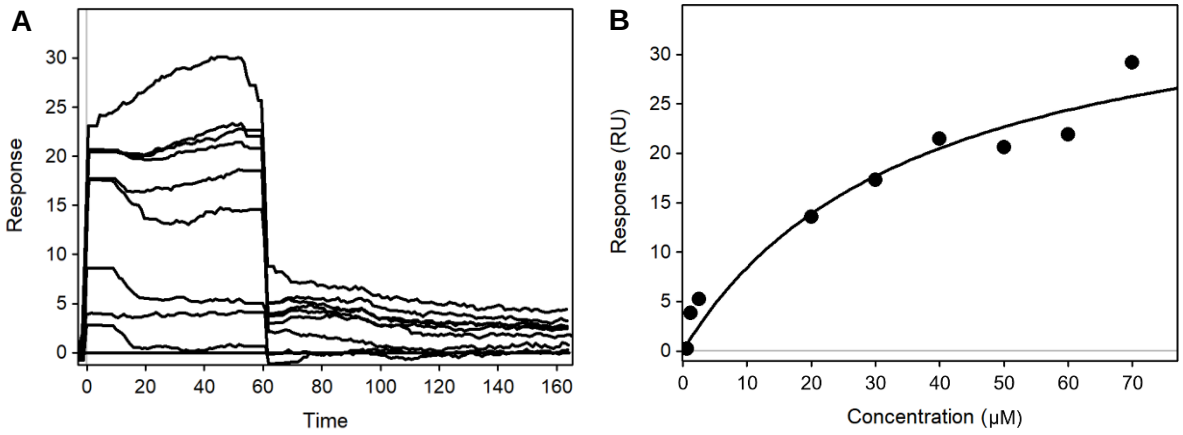

Supplementary Figure 152 (A) Overlay of sensorgrams of **1** injected at concentrations 1.25−70 µM over an immobilized ΔmtDXPS; (B) Fitting of responses at equilibrium according to 1:1 Langmuir binding model (K_D: 40 ± 10 µM).

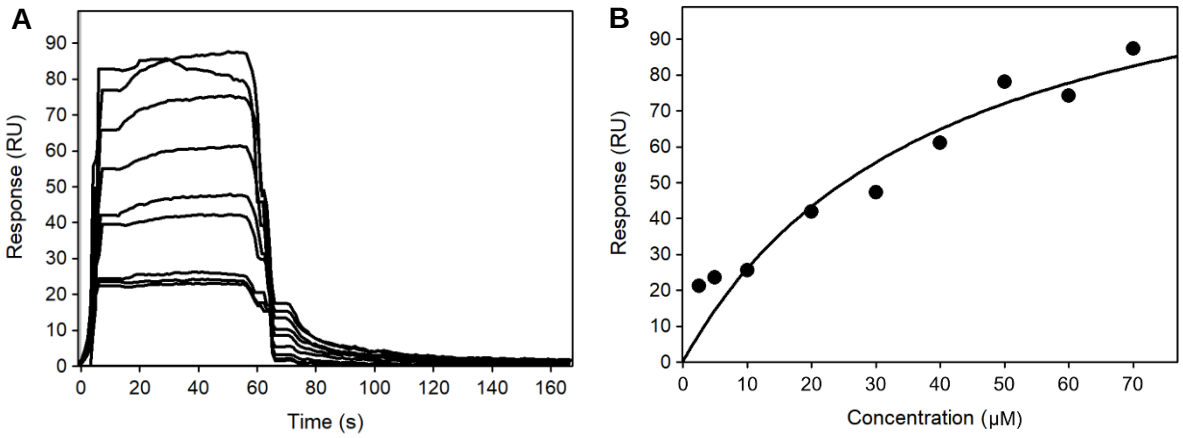

Supplementary Figure 153 (A) Overlay of sensorgrams of **2** injected at concentrations 2.5−70 μM over an immobilized ΔmtDXPS; (B) Fitting of responses at equilibrium according to 1:1 Langmuir binding model (K_D: 40 ± 10 μM).

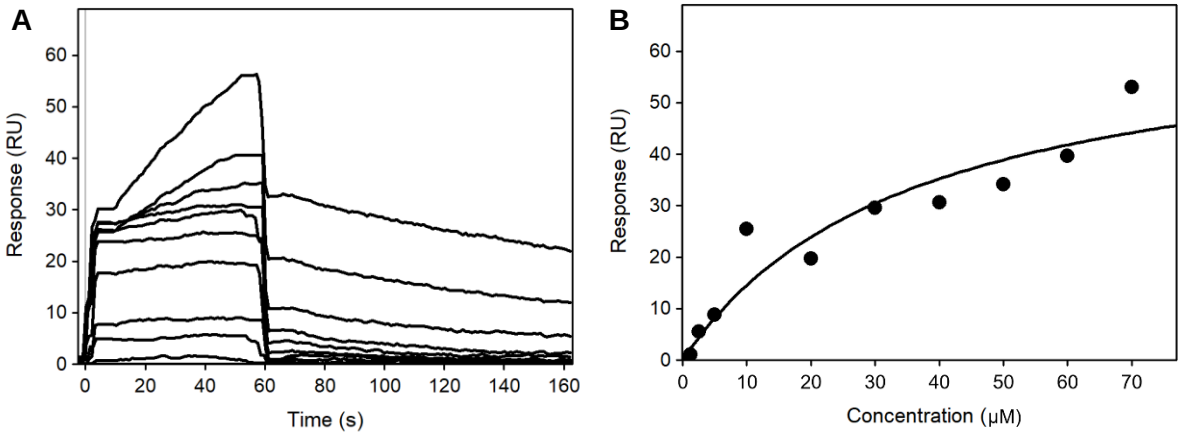

Supplementary Figure 154 (A) Overlay of sensorgrams of **3** injected at concentrations 1.25−70 μM over an immobilized ΔmtDXPS; (B) Fitting of responses at equilibrium according to 1:1 Langmuir binding model (K_D: 40 ± 10 μM).

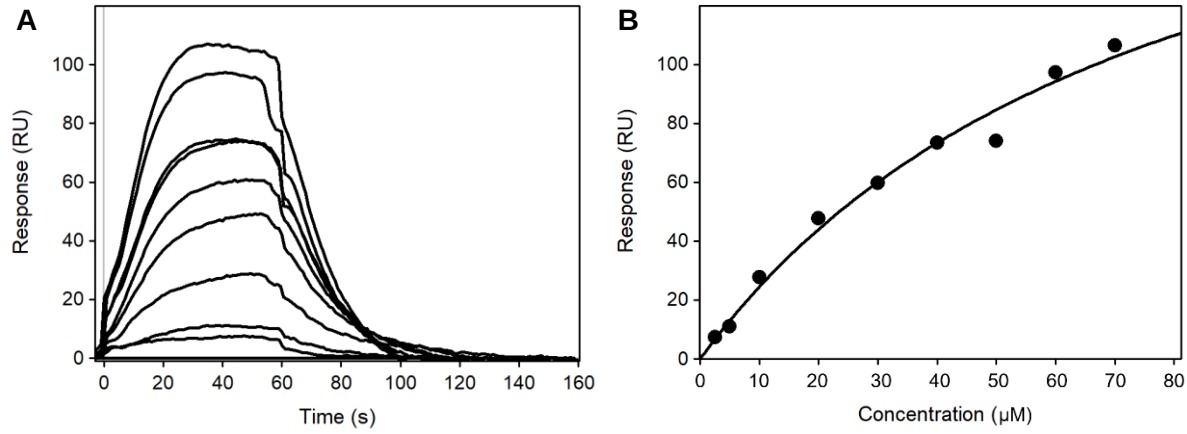

Supplementary Figure 155 (A) Overlay of sensorgrams of **4** injected at concentrations 2.5−70 μM over an immobilized ΔmtDXPS; (B) Fitting of responses at equilibrium according to 1:1 Langmuir binding model (K_D: 80 ± 10 μM).

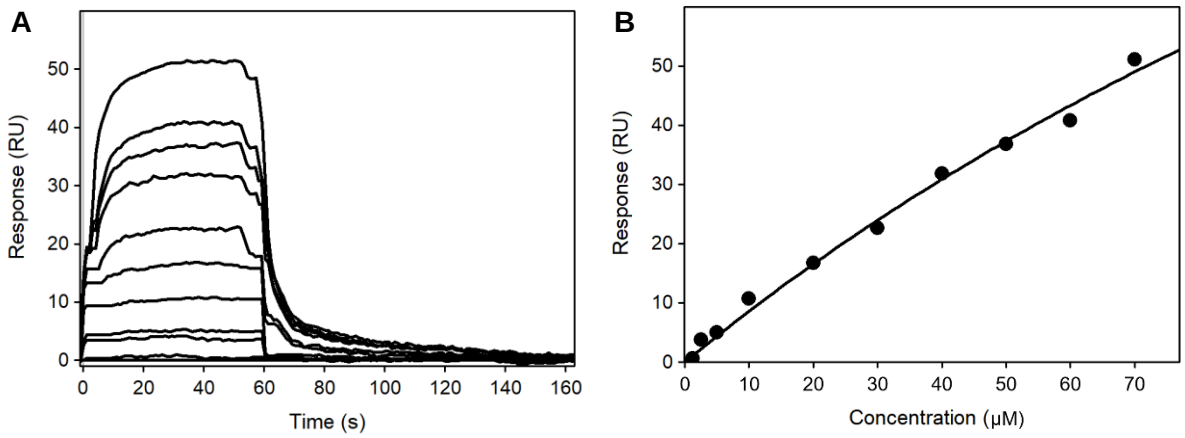

Supplementary Figure 156 (A) Overlay of sensorgrams of **5** injected at concentrations 1.25−70 μM over an immobilized ΔmtDXPS.; (B) Fitting of responses at equilibrium according to 1:1 Langmuir binding model (K_D: 250 ± 20 μM).

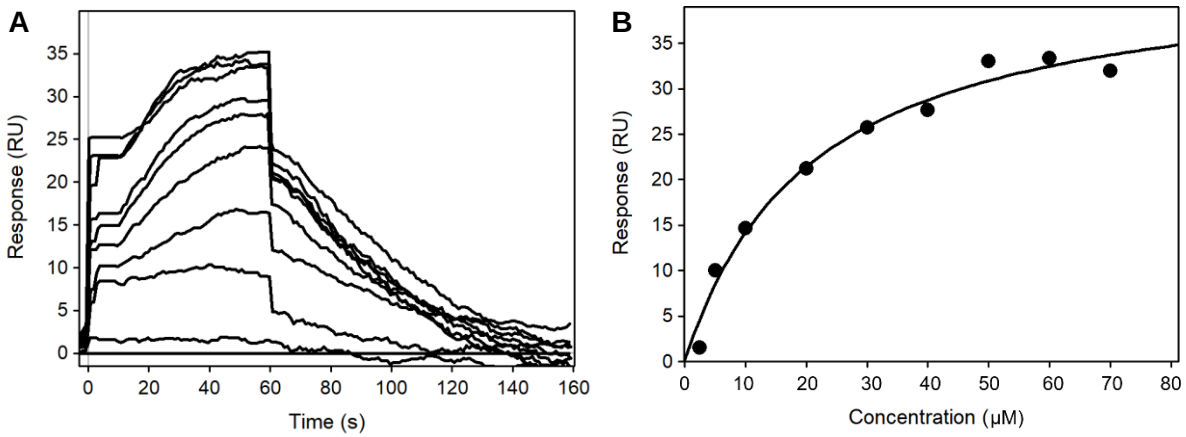

Supplementary Figure 157 (A) Overlay of sensorgrams of **6** injected at concentrations 2.5−70 μM over an immobilized ΔmtDXPS; (B) Fitting of responses at equilibrium according to 1:1 Langmuir binding model (K_D: 21 ± 3 μM).

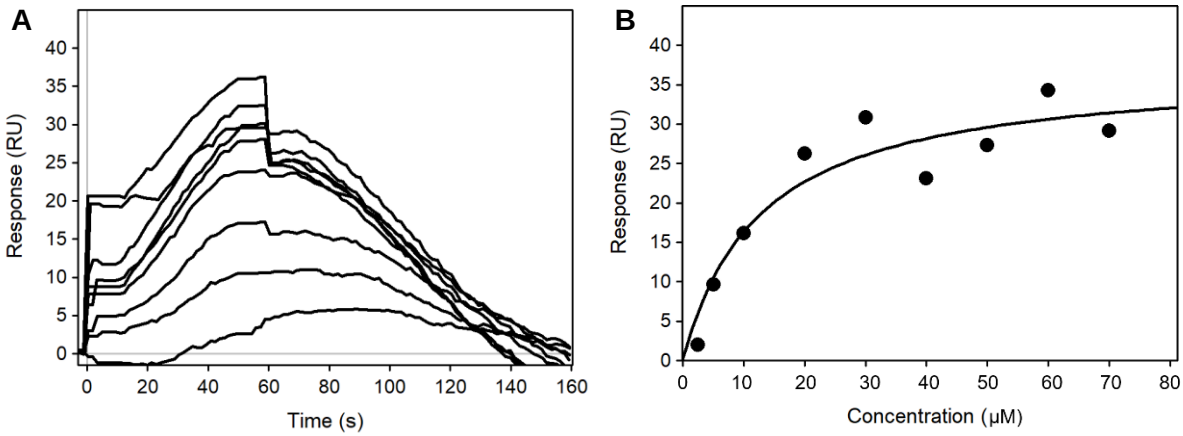

Supplementary Figure 158 (A) Overlay of sensorgrams of **7** injected at concentrations 2.5−70 μM over an immobilized ΔmtDXPS; (B) Fitting of responses at equilibrium according to 1:1 Langmuir binding model (K_D: 13 ± 3 μM).

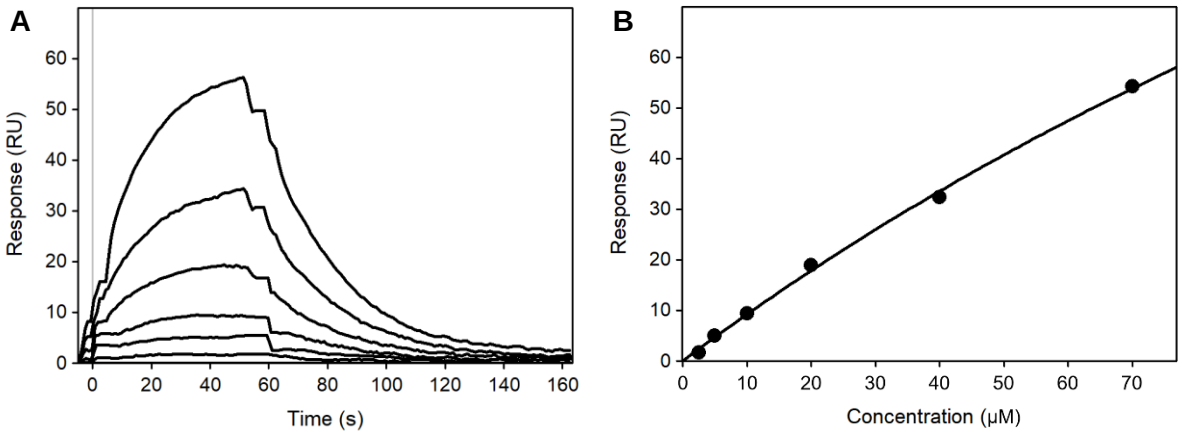

Supplementary Figure 159 (A) Overlay of sensorgrams of **8** injected at concentrations 2.5−70 μM over an immobilized ΔmtDXPS; (B) Fitting of responses at equilibrium according to 1:1 Langmuir binding model (K_D: 230 ± 20 μM).

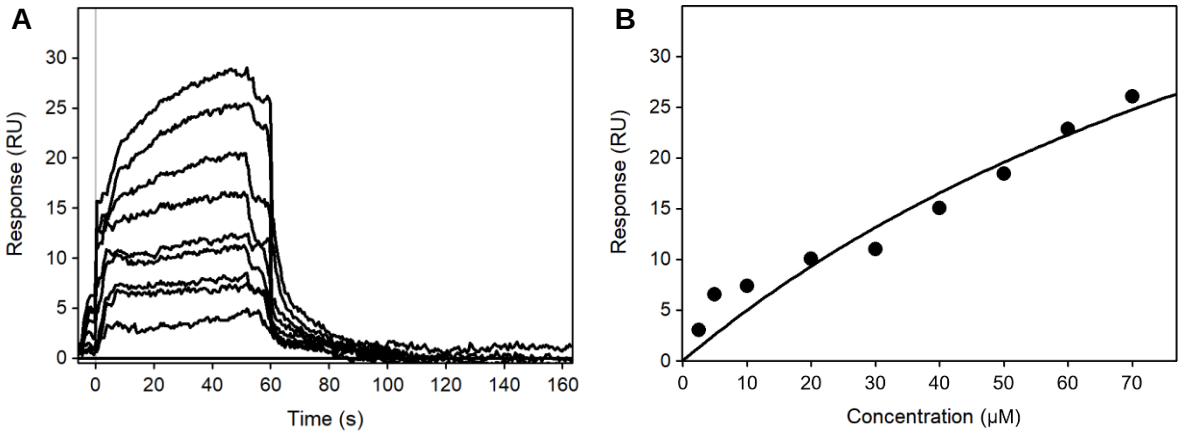

Supplementary Figure 160 (A) Overlay of sensorgrams of **9** injected at concentrations 2.5−70 μM over an immobilized ΔmtDXPS; (B) Fitting of responses at equilibrium according to 1:1 Langmuir binding model (K_D: 140 ± 50 μM).

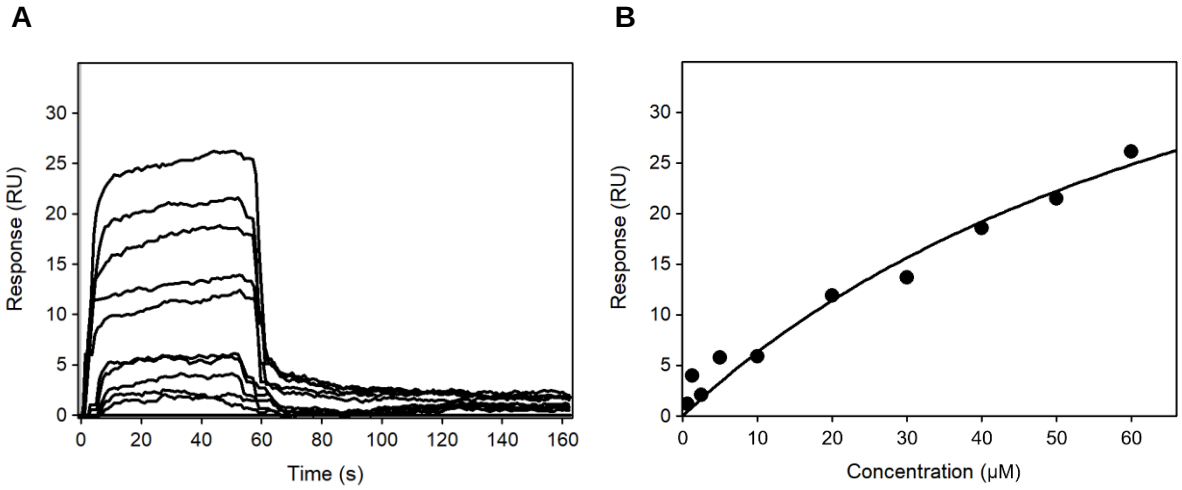

Supplementary Figure 161 (A) Overlay of sensorgrams of **11** injected at concentrations 0.625−60 μM over an immobilized ΔmtDXPS; (B) Fitting of responses at equilibrium according to 1:1 Langmuir binding model (K_D: 90 ± 30 μM).

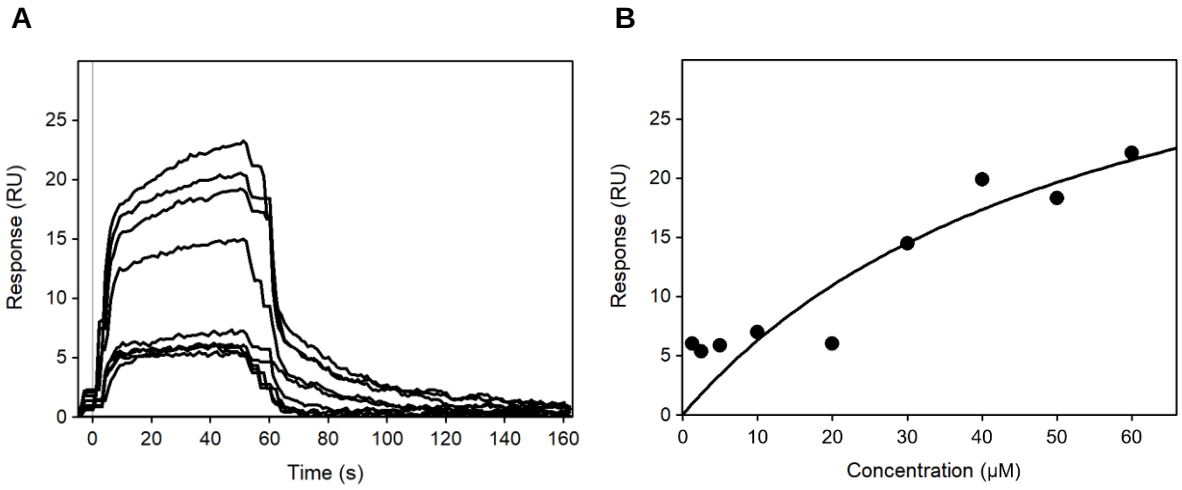

Supplementary Figure 162 (A) Overlay of sensorgrams of **12** injected at concentrations 1.25−60 μM over an immobilized ΔmtDXPS; (B) Fitting of responses at equilibrium according to 1:1 Langmuir binding model (K_D: 60 ± 20 μM).

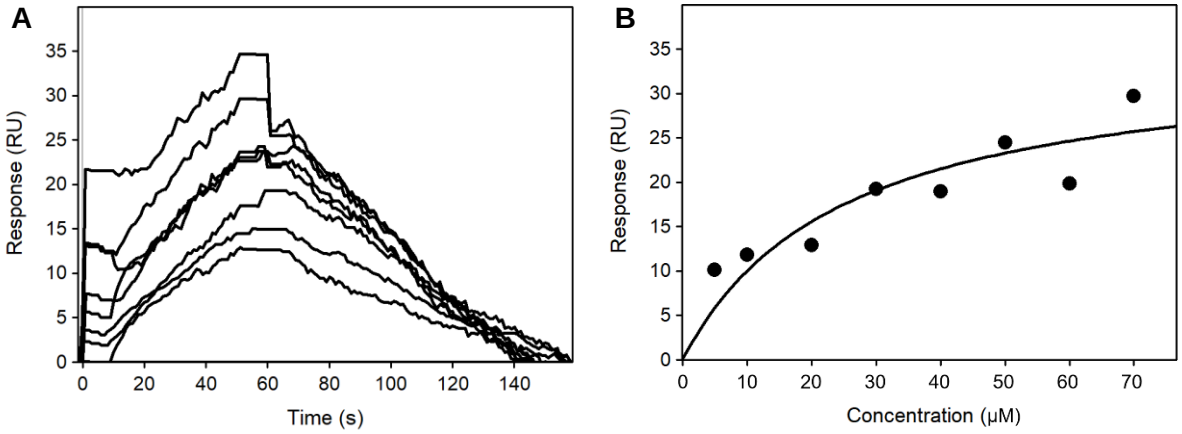

Supplementary Figure 163 (A) Overlay of sensorgrams of **21** injected at concentrations 5−70 μM over an immobilized ΔmtDXPS; (B) Fitting of responses at equilibrium according to 1:1 Langmuir binding model (K_D: 25 ± 8 μM).

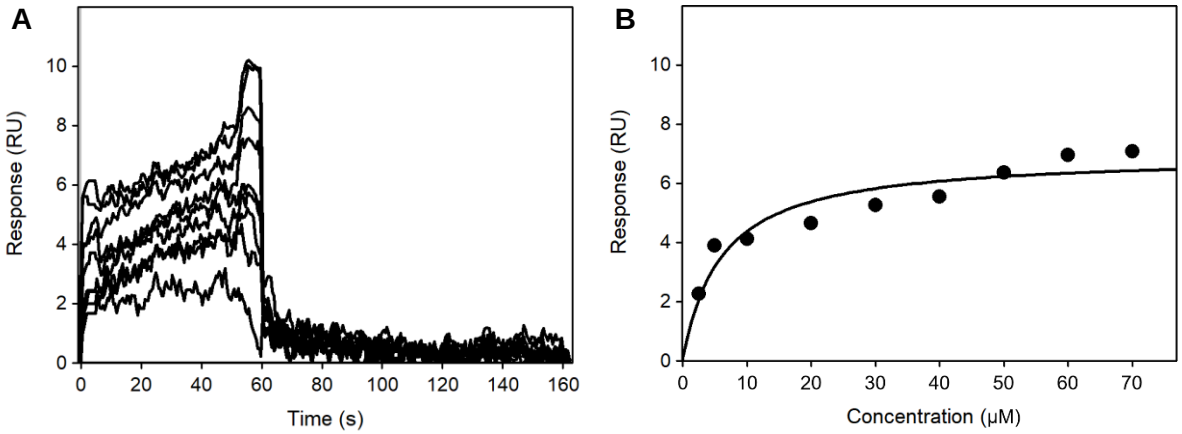

Supplementary Figure 164 (A) Overlay of sensorgrams of **22** injected at concentrations 2.5−70 μM over an immobilized ΔmtDXPS; (B) Fitting of responses at equilibrium according to 1:1 Langmuir binding model (K_D: 6 ± 1 μM).

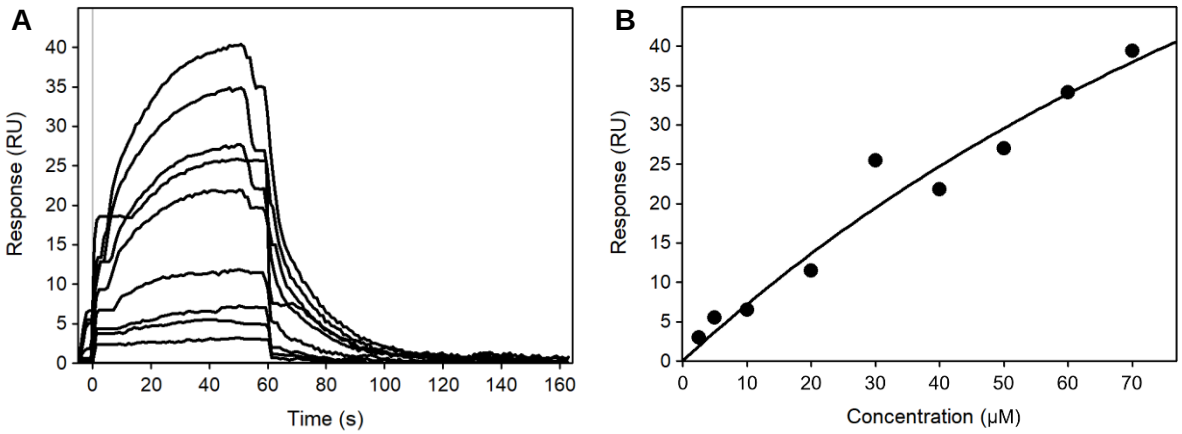

Supplementary Figure 165 (A) Overlay of sensorgrams of **23** injected at concentrations 2.5−70 μM over an immobilized ΔmtDXPS. (B) Fitting of responses at equilibrium according to 1:1 Langmuir binding model (K_D: 160 ± 40 μM)

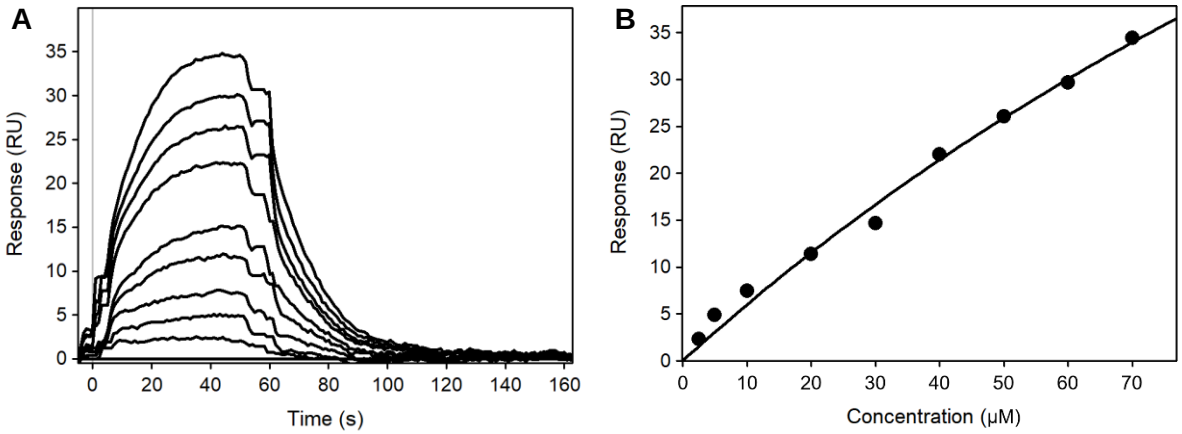

Supplementary Figure 166 (A) Overlay of sensorgrams of **24** injected at concentrations 2.5−70 μM over an immobilized ΔmtDXPS; (B) Fitting of responses at equilibrium according to 1:1 Langmuir binding model (K_D: 250 ± 60 μM).

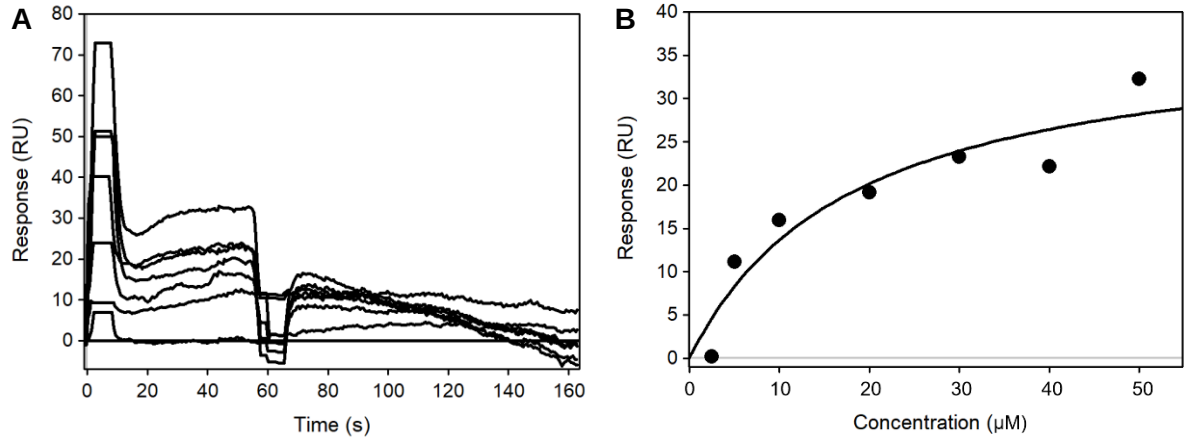

Supplementary Figure 167 (A) Overlay of sensorgrams of **25** injected at concentrations 2.5−50 μM over an immobilized ΔmtDXPS; (B) Fitting of responses at equilibrium according to 1:1 Langmuir binding model (K_D: 20 ± 4 μM).

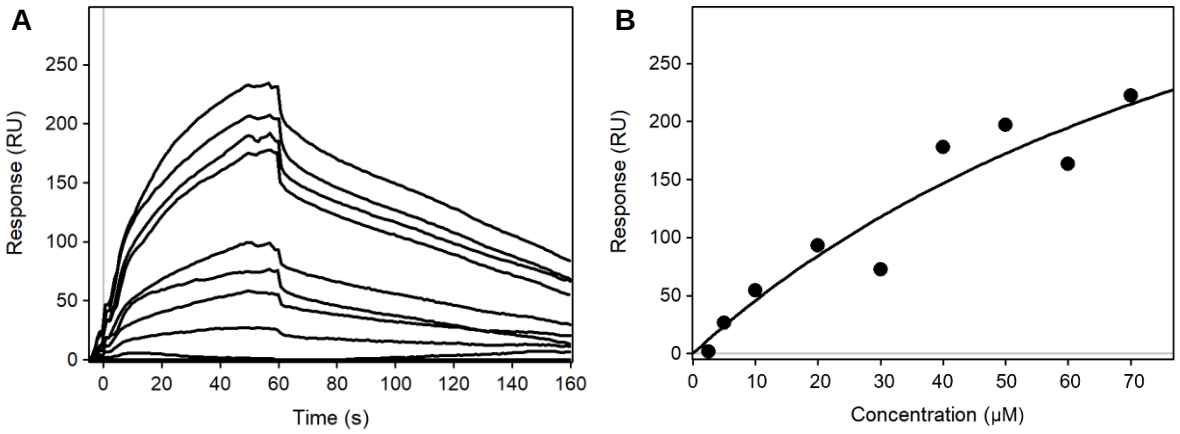

Supplementary Figure 168 (A) Overlay of sensorgrams of **26** injected at concentrations 2.5−70 μM over an immobilized ΔmtDXPS; (B) Fitting of responses at equilibrium according to 1:1 Langmuir binding model (K_D: 110 ± 40 μM).

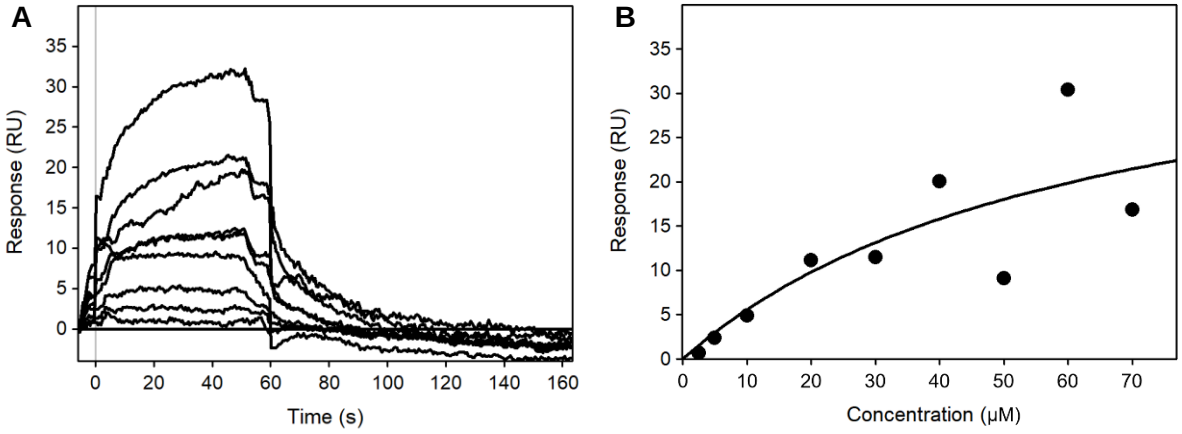

Supplementary Figure 169 (A) Overlay of sensorgrams of **35** injected at concentrations 2.5−70 μM over an immobilized ΔmtDXPS; (B) Fitting of responses at equilibrium according to 1:1 Langmuir binding model (K_D: 60 ± 20 μM).

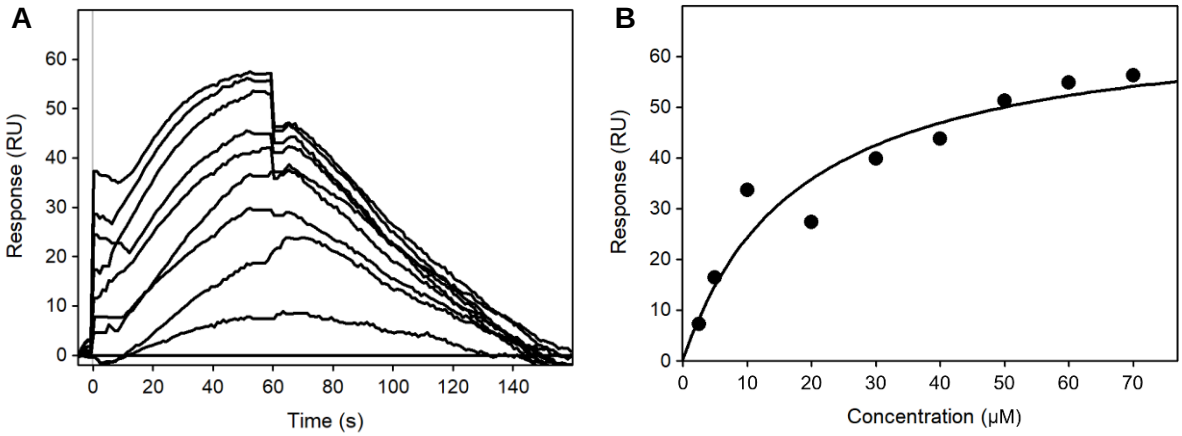

Supplementary Figure 170 (A) Overlay of sensorgrams of **37** injected at concentrations 2.5−70 μM over an immobilized ΔmtDXPS; (B) Fitting of responses at equilibrium according to 1:1 Langmuir binding model (K_D: 18 ± 3 μM).

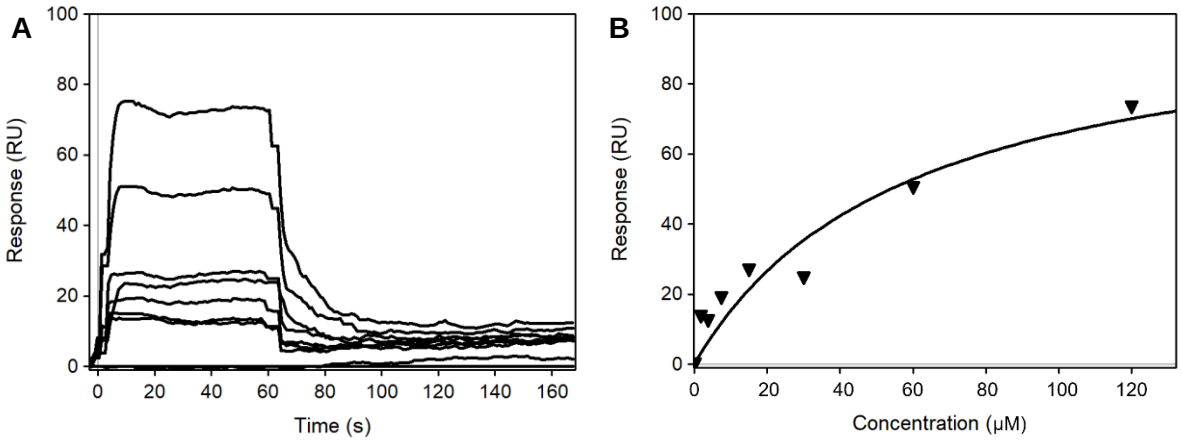

Supplementary Figure 171 (A) Overlay of sensorgrams of **38** injected at concentrations 0.2−120 μM over an immobilized dmtDXS; (B) Fitting of responses at equilibrium according to 1:1 Langmuir binding model (K_D: 60 ± 20 μM).

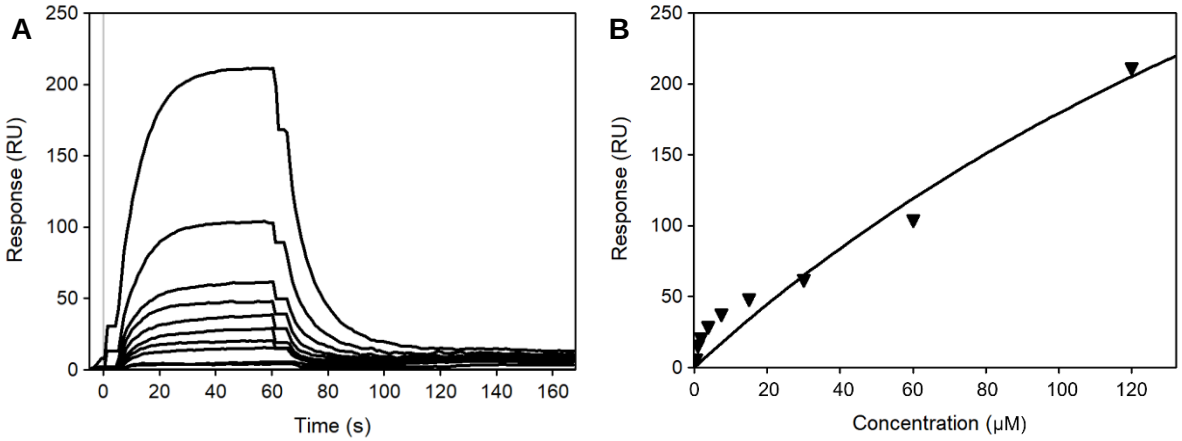

Supplementary Figure 172 (A) Overlay of sensorgrams of **39** injected at concentrations 0.2−120 μM over an immobilized dmtDXS; (B) Fitting of responses at equilibrium according to 1:1 Langmuir binding model (K_D: 260 ± 20 μM).

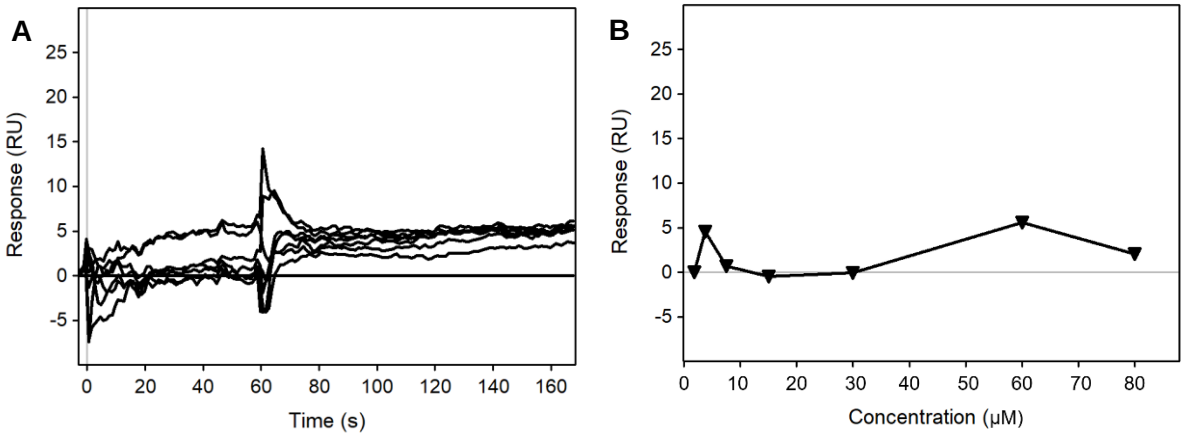

Supplementary Figure 173 (A) Overlay of sensorgrams of **40** injected at concentrations 1.9−80 μM over an immobilized dmtDXS; (B) Responses at equilibrium are concentration-independent and could not be fitted to Langmuir nor Hill binding model, indicating no significant binding.

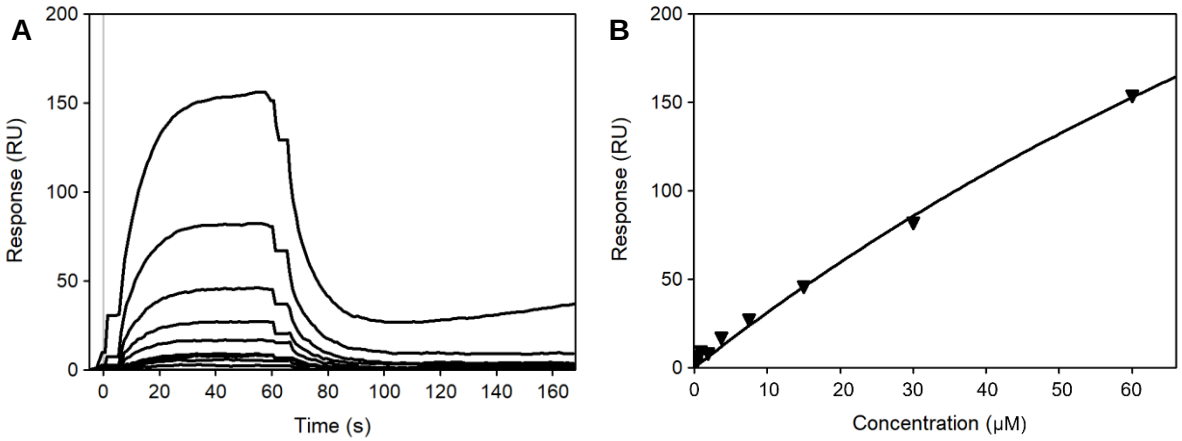

Supplementary Figure 174 (A) Overlay of sensorgrams of **41** injected at concentrations 0.2−60 µM over an immobilized dmtDXS; (B) Fitting of responses at equilibrium according to 1:1 Langmuir binding model (K_D: 210 ± 50 µM).

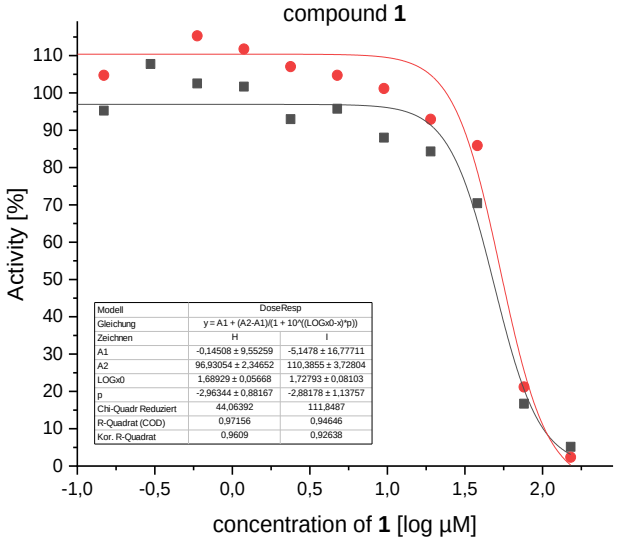

Supplementary Figure 175 Enzymatic activity of the enzyme drDXPS at different concentrations of compound **1**. Individual IC_{50} values are 53.4 ± 9.9 and 48.8 ± 6.3 µM; mean **IC_{50}: 51.2 ± 3.1 µM**. Triton X-100 was used in the assay.

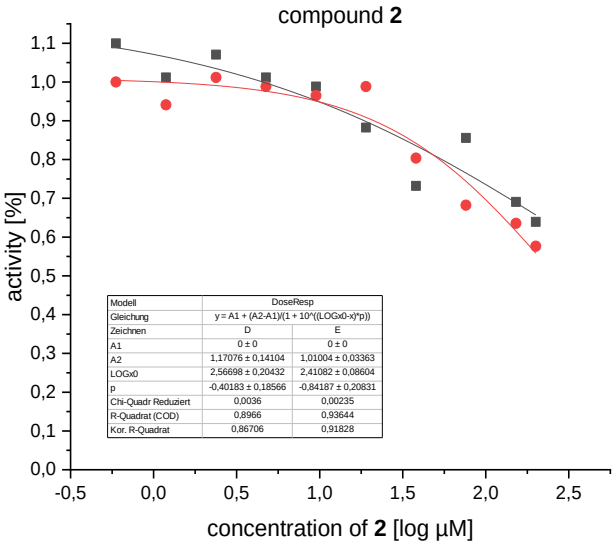

Supplementary Figure 176 Enzymatic activity of the drDXPS at different concentrations of compound **2**. Full inhibition could not be reached due to solubility limitations. Inhibition at 200 µM is 39.3 ± 4.4%, derived inhibition at 120 µM is 30.9 ± 3.6%. Triton X-100 was used in the assay.

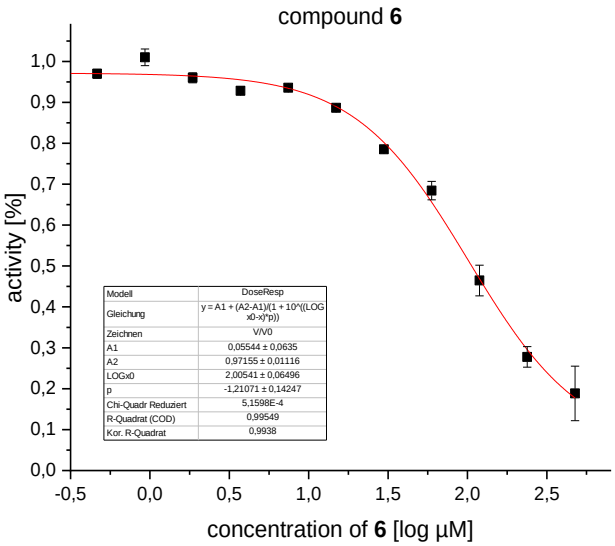

Supplementary Figure 177 Enzymatic activity of the enzyme drDXPS at different concentrations of compound **6**. Duplicates were averaged and fitted together, mean **IC_{50}: 101.3 ± 15.1 µM**. Triton X-100 was used in the assay.

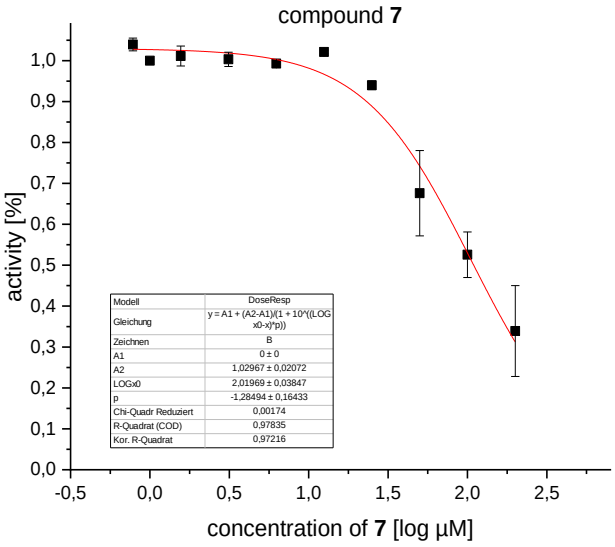

Supplementary Figure 178 Enzymatic activity of the enzyme drDXPS at different concentrations of compound **7**. Duplicates were averaged and fitted together, full inhibition could not be reached due to solubility limitations. Assuming full inhibition at high concentrations, an **IC_{50} of 104.6 ± 9.3 µM** was estimated. Triton X-100 was used in the assay.

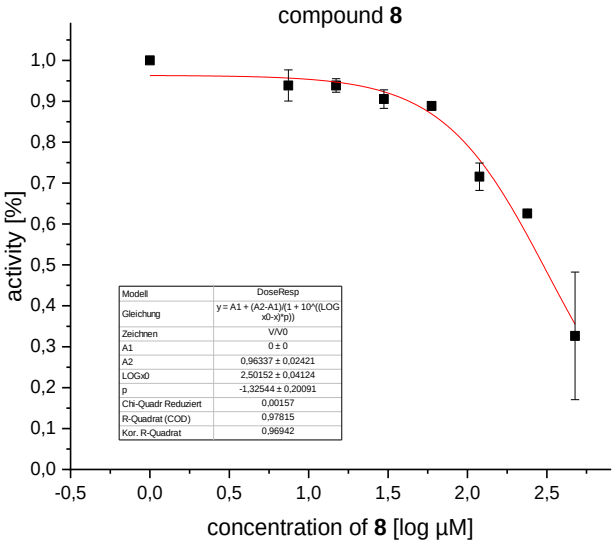

Supplementary Figure 179 Enzymatic activity of the enzyme drDXPS at different concentrations of compound **8**. Duplicates were averaged and fitted together, full inhibition could not be reached due to solubility limitations. Assuming full inhibition at high concentrations, an **IC_{50} of 317.3 ± 30.1 µM** was estimated. Triton X-100 was used in the assay.

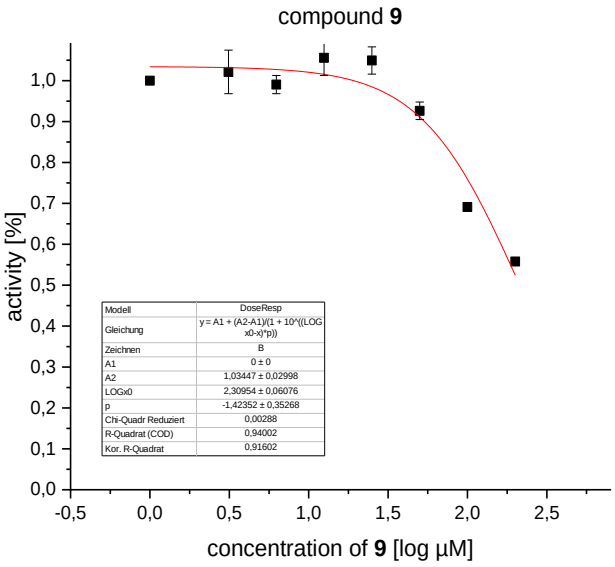

Supplementary Figure 180 Enzymatic activity of the enzyme drDXPS at different concentrations of compound **9**. Duplicates were averaged and fitted together, full inhibition could not be reached due to solubility limitations. Inhibition at 200 µM is 45.3%, derived inhibition at 120 µM is 30.1%. Triton X-100 was used in the assay.

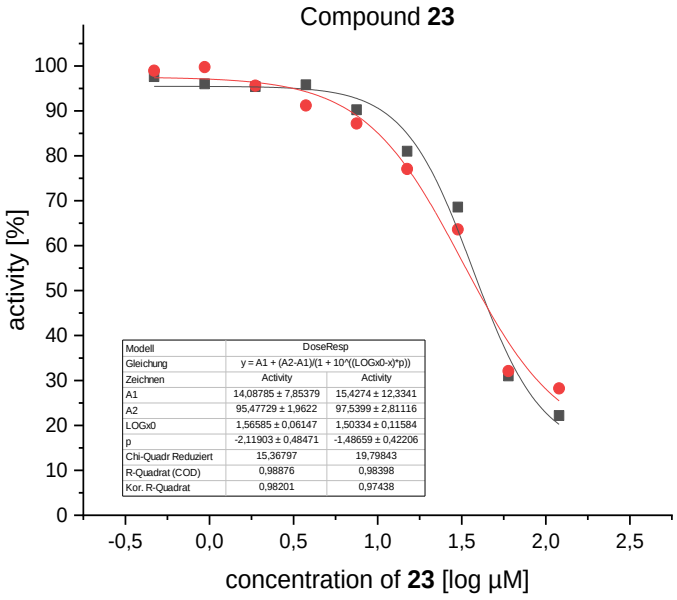

Supplementary Figure 181 Enzymatic activity of the drDXPS at different concentrations of compound **23**. Individual IC_{50} values are 36.8 ± 5.2 and 31.8 ± 8.5 µM; mean **IC_{50}: 34.3 ± 3.5 µM.**

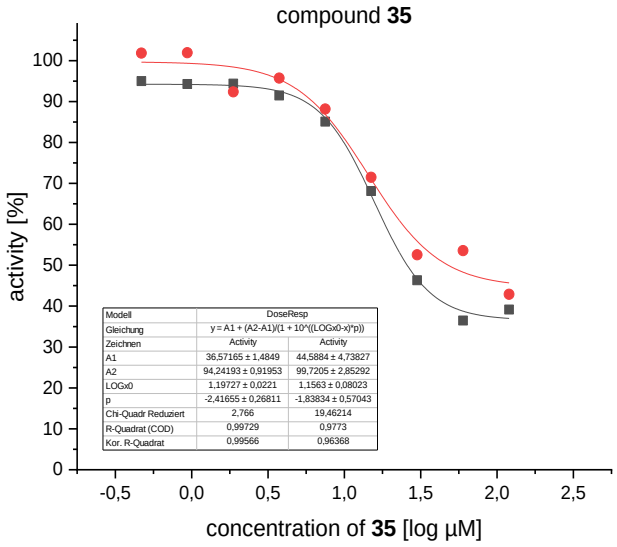

Supplementary Figure 182 Enzymatic activity of the drDXPS at different concentrations of compound **35**. Individual IC_{50} values are 15.75 and 14.33 µM. The compound seems to be a partial inhibitor, as the residual activity of the enzyme is 40 %.

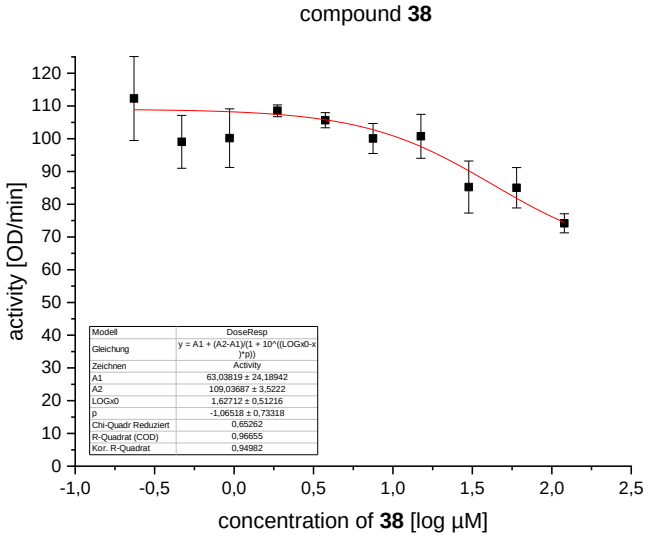

Supplementary Figure 183 Enzymatic activity of the drDXPS at different concentrations of compound **38**. Full inhibition could not be reached. Inhibition at 120 µM is 25.8 ± 2.9%.

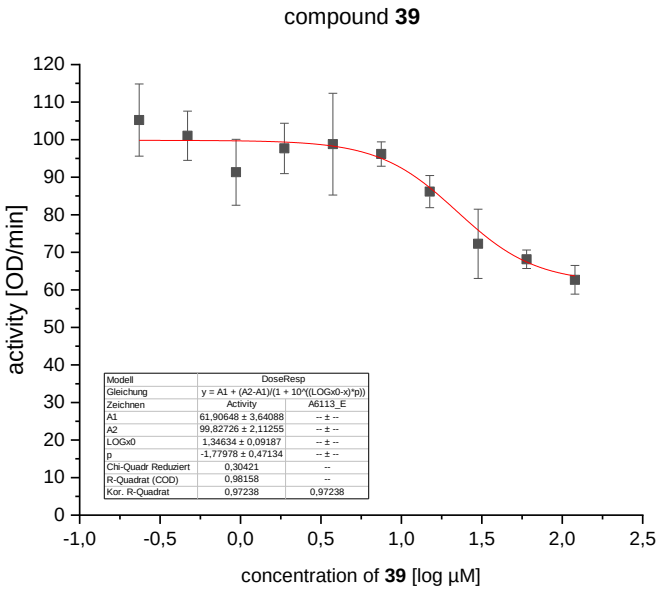

Supplementary Figure 184 Enzymatic activity of the drDXPS at different concentrations of compound **39**. Full inhibition could not be reached. Inhibition at 120 µM is 37.3 ± 3.8%

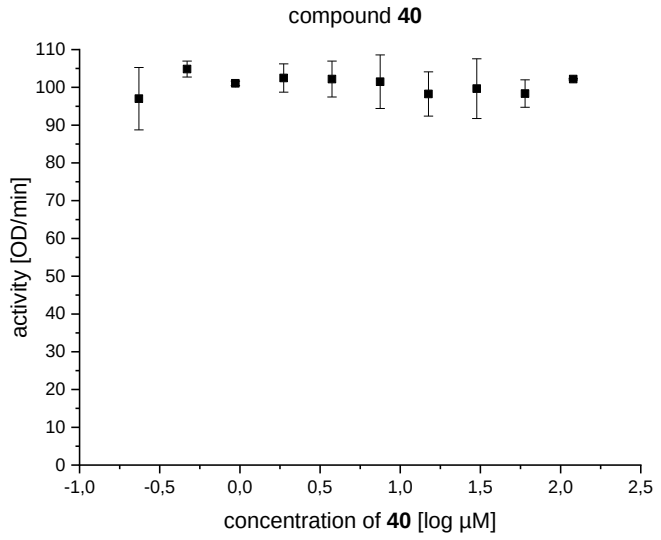

Supplementary Figure 185 Enzymatic activity of the drDXPS at different concentrations of compound **40**. Full inhibition could not be reached. Inhibition at 120 µM is 0 %

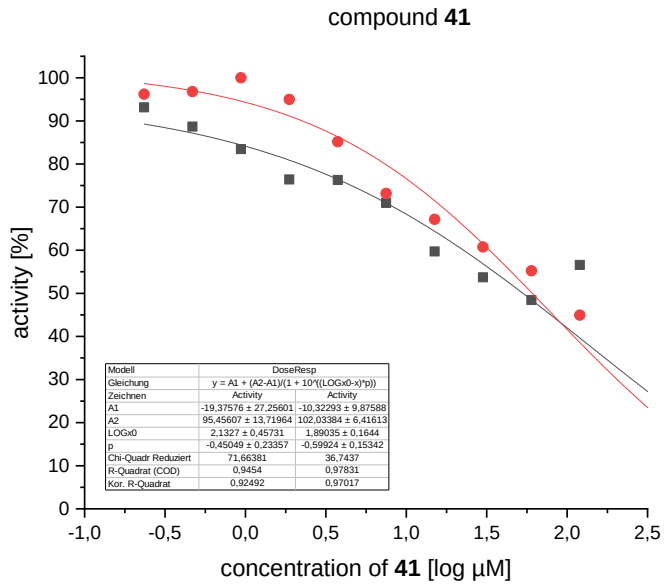

Supplementary Figure 186 Enzymatic activity of the drDXPS at different concentrations of compound **41**. Full inhibition could not be reached. Inhibition at 60 µM is 48.2 ± 3.4% and at 120 µM is 49.2 ± 5.8%. Assuming full inhibition at high concentrations, an **IC_{50} of 99 ± 2 µM** was estimated.

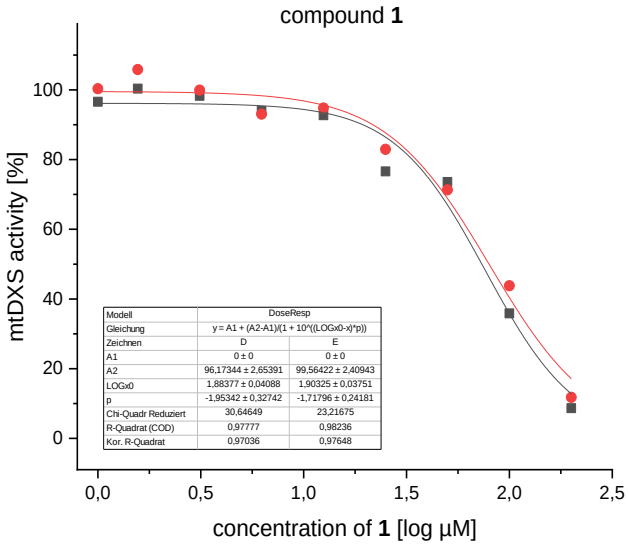

Supplementary Figure 187 Enzymatic activity of the mtDXPS at different concentrations of compound **1**. Individual IC_{50} values are 80.0 ± 6.9 µM and 76.5 ± 7.2 µM; mean **IC_{50}: 78.3 ± 2.5 µM**. Triton X-100 was used in the assay.

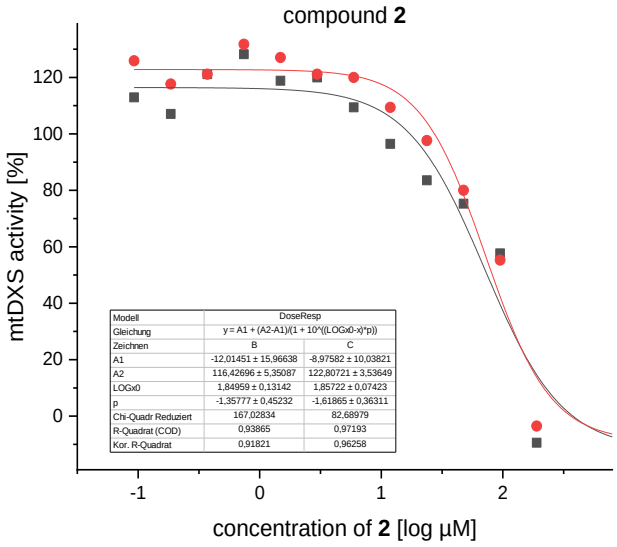

Supplementary Figure 188 Enzymatic activity of the mtDXPS at different concentrations of compound **2**. Individual IC_{50} values are 70.7 ± 21.4 and 72.0 ± 12.3 µM; **IC_{50}: 71.3 ± 0.99 µM.** Triton X-100 was used in the assay.

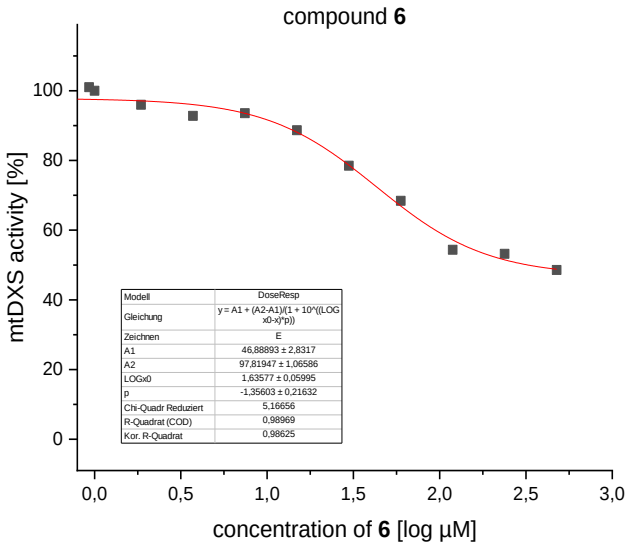

Supplementary Figure 189 Enzymatic activity of the mtDXPS at different concentrations of compound **6**. IC_{50}: 43.1 µM at the residual activity of 50 %. Triton X-100 was used in the assay.

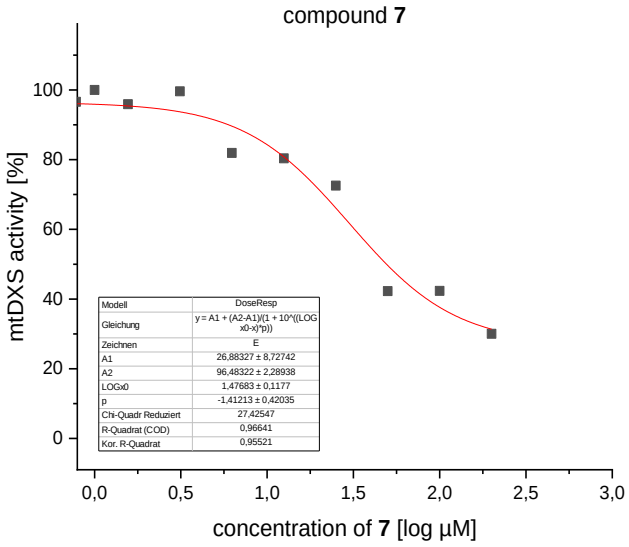

Supplementary Figure 190 Enzymatic activity of the mtDXPS at different concentrations of compound **7**. IC_{50}: 30 µM at the residual activity of 30 %. Triton X-100 was used in the assay.

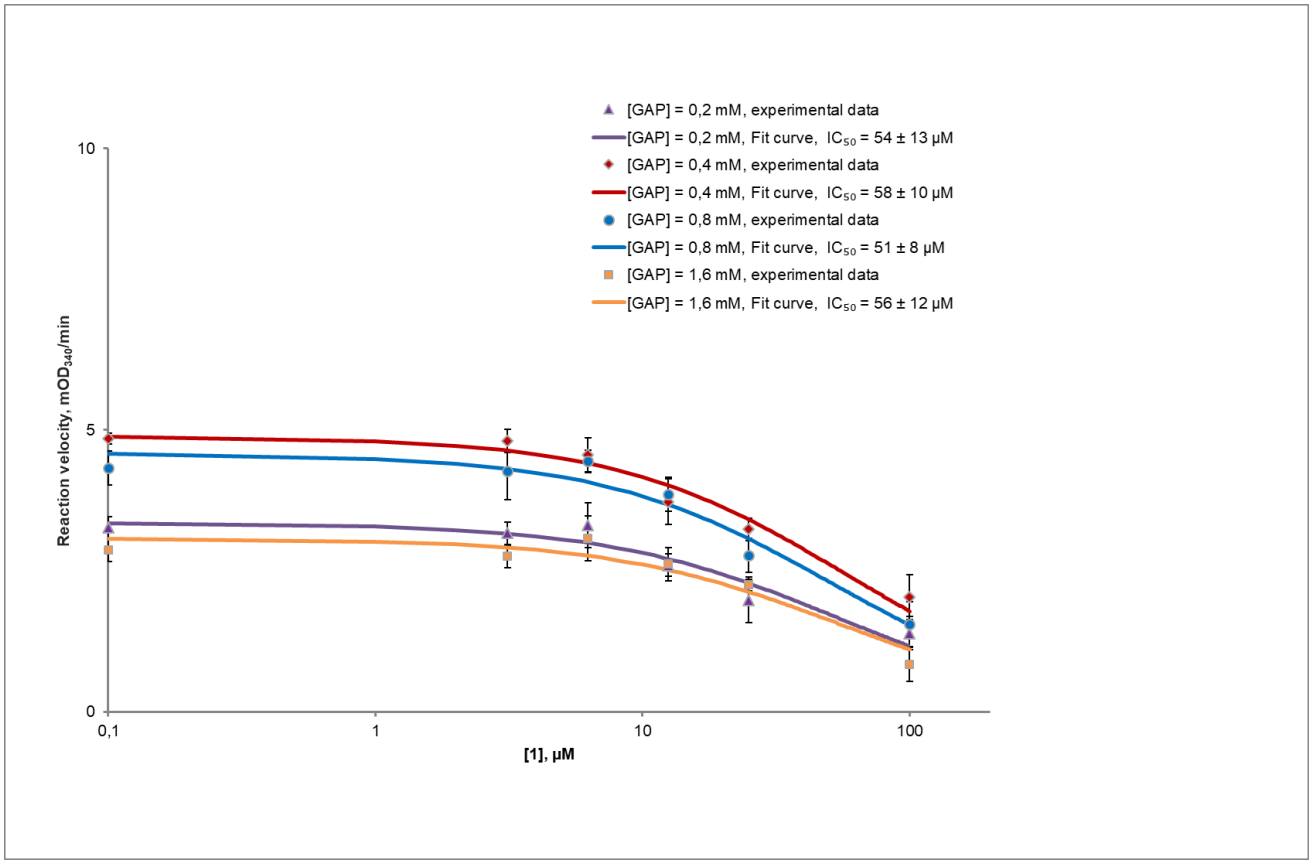

Supplementary Figure 191 Inhibition of drDXPS by **1** at different concentrations of D/L-GAP.

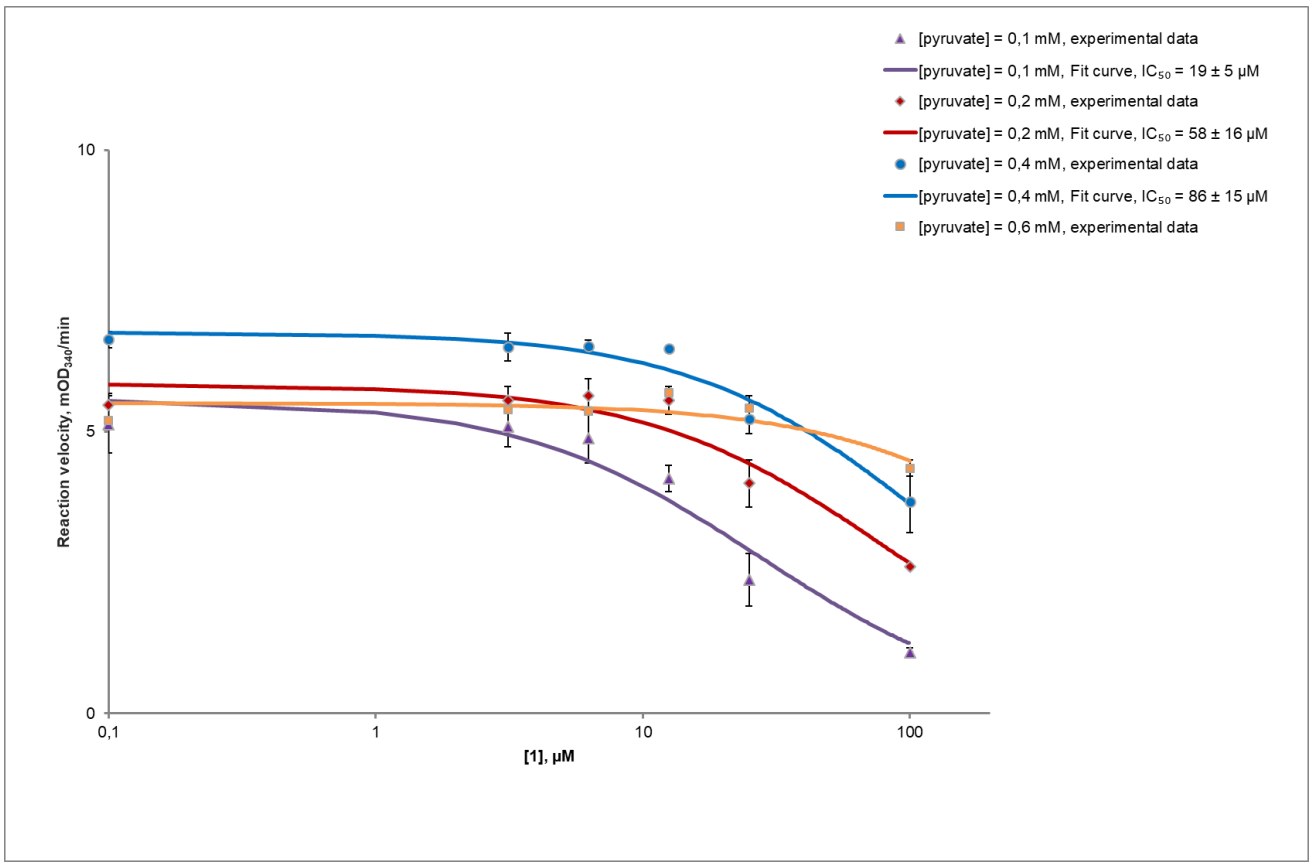

Supplementary Figure 192 Inhibition of drDXPS by **1** at different concentrations of pyruvate.

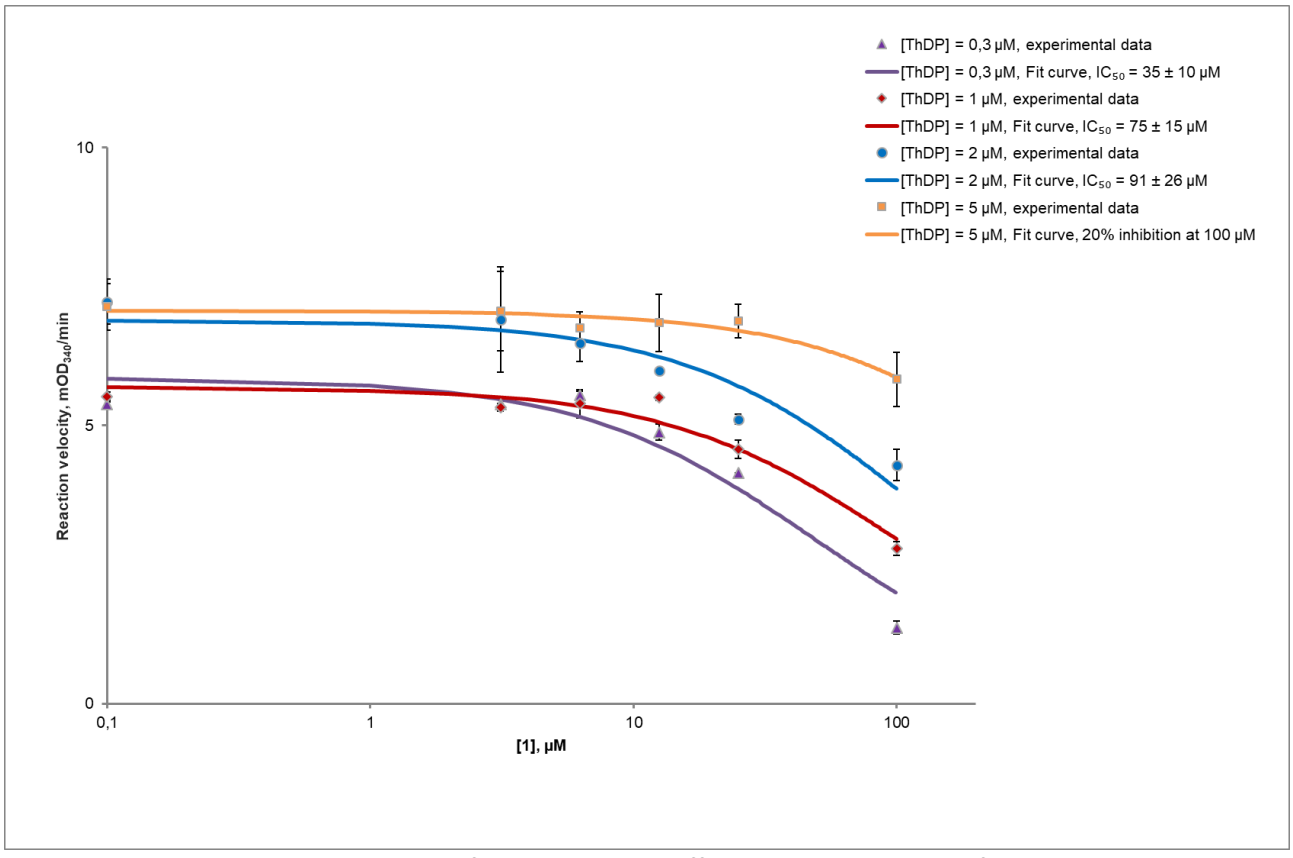

Supplementary Figure 193 Inhibition of drDXPS by **1** at different concentrations of ThDP.

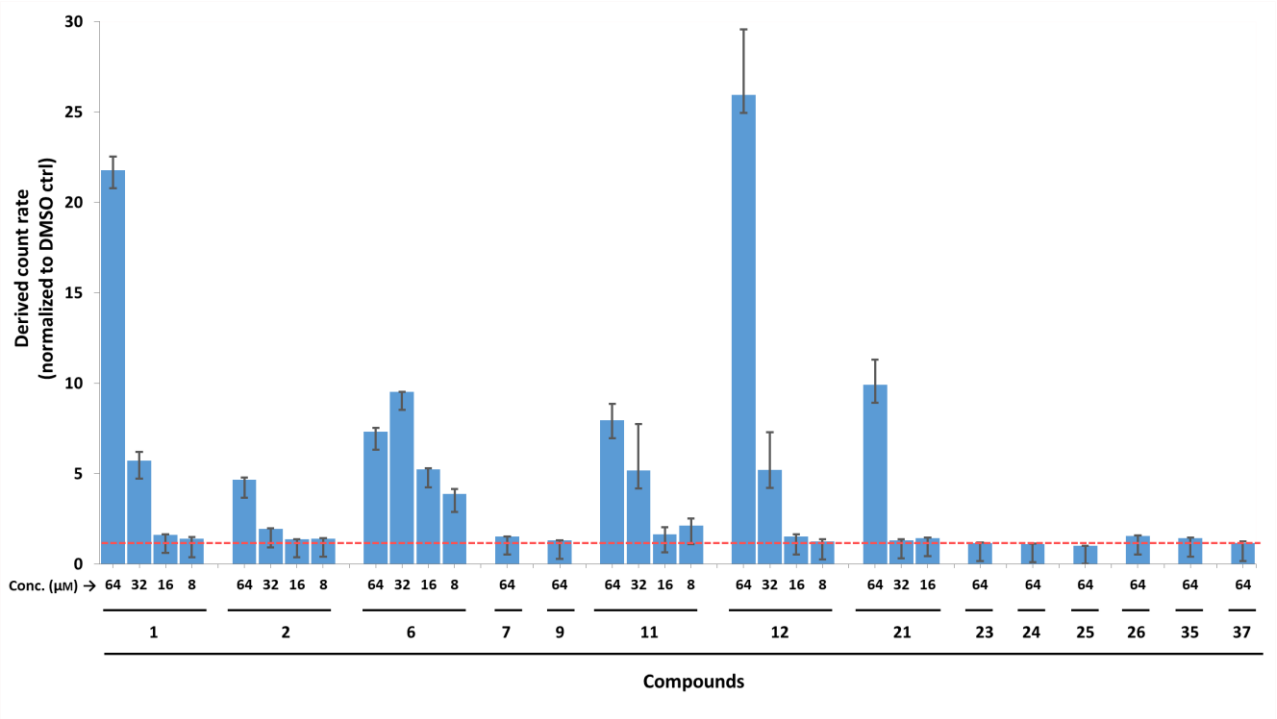

Supplementary Figure 194 Dynamic light scattering (DLS) measurements of DCC hits.

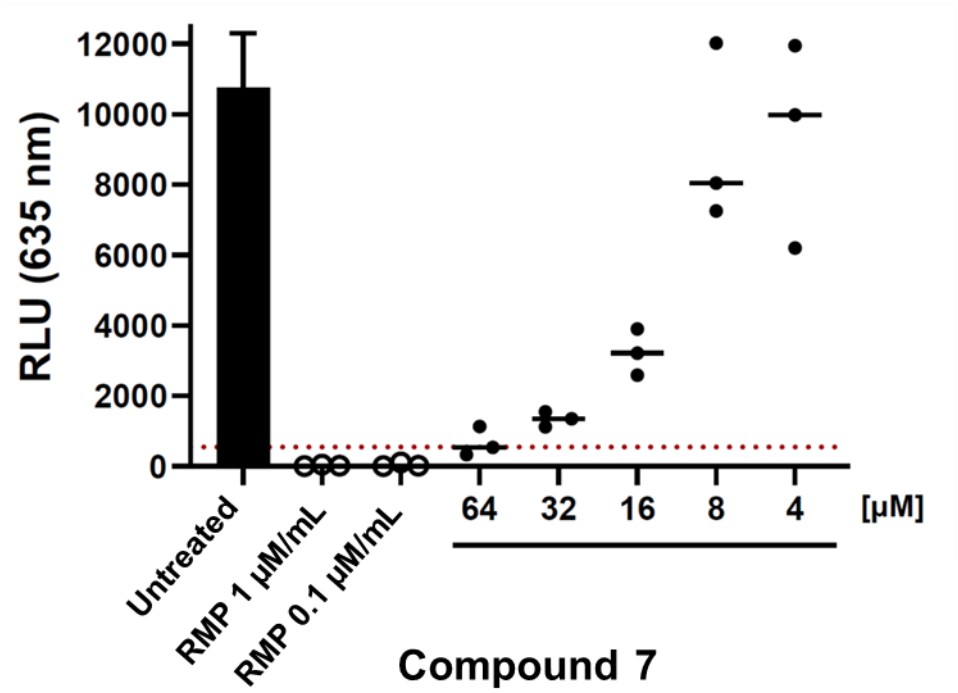

Supplementary Figure 195 Growth inhibition of *M. tuberculosis* (H37Rv) bacteria at different concentrations of compound **7** for MIC analysis.

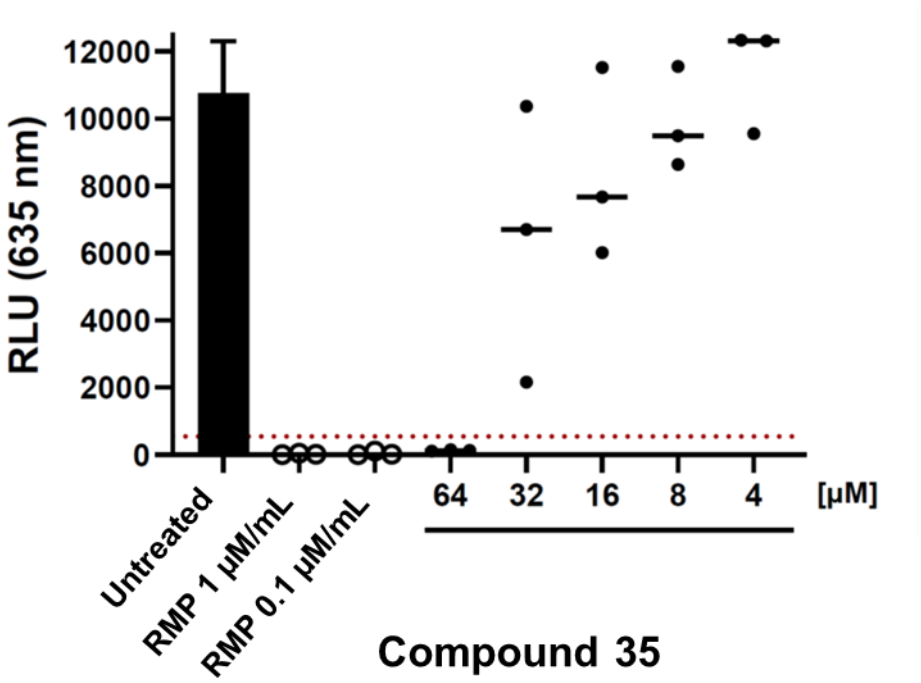

Supplementary Figure 196 Growth inhibition of *M. tuberculosis* (H37Rv) bacteria at different concentrations of compound **35** for MIC analysis.

SUPPLEMENTARY REFERENCES

1 P. Frei, L. Pang, M. Silbermann, D. Eriş, T. Mühlethaler, O. Schwardt and B. Ernst, *Chem. Eur. J.,* 2017, **23**, 11570.
2 P. Frei, R. Hevey, B. Ernst, *Chem. Eur. J.* 2019, **25**, 60.
3 S. Xiang, G. Usunow, G. Lange, M. Busch, L. Tong, *J. Biol. Chem.,* 2007, **282**, 2676.
4 LeadIT version 2.3.2; BioSolveIT GmbH, Sankt Augustin, Germany, www.biosolveit.de/LeadIT, **2017**.
5 K. Stierand, M. Rarey, *ACS Med. Chem. Lett.*, 2010, **1**, 540.
6 SeeSAR version 10.1; BioSolveIT GmbH, Sankt Augustin, Germany, www.biosolveit.de/SeeSAR, **2020**.
7 N. N. Farshori, A. Rauf, M. A. Siddiqui, E. S. Al-Sheddi and M. M. Al-Oqail, *Arab. J. Chem*, 2017, **10**, S2853
8 T. Masini, J. Pilger, B. S. Kroezen, B. Illarionov, P. Lottmann, M. Fischer, C. Griesinger, A. K. H. Hirsch, *Chem. Sci.*, 2014, **5**, 3543
9 S. Hecht, J. Wungsintaweekul, F. Rohdich, K. Kis, T. Radykewicz, C. A. Schuhr, W. Eisenreich, G. Richter and A. Bacher, *J. Org. Chem.*, 2001, **66**, 7770.
10 W. A. M. Elgaher, M. Fruth, M. Groh, J. Haupenthal, R. W. Hartmann, *RSC Adv.*, 2014, **4**, 2177
11 A. Zelmer, P. Carroll, N. Andreu, K. Hagens, J. Mahlo, N. Redinger, B. D. Robertson, S. Wiles, T. H. Ward, T. Parish, J. Ripoll, G. J. Bancroft and U. E. Schaible, *J Antimicrob. Chemother.*, 2012, **67**, 1948.
12 K. Kolbe, L. Möckl, V. Sohst, J. Brandenburg, R. Engel, S. Malm, C. Bräuchle, O. Holst, T. K. Lindhorst, N. Reiling, *ChemBioChem*, 2017, **18**, 1172.
13 A. Michelucci, T. Cordes, J. Ghelfi, A. Pailot, N. Reiling, O. Goldmann, T. Binz, A. Wegner, A. Tallam, A. Rausell, M. Buttini, C. L. Linster, E. Medina, R. Balling and K. Hiller, *Proc. Natl. Acad. Sci.,* 2013, **110**, 7820.
14 D. H. Schwarz, W. A. M. Elgaher, K. Hollemeyer, A. K. H. Hirsch and G. Wenz, *J. Mater. Chem. B*, 2019, **7**, 6148.
15 P. Kirsch, V. Jakob, W. A. M. Elgaher, C. Walt, K. Oberhausen, T. F. Schulz and M. Empting *ACS Chem. Biol.*, 2020, **15**, 388.
16 A. M. Hartman, V. R. Jumde, W. A. M. Elgaher, E. M. Te Poele, L. Dijkhuizen and A. K. H. Hirsch, *ChemMedChem*, 2021, **16**, 113.
17 A. Marcozzi, T. Masini, D. Zhu, D. Pesce, B. Illarionov, M. Fischer, A. Herrmann, A. K. H. Hirsch, *ChemBioChem,* 2018, **19**, 58.
18 P. Kuzmic, *Anal. Biochem.*, 1996, **237**, 260.